ZooKeys 1043: 1–20 (2021)
doi: 10.3897/zookeys.1043.66992
https://zookeys.pensoft.net

RESEARCH ARTICLE

A peer-reviewed open-access journal
ZooKeys
Launched to accelerate biodiversity research

Molecular and morphological systematics of a new, reef forming, cupped oyster from the northern Arabian Gulf: *Talonostrea salpinx* new species

Manal Al-Kandari[1], P. Graham Oliver[2], Daniele Salvi[3]

1 *Ecosystem-Based Management of Marine Resources, Environment and Life Sciences Research Center, Kuwait Institute for Scientific Research, Hamad Al-Mubarak Street, Building 900004, Area 1, Raas Salmiya, Kuwait* **2** *National Museum of Wales, Cathays Park, Cardiff CF10 3NP, UK* **3** *Department of Health, Life & Environmental Sciences - University of L'Aquila, Via Vetoio snc, 67100, L'Aquila-Coppito, Italy*

Corresponding author: Daniele Salvi (danielesalvi.bio@gmail.com)

Academic editor: Pavel Stoev | Received 6 April 2021 | Accepted 10 May 2021 | Published 10 June 2021

http://zoobank.org/0FC6C437-4834-4E5F-999E-218D9CA14593

Citation: Al-Kandari M, Oliver PG, Salvi D (2021) Molecular and morphological systematics of a new, reef forming, cupped oyster from the northern Arabian Gulf: *Talonostrea salpinx* new species. ZooKeys 1043: 1–20. https://doi.org/10.3897/zookeys.1043.66992

Abstract

The rocky northern shores of Kuwait and those of the western, inner shores of Kuwait Bay are dominated by a small, densely encrusting oyster. The identity of this oyster has never been confirmed and was mistaken previously for a small *Saccostrea*. The shell morphology suggests that this species belongs to the subfamily Crassostreinae, but within that subfamily, the presence of marginal erect trumpet-shaped projections is so far unique. Phylogenetic analyses based on mitochondrial DNA sequence data confirmed that this species belongs to the Crassostreinae and has a sister position to the clade including *Talonostrea talonata* and *T. zhanjiangensis*. Genetic distance between this species and *Talonostrea* species is remarkably high, being ~20% for the cytochrome oxidase I gene and ~7% for the 16S rRNA gene. Based on morphological and molecular analyses, this oyster is therefore described here as *Talonostrea salpinx* Oliver, Salvi & Al-Kandari, **sp. nov.** Shell morphology is shown to be variable, and the different forms encountered are described. The wider distribution and origins of this species, whether native or introduced, are discussed.

Keywords

COI, *cox1*, Crassostreinae, crassostreine oyster, DNA sequences, Kuwait, morphology, Ostreidae, 16S rRNA

Introduction

The invertebrate fauna of the northern Arabian Gulf and that of Kuwait has a relatively recent investigation period as evidenced by the dearth of specific literature cited by Jones (1986). While Kuwait and the Arabian Gulf were famous for the pearl fishing industry (Al-Shamlān 2000) and molluscs have been exploited for food for thousands of years (Cataliotti-Valdina 1990; Prieur 2011), the scientific investigation only dates from the 1980s (Al-Bakri et al. 1985). Although famous for pearl oysters (*Pinctada*), true oysters (Ostreidae) are a prominent feature of some shores, particularly around the island of Boubyan (Omar and Roy 2014). The island of Boubyan is listed as a potential world heritage site (https://whc.unesco.org/en/tentativelists/6257/) and is important for breeding and migratory birds such as the Crab Plover. Its waters are home to cetaceans including humpback dolphins, bottlenose dolphins, common dolphins and finless porpoises. Isolated oyster reefs are cited as an important ecological feature (Omar and Roy 2014) around the island of Boubyan where they are known locally as 'bogar boubyan' or 'Boubyan cows' due to their resemblance to a herd of cattle. These isolated reefs of oysters (Fig. 1E–F) appear at low water where they pose a risk to shipping. These oysters were tentatively identified as *Saccostrea cucullata* (Born, 1778) in Omar and Roy (2014). The earliest checklist for the Mollusca of Kuwait (Glayzer, Glayzer and Smythe 1984) also lists the dominant oyster at Khor Al-Subiyah (adjacent to Boubyan Island) as *Saccostrea cucullata*.

Over the years 2014 to 2018, the Kuwait Institute for Scientific Research carried out a survey of the Kuwait's intertidal fauna and the results for the Mollusca were published in 2020 (Al-Kandari et al. 2020). Two oyster species were common components of the upper and mid intertidal zone. On the eastern coast of Kuwait Bay and the southern coast of the mainland, *Saccostrea* was common and tentatively identified as *S. cucullata* (Born, 1778). Extensive aggregations of a second, small, oyster were found in Khor Al-Subiyah, adjacent to Boubyan Island, where the upper beach rock is entirely covered by oysters (Fig. 1A, B), extending for many tens of meters. The 'bogar Boubyan' mounds were also confirmed to be the same oyster but were not identified as *Saccostrea* but as a species of *Crassostrea*, the lack of marginal chomata confirming the identification. Similar oysters were also found in abundance on the inner Kuwait Bay shores, especially around the peninsula at Ashairij and the Umm Al-Namil Island (Fig. 1C, D).

Glayzer, Glayzer and Smythe (1984) mentions an unidentified *Crassostrea* from the south of Kuwait at An Niggalyat but list the dominant oyster at Khor Al-Subiyah and Ashairij as *Saccostrea cucullata*. Given that Kathleen Smythe in particular was well acquainted with the Arabian fauna, it is somewhat surprising that she did not recognize the presence of two genera of intertidal oysters. Jones (1986) lists the dominant oyster as *Crassostrea margaritacea* (Lamarck), now *Striostrea margaritacea* (Lamarck, 1819), but he notes that the identification is tentative. From the description given, with shells reaching 100 mm, it seems probable that Jones (1986) was describing *Saccostrea*; *Striostrea* has not been recognized from the northern Gulf. The tentative and incomplete

Figure 1. Oyster beds and reefs in northern Kuwait **A, B** Khor Al-Subiyah **C, D** Ashairij **E, F** Boubyan Island (North Khor Al-Subiyah).

recognition of intertidal oysters of Kuwait by previous authors perhaps illustrates the problematic nature of identifying oysters from their shells alone.

Given that these oysters are key components of the intertidal communities and are cited as a feature for a potential world heritage reserve, their precise identity is important. Consequently, the senior author within Kuwait Institute for Scientific Research (KISR) embarked upon a project to more precisely identify all oyster species in Kuwait based on both morphology and molecular data. Such an integrative taxonomic approach is essential for robust taxonomic identification and systematic assessment of oysters. Indeed, difficulties in identifying and classifying oysters based on a morphological diagnosis extend beyond the species level, up to the genus and subfamily ranks

(Salvi et al. 2014; Raith et al. 2016; Salvi and Mariottini 2021) because their morphology is extremely simplified and affected by high levels of phenotypic plasticity (e.g., Liu et al. 2011).

This paper concerns the identity of the oyster listed as *Crassostrea* sp., by Al-Kandari et al. (2020) from Khor Al-Subiyah and Ashairij; future papers will attend to other species including those in the genera *Saccostrea*, *Booneostrea*, *Ostrea* and *Hyotissa*.

Materials and methods

Sampling

Representative samples of all shell morphs were collected during the KISR intertidal survey of 2014–2017 (Al-Kandari et al. 2020) and in 2019 further samples were collected specifically for tissue extraction for the molecular study.

The sampling sites for the oysters considered here are indicated on the map (Fig. 2) and listed in Table 1. Specimens were levered open and the adductor muscle and mantle were excised whole or in part and fixed in 100% ethanol.

Molecular analysis

Total genomic DNA was extracted from 24 alcohol-preserved tissues following standard high-salt protocols (Sambrook et al. 1989). Two mitochondrial gene fragments were amplified by polymerase chain reaction (PCR), the cytochrome oxidase subunit I (*cox1*) and the 16S rRNA (16S). Primers and PCR protocols used for the ampli-

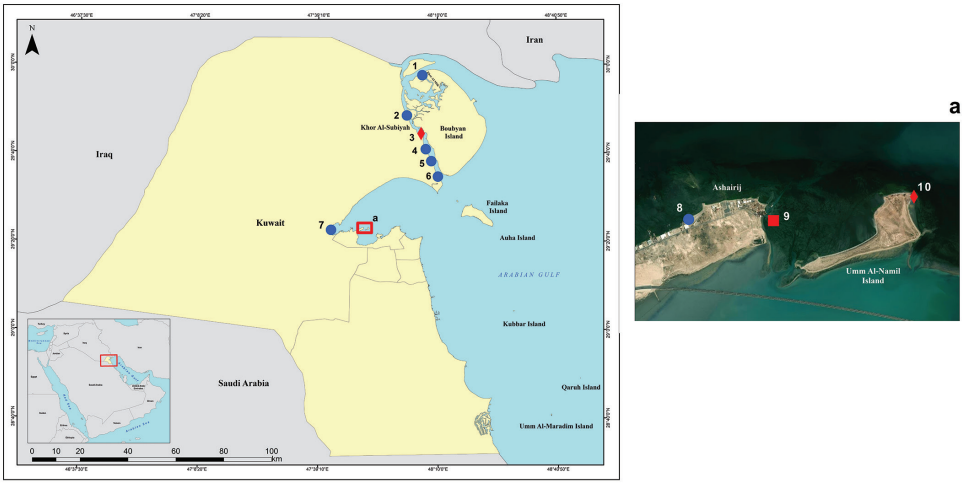

Figure 2. Map of Kuwait indicating known distribution of *Talonostrea salpinx* sp. nov. Blue circle for field records, red diamond for cited material, red square for type locality. Details of localities are given in Table 1.

fication are described in previous studies (Salvi et al. 2010; Crocetta et al. 2015). Sequencing of PCR products were carried out by the company GENEWIZ (https://www.genewiz.com), using the same primers employed for amplification. Details on sample data and GenBank accession numbers of sequences generated in this study are provided in Table 2 where we also indicated the GenSeq nomenclature for genetic sequences based on the reliability of the taxonomic identification of the source

Table 1. Sampling transects and localities of the intertidal oysters studied.

Transect	Location Name	Coordinates	Date	References
1	Khor Al-Milh	29.961222, 48.101151	2004–2005	Omar and Roy 2014
2	Boubyan Island (north Khor Al-Subiyah)	29.809521, 48.034599	17.12.2015	Al-Kandari et al. 2020
3	Khor Al-Subiyah (Al Maghasil)	29.74127, 48.09567	23.11.2014	Al-Kandari et al. 2020 and Revisited
4	Khor Al-Subiyah (Al-Alaimah)	29.68225, 48.115972	12.2019	Visited
5	Khor Al-Subiyah (Shumaymah)	29.65672, 48.13083	24.11.2014	Al-Kandari et al. 2020 and Revisited
6	Khor Al-Subiyah (Ras Himar)	29.578667, 48.16803	25.11.2014	Visited
7	Ras Kadmah (Al-Kuwaisat)	29.37795, 47.708	17.11.2014	Al-Kandari et al. 2020
8	Kuwait Bay (Ashairij)	29.38412, 47.83653	03.02.2014	Al-Kandari et al. 2020
9	Between Ashairij and Umm Al-Namil Island	29.383944, 47.849556	29.03.2021	Visited
10	Umm Al-Namil Island	29.38687, 47.87075	29.03.2021	Visited

Table 2. Genbank accession number, mitochondrial haplotype and GenSeq nomenclature (after Chakrabarty et al. 2013) for genetic sequences obtained from voucher specimens of *Talonostrea salpinx* sp. nov. analysed in this study (na: mitochondrial haplotype not available because the *cox1* sequence was not obtained).

Specimen Catalogue #	Locality	GenBank accession number		Haplotype	GenSeq Nomenclature
		cox1	16S		
NMW.Z.2021.009.001 (holotype)	Between Ashairij and Umm Al-Namil Island	MZ126560	MZ099713	Hap1	genseq-1 cox1, 16S
NMW.Z.2021.009.002/1 (paratype)		MZ126561	MZ099714	Hap9	genseq-2 cox1, 16S
NMW.Z.2021.009.002/2 (paratype)		MZ126562	MZ099715	Hap10	genseq-2 cox1, 16S
NMW.Z.2021.009.002/3 (paratype)		MZ126563	MZ099716	Hap1	genseq-2 cox1, 16S
NMW.Z.2021.009.002/4 (paratype)		MZ126564	MZ099717	Hap11	genseq-2 cox1, 16S
NMW.Z.2021.009.002/5 (paratype)		MZ126565	MZ099718	Hap1	genseq-2 cox1, 16S
NMW.Z.2021.009.002/6 (paratype)		MZ126566	MZ099719	Hap12	genseq-2 cox1, 16S
NMW.Z.2021.009.002/7 (paratype)		MZ126567	MZ099720	Hap1	genseq-2 cox1, 16S
NMW.Z.2021.009.002/8 (paratype)		MZ126568	MZ099721	Hap1	genseq-2 cox1, 16S
NMW.Z.2021.009.002/9 (paratype)		–	MZ099722	na	genseq-2 16S
NMW.Z.2021.009.002/10 (paratype)		–	MZ099723	na	genseq-2 16S
NMW.Z.2021.009.002/11 (paratype)		MZ126569	MZ099724	Hap13	genseq-2 cox1, 16S
NMW.Z.2021.009.004/1 (paratype)	Khor Al-Subiyah	MZ126570	MZ099725	Hap1	genseq-2 cox1, 16S
NMW.Z.2021.009.004/2 (paratype)		MZ126571	MZ099726	Hap2	genseq-2 cox1, 16S
NMW.Z.2021.009.004/3 (paratype)		MZ126572	MZ099727	Hap3	genseq-2 cox1, 16S
NMW.Z.2021.009.004/4 (paratype)		MZ126573	MZ099728	Hap1	genseq-2 cox1, 16S
NMW.Z.2021.009.004/5 (paratype)		MZ126574	MZ099729	Hap4	genseq-2 cox1, 16S
NMW.Z.2021.009.004/6 (paratype)		MZ126575	MZ099730	Hap5	genseq-2 cox1, 16S
NMW.Z.2021.009.004/7 (paratype)		MZ126576	MZ099731	Hap1	genseq-2 cox1, 16S
NMW.Z.2021.009.004/8 (paratype)		MZ126577	MZ099732	Hap6	genseq-2 cox1, 16S
NMW.Z.2021.009.004/9 (paratype)		MZ126578	MZ099733	Hap1	genseq-2 cox1, 16S
NMW.Z.2021.009.004/10 (paratype)		MZ126579	MZ099734	Hap7	genseq-2 cox1, 16S
NMW.Z.2021.009.004/11 (paratype)		MZ126580	MZ099735	Hap8	genseq-2 cox1, 16S
NMW.Z.2021.009.004/12 (paratype)		MZ126581	MZ099736	Hap1	genseq-2 cox1, 16S

specimens following Chakrabarty et al. (2013). Sequences of both gene fragments were obtained for 22 specimens, whereas for two specimens only 16S sequences were obtained (Table 2). These newly generated sequences were aligned with sequences of 46 oyster species obtained from GenBank and used in a recent phylogenetic assessment of the family Ostreidae (Salvi and Mariottini 2017; see Table 1 of Salvi and Mariottini 2017 for GenBank accession numbers). Multiple sequence alignments were performed with MAFFT v.7 (Katoh and Standley 2013) using the E-INS-i iterative refinement algorithm (alignments available on request from the authors). Genetic distance (uncorrected *p*-distance) between samples analysed in this study and sequences of oyster species obtained from GenBank were calculated with MEGA v.7 (Kumar et al. 2016).

Phylogenetic relationships were inferred by the Bayesian Inference method in BEAST 2.6.3 (Bouckaert et al. 2019) using the best models of nucleotide substitution selected by JModelTest 2.1.1 (Darriba et al. 2012) under the corrected Bayesian Information Criterion (*cox1*: HKY+G; 16S: GTR+I+G). We unlinked substitution models and clock models of gene partitions, and we linked the tree model across gene partitions. We used the Relaxed Uncorrelated Lognormal Clock model and the Yule process of speciation as tree prior. Two independent runs of 150 million generations were performed, sampling parameters every 15,000 generations. Results were analysed with Tracer 1.7 (Rambaut et al. 2018) to check the runs for convergence (burn-in = 25%). Runs were combined with LogCombiner and a consensus tree representing the posterior distribution was obtained in TreeAnnotator. Nodal support was estimated as Bayesian posterior probability (BPP).

Results

Molecular analysis

Mitochondrial sequences of the oysters from Khor Al-Subiyah and Ashairij represent 13 haplotypes differing from each other by one to three nucleotide substitutions occurring at 17 sites. Given their very limited genetic divergence, all 24 specimens analysed represent a single taxon. Phylogenetic analyses resolve the position of this taxon within the subfamily Crassostreinae as sister to the clade formed by *Talonostrea talonata* and *T. zhanjiangensis* (Fig. 3). This relationship received high statistical support (BPP ≥ 0.99). Genetic distances based on *cox1* between this new taxon and *Talonostrea*, *Magallana* and *Crassostrea* species range from 19 to 20.5%, 17.3 to 20%, and 21.9 to 24.2%, respectively. Genetic distances based on 16S between this new taxon and *Talonostrea*, *Magallana* and *Crassostrea* species range from 6 to 6.9%, 8.1 to 11%, and 16.5 to 21.1%, respectively.

Based on morphological and molecular assessments we assign these oysters to a new *Talonostrea* species that is described in the following section.

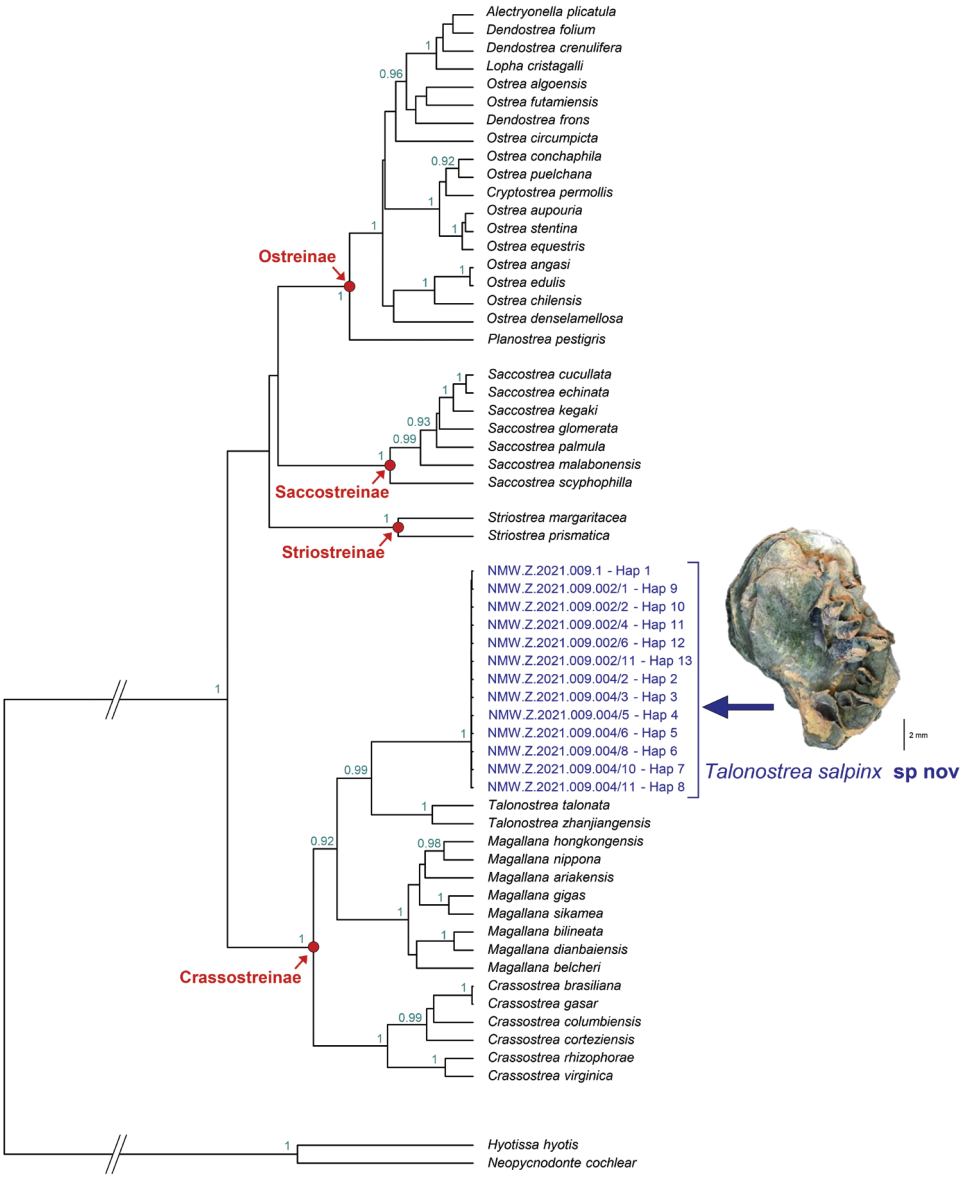

Figure 3. Bayesian phylogenetic tree based on *cox1* and 16S DNA sequence data. Bayesian posterior probability higher than 0.9 are reported in correspondence of the nodes.

Systematics

Ostreoidea Rafinesque, 1815
Ostreidae Rafinesque, 1815
Crassostreinae Scarlato & Starabogatov, 1979

Talonostrea X.-X. Li & Z.-Y. Qi, 1994

Type species. *Talonostrea talonata* X.-X. Li & Z.-Y. Qi, 1994

Nominal species included. *Crassostrea zhanjiangensis* X.-Y. Wu, S. Xiao & Z. Yu, 2013

Definition. The genus *Talonostrea* was first defined on morphological characters alone and was then monotypic, the type species *T. talonata* being described simultaneously by Li and Qi (1994). The oyster took the common name of the 'cat's paw oyster' referring to the folded and broadly digitate margin of the upper valve. This contrasts with *T. zhanjiangensis* and *T. salpinx* (described below), where the upper valve is flat with or without narrow fluted extensions. *Talonostrea salpinx* has the unique feature of possessing trumpet-shaped marginal projections. The shell, therefore, offers few if any defining characters. The anatomical character of a separated style sac observed in *T. talonata* has not been confirmed in *T. zhanjiangensis* and at this time, we cannot be sure if this character is an apomorphy of *T. talonata* or a synapomorphy of the genus as a whole. The anatomical arrangement in *T. salpinx* (see below) agrees with that of *T. talonata* as illustrated in Cavaleiro et al. (2019) and therefore does suggest that this is a defining feature of *Talonostrea*. As the anatomy of *T. zhanjiangensis* has not been described, the genus *Talonostrea* is confirmed on molecular data alone (Salvi and Mariottini 2017) but it is possible that the separate style sac/mid gut character will prove to be a synapomorphy of the genus.

Talonostrea salpinx Oliver, Salvi & Al-Kandari, sp. nov.

http://zoobank.org/533F31DC-1107-432E-BA79-279793A7C81F

Material examined. All type material deposited in the National Museum of Wales (NMW.Z) Kuwait • 20 + specimens in two clumps; Kuwait Bay, between Ashairij and Umm Al-Namil Island; 29.382423°N, 47.851735°E; intertidal as clumps on rocks and stones; 30 Nov 2019; PG Oliver leg. (Fig. 4). ***Holotype*** (Shell h in Fig. 4A–C) Kuwait • 1 shell; same collection data as for preceding; NMW.Z.2021.009.001; lower valve length 39.1mm, upper valve length 33.1 mm. ***Paratypes*** (Fig. 4D, to illustrate variation in internal colouration only) Kuwait • 11 specimens used in sequencing; collection data as for preceding; NMW.Z. 2021. 009.002/1–11.

Other material. Kuwait • remainder of shells in clumps; same collection data as for preceding; NMW.Z.2021.009.003. Kuwait • 20 + specimens in three clumps; Khor Al-Subiyah, Al Maghasil; 29.74127°N, 48.09567°E; upper intertidal reef forming on beach rock; 15 Nov 2015 and Dec 2019; PG Oliver leg. (Fig. 5). ***Paratypes.*** Kuwait • 12 specimens used in sequencing; collection data as for preceding; NMW.Z.2021.009.004/1–12. ***Paratypes.*** Kuwait • remainder of shells in clumps; same collection data as for preceding, NMW.Z.2021.009.005 (Fig. 5A, B, E). Kuwait • 50 + specimens; Kuwait Bay, Umm Al-Namil island; 29.38687°N, 47.87075°E; on stones, cobbles and rock in the upper intertidal; 29 March 2021; Manal Al-Kandari leg. ***Paratypes.*** Kuwait • 12 specimens; collection data as for preceding; NMW.Z.2021.009.006 (Fig. 6A–C) including shells from dissections.

Type locality. Kuwait, Kuwait Bay, between Ashairij and Umm Al-Namil Island, 29.382423°N, 47.851735°E, intertidal attached to rocks and cobbles, 30 Nov 2019, PG Oliver leg.

Derivation of name. *salpinx*, Greek, a trumpet; referring to the marginal trumpet-shaped projections typical of this species

Description. (**Type series from Ashairij**) Maximum size recorded 41 mm. Specimens of all sizes found growing on or among others creating dense clumps. Shells thin but robust. The lower (left) valve openly cupped, umbonal cavity shallow (Fig. 4B). Margins undulating, slightly raised, roundly digitate and occasionally drawn out into blunt spines. The attachment area is large, furnished with spines and foliations. The inner shell layer is white with brown to black pigmented adductor scars.

Upper (right) valve smaller than and fitting into lower valve (Fig. 4A). Rather flat but undulating, nacreous free margin very narrow. Outline variable, mostly oval some irregularly subquadrate to lingulate. External surface often worn smooth, or weakly foliaceous but not raised into commarginal frills. Occasional shells have open trumpet-shaped projections arising from the margins (Fig. 4E); these are formed by convoluted folding and do not form an entire tube. These trumpet-shaped spines are found mostly in small shells in sheltered sites. Hinge relatively narrow, ligament alivincular, amphidetic; dorsal area not greatly elongated. Chomata absent. External colouration mostly obscured by surface algae but pale grey, some with traces of purple radial streaks, these more prominent in small shells (Fig. 4F). The inner shell layer mostly white, inner margin frequently tinged with pale orange and dark grey, crescentic adductor scar mostly black, some brown, some lacking colour except for a dark ventral rim (Fig. 4C, D)

(**Paratype series from Khor Al-Subiyah**) (Fig. 5A–E) Maximum size recorded 30 mm. Specimens of all sizes forming a continuous reef over beach rock. The shells are thin but not fragile.

The lower valve is deeply cupped often with a deeper umbonal cavity related to the extension of the dorsal hinge plate. Attachment area over most of lower valve with interlocking spines and foliations. Outline is mostly oval but can be distorted into many shapes from lingulate to subcircular; the free margin is upturned, weakly convoluted with short blunt spines; except where growing in sheltered or uncrowded condition where the margins can be greatly extended into spathulate spines (Fig. 5C). Chomata are absent. The ligament is alivincular, the dorsal plate often elongated usually amphidetic but coiling in some. The inner shell layer colour white; adductor scar crescentic reddish-brown to dark brown/black in colour, colouration often extending into the umbonal cavity.

Upper valve smaller than, and fitting into lower valve. Rather flat but undulating, nacreous free margin very narrow slightly elevated. External surface weakly foliaceous but not raised into commarginal frills. Shells sheltered among others and juveniles frequently display open trumpet-shaped projections as above (Fig. 5D). External colouration is mostly obscured by algal growth but is underlying greyish-beige; juvenile shells and those in sheltered positions may have coloured radial bands of a purple-black

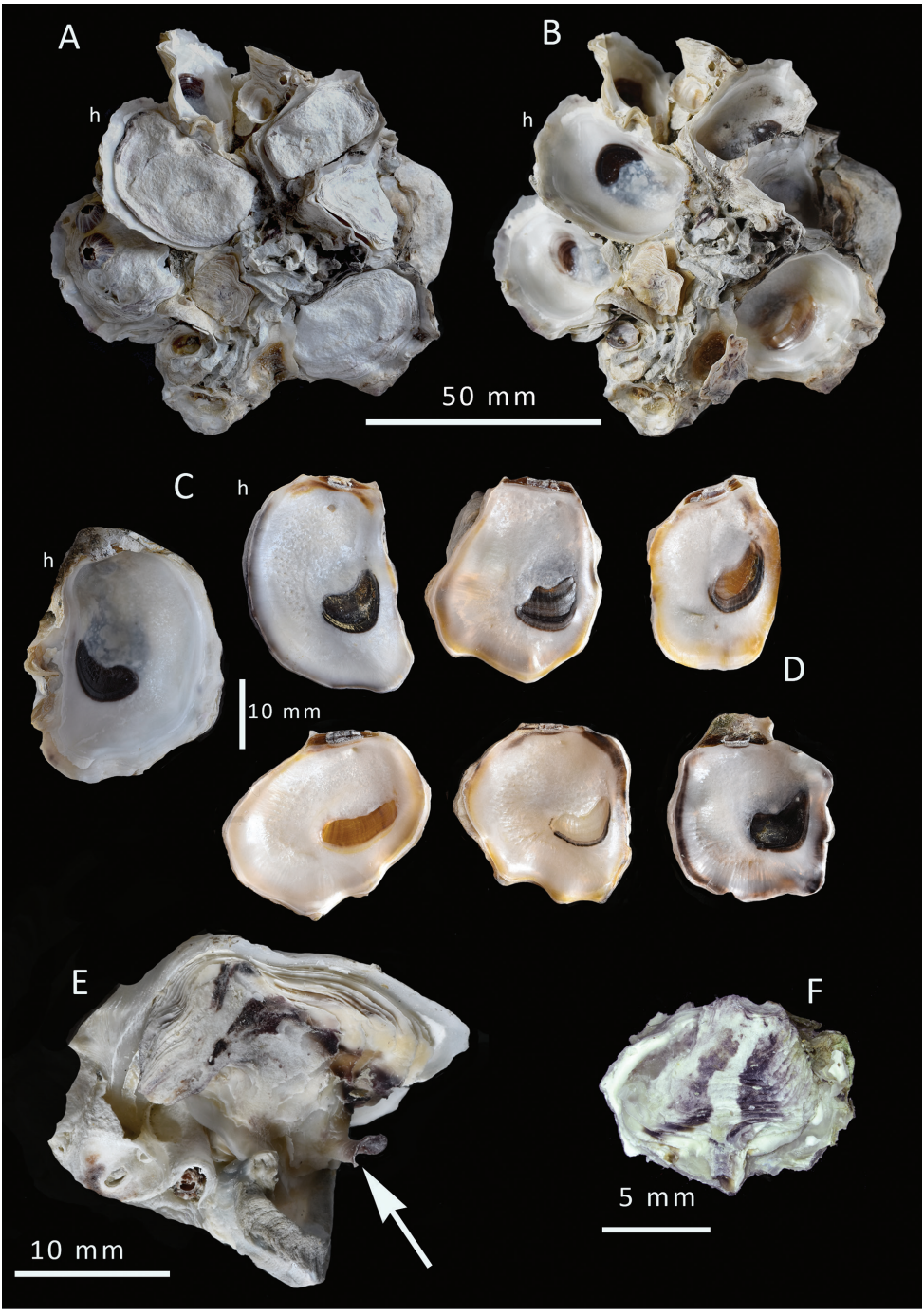

Figure 4. *Talonostrea salpinx* sp. nov. from Ashairij **A, B** clump with and without upper valves, shell h is holotype **C** inner views of lower and upper valves of holotype, NMW.Z. 2021.009. 001 **D** inner views of upper valves of five paratypes showing variation in shape and colouration, NMW.Z.009.002 **E** upper valve with a trumpet shapes projection, arrowed **F** a small upper valve showing radial purple-black colour banding.

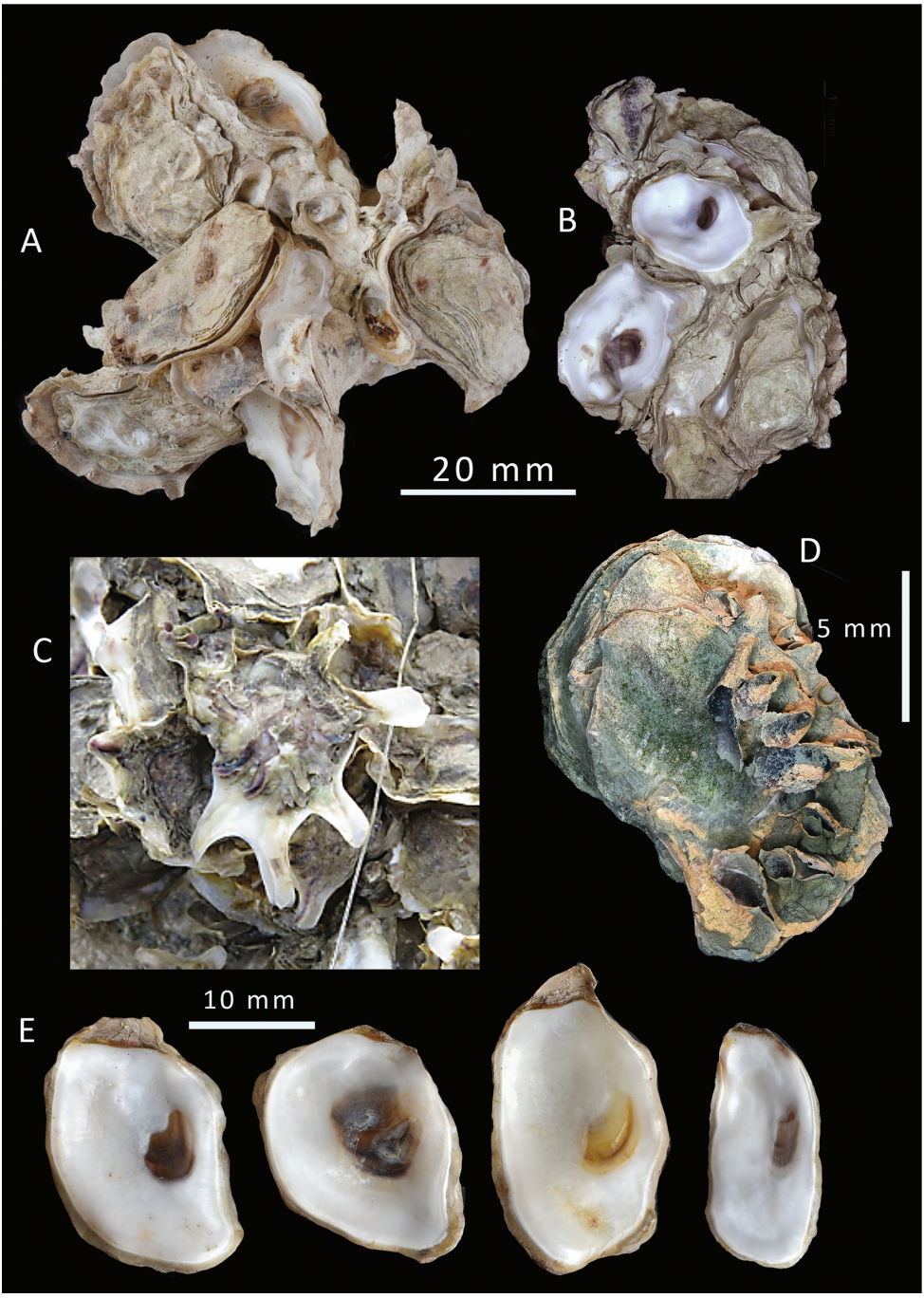

Figure 5. *Talonostrea salpinx* sp. nov. Paratypes from Khor Al-Subiyah, NMW.Z.2021.009.005 **A, B** clump with and without upper valves **C** in situ photograph of a shell from a sheltered position **D** small upper valve with an array of trumpet-shaped projections along margin **E** Inner views of four shells showing variation in shape and internal colouration.

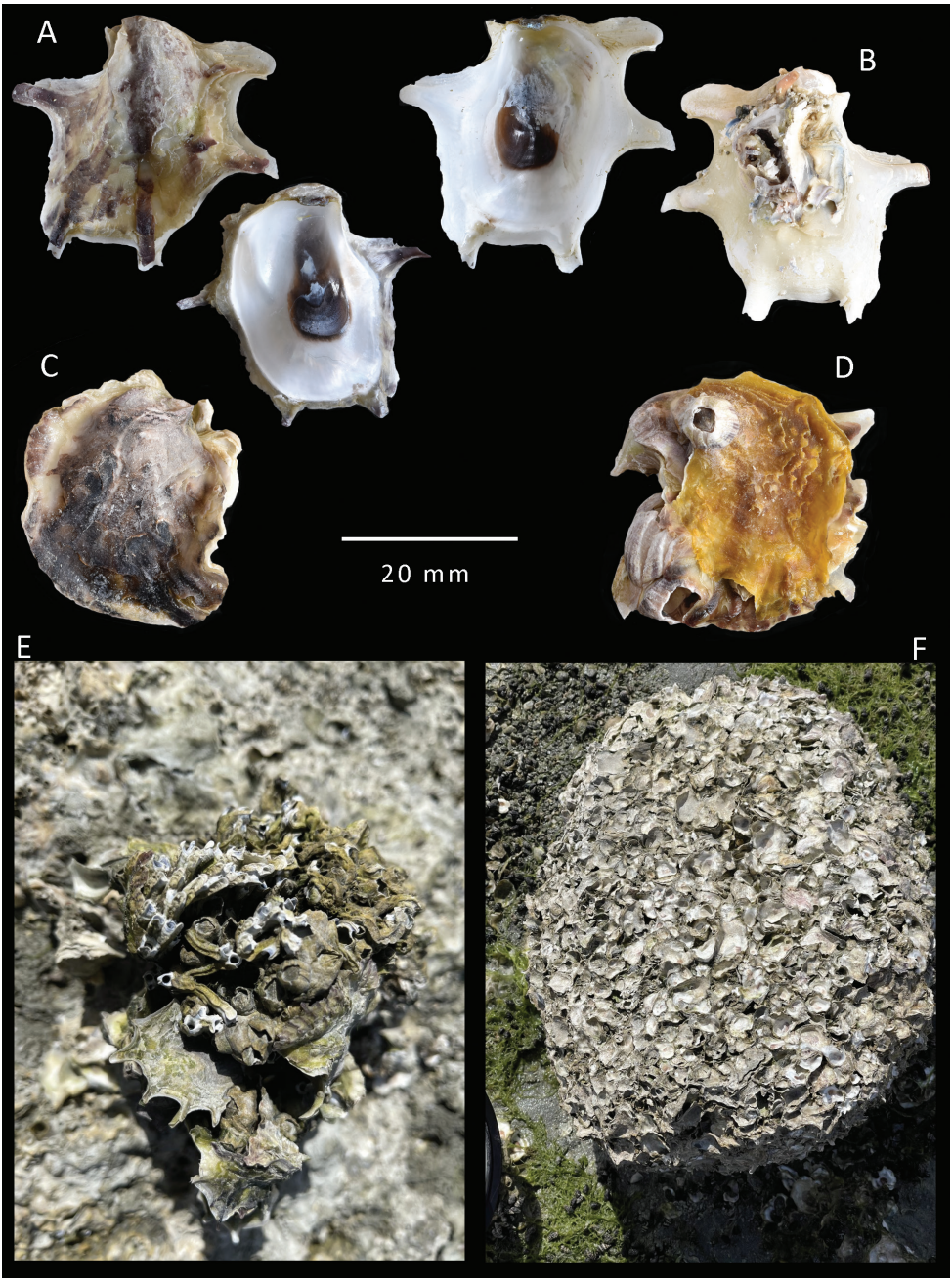

Figure 6. *Talonostrea salpinx* sp. nov. shells from Umm Al-Namil **A, B** external and internal views of a shell with marginal fluted spines, Paratypes NMW.Z.2021.009.006/ **C, D** Paratypes, NMW.Z.2021.009.006/2–3, shells of differing colours and lacking marginal fluted spines **E** clump of shells some with fluted spines associated with the tubeworm *Spirobranchus kraussi* (Baird, 1864) and the barnacle *Amphibalanus amphitrite* (Darwin, 1854). F, rock encrusted with irregular shaped shells mostly lacking fluted spines.

hue (Fig. 5C). Chomata are absent. The inner shell layer is white with the crescentic adductor scar brown to brown-black in colour (Fig. 5E).

(**Paratype series from Umm Al-Namil**) (Fig. 6A–D) Maximum size recorded 35 mm. Specimens of all sizes are found attached in clumps (Fig. 6E) to stones and cobbles or encrusting rocks (Fig. 6F). While most of these are identical to the type series (Fig. 6F) those from sheltered sites are rather thin, may have marginal extensions that are easily broken and often exhibit a more vivid colouration.

Attachment area small, free area with 5–7 prominent folds extending as furrowed spines (Fig. 6B). Outline is mostly oval but can be distorted into many shapes from lingulate to subcircular. Chomata absent. The ligament alivincular, dorsal plate often elongated usually amphidetic but coiling in some. The inner shell layer colour white: adductor scar crescentic reddish-brown to dark brown/black in colour, colouration often extending into the umbonal cavity (Fig. 6B).

Upper valve smaller than, and fitting into lower valve. Rather flat but undulating, nacreous free margin narrow, slightly elevated and extended as spines (Fig. 6A) fitting into furrows of lower valve. External surface weakly foliaceous, not raised into commarginal frills. External colouration ranging from uniformly dull grey, dirty white, to beige with purple-brown radial stripes extending onto spines (Fig. 6A); few golden brown (Fig. 6D) to purple-black all over (Fig. 6C). Chomata absent. Nacreous layer white with the crescentic adductor scar brown to brown-black in colour (Fig. 6A).

Anatomy (Fig. 7). Preserved specimens from Umm Al-Namil were opened by severing the ligament, levering the upper valve open slightly and then slicing the adductor muscle to free the upper valve. The animals were then dissected by sequentially removing the mantle (Fig. 7A), the ctenidia and finally dissecting into the visceral mass removing gonad and digestive diverticula tissue to reveal the alimentary system (Fig. 7B). Tissues have been stained in Methyl Blue to aid contrast.

The mantle in its preserved and contracted condition shows an array of radial folds (Fig. 7B). Mantle edge free except at the ventral margin where it is joined to the ctenidium. Mantle edge with three folds, middle fold with short pigmented, tuberculated, tentacles typically arranged with a one large one small pattern (Fig. 7C), inner fold with simple smooth unpigmented tentacles all of equal size and shape (Fig. 7C).

Adductor muscle crescent shaped in a posterior ventral position; pericardium immediately dorsal to it (Fig. 7A). Ctenidium of two reflected demibranchs (Fig. 7A), filamental rods bundled into groups of 10–12 by longitudinal and transverse junctions (Fig. 7F). Labial palps triangular, inner faces entirely with sorting ridges, oral groove smooth, short (Fig 7E).

Alimentary system (Fig. 7B) of large stomach within visceral mass dorsal of pericardium, surrounded by digestive diverticula; oesophagus enters dorsally; mid gut and style sac open on lower anterior side of visceral mass; style sac long, curving ventrally towards adductor muscle; mid gut running towards the posterior below the stomach and then hind gut travels on the posterior side dorsally before plunging under the stomach, curving ventrally, appearing through the pericardium and running as rectum around posterior of adductor muscle; anus simple slightly elevated (Fig. 7D).

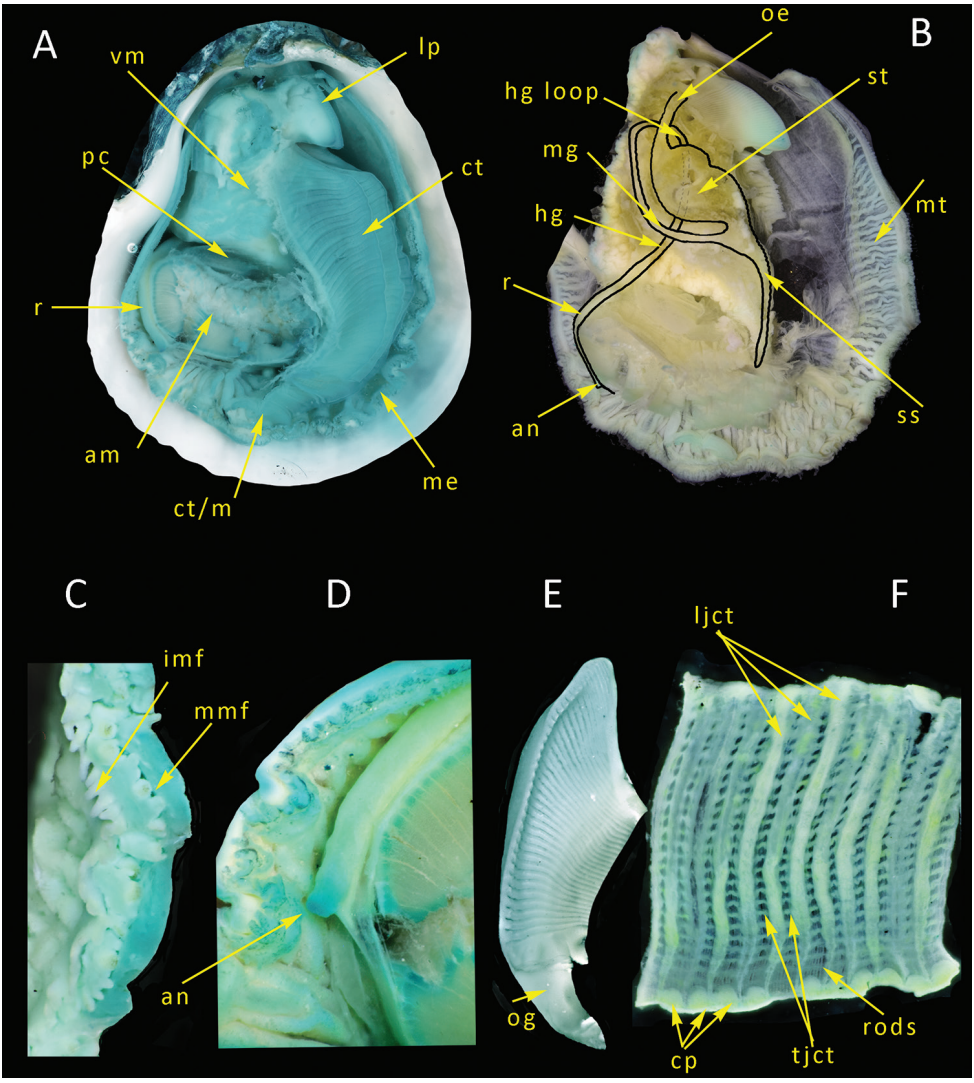

Figure 7. Anatomy of *Talonostrea salpinx* sp. nov. **A** gross view after removal of upper (right) valve **B** gross view including route of alimentary canal after removal of ctenidia, gonad and digestive diverticula **C** mantle edge **D** rectum and anus **E** excised labial palp **F** portion of ctenidium showing fine structures. Abbreviation: am, adductor muscle; an, anus; cp, ciliated pad; ct, ctenidium; ct/m, ctenidium mantle edge junction; hg, hind gut; hg loop, hind gut loop behind stomach; imf, inner mantle fold; ljct, longitudinal junction; lp, labial palp; me, mantle edge; mg, mid gut; mmf, middle mantle fold; mt, mantle; oe,oesophagus; og, oral groove; pc, pericardium; r, rectum; rods, ctenidial filaments; s, stomach; ss, style sac; tjct, transverse junction; vm, visceral mass.

Habitat. *Talonostrea salpinx* is an oyster of the upper and middle shores living attached to exposed hard substrates. Extensive oyster growth is seen in Khor Al-Subiyah and the western end of Kuwait Bay. The waters of these localities are highly turbid and often hypersaline (Al-Yamani et al. 2004), the intertidal environment is further stressed

by experiencing a summer air temperature maximum of 50°C and a winter minimum occasionally as low as 0°C. The summer salinity at Ashairij has been measured at 47 ppt whereas to the south it is around 45 ppt (Pokavinich et al. 2013). In Khor Al-Subiyah the salinity can be variable depending on the discharge from the Tigris and Euphrates rivers through the Shatt el Arab (Omar and Roy 2014). The indications are that *T. salpinx* can survive multiple extremes of turbidity, air temperature and salinity.

Distribution. *Talonostrea salpinx* has been found or recorded from a number of locations other than that cited in Material examined. The current distribution can be summarised as the south-eastern area of Kuwait Bay, from Raz Kazmah to Umm Al-Namil Island where extensive fields are present, and the oysters are attached to low rocks and loose cobbles. Throughout Khor Al-Subiyah, including Khor Al-Milh adjacent to Warbah Island in the very north of Boubyan, where oysters form intertidal reefs and mounds. It has also been found at an unlisted locality in Iran (see Discussion).

Remarks. The shell morphology of *T. salpinx* is in keeping with other crassostreines in lacking any chomata. Unusual for the subfamily is the presence of the trumpet-shaped marginal projections as these are not recorded for any other Indo-Pacific *Magallana* or *Talonostrea* nor indeed for any Atlantic *Crassostrea* (Inaba and Torigoe 2004). The adductor scar is strongly pigmented in the larger shells, a character not shared by *T. talonata* but present in *T. zhanjiangensis*.

Talonostrea talonata is known as the 'cat's paw oyster' (Li and Qi 1994; Cavaleiro et al. 2019) due to it having a strongly ridged and digitate upper valve and in this feature is very different from *T. salpinx.* The only other *Talonostrea* is *T. zhanjiangensis* Wu et al. 2013. and here there is greater similarity with *T. salpinx* in having a weakly undulating cupped lower valve and a rather flat featureless upper valve but lacking trumpet-shaped marginal projections. Due to the more rounded upper valve, *T. zhanjiangensis* has been given the common name of the "cats ear oyster" (Wu et al. 2013), perhaps *T. salpinx* should be known as the 'tufted cat's ear oyster' in reference to the marginal projections.

The morphology and molecular results of *T. salpinx* clearly indicate that this new species belongs to the Pacific cupped oyster lineage, with a closer affinity to the Chinese species of *Talonostrea* rather than to the more widespread *Magallana* species. This is supported also in the morphology where both *T. salpinx* and *T. talonata* share the character of the style sac and mid gut being separate for most of their lengths while in *Magallana* and *Crassostrea* the mid gut and style sac run together. A discrepancy between the route of the mid gut as illustrated by Li and Qi (1994) and that of Cavaleiro et al. (2019) for *T. talonata* exists. In Li and Qi (1994) the mid gut of *T. talonata* is shown running to the anterior before curving over the face of the stomach whereas in Cavaleiro et al. (2019), and in *T. salpinx*, the mid gut runs toward the posterior. Without Chinese specimens to dissect we are unable to tell if the difference is real or an artifact in the illustration by Li and Qi (1994). The detailed anatomy of *T. zhanjiangensis* has never been described. Torigoe (1981) described the mantle tentacles of the major genera noting that for the inner fold of Crassostreinae the tentacles are arranged in an alternating large-small pattern but in *T. salpinx* the inner mantle fold tentacles are all of the same size. The mantle tentacle arrangement has not been described for other *Talonostrea* species. Genetic distance between *T. salpinx* and the other two *Talonostrea*

species is remarkably high (~20% and ~7% for *cox1* and 16S genes respectively). Such a high genetic divergence combined with a unique morphology might justify the assignment of this new species to a distinct genus of Crassostreinae. However, we believe that its assignment to the genus *Talonostrea* is a more conservative approach as it avoids erecting a monotypic genus. This study emphasizes once again that our knowledge of the evolutionary diversity of oysters is far from complete and that molecular data are essential for a robust taxonomic identification and classification of oyster taxa.

Discussion

It is perhaps surprising that the Kuwait oyster belongs to the genus *Talonostrea* as that genus has its distribution centred on China rather than to the more widespread *Magallana*. Some northern Gulf bivalves, such as *Congetia chesnyi* (Oliver & Chesney, 1994) and *Protapes cor* (Sowerby, 1853) are not found further south in the Gulf but occur again in Pakistan and northern India. One might have expected the Kuwait oyster to be allied to species such as *Magallana bilineata* (Röding, 1798) or *M. cuttackensis* (Newton & Smith, 1912), both widely recorded from the west coast of India and Pakistan, and the former also found as a non-native in eastern Australia (Willan et al. 2021). Comparison of 16S rRNA sequences generated in this study for *T. salpinx* with sequences available from GenBank indicate that the same taxon has been found in Iran but was not identified (GenBank accession numbers HF549037–HF549058). Sequence identity between oysters from Kuwait and oysters from Iran is between 99.3 and 100%. Currently *T. salpinx* is restricted to the northern Arabian Gulf and is perhaps endemic to this region. The lack of presence records for *T. salpinx* outside the northern Gulf might be explained by the fact that this species has been overlooked (or become extinct) from a wider range or that it originated *in situ*. This latter hypothesis requires a rapid rate of speciation as the Arabian Gulf was dry at the last glacial maximum some 18, 000 years ago with the present shoreline reached some 6000 years ago (Lambeck 1996). Based on the observed phylogenetic divergence of *T. salpinx* with *T. talonata* or *T. zhanjiangensis,* their separation is likely to be several million years old as deduced by comparison of branch lengths within Crassostreinae as estimated in this study and in previous phylogenetic analyses implementing molecular clock models (the estimated divergence between *Magallana* and *Crassostrea* is of 66–102 Mya according to Ren et al. 2010). However, it is not possible to exclude the fact that an unknown sister species of *T. salpinx* occurs elsewhere.

Talonostrea talonata has now been recognised in Peru, Brazil and Argentina, indicating that *Talonostrea* can be invasive (Cavaleiro et al. 2019). If *T. salpinx* is alien in the Arabian Gulf, then its origins are unknown and at this time we have little data on the age of the oyster reef at Khor Al-Subiyah or the oyster field at Ashairij. Al-Bakri et al. (1985) includes photographs of the oyster reefs in Khor Al-Subiyah and the oyster field at Ashairij and these illustrate how extensive and well developed the reefs were at that time (Fig. 8). Given that the oyster mounds had been given the colloquial name of bogar Boubyan (cows) one would surmise that they were a long-time feature of the landscape. Marine invertebrate invasions are often cited as a result of transport of larvae

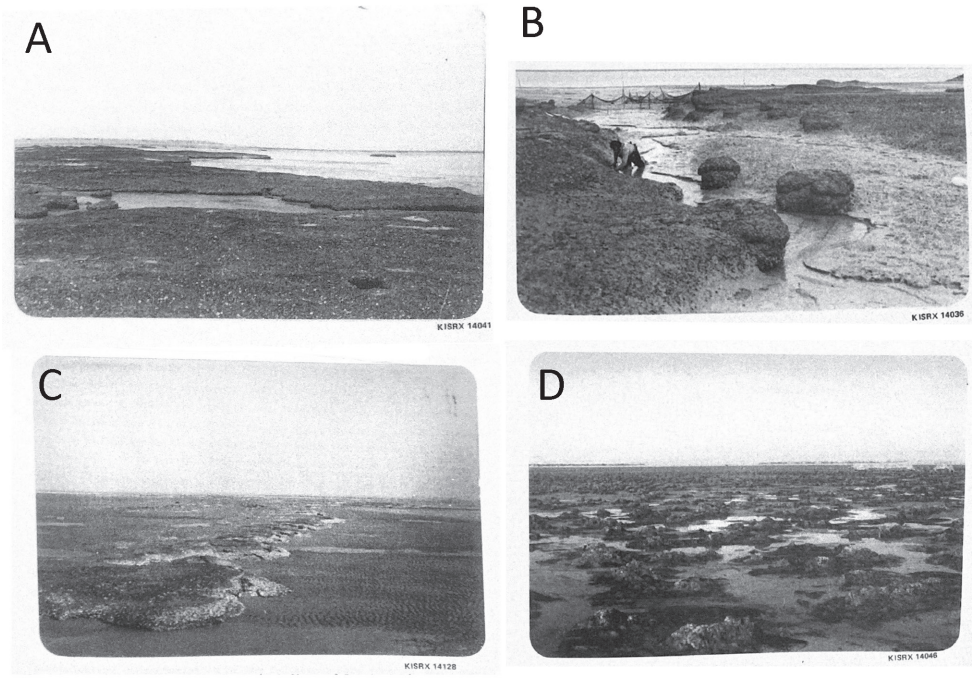

Figure 8. Photographs of *Talonostrea salpinx* sp. nov. beds and reefs from Al-Bakri et al. 1985 **A–C** reefs and beds in Khor Al-Subiyah **D** oyster field at Al-Memlahah, south-eastern end of Kuwait Bay.

in ballast water (Gonçalves 2013) but in Kuwait relatively few (fourteen) invasive organisms have been recognised (Al-Yamani, Skryabin and Subba Rao 2015). These latter authors cite the extreme environment of the northern Gulf preventing colonization by many species of fauna and flora and this might suggest that *T. salpinx* is not an invasive species. However, it is apparent that *T. salpinx* thrives in these conditions and is well adapted to great variations in water quality suggesting to us that it is a native species.

Acknowledgements

The authors wish to thank all those who made it possible to collect the specimens for this study including Henk Dekker who accompanied us in 2019. We thank Matteo Garzia and Emanuele Berrilli at Salvi's lab (University of L'Aquila) for their valuable molecular laboratory work. PGO wishes to thank Kenji Torigoe for his literature gift; to Bangor University for continuing electronic access to their library; to Harriet Wood of the National Museum of Wales for handling registration of the type material. Gratitude goes to the Kuwait Petroleum Corporation (KPC) and the Kuwait Institute for Scientific Research (KISR) for providing financial support and facilitating this research. Special thanks go to Muneera Aljeri (KISR) to prepare the GIS map and all KISR staff of project FM075C for their help in sampling, including Dr Valeriy Skryabin for photographing oyster habitats.

References

Al-Bakri D, Foda M, Behbehani M, Khalaf F, Shublaq W, El-Sayed, MI, Al-Sheikh Z, Kittaneh W, Khuraibit A, Al-Kadi A (1985) Environmental Assessment of the Intertidal Zone of Kuwait. Kuwait Institute for Scientific Research, Kuwait.

Al-Kandari M, Oliver PG, Chen W, Skryabin V, Raghu M, Bishop J, Hussain S, Al-Jazzaf S, Yousif A (2020) Diversity and distribution of the intertidal Mollusca of the State of Kuwait, Arabian Gulf. Regional Studies in Marine Science 33: 1–19. https://doi.org/10.1016/j.rsma.2019.100905

Al-Shamlān SM (2000) Pearling in the Arabian Gulf. A Kuwaiti Memoir. The London Centre of Arab Studies, 199 pp.

Al-Yamani F, Bishop J, Essa RM, Al-Husaini M, Al-Ghadban AN (2004) Oceanographic Atlas of Kuwait's Waters. Safat, Kuwait. Kuwait Institute for Scientific Research and Environment Public Authority, 203 pp.

Al-Yamani F, Skryabin V, Subba Rao VD (2015) Suspected ballast water introductions in the Arabian Gulf, Aquatic Ecosystem Health & Management 18: 3, 282–289. https://doi.org/10.1080/14634988.2015.1027135

Bouckaert R, Vaughan TG, Barido-Sottani J, Duchêne S, Fourment M, Gavryushkina A, Heled J, Jones G, Kühnert D, Maio DN, Matschiner M, Mendes FK, Müller NF, Ogilvie HA, Plessis L, Popinga A, Rambaut A, Rasmussen D, Siveroni I, Suchard MA, Chieh-Wu H, Xie D, Zhang C, Stadler T, Drummond AJ (2019) BEAST 2.5: An advanced software platform for Bayesian evolutionary analysis. PLoS Computational Biology 15(4): e1006650. https://doi.org/10.1371/journal.pcbi.1006650

Cataliotti-Valdina J (1990) Les coquillages de Failaka. Failaka, fouilles françaises 1986–1988. Sous la direction de Yves Calvet et Jeacqueline Gachet. Lyon: Maison de l'Orient et de la Méditerranée Jean Pouilloux. Travaux de la Maison de l'Orient 18: 71–84.

Cavaleiro NP, Lazoski C, Tureck CR, Melo CMR, do Amaral VS, Lomovasky BJ, Absher, TM, Solé-Cava AM (2019) *Crassostrea talonata*, a new threat to native oyster (Bivalvia: Ostreidae) culture in the Southwest Atlantic. Journal of Experimental Marine Biology and Ecology 511: 91–99. https://doi.org/10.1016/j.jembe.2018.11.011

Chakrabarty P, Warren M, Page LM, Baldwin CC (2013) GenSeq: An updated nomenclature and ranking for genetic sequences from type and non-type sources. ZooKeys 346: 29–41. https://doi.org/10.3897/zookeys.346.5753

Crocetta F, Mariottini P, Salvi D, Oliverio M (2015) Does GenBank provide a reliable DNA barcode reference to identify small alien oysters invading the Mediterranean Sea? Journal of the Marine Biological Association of the United Kingdom 95: 111–122. https://doi.org/10.1017/S0025315414001027

Darriba D, Taboada GL, Doallo R, Posada D (2012) jModelTest 2: more models, new heuristics and parallel computing. Nature Methods 9: e772. https://doi.org/10.1038/nmeth.2109

Glayzer BA, Glayzer DT, Smythe KR (1984) The marine molluscs of Kuwait, Arabian. Gulf. Journal of Conchology 31: 311–330.

Gonçalves AA (2013) Bioinvasion through ballast water: a global concern. Journal of Ocean Technology 8 (special): 88–188.

Inaba A, Torigoe K (2004) Oysters in the world. Part 2. Systematic description of the Recent oysters. Bulletin of the Nishinomiya Shell Museum 3: 1–63.

Jones DA (1986) A Field Guide to the Seashores of Kuwait and the Arabian Gulf. University of Kuwait & Blandford Press, 192 pp.

Katoh K, Standley DM (2013) MAFFT multiple sequence alignment software version 7: improvements in performance and usability. Molecular biology and evolution 30: 772–780. https://doi.org/10.1093/molbev/mst010

Kumar S, Stecher G, Tamura K (2016) MEGA7: Molecular Evolutionary Genetics Analysis version 7.0 for bigger datasets. Molecular Biology and Evolution 33: 1870–1874. https://doi.org/10.1093/molbev/msw054

Lambeck K (1996) Shoreline reconstructions for the Persian Gulf since the last glacial maximum. Earth and Planetary Science Letters 142: 43–57. https://doi.org/10.1016/0012-821X(96)00069-6

Li X, Qi Z (1994) Studies on the comparative anatomy, systematic classification and evolution of Chinese oysters (In Chinese). Studia Marina Sinica 35: 143–173.

Liu J, Li Q, Kong L, Yu H, Zheng X (2011) Identifying the true oysters (Bivalvia: Ostreidae) with mitochondrial phylogeny and distance-based DNA barcoding. Molecular Ecology Resources 11: 820–830. https://doi.org/10.1111/j.1755-0998.2011.03025.x

Omar SAS, Roy WY (2014) Ecology and environment of Boubyan Island in Kuwait. KISR Kuwait and Ross Publishing USA, 292 pp.

Pokavanich T, Polikarpov I, Lennox A, Al-Hulail F, Al-Said T, Al-Enezi E, Al-Yamani F, Stokozov N, Shuhaibar B (2013) Comprehensive investigation of summer hydrodynamic and water quality characteristics of desertic shallow water body: Kuwait Bay. Proceedings of the 7th International Conference on Coastal Dynamics (Arcachon, France), 1253–1264.

Prieur A (2011) Inventory, faunal distribution and use of the malacofauna from Tell Akkaz (Kuwait). In: Gachet-Bizollon J (Ed.) Tell Akkaz in Kuweit. Tome maison de l"orient 57: 379–390.

Raith M, Zacherl DC, Pilgrim EM, Eernisse DJ (2016) Phylogeny and species diversity of Gulf of California oysters (Ostreidae) inferred from mitochondrial DNA. American Malacological Bulletin 33: 263–283. https://doi.org/10.4003/006.033.0206

Rambaut A, Drummond AJ, Xie D, Baele G, Suchard MA (2018) Posterior summarisation in Bayesian phylogenetics using Tracer 1.7. Systematic Biology 67: 901–904. https://doi.org/10.1093/sysbio/syy032

Ren J, Liu X, Jiang F, Guo X, Liu B (2010) Unusual conservation of mitochondrial gene order in *Crassostrea* oysters: evidence for recent speciation in Asia. BMC Evolutionary Biology 10: e394. https://doi.org/10.1186/1471-2148-10-394

Salvi D, Bellavia G, Cervelli M, Mariottini P (2010) The analysis of rRNA Sequence-Structure in phylogenetics: an application to the family Pectinidae (Mollusca, Bivalvia). Molecular Phylogenetics and Evolution 56: 1059–1067. https://doi.org/10.1016/j.ympev.2010.04.025

Salvi D, Macali A, Mariottini P (2014) Molecular phylogenetics and systematics of the bivalve family Ostreidae based on rRNA sequence-structure models and multilocus species tree. PLoS ONE 9: e108696. https://doi.org/10.1371/journal.pone.0108696

Salvi D, Mariottini P (2017) Molecular taxonomy in 2D: A novel ITS2 rRNA sequence-structure approach guides the description of the oysters' subfamily Saccostreinae and the genus *Magallana* (Bivalvia: Ostreidae). Zoological Journal of the Linnean Society 179: 263–276. https://doi.org/10.1111/zoj.12455

Salvi D, Mariottini P (2021) Revision shock in Pacific oysters taxonomy: the genus *Magallana* (formerly *Crassostrea* in part) is well-founded and necessary. Zoological Journal of the Linnean Society 192: 43–58. https://doi.org/10.1093/zoolinnean/zlaa112

Sambrook J, Fritsch EF, Maniatis T (1989) Molecular Cloning: A Laboratory Manual. 2nd ed. New York: Cold Spring Harbor Press, 1695pp.

Torigoe K (1981) Oysters in Japan. Journal of science of the Hiroshima University Ser B, Div. 1 (Zoology) 29(2): 291–347.

Willan RC, Nenadic N, Ramage A, McDougall C (2021) Detection and identification of the large, exotic, crassostreine oyster *Magallana bilineata* (Röding, 1798) in northern Queensland, Australia. Molluscan Research. https://doi.org/10.1080/13235818.2020.1865515

Wu X, Xiao S, Yu Z (2013) Mitochondrial DNA and morphological identification of *Crassostrea zhanjiangensis* sp. nov. (Bivalvia: Ostreidae): a new species in Zhanjiang, China. Aquatic Living Resources 26: 273–280. https://doi.org/10.1051/alr/2013065

ZooKeys 1043: 21–31 (2021)
doi: 10.3897/zookeys.1043.65223
https://zookeys.pensoft.net

RESEARCH ARTICLE

A peer-reviewed open-access journal
ZooKeys
Launched to accelerate biodiversity research

Two new species of the family Megalyridae (Hymenoptera) from China

Hua-yan Chen[1], Bo-jing Liuhe[2], Xiao Zhang[1]

1 *State Key Laboratory of Biocontrol, School of Life Sciences / School of Ecology, Sun Yat-sen University, Guangzhou 510275, China* **2** *Kunming Daqiuyin Technology Co., Ltd, Kunming 650051, China*

Corresponding author: Xiao Zhang (zhangxiaofossil@163.com)

Academic editor: Andreas Köhler | Received 28 February 2021 | Accepted 31 May 2021 | Published 10 June 2021

http://zoobank.org/F2CE5635-A15F-471E-BDB1-8F2778CC695F

Citation: Chen H-y, Liuhe B-j, Zhang X (2021) Two new species of the family Megalyridae (Hymenoptera) from China. ZooKeys 1043: 21–31. https://doi.org/10.3897/zookeys.1043.65223

Abstract

Two new species of the small and rarely collected family Megalyridae are described from China: *Carminator daliensis* Chen & Liuhe, **sp. nov.** from Yunnan and *Ettchellsia hainanensis* Chen & Liuhe, **sp. nov.** from Hainan. A key to megalyrid species of China is provided. The biogeographical implication of the new taxa is discussed.

Keywords

Megalyroidea, Oriental Region, parasitic wasps, taxonomy

Introduction

Megalyridae is a small family of parasitic wasps, which, as far as known, parasitize the larvae of wood-boring beetles (Coleoptera) and more rarely mud-nesting Sphecidae (Hymenoptera) (Shaw 1990a; Naumann 1987). So far, only 62 species have been described worldwide (Binoy et al. 2020; Mita and Shaw 2020). Although rarely collected, these wasps have nevertheless been reported from most of the major biogeographic regions worldwide, with the exception of the Nearctic (Vilhelmsen et al. 2010). Most megalyrid species occur in the tropics and subtropics of the Southern Hemisphere (Vilhelmsen et al. 2010; Binoy et al. 2020). While most Asian species of megalyrids have highly restricted distribution ranges (Mita and Konishi 2011), there

is one notable exception, *Megalyra fasciipennis* Westwood, which occurs widely in Australia and Tasmania and has been reported as accidentally introduced into South Africa and India (Binoy et al. 2020). The biogeography of megalyrids has attracted increasing attention in recent years (Shaw 1990b; Vilhelmsen et al. 2010; Mita and Konishi 2011). Therefore, an intensive field survey of megalyrids is of interest towards better understanding the diversity and distributional patterns of these wasps. Previously, *Carminator cavus* Shaw from Taiwan and *Ettchellsia sinica* He from Yunnan were the only two megalyrids described from China (Shaw 1988; He 1991). In this study, we describe two additional new species of Megalyridae from southern China.

Materials and methods

All specimens are deposited in the collections of the Museum of Biology, Sun Yat-sen University, Guangzhou, China (**SYSBM**). The morphological terms generally follow that of Shaw (1988, 1990b), and the nomenclature of the sculpture and texture of the integument follows Harris (1979). Images and measurements were made using a Nikon SMZ25 microscope with a Nikon DS-Ri 2 digital camera system. Images were post-processed with Abobe Photoshop CS6 Extended.

The following abbreviations are used:

A1–A14 antennomere 1 to 14;
OOL shortest distance from the outer edge of a lateral ocellus to the compound eye;
LOL shortest distance between the inner edges of the lateral ocellus and the median ocellus;
POL distance between the inner edges of the lateral ocelli.

Results

Key to species of Megalyridae of China

1 Posterior ocular orbits without groove (Fig. 1F); forewing with vein Rs between Rs + M and r-rs absent, apical segment of Rs absent or spectral (Fig. 2D)..... **2**

– Posterior ocular orbits with groove (Fig. 3E); forewing with vein Rs between Rs + M and r-rs tubular, apical segment of Rs tubular, arched towards stigma (Fig. 4D)..... **3**

2 Median strip on frons distinctly deeper than longitudinal striae; ventral margin of mesepisternum swollen, more or less rounded ..... ***Carminator cavus* Shaw**

– Median strip on frons indistinct, not deeper than longitudinal striae (Fig. 1C); ventral margin of mesepisternum flat (Fig. 2B) ..... ***Carminator daliensis* Chen & Liuhe, sp. nov.**

3 Frons irregularly rugose (Fig. 3C); clypeus largely punctate rugose; POL distinctly longer than OL (Fig. 3D); 5th metasomal tergite smooth (Fig. 4C)....
.....***Ettchellsia hainanensis*** **Chen & Liuhe, sp. nov.**

– Frons coarsely reticulate; clypeus dorsal half finely punctate, ventral half smooth; POL shorter than OL; 5th metasomal tergite finely transversely rugulose .....***Ettchellsia sinica*** **He**

Carminator Shaw, 1988

Carminator Shaw 1988: 102; Shaw 1990b: 572; Mita et al. 2007: 202; Vilhelmsen et al. 2010: 663; Mita and Konishi 2011: 109. Type species: *Carminator ater* Shaw, 1988.

Diagnosis. *Carminator* is diagnosed by the following morphological characters: shallow subantennal groove, mandible stout and with five teeth, head prognathous, wing venation reduced and pterostigma absent, fore tibia with a comb of stout spines, ovipositor strongly arched (Shaw 1990b).

Biology. Little is known about the biology of *Carminator*, but these wasps have been suspected to be parasitoids of wood-boring larvae of Coleoptera (Mita and Konishi 2011).

Distribution. Oriental, Australasian, and eastern Palaearctic regions.

Carminator daliensis Chen & Liuhe, sp. nov.

http://zoobank.org/AB8033B3-FEB2-4309-AEC6-08E2572B4991
Figures 1, 2

Diagnosis. Head longer than wide (Fig. 1D); frons entirely costate, median strip of frons shallow and smooth (Fig. 1C); postgena entirely obliquely striate (Fig. 1E); occipital ridge strongly arched (Fig. 1F); mandible with five blunt, subtriangular teeth (Fig. 1C); propleuron elongate, forming "neck" (Fig. 1E); prosternum without median groove (Fig. 1E); fore tibia with two rows of stout spines (nine + seven) arranged in a V shape (Fig. 2E); branching point between R1 and 2r of forewing not thickened (Fig. 2D).

Description. Female (holotype). Body length 4.4 mm. *Color*. Body black; mandible reddish black; pedicel and first four flagellomeres dark brown, remainders of antenna black; legs black with tibiae dark brown to black and tarsus brown; wings tinged with brown and forewing veins dark brown; ovipositor sheath brown; ovipositor reddish brown.

Head (Fig. 1C–F) 1.1× longer than wide in dorsal view, widely smooth with scattered punctures, punctures denser on gena and vertex; frons costate along lower margin, with about 12 longitudinal costae, punctures present among costae; median strip shallow and smooth; outer margin of frons without granulated area; posterior margin

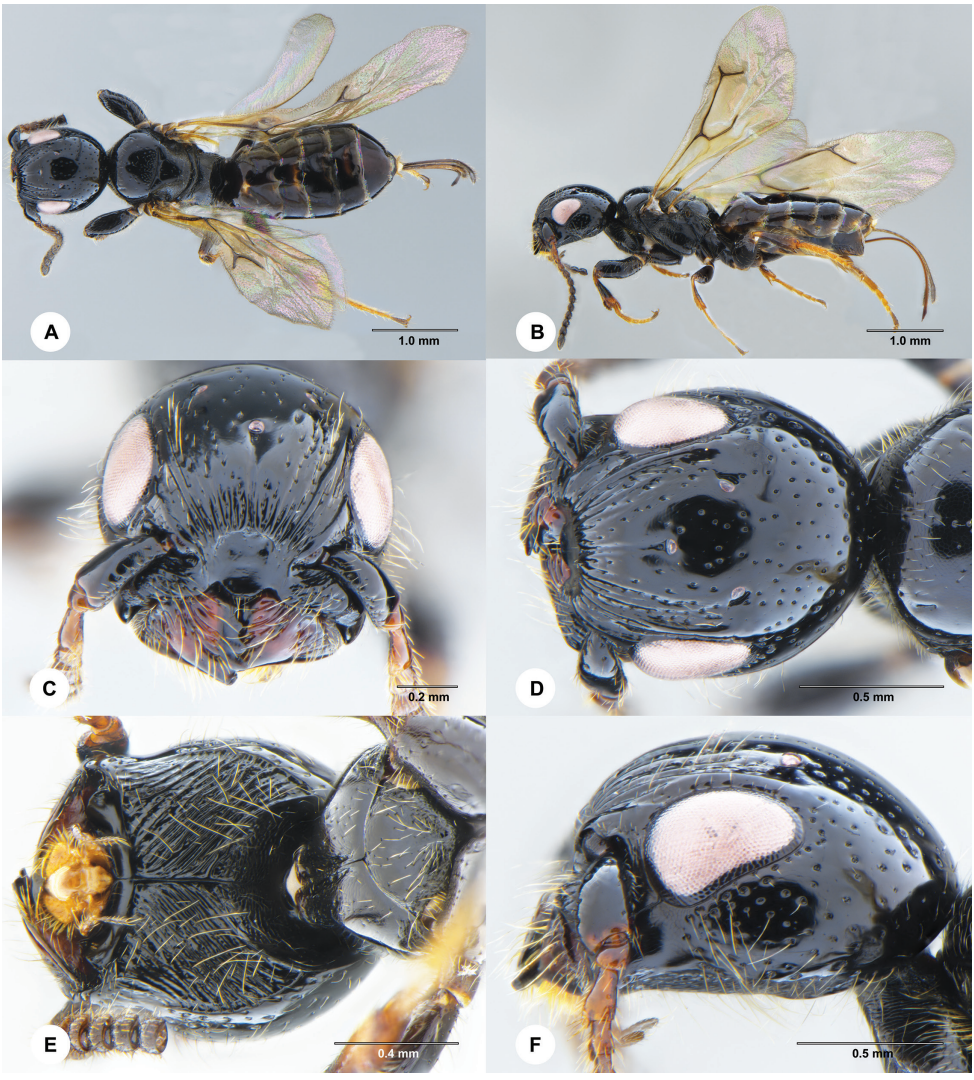

Figure 1. *Carminator daliensis* Chen & Liuhe, sp. nov., female, holotype (SCAU 3049430) **A** habitus, dorsal **B** habitus, lateral **C** head, frontal **D** head, dorsal **E** head and prothorax, ventral **F** head and pronotum, lateral.

of frons slightly convex, higher than level of clypeus; punctures on gena and vertex denser; malar space below antennal insertion obliquely striate, with scattered punctures; posterior carina of subantennal groove present; lower margin of gena (as genal ridge in Mita and Konishi 2011) simple, not forming a blunt angle; postgena entirely obliquely striate; vertex wide, without a coronet behind lateral ocelli; occipital ridge arched; clypeus smooth, posterior margin rounded; a groove parallel to inner orbit of eye; eye with scattered short setae; ocelli forming large obtuse triangle; POL = 6.5; OL = 4.9; OOL = 3.2; mandible with five blunt subtriangular teeth, basal part swollen, outer margin flat; antenna (Fig. 2G) with A1–A3 weakly flattened, A4–A14 strongly flattened, covered with numerous short to long setae; length/width ratio of antennal

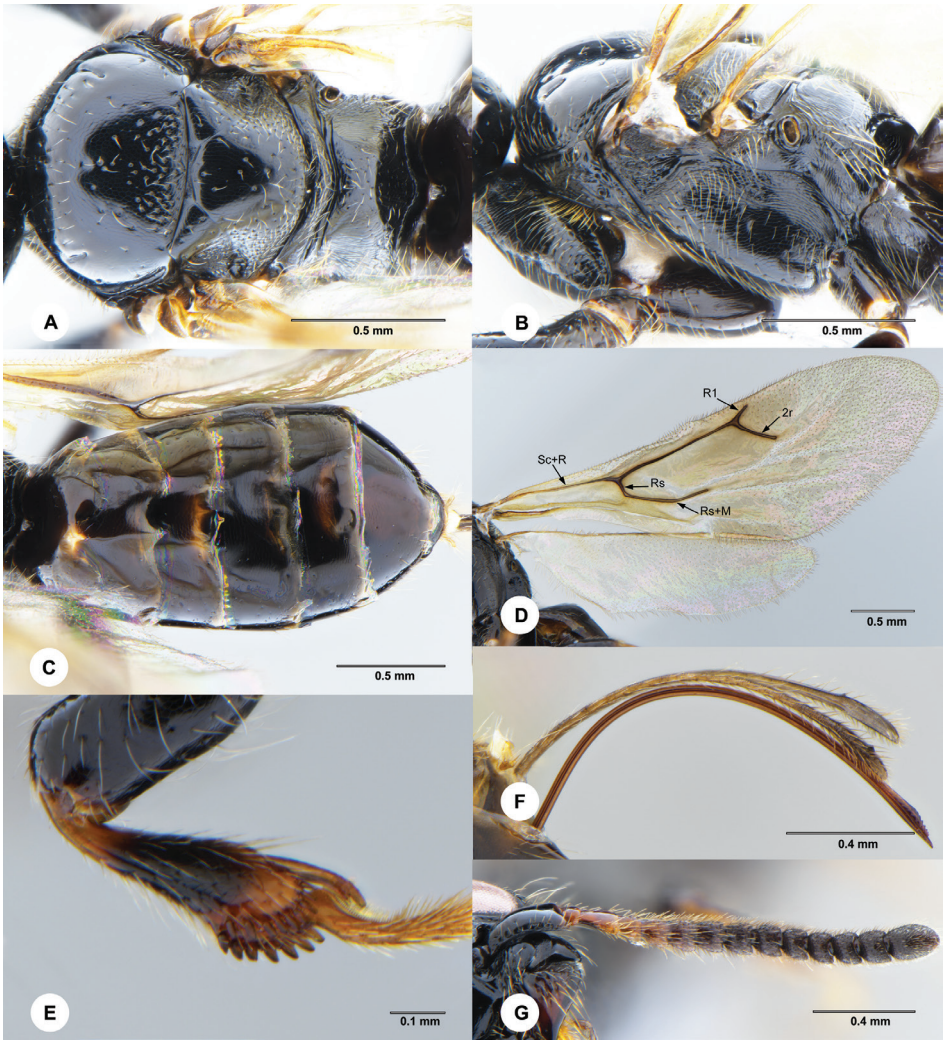

Figure 2. *Carminator daliensis* Chen & Liuhe, sp. nov., female, holotype (SCAU 3049430) **A** mesosoma, dorsal **B** mesosoma, lateral **C** metasoma, dorsal **D** wings **E** fore tibia, inner face **F** ovipositor and ovipositor sheath, lateral **G** antenna, dorsal.

segments: 6.4:2.0, 1.3:1.3, 3.0:1.5, 1.8:1.9, 2.0:2.1, 2.2:2.5, 2.2:2.5, 2.2:2.5, 2.2:2.4, 2.1:2.4, 1.8:2.3, 2.1:2.5, 2.2:2.6, and 4.4:2.7.

Mesosoma (Figs 1E, F, 2A, B). Pronotum shagreened to rugulose; propleuron dorsally shagreened, ventrally coriaceous, elongate, forming "neck"; median groove of prosternum absent; setae on propleuron and prosternum dense; mesoscutum largely smooth with sparse, small punctures anteriorly and laterally, coriaceous to finely punctate rugulose posteriorly, median mesoscutal sulcus weakly developed and only present anteriorly; admedian lines absent, parapsides short and present anterolaterally; mesoscutum convex, 0.65× as long as wide; mesoscutellum 0.57× as long as wide, coriaceous with sparse puntures medially, finely and desenly punctate laterally; anterior margin of

axillae broadly separated; mesopleuron rugulose dorsally, largely shagreened or coriaceous ventrally; epicnemial sulcus obscure; ventral margin of episternum forming blunt angle; episternal scrobe with a weak depression; pleural sulcus complete; metanotum narrow, strongly shagreened, without punctures; metapleuron swollen anteriorly, covered with long setae; propodeum with posterior propodeal carina distinct, area anterior to posterior propodeal carina largely shagreened with sparse small punctures medially, area posterior to posterior propodeal carina smooth.

***Legs*.** Fore tibia flat, with two rows of stout spines arranged in a V shape (Fig. 2E); fore tarsomeres with ratios: 7.3:2.6:2.1:1.6:3.8; hind tarsomeres with ratio: 5.4:1.9:1.4:1.0:3.7.

Wings (Fig. 2D). Forewing with vein Sc + R branching into veins R and Rs; R1/2r = 0.4; branching point between veins R1 and 2r not thickened; Rs/(Rs + M) = 0.18.

Metasoma (Fig. 2C, F) subcylindrical, widest at metasomal segment 4; terga and sterna faintly shagreened to smooth; tergite 1 0.43 × as long as wide; ovipositor sheath 0.9× as long as ovipositor; setae on ovipositor sheath longer than diameter of ovipositor; apex of ovipositor sharp.

Variation. The body length of the paratype female is 4.2 mm, and other characters are similar to the holotype.

Male. Unknown.

Etymology. The specific epithet refers to the locality (Dali) where the type specimens were collected. It should be treated as a noun in apposition.

Material examined. ***Holotype***, female, China: Yunnan, Dali, Yunlong County, 3063 m a.s.l., forest, 21°51'23"N, 99°14'10"E, 12–27.ix.2020, Malaise trap, SCAU 3049430 (SYSBM). ***Paratype*:** 1 female, same collecting data as holotype, SCAU 3049431 (SYSBM).

Distribution. Oriental region, China, Yunnan Province.

Ettchellsia Cameron, 1909

Ettchellsia Cameron 1909: 208; Baltazar 1961: 219; He 1991: 475; Mita and Shaw 2012: 101. Type species: *Ettchellsia piliceps* Cameron, 1909 (by monotypy).

Diagnosis. Posterior ocular orbits with groove and carina present; posterior border of mesopleuron smooth, without a row of foveae; propodeum with unique pattern of longitudinal carinae; forewing fuscous or with fuscous banding pattern; forewing with vein Rs between Rs + M and r-rs tubular for at least a short distance, apical segment of Rs tubular, arched towards stigma, M+ Cu and distal segments of Cu absent or at most spectral; Hind tibia rugose and with erect setae. Additional diagnostic characters for the genus were provided by Shaw (1990b), Vilhelmsen et al. (2010), and Mita and Shaw (2012).

Biology. No biological data for *Ettchellsia* species are available; however, these wasps have long been suspected to be idiobiont ectoparasitoids that attack beetle larvae (Shaw 1990b).

Distribution. Oriental region.

***Ettchellsia hainanensis* Chen & Liuhe, sp. nov.**
http://zoobank.org/0DE06E91-FC9A-43C8-88FF-36C2FCA1CCCF
Figures 3, 4

Diagnosis. Frons irregularly rugose (Fig. 3C); clypeus largely punctate rugose (Fig. 3C); vertex posterior to lateral ocellus smooth anteriorly and reticulate-rugose posteriorly (Fig. 3D); gena smooth (Fig. 3E); metanotum puncate and setose medially (Fig. 4A); median propodeal region not narrowed (Fig. 4A); metasoma (Fig. 4C) smooth except tergite 6 largely coriaceous.

Description. Female (holotype). Body length 4.9 mm. *Color*. Head black, mesosoma largely black except mesoscutum and axill reddish brown and tegula brown, metasoma mainly black with posterior margin of terga dark brown; mandible dark brown with teeth darker; antenna brown to dark brown with apical flagellomeres paler; trochanters and tarsi of fore and mid legs pale yellow, remainders of the legs brown to dark brown; trochanter and tarsus of hind leg brown, femur dark brown to black, coxa and tibia black; dorsal surface of hind tibia with both white and black long setae; basitarsus with white long setae; forewing with four transverse dark brown bands; ovipositor sheath black; ovipositor reddish brown.

Head (Fig. 3C–E) 1.5× wider than long in dorsal view, covered with long black erect setae and relatively short decumbent white setae; frons irregularly rugose; vertex convex, with ocellar triangle smooth, except by a median row of longitudinal punctures, area between ocelli and eyes smooth with a row of longitudinal punctures arising from lateral ocellus and parallel to orbit; vertex posterior to lateral ocellus smooth anteriorly and reticulate-rugose posteriorly; POL = 4.7; OL = 3.4; OOL = 4.0; eye margined posteriorly by a groove and a single postocular oribital carina, the groove smooth anteriorly and foveate posteriorly; gena smooth; occipital carina foveate; clypeus largely punctate rugose, apical margin slightly incise medially; mandible with 3 teeth; antenna filiform, A3–A6th flagellomeres subequal and the longest, remainder flagellomeres becoming shorter.

Mesosoma (Fig. 4A, B) covered with short decumbent white setae; scattered, long, erect, black setae present on mesonotum; mesoscutum humped, anterior surface smooth, dorsal surface largely smooth with fine punctures, median mesoscutal sulcus present and foveate, lateral carina of anterior surface present; axilla and mesoscutellum largely smooth with fine punctures; metanotum puncate and setose medially; propodeum with pairs of median, submedian, and lateral longitudinal carinae; median propodeal region not narrowed, with four complete and two incomplete transverse carinae, posterior margin producing dorsally; submedian region with two complete transverse carinae; lateral region with four complete transverse carinae.

Legs (Figs 3B, 4E). Hind femur punctate and rugose medially; hind tibia longitudinally rugose; hind tibia covered with both white and black long erect setae, longer than the width of the hind tibia; basitarsus covered with white long erect setae, longer than the width of the hind tibia.

Wings (Fig. 4D). Forewing with vein M 1.9× basal part of vein RS; erect setae on vein C 0.5× those on vein Sc+R and A.

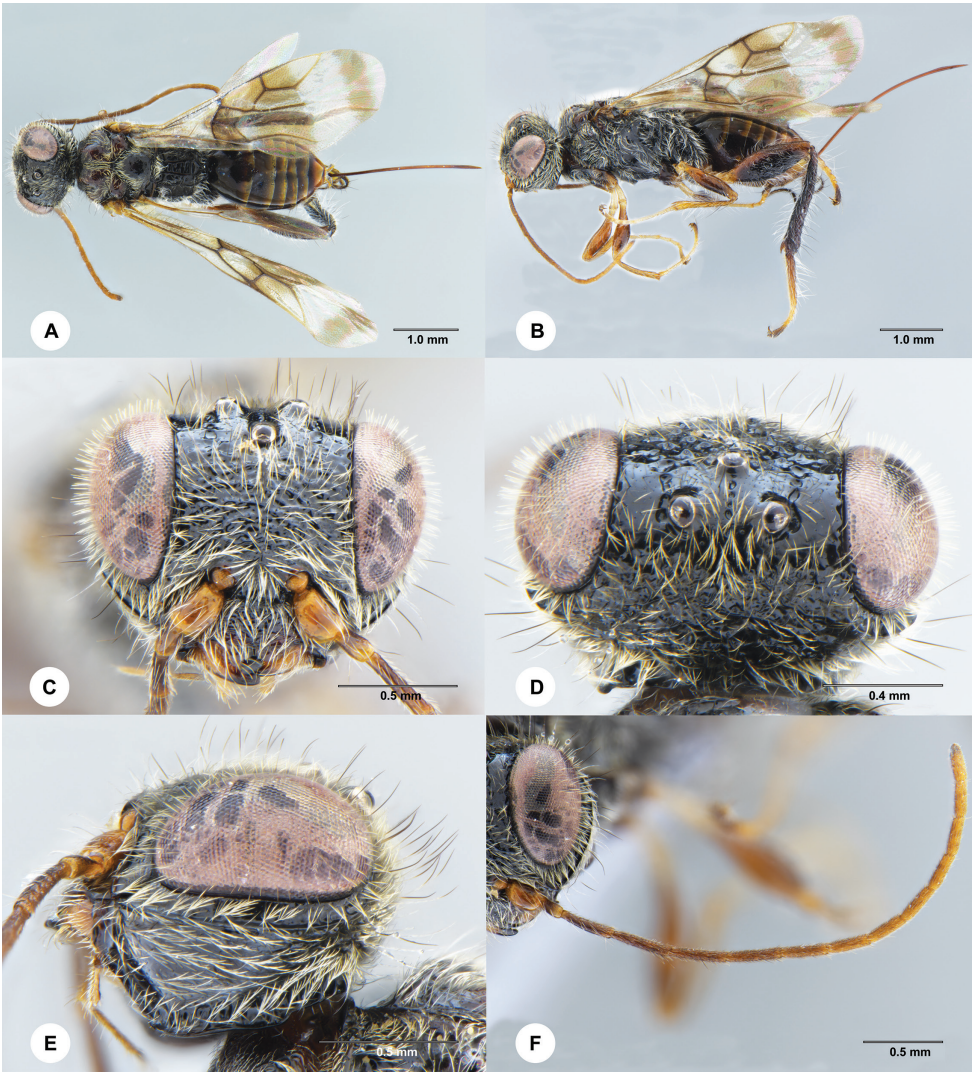

Figure 3. *Ettchellsia hainanensis* Chen & Liuhe, sp. nov., female, holotype (SCAU 3049429) **A** habitus, dorsal **B** habitus, lateral **C** head, frontal **D** head, dorsal **E** head, lateral **F** antenna.

Metasoma (Fig. 4C) smooth except tergite 6 largely coriaceous; ovipositor 1.76× mesosoma length, apex with small teeth and single knob.

Variation. The body length of the paratype female 5.0 mm; antenna dark brown to black; mesoscutellum reddish brown; median propodeal region with seven complete transverse carinae; other characters similar to the holotype.

Male. Unknown.

Etymology. The specific epithet refers to Hainan Island, where the type locality is located. It is treated as a noun in apposition.

Figure 4. *Ettchellsia hainanensis* Chen & Liuhe, sp. nov., female, holotype (SCAU 3049429) **A** mesosoma, dorsal **B** mesosoma, lateral **C** metasoma, dorsal **D** wings **E** hind leg, lateral **F** apical ovipositor, lateral.

Material examined. ***Holotype***, female, China: Hainan, Qiongzhong, Mount Limushan, 19°10.771'N, 109°46.225'E, 20–22.vii.2020, forest, sweep, Huayan Chen, SCAU 3049429 (deposited in SYSBM). ***Paratype*****:** 1 female, China: Hainan, Qiongzhong, Mount Limushan, 19°10'23.28"N, 109°46'40.79"E, 30.xi–31.xii.2020, forest, Malaise trap, Longlong Chen, SCAU 3042295 (SYSBM).

Distribution. Oriental region, China, Hainan Province.

Remarks. *Ettchellsia hainanensis* is most similar to *E. sinica* He, which was previously described based on a single female from Yunnan of China, but *E. hainanensis* can

be distinguished from *E. sinica* by the following characters: frons irregularly rugose (Fig. 3C); clypeus largely punctate rugose (Fig. 3C); POL distinctly longer than OL (Fig. 3D); metasomal tergite 5 smooth (Fig. 4C). We contacted the curators of the Hymenoptera collection of Zhejiang University (previously known as Zhejiang Agricultural University) where the holotype of *E. sinica* claimed to be deposited, but they failed to find the type. If the holotype were confirmed to be lost, a neotype of the species may need to be designated based on a specimen collected from the type locality in the future.

Dicussion

Mita and Shaw (2012) have suggested that species diversity of megalyrids from the Southeast Asia is still undersampled and intensive study is required. Additional discoveries from this region would help us better understand the biogeography and eveolutionary history of Megalyridae.

Species of *Carminator* mainly occur in Southeast Asia. Morphologically, *C. daliensis* is most similar to *C. affinis* Shaw, but the former can be distinguished by its smaller size and that frons entirely costate (only laterally costate in *C. affinis*) and prosternum without median groove (prosternum with median groove in *C. affinis*). *Carminator daliensis* is also similar to *C. ater* in having frons entirely costate, but the vertex is largely smooth with sparse punctures and the dorsal carina of subantennal groove is present. Geographically, *C. daliensis* is close to *C. affinis* from Malaysia and *C. ater* from Thailand (Shaw 1988). According to Mita and Konishi (2011), *Carminator* is a monophyletic taxon, with *C. affinis* as the sister group to the rest of the genus. So, the discovery of *C. daliensis* and its morphological similarity to *C. affinis* might serve as additional evidence that the common ancestor of the extant *Carminator* species was probably present in the Oriental–Australian transition zone and subsequently species dispersed northward as far as Japan (Mita and Konishi 2011).

So far, including the *E. hainanensis* described here, *Ettchellsia* species have mainly been found in the Indomalayan region (Mita and Shaw 2012). Unidentified species of *Ettchellsia* were reported from Taiwan (Shaw 1990b; Vilhelmsen et al. 2010) where the northernmost record of the genus is located. Further biogeographical and phylogenetic analyses of *Ettchellsia* will be desired in the future when additional new species and distributional records are found.

Acknowledgements

We thank Dr Shi-xiao Luo (South China Botanical Garden, Chinese Academy of Sciences) for providing a specimen of *Ettchellsia*. We are grateful to the subject editor, Andreas Köhler, and to Toshiharu Mita, Scott Shaw, and the other two anonymous reviewers who greatly contributed to the improvement of this paper. This material is based upon work supported in part by the Guangdong Basic and Applied Basic Research Foundation (2019A1515110610).

References

Binoy C, Shaw SR, Kumar PG, Santhosh S, Nasser M (2020) First discovery of a long-tailed wasp from the Indian subcontinent (Hymenoptera: Megalyroidea: Megalyridae). International Journal of Tropical Insect Science 40: 751–758. https://doi.org/10.1007/s42690-020-00126-7

Harris RA (1979) A glossary of surface sculpturing. Occasional Papers in Entomology, State of California Department of Food and Agriculture 28: 1–31.

He J-H (1991) A new species of the genus *Ettchellsia* Cameron (Hymenoptera: Ichneumonoidea, Megalyridae). Acta Entomologica Sinica 34: 475–477.

Mita T, Konishi K (2011) Biogeography and phylogeny of *Carminator* (Hymenoptera: Megalyridae). Systematic Entomology 36: 569–581. https://doi.org/10.1111/j.1365-3113.2010.00548.x

Mita T, Konishi K, Terayama M, Yamane S (2007) Two new species of the genus *Carminator* Shaw from Japan, the northernmost record of extant Megalyridae (Hymenoptera). Entomological Science 10: 201–208. https://doi.org/10.1111/j.1479-8298.2007.00213.x

Mita T, Shaw SR (2020) A taxonomic study of *Dinapsis* Waterson, 1922 from Madagascar (Hymenoptera: Megalyridae, Dinapsini): crested wasps of the hirtipes species-group. Zootaxa 4858: 071–084. https://doi.org/10.11646/zootaxa.4858.1.4

Naumann ID (1987) A new megalyrid (Hymenoptera: Megalyridae) parasitic on a sphecid wasp in Australia. Journal of the Australian Entomological Society 26: 215–222. https://doi.org/10.1111/j.1440-6055.1987.tb00289.x

Shaw SR (1988) *Carminator*, a new genus of Megalyridae (Hymenoptera) from the Oriental and Australian regions, with a commentary on the definition of the family. Systematic Entomology 13: 101–113. https://doi.org/10.1111/j.1365-3113.1988.tb00233.x

Shaw SR (1990a) A taxonomic revision of the long-tailed wasps of the genus *Megalyra* Westwood (Hymenoptera: Megalyridae). Invertebrate Taxonomy 3: 1005–1052. https://doi.org/10.1071/IT9891005

Shaw SR (1990b) Phylogeny and biogeography of the parasitoid wasp family Megalyridae (Hymenoptera). Journal of Biogeography 17: 569–581. https://doi.org/10.2307/2845141

Vilhelmsen L, Perrichot V, Shaw SR (2010) Past and present diversity and distribution in the parasitic wasp family Megalyridae (Hymenoptera). Systematic Entomology 35: 658–677. https://doi.org/10.1111/j.1365-3113.2010.00537.x

ZooKeys 1043: 33–59 (2021)
doi: 10.3897/zookeys.1043.68316
https://zookeys.pensoft.net

RESEARCH ARTICLE

A peer-reviewed open-access journal
ZooKeys
Launched to accelerate biodiversity research

Two species? – Limits of the species concepts in the pygmy grasshoppers of the *Tetrix bipunctata* complex (Orthoptera, Tetrigidae)

Valentin Moser[1], Hannes Baur[2,3], Arne W. Lehmann[4], Gerlind U. C. Lehmann[5]

1 *Ochsengasse 66, 4123 Allschwil, Switzerland* **2** *Department of Invertebrates, Natural History Museum Bern, Bernastrasse 15, 3005 Bern, Switzerland* **3** *Institute of Ecology and Evolution, University of Bern, Baltzerstrasse 6, 3012 Bern, Switzerland* **4** *Specialist Interest Group Tetrigidae (SIGTET), Friedensallee 37, 14532 Stahnsdorf, Germany* **5** *Department of Biology, Evolutionary Ecology, Humboldt University Berlin, Invalidenstrasse 110, 10115 Berlin, Germany*

Corresponding authors: Valentin Moser (valentinmoser@hotmail.com); Hannes Baur (hannes.baur@nmbe.ch)

Academic editor: Tony Robillard | Received 5 May 2021 | Accepted 25 May 2021 | Published 11 June 2021

http://zoobank.org/4071CDCD-41CA-4516-965E-9FBC0B31394D

Citation: Moser V, Baur H, Lehmann AW, Lehmann GUC (2021) Two species? – Limits of the species concepts in the pygmy grasshoppers of the *Tetrix bipunctata* complex (Orthoptera, Tetrigidae). ZooKeys 1043: 33–59. https://doi.org/10.3897/zookeys.1043.68316

Abstract

Today, integrative taxonomy is often considered the gold standard when it comes to species recognition and delimitation. Using the *Tetrix bipunctata* complex, we here present a case where even integrative taxonomy may reach its limits. The *Tetrix bipunctata* complex consists of two morphs, *bipunctata* and *kraussi*, which are easily distinguished by a single character, the length of the hind wing. Both morphs are widely distributed in Europe and reported to occur over a large area in sympatry, where they occasionally may live also in syntopy. The pattern has led to disparate classifications, as on the one extreme, the morphs were treated merely as forms or subspecies of a single species, on the other, as separate species. For this paper, we re-visited the morphology by using multivariate ratio analysis (MRA) of 17 distance measurements, checked the distributional data based on verified specimens and examined micro-habitat use. We were able to confirm that hind wing length is, indeed, the only morphological difference between *bipunctata* and *kraussi*. We were also able to exclude a mere allometric scaling. The morphs are, furthermore, largely sympatrically distributed, with syntopy occurring regularly. However, a microhabitat niche difference can be observed. Ecological measurements in a shared habitat confirm that *kraussi* prefers a drier and hotter microhabitat, which possibly also explains the generally lower altitudinal distribution. Based on these

results, we can exclude classification as subspecies, but the taxonomic classification as species remains unclear. Even with different approaches to classify the *Tetrix bipunctata* complex, this case is, therefore, not settled. We recommend continuing to record *kraussi* and *bipunctata* separately.

Keywords
Allometry, integrative taxonomy, morphometry, Orthoptera, species delimitation, Tetrigidae, *Tetrix*

Introduction

Species concepts shape the way we see an individual from a given population. Species are the fundamental unit in evolutionary biology (Coyne and Orr 2004) and it is, therefore, important to apply the species status to the best of our current knowledge (Sites and Marshall 2004). Species discovery and description remain a core priority of taxonomic research and critical reflection of current practice is called for (Yeates et al. 2011). Traditionally, species were mostly based on morphological characters. With the advance of technology and easier access to genomes, species classification criteria have diversified (Wägele 2005; Zachos 2016). To generalise species classification and comparability, attributes, such as morphology, genetics, behaviour and ecology are treated as evidence (Dayrat 2005; Will et al. 2005; De Queiroz 2007; Yeates et al. 2011). However, there are still cases where the assignment is difficult, even when using a variety of data. Here, we present such a case in the Pygmy Grasshopper of the family Tetrigidae.

The *Tetrix bipunctata* complex is an intriguing case: *T. bipunctata* (Linnaeus, 1758) and *T. kraussi* Saulcy, 1888 (see Evenhuis 2002 for year of publication) are two widely distributed European Orthoptera of the family Tetrigidae. They are considered morphologically very similar, except for a striking hind wing dimorphism. In the morph *bipunctata*, the hind wing is said to be at least 2.5 times as long as the length of the tegmen, whereas in the morph *kraussi*, it is only about twice as long as the tegmen (sometimes also called tegmentulum, Fig. 1) (Fischer 1948; Schulte 2003; Baur et al. 2006; Lehmann and Landeck 2011; Sardet et al. 2015a).

The status of the two morphs has always been controversial. Fischer (1948) recognised ecological differences and suggested to treat them as species, but this view was later challenged. For example, the morphs were treated only as infrasubspecific taxa by Kevan (1953) and Harz (1957, 1975), but also as subspecies by Nadig (1991). Based on several syntopic occurrences (Schulte 2003), Lehmann (2004) suggested to raise the morphs to species status, a view that has since been widely adopted (Baur et al. 2006; Default and Morichon 2015; Sardet et al. 2015b; Zuna-Kratky et al. 2017; Willemse et al. 2018; Cigliano et al. 2021), with some exceptions (Wranik et al. 2008; Pfeifer et al. 2011; Massa et al. 2012; Bellmann et al. 2019; Fischer et al. 2020)

Some authors have suggested that there are further morphological characters besides the hind wing that would allow us to distinguish the two morphs. Koch and Meineke (in Schulte 2003) state that, not only the length of the hind wing, but also the extent of the tegmen and the height of the pronotum significantly differ between the two morphs. Schulte (2003) used a sex-specific ratio of hind wing length to pronotum

Figure 1. The 20 characters measured on 273 females of *Tetrix bipunctata* and *kraussi*. Measurements indicated by yellow lines. In all cases, a single photo was taken with reference points exactly placed in the focal plane. For character definitions, see Table 1.

length to determine the morphs. Furthermore, it was suggested that *bipunctata* is, on average, slightly larger and the pronotum more strongly arched (e.g. Baur et al. 2006).

No genetic differences have been found so far, as the two morphs form a single cluster when compared using COI barcoding (Hawlitschek et al. 2017).

In this study, we examine the morphs *bipunctata* and *kraussi* and discuss their status, based on new data from: (1) multivariate morphometry, (2) biogeography in Central Europe and (3) microhabitat niche use in syntopy.

1) Concerning morphological characters, we address the following questions:

– Are further characters – besides wing length – important for the separation of *bipunctata* and *kraussi* and to what extent? Some authors claim that body proportions seem to differ; however, nobody has ever tried to quantify those traits.

– What are the best shape characters for separating *bipunctata* and *kraussi*? As mentioned before, so far only a single ratio, hind wing length to tegmen length (either by taking into account the entire hind wing length or just the part projecting beyond the tegmen), has been used regularly. A morphometric analysis thus might reveal some more reliable ratios.

– Despite the evidence for two distinct morphs (Fischer 1948; Schulte 2003), specimens with intermediate wing ratios have been reported by Nadig (1991). Therefore, we re-examined Nadig's collection including the specimens in question.

– How much allometry is present? Size-dependent variation in the adult stage (static allometry, see Gould 1966; Klingenberg 2008, 2016; Anichini et al. 2017; Rebrina et al. 2020) plays a major role in such investigations, but so far, it has been neglected in this complex. Here, we analyse which characters and character ratios correlate with body size.

2) Biogeography

Due to the uncertain taxonomic situation, the distribution is far from settled, as many authors have not differentiated between *bipunctata* and *kraussi.* Furthermore, a substantial number of misidentifications have been published for *Tetrigidae* (own results, compare Lehmann et al. 2017). To establish a firm database for the distribution, we studied specimens from European Museums, complemented by private collections. The material from six central European countries added up to 663 specimens. This allows us to analyse the distribution and especially the level of sympatry and even syntopy. Furthermore, we study the altitudinal range separately for *bipunctata* and *kraussi*.

3) Ecology of habitat use at a syntopic population in Brandenburg

The segregated distribution of *bipunctata* and *kraussi* is interpreted as an ecological separation (Fischer 1948; Lehmann 2004). To test for differential habitat use, we studied microhabitat niches in a syntopic population discovered in southern Brandenburg (Lehmann and Landeck 2011).

Materials and methods

Identification of specimens

Below, we consistently refer to the morphs as "*bipunctata*" and "*kraussi*" and treat them in the sense of operational taxonomic units. For the assignment of specimens to morphs, we adopted the identifications found on the labels in the Swiss collections. This was mainly the case for specimens in Nadig's collection, also with respect to what

he considered as intermediate specimens. In all other instances we followed current practice (Schulte 2003; Lehmann 2004; Baur et al. 2006) and calculated the ratio of the full hind wing length to tegmen length: ≥ 2.5 = *bipunctata*, < 2.5 = *kraussi* (corresponding to the ratio of the protruding part of hind wing length to tegmen length of ≥ 1.5 and < 1.5, respectively). The same threshold was applied for a very few specimens that had obviously been misidentified by Nadig. The assignment of specimens was done before we performed any of the analyses reported below. As mentioned in the Introduction, *bipunctata* and *kraussi* have traditionally been separated by this ratio, which is why we refer to it as the "standard ratio" below.

1) Morphometry

Character measurements

We measured 20 characters from all over the body to cover the most relevant variation in size and shape between *bipunctata* and *kraussi*. The selection of characters was based on Harz (1975), Devriese (1996), Tumbrinck (2014) and our own expertise. Characters are shown in Fig. 1, definitions being given in Table 1. An overview of the basic descriptive statistics for each measurement (in mm) and morph, as well as the sample sizes is given in Appendix 2. We base our morphometric study on females because they were available in larger numbers. A further strength of using females is their larger body size, making measurements easier and faster. The majority of specimens originated from the collection Nadig (in Muséum d'histoire naturelle, Geneva, Switzerland, MHNG), the rest consisting of older material collected by Baur (in coll. Nadig) and some specimens collected in 2015 (also in Naturhistorisches Museum Bern, Switzerland, NMBE). We included 273 females from various populations in Central Europe, mainly from the Alps and the Jura (Table 2).

Each character was photographed with a Keyence VHX 2000 digital microscope and a VH-Z20R/W zoom lens at different magnification, depending on the size of the body part (see Table 1). For most measurements, we ensured that the reference points were placed exactly in the focal plane. Only one character, pronotum height (prn.h), was exceptional in that the reference points were not exactly in the same focal distance; here also, just a single photo was necessary, because the depth of field was sufficiently large. Moser took the photographs and measured the distances using ImageJ v.1.49r (Schneider et al. 2012); body parts on the images were zoomed in 3–4 times before measuring. Three characters were eventually omitted from the morphometric analysis (explained in Appendix 1), because of strong individual variation (pronotum height) or wear (2nd and 3rd pulvillus length), so that the final data contained 17 characters.

Multivariate ratio analysis of the body measurements

For the data analysis, we applied multivariate ratio analysis (MRA) (Baur and Leuenberger 2011). MRA comprises several tools related to standard multivariate methods,

Table 1. Abbreviation, name, definition and magnification (on Keyence digital microscope) of the 20 measurements used for the morphometric analyses of *Tetrix bipunctata* complex females. General morphology follows Lawrence et al. (1991) and the morphological terminology for pronotal carinae is adopted from Devriese (1996).

No.	Abbrev.	Character name	Character definition	Magnification
1	bt3.l	Basitarsus length	Length of basitarsus of hind tarsus, from proximal expansion to apex, outer aspect along ventral side	150
2	eye.b	Eye breadth	Greatest breadth of eye, lateral view	150
3	eye.h	Eye height	Greatest height of eye, lateral view	150
4	fl5.b	5th flagellomere breadth	Greatest breadth of 5th flagellomere, dorsal (inner) aspect	150
5	fl5.l	5th flagellomere length	Greatest length of 5th flagellomere, dorsal (inner) aspect	150
6	fm2.b	Mid-femur breadth	Greatest breadth of mid-femur, lateral view	100
7	fm2.l	Mid-femur length	Length of mid-femur, from proximal emargination of trochanter to emargination of knee, lateral view	100
8	fm3.b	Hind femur breadth	Greatest breadth of hind femur, lateral view	30
9	fm3.l	Hind femur length	Length of hind femur, from proximal edge to tip of knee disc, lateral view	30
10	fro.h	Frons height	Height of frons, from lower margin of clypeus to lower margin of eye orbit, frontal view	100
11	hea.b	Head breadth	Greatest breadth of head, dorsal view	100
12	hwi.l	Hind wing length	Length of hind wing, from proximal edge of tegmen to tip of hind wing, in situ. *Remark*: Very often, only the part protruding below the tegmen has been considered. Unfortunately, the measurement is then critically dependent on the position of the tegmen, which is often displaced relative to the hind wing. We, therefore, preferred the entire hind wing length, which can be measured rather more reliably	30
13	prn.b	Pronotum breadth	Greatest breadth of pronotum, dorsal view	30
14*	prn.h	Pronotum height	Greatest height of pronotum, from carina humeralis at level of proximal edge of tegmen to highest point of carina medialis, exact lateral view	30
15	prn.l	Pronotum length	Length of pronotum, from anterior margin to the tip of the posterior pronotal process, dorsal view along carina medialis	30
16*	pu2.l	2nd pulvillus length	Length of 2nd pulvillus on basitarsus of hind tarsus, from its proximal notch to distal notch, outer aspect	150
17*	pu3.l	3rd pulvillus length	Length of 3rd pulvillus on basitarsus of hind tarsus, from its proximal notch to distal notch, outer aspect	150
18	teg.b	Tegmen breadth	Greatest breadth of sclerotised part of tegmen, outer aspect	100
19	teg.l	Tegmen length	Length of fore wing, from proximal edge of tegmen to tip of fore wing, outer aspect	100
20	vrt.b	Vertex breadth	Shortest breadth of vertex, dorsal view. Together with head breath, this covers also potential differences in eye breath.	100

* Character omitted in morphometric analyses, see Appendix 1.

Table 2. Overview on *Tetrix bipunctata* complex populations (females only) included in the morphometric analyses. Most specimens are from the Nadig collection in MHNG.

Country	Population
AT	Kärnten
CH	BE Beatenberg
CH	BE/JU Jura
CH	GR Oberengadin
CH	GR Schams
CH	GR Unterengadin
CH	UR Urnerboden
DE	S-Bayern
DE	Schwarzwald
IT	Chiavenna
IT	Como
IT	Gardasee
IT	S-Tirol E/Mittenwald
IT	Trentino

such as principal component analysis (PCA) and linear discriminant analysis (LDA). Contrary to the normal application of these methods, MRA allows the interpretation of size and shape in a manner that is entirely consistent with the customary usage of body lengths and body ratios in taxonomy, for instance, in descriptions and diagnoses. Examples of the application of different MRA tools may be found in various papers (László et al. 2013; Baur et al. 2014; Ali et al. 2016; Huber and Schnitter 2020; Le et al. 2020; Selz et al. 2020). Here, we first calculated a general measure of size, "isosize", which we obtained by calculating for each specimen the geometric mean of all measurements. We then performed a PCA on a data matrix, where we divided each value by isosize, thus entirely removing differences in isometric size. To distinguish this particular type of PCA from the usual one based on just log-transformed raw data (Jolicoeur 1963), we called it "shape PCA" below.

Very often shape correlates with size, which corresponds to the well-known phenomenon of allometry. In the case of specimens belonging to the same stage, in our case adults, we are talking of static allometry (Gould 1966). Static allometric variation might furthermore be intraspecific, i.e. amongst members of the same species or interspecific, i.e. between species (Klingenberg 2008, 2016). The nature of allometry is often similar for some species, but sometimes, it also differs in extent and direction (Rebrina et al. 2020). It is important to note that intraspecific allometry may obscure the differences in body ratios. Interspecific allometry, on the other hand, may sometimes simulate differences, where only allometric scaling, the shift along a common allometric axis is present (Gould 1966; Seifert 2002; Warton et al. 2006; Klingenberg 2008, 2016).

For a sensible interpretation of morphometric results, it is therefore essential to consider allometric variation. In many studies, such variation is simply removed from the data by various "correction" procedures (Bartels et al. 2011; Sidlauskas et al. 2011). This, for instance, is also what happens when a PCA is used in a "normal" manner. Here, the first PC comprises size, as well as all the shape variation that correlates with size, thus removing allometry from the second and all subsequent PCs (but not necessarily removing isometric size differences) (Jolicoeur 1963; Baur and Leuenberger 2011). Unfortunately, this approach does not tell us anything about the nature of allometric variation. In contrast, by applying a shape PCA within the analytical framework of MRA, allometry is not at all removed but *uncovered* by plotting shape axes (e.g. shape PCs or some body ratios) against isosize. Such plots reveal useful information about the strength and direction of allometry, which may vary between the different shape axes, as well as between groups (Mosimann 1970; Klingenberg 2016). Below, we are making use of such plots for analysing our *Tetrix* data.

We first performed a series of shape PCAs to see how well the morphs were supported by variation in shape. A shape PCA shows in very few axes (usually just the first one or two shape PCs are important) the unconstrained pattern of variation in the data. A PCA type of analysis is convenient here, as it does not require *a priori* assignment of specimens to a particular group, but assumes that all belong to a single group. We could thus avoid bias with respect to groupings (Pimentel 1979; Baur and Leuenberger 2011).

We, furthermore, employed the PCA ratio spectrum that allows an easy interpretation of shape PCs in terms of body ratios. In a PCA ratio spectrum, the eigenvector coefficients of all variables are arranged along a vertical line. Ratios calculated from variables lying at the opposite ends of the spectrum have the largest influence on a particular shape PCA; ratios from variables lying close to each other or in the middle of the graph are negligible (Baur and Leuenberger 2011; Baur et al. 2014). As usually only few variables are located at the ends, the most important variation may be spotted at a glance.

The situation changes once we specifically ask for differences *between* groups. For this question, we use a method where the groups are specified *a priori*. In the morphometry of distance measurements, such methods are usually based on linear discriminant analysis (LDA) (e.g. Hastie et al. 2009). Here, we applied a particular method of the MRA tool kit, the LDA ratio extractor (see Baur and Leuenberger 2011 for how this algorithm works). This allows the user to find the best ratio for separating two groups. Note that the algorithm not just extracts them according to discriminating power, it also ensures that successive ratios (best, second best etc.) are least correlated (Baur and Leuenberger 2011).

We used the R language and environment for statistical computing for data analysis, version 4.0.3 (R Core Team 2020). For MRA, we employed the R-scripts provided by Baur and Leuenberger (2020) on Zenodo. ANOVAs were calculated using "summary(aov())" and by using the default settings. Scatterplots were generated with the package "ggplot2" (Wickham 2016). Naturally, not all specimens in the collection were complete, which means that 95 specimens lacked one body part or another. In order to be able to include all specimens in the multivariate analyses, missing values were imputed with the R package "mice" (Buuren and Groothuis-Oudshoorn 2011), using the default settings of the function "mice()".

Raw data in millimetres and the complete set of photographs with measurements, as well as the R-scripts used for the analyses, are available in a data repository on Zenodo (Moser and Baur 2021).

2) Biogeography

Given the high level of erroneous Tetrigidae determinations in collections, we refrain from incorporating published records. Instead, we concentrate on specimens studied by ourselves from several European Museums and private collections (Table 3).

Specimens were assigned to each morph by calculating the standard ratio (see above). After eliminating erroneous determinations by our precursors, nymphs and a single specimen of the f. macroptera which cannot be associated with either *bipunctata* or *kraussi* so far, we were able to include 660 specimens from the six Central Europe countries Germany, Netherlands, Switzerland, Austria, Italy and Slovenia (Suppl. material 1: Table S1: table of localities). Geographic coordinates and altitude were

Table 3. List of Museums and private collections with material of *bipunctata* and *kraussi* studied for the biogeography pattern. Museum codes are unified using the NCBI database (https://www.ncbi.nlm.nih.gov/biocollections/), see also Sharma et al. (2018). An exception is the Naturhistorisches Museum Bern, where we take the code used by the Museum NMBE instead of the NCBI code NHMBe.

Code	Institution
DEI	Senckenberg Deutsches Entomologisches Institut
MHNG	Muséum d'Histoire Naturelle, Geneva
MNHN	Muséum National d'Histoire Naturelle (Paris)
NMBE	Naturhistorisches Museum Bern
NHMV	Müritzeum / Naturhistorische Landessammlungen für Mecklenburg-Vorpommern
NHMW	Naturhistorisches Museum Wien
NKML	Naturkundemuseum Leipzig
SMNG	Senckenberg Museum für Naturkunde Görlitz
ZMA	Universiteit van Amsterdam, Zoologisch Museum
ZMB	Museum für Naturkunde Berlin
ZSM	Zoologische Staatssammlung München
Collectio Gatz	Katharina Gatz, Berlin, Germany
Collectio Gomboc	Stanislav Gomboc, Kranj,Slovenia
Collectio Hochkirch	Prof. Axel Hochkirch, Trier, Germany
Collectio Karle-Fendt	Alfred Karle-Fendt, Sonthofen, Germany
Collectio Landeck	Ingmar Landeck, Finsterwalde, Germany
Collectio Lehmann	Dr. Arne Lehmann, Stahnsdorf, Germany
Collectio Muth	Martin Muth, Kempten, Germany

extracted from specimen labels or using standard internet sources. We analysed the biogeography stratified for *bipunctata* and *kraussi* with an emphasis on the level of sympatry and syntopy. Furthermore, we studied the altitudinal range over the north-south gradient from the northern lowlands of Germany southwards to Italy and Slovenia.

For the generation of the map, we used QGis 3.10.13-A Coruna and the Natural Earth Data (https://www.naturalearthdata.com/about/terms-of-use/, https://www.openstreetmap.org/copyright, OpenStreetMap contributors).

3) Microhabitat niches

In a syntopic population in Brandenburg (2.5 km E of Theisa 51.542°N, 13.503°E), the microhabitat use was studied for four months from May to August 2015 by Katharina Gatz, supervised by G.U.C. Lehmann. By slowly walking through the habitat, individuals were located either sitting or jumping from a retraceable spot. At the point of origin, a little flag was placed and the animal afterwards caught with the help of a 200 ml plastic vial (Greiner BioOne) (Fig. 8). To document the microhabitat, Katharina Gatz measured the percentage of vegetation cover and the mean vegetation height in a radius of 10 centimetres around the flag. Individuals were here also determined using the standard ratio (see above). Microhabitat niche use was available for 34 adults determined as *kraussi* and 14 *bipunctata*. Habitat data for nymphs were excluded, as the wings are not fully developed, thus preventing determination.

Results

Measurement data

Appendix 2 gives the descriptive statistics for each measurement (in mm) and morph as well as the sample sizes.

Analysis using shape PCA

We first performed a series of shape PCAs to see how well the morphs were supported by variation in shape and which body ratios were responsible for separation (Fig. 2).

In the scatterplot of the first against second shape PC, the individuals were almost perfectly separated along the first shape PC, but entirely overlapping along the second (Fig. 2A). For the interpretation of the first shape PC, we must now have a look at its PCA ratio spectrum (Fig. 2B). With this graph, we are able to read off the most important character ratios at a glance, as just those ratios are relevant that include characters lying at the opposite ends of the spectrum (in Fig. 2B, C, the only ones labelled). So, for the first shape PC, these were hind wing length (hwi.l) at the upper end and 5th flagellomere length (fl5.l) at the lower end. Hence, the ratio hwi.l/fl5.l should normally be considered as the most important one. However, here the PCA ratio spectrum was noteworthy, insofar as we had, at the one end, a single character (hwi.l), whereas the other 16 characters were densely packed at the other end of the spectrum. Such an asymmetrical ratio spectrum is exceptional, since we usually observe a more symmetrical character dispersion, with few characters at the tips and the rest around the middle. Indeed, the strong asymmetry, in this

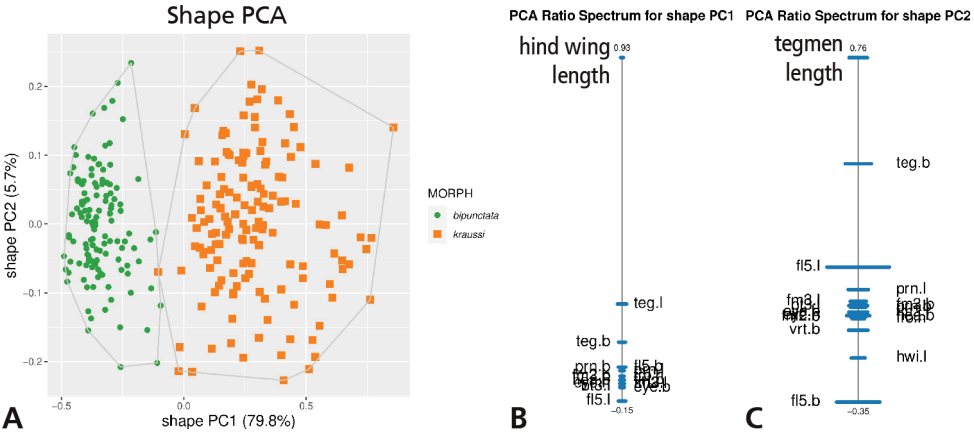

Figure 2. Shape principal component analysis (shape PCA) of 273 females of *Tetrix bipunctata* and *kraussi* **A** analysis including 17 variables, scatterplot of first against second shape PC; in parentheses the variance explained by each shape PC **B** PCA ratio spectrum for first shape PC **C** PCA ratio spectrum for second shape PC. Horizontal bars in the ratio spectra represent 68% bootstrap confidence intervals, based on 1000 replicates; only the most important characters are indicated in ratio spectra.

particular case, profoundly influenced our interpretation. It quite simply implied that *any* ratio formed with hind wing length would result in a similar separation of the morphs! Perhaps the weakest separation should be expected from the ratio hwi.l/teg.l, because tegmen length was represented in the ratio spectrum by the bar that was a bit distant from the remaining characters at the lower end and also closest to hind wing length.

With respect to the second shape PC, the situation is quite different as there is broad overlap between *bipunctata* and *kraussi*. According to its PCA ratio spectrum (Fig. 2C), tegmen length (teg.l) to 5th flagellomere breadth (fl5.b) emerged as the most important ratio. Any ratio formed with teg.l and one of the characters in the lower third of the spectrum give a similar result, as this ratio spectrum was also notably asymmetrical. Note that the overlap which we observed in morphs did not necessarily mean that none of these ratios contributed to their differentiation (see below under Extracting best ratios), but their relevance was lower. This is also reflected by the variation explained in the respective shape PCs; the first shape PC explained almost 80% of the variance, the rest less than 6% (see Fig. 2A).

Allometry

Plotting isosize against the first shape PC revealed that intraspecific allometry was weak in *bipunctata* and moderate in *kraussi* (Fig. 3). We were able to exclude a mere allometric scaling, because the morphs extensively overlapped in isosize, even though *bipunctata* was larger on average (ANOVA: $F_{1,271} = 88.96$, $p < 0.001$).

Extracting best ratios

The LDA ratio extractor found hind wing length to mid-femur length as the best ratio for separating *bipunctata* from *kraussi*. This ratio was indeed more powerful than

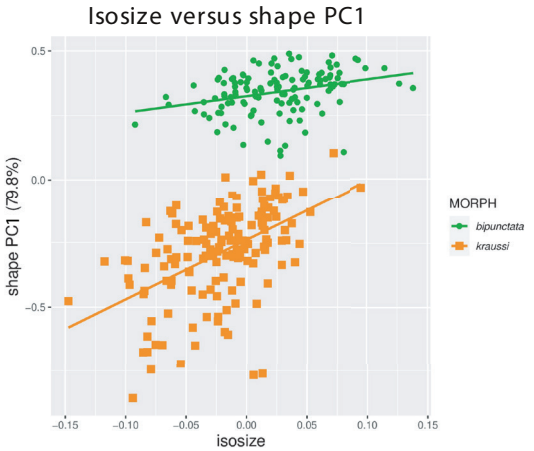

Figure 3. Analysis of allometric variation in 273 females of *Tetrix bipunctata* and *kraussi*. Scatterplot of isosize against first shape PC.

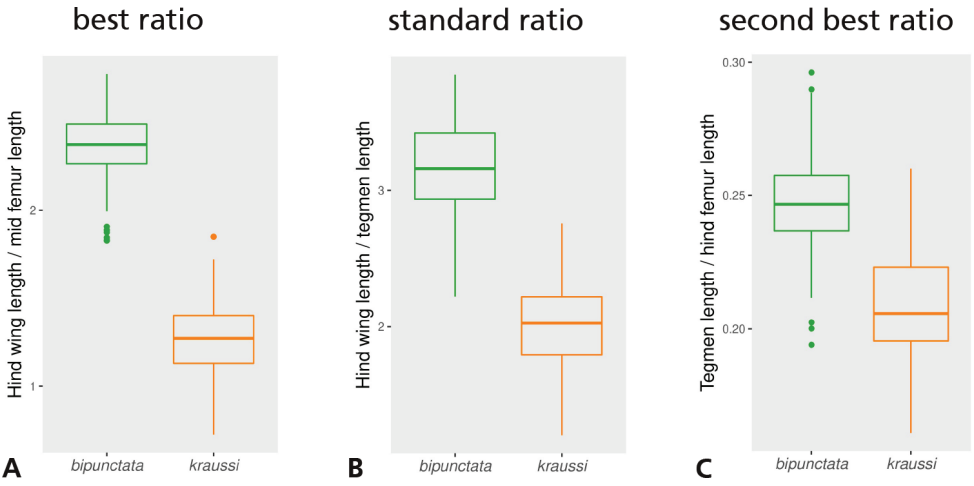

Figure 4. Boxplots of body ratios of 273 females of *Tetrix bipunctata* and *kraussi* **A** hind wing length to mid-femur length, the ratio selected by the LDA ratio extractor as the best ratio for separating the morphs **B** hind wing length to tegmen length, the standard ratio used for discrimination **C** tegmen length to hind femur length, the second best ratio found by the LDA ratio extractor (actually the best ratio when hind wing length is omitted). Means in all plots significantly different (ANOVA, $p < 0.001$).

the standard ratio (compare Fig. 4A, B). In contrast, the second-best ratio found by the ratio extractor, tegmen length to hind femur length, separated the morphs much less well (Fig. 4C). However, once hind wing length was omitted, this ratio had the best discrimination power. It was also more weakly correlated with the other two ratios and thus stood for another direction in the data. This direction only revealed differences in mean (ANOVA: $F_{1,271} = 795$, $p < 0.001$), but otherwise the morphs were largely overlapping.

The specimens considered as "Nadig intermediates" ("Zwischenformen") are found in both groups. In the plot with the best ratio (Fig. 5A), these specimens were nested within each morph and, therefore, cannot be considered intermediates. In the other plot, including the standard ratio (Fig. 5B), many intermediates emerged in or near the zone of overlap.

Biogeography

In total, 660 specimens from 286 localities could be included into our biogeographic analysis (Suppl. material 1: Table S1). We were able to include a slightly higher number of records for *kraussi*, with 403 individuals from 170 localities, than for *bipunctata* with 257 individuals from 116 localities. The general distribution pattern is largely overlapping; both *bipunctata* and *kraussi* occur in Central Europe sympatrically over much of the range (Fig. 6). However, this sympatric distribution is not perfect. In the northern lowlands area of the Netherlands, the German Federal States,

Figure 5. Scatterplots of isosize against body ratios of 273 females of *Tetrix bipunctata* and *kraussi*, showing the position of intermediate specimens **A** isosize against ratio of hind wing length to mid-femur length, the best ratio for separation of morphs **B** isosize against ratio of hind wing length to tegmen length, the standard ratio for discrimination (see Fig. 4). The 11 specimens considered by Nadig (1991) as "Zwischenformen" marked by black triangles.

Mecklenburg-Western Pomerania (Mecklenburg-Vorpommern) and ¾ of northern Brandenburg, only *bipunctata* individuals are found. All those records are below 121 m altitude, i.e. in the planar altitudinal belt. In contrast, the northernmost records of *kraussi* are from the mountainous Harz in Sachsen-Anhalt. From here, *kraussi* occurs largely sympatrically with *bipunctata* over the Central German Uplands. Given the general overlap, the low number of shared populations is notable; we identified only five syntopic localities for our German sample (two in southern Brandenburg, Thuringia Hainleite, Thuringia Kyffhäuser and Sachsen-Anhalt Balgstädt Tote Täler). In a large part of the Alps, *bipunctata* and *kraussi* are sympatric over much of their range. In Switzerland, we found syntopic populations occurring at medium altitude, especially pronounced in the Canton Bern with four out of five populations being syntopic, followed by the Jura with two out of six populations. In Beatenberg (Bernese Alps), the *bipunctata* to *kraussi* ratio was 5/9 and in Orvin (Jura), one *bipunctata* to 14 *kraussi* (Moser and Baur 2021). However, in the southern Alps, only *kraussi* occurs; all individuals from Istria up north to Carinthia (Kärnten) and Styria (Steiermark) in Austria and all prealpine populations in Italy, extending into the Ticino in Switzerland, belong to *kraussi*. Despite the large sympatric occurrence, a notable difference exists in the inhabited altitude. Segregated for the Federal States in Germany and the Alpine countries, *bipunctata* inhabits, on average, the higher altitudes (Fig. 7). The difference is especially clear in our samples from Austria and Bavaria, but is also found in seven out of ten regions with overlapping populations. In Slovenia, where only *kraussi* occurs, its altitudinal range is comparable to the *bipunctata* range found north of the Alps in Bavaria.

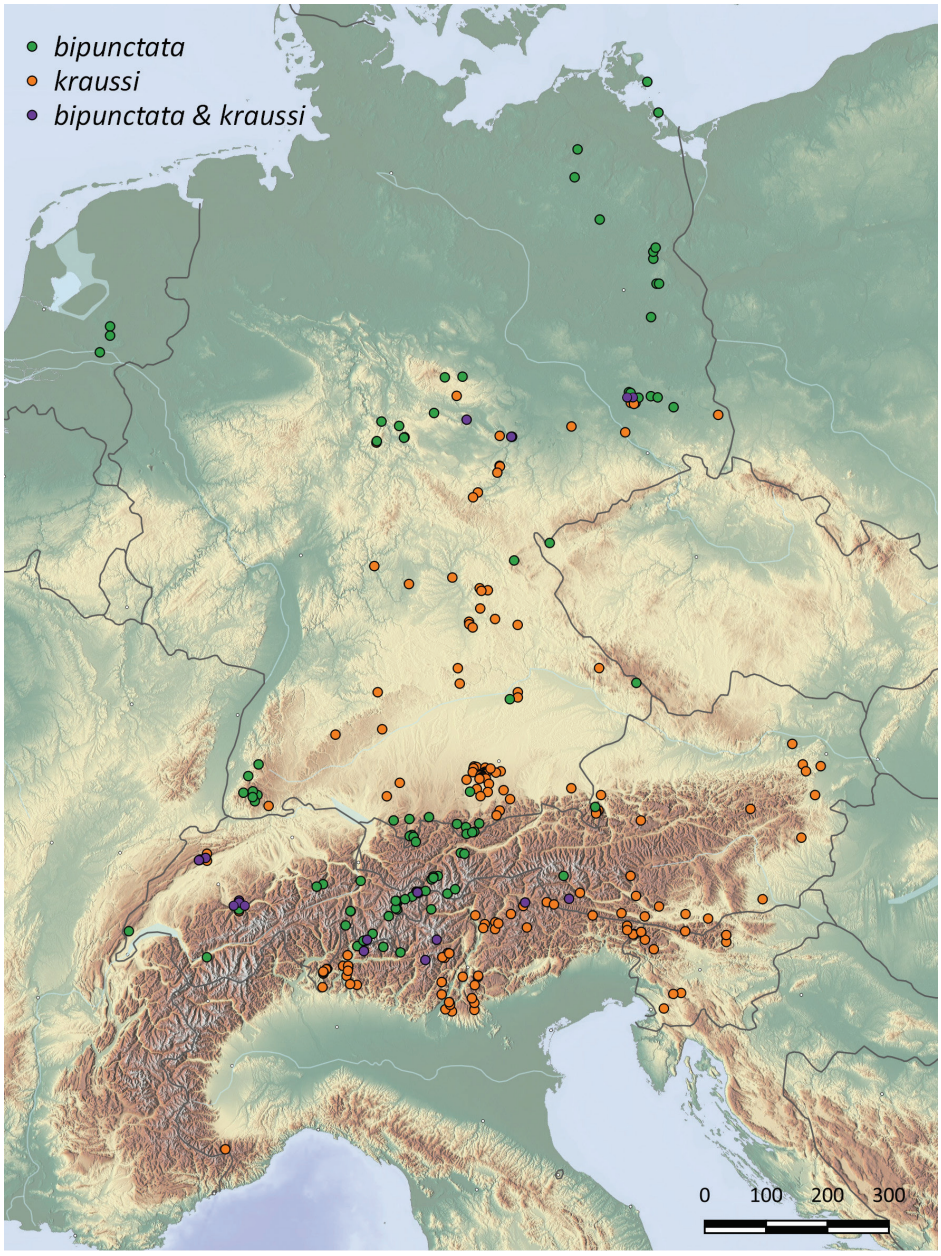

Figure 6. Distribution of 260 localities with records of *Tetrix bipunctata* (green dots), *kraussi* (orange dots) and syntopic populations (purple dots), mapped for six central European countries. Map generated using Natural Earth Data https://www.naturalearthdata.com/about/terms-of-use/.

Microhabitat niches

In the syntopic population in Brandenburg, adults of *bipunctata* and *kraussi* show separated microhabitat niche use. While *bipunctata* adults preferentially inhabit denser

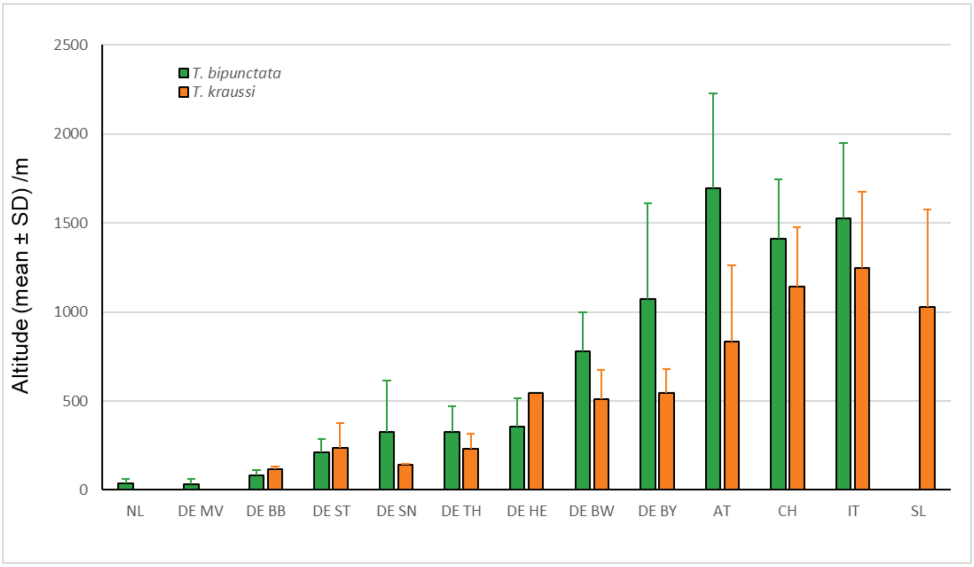

Figure 7. Altitudinal distribution (mean ± SD) of 286 populations of *Tetrix bipunctata* (green) and *kraussi* (orange) segmented for five Central European countries and eight Federal States in Germany. Regions are grouped along the north-south axis, NL = The Netherlands, DE = Germany: DE MV = Mecklenburg-Vorpommern, DE BB = Brandenburg, DE ST = Sachsen-Anhalt, DE SN = Sachsen, DE TH = Thüringen, DE HE = Hessen, DE BW = Baden-Württemberg, DE BY = Bayern, AT = Austria, CH = Switzerland, IT = Italy, SL = Slovenia.

Figure 8. Characteristic microhabitats of *Tetrix bipunctata* (left) and *kraussi* (right) at the syntopic population at Theisa, southern Brandenburg.

vegetation with higher plants (Fig. 8a), the more open areas with less tall plants are inhabited by *kraussi* (Fig. 8b). These spots occur side-by-side in the forest aisle at Theisa in Southern Brandenburg.

Microhabitats of *bipunctata* had a mean vegetation cover of 70 ± 18%, nearly twice as dense as the vegetation at *kraussi* spots (40 ± 7%) (Fig. 9). This difference in vegeta-

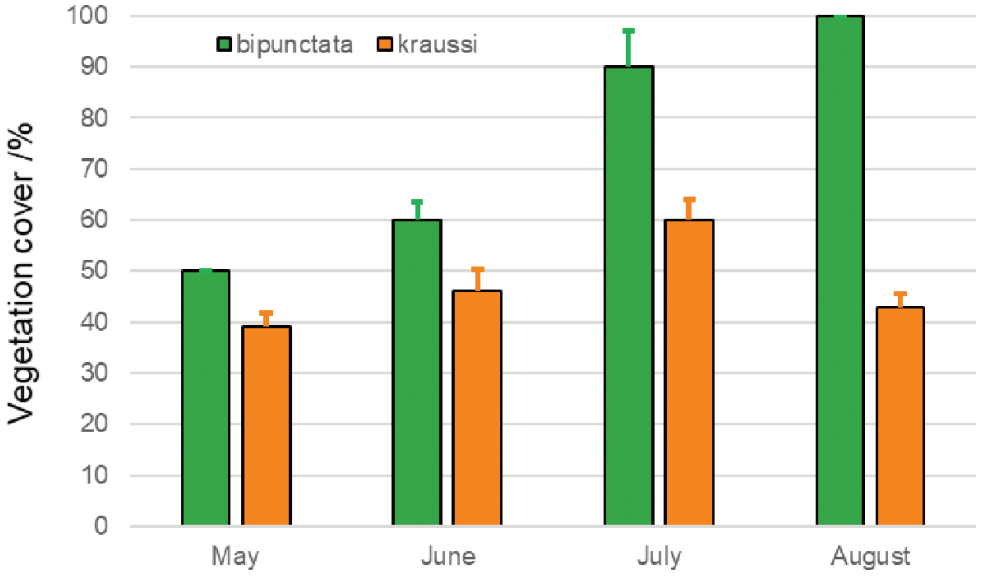

Figure 9. Vegetation cover in percent (mean ± SD) at spots of 10 cm diameter with records of adult *Tetrix bipunctata* and *kraussi* at the syntopic population at Theisa, southern Brandenburg.

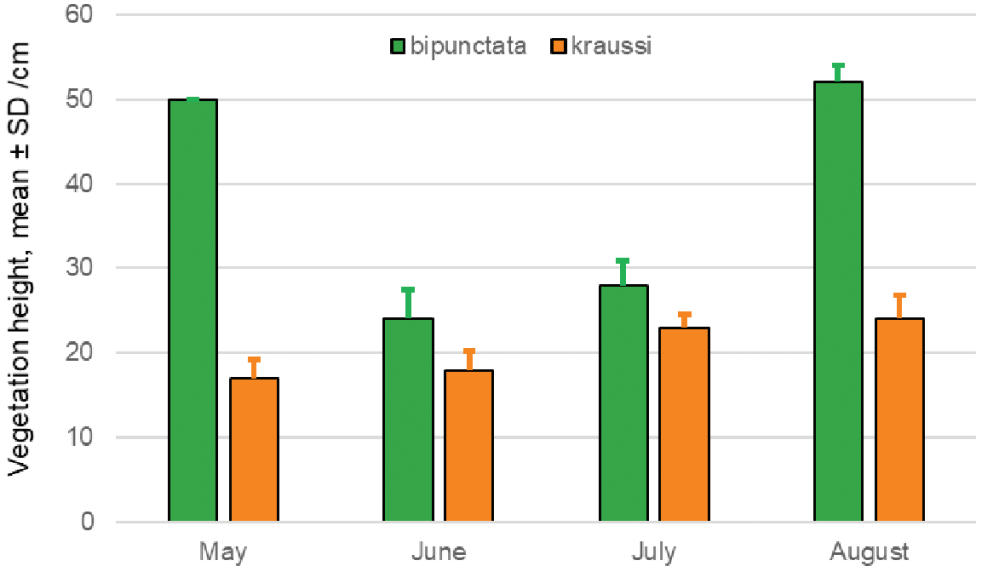

Figure 10. Vegetation height (mean ± SD) at spots of 10 cm diameter with records of adult *Tetrix bipunctata* and *kraussi* at the syntopic population at Theisa, southern Brandenburg.

tion cover was significant between morphs (two-way ANOVA: $F_{1,47} = 455.77$, $p < 0.001$) and between months (ANOVA: $F_{3,45} = 86.33$, $p < 0.001$). Even if the preference for more dense vegetation cover increases for *bipunctata* over the season, this shift was not significant, as indicated by the interaction term (ANOVA: $F_{3,45} = 2.16$, $p = 0.11$).

The vegetation at sites inhabited by *bipunctata* adults was on average 27 cm ± 12 cm tall, nearly twice as high as the plants at patches with *kraussi* occurrence (16 cm ± 4 cm) (Fig. 10). The difference is significant between morphs (two-way ANOVA: $F_{1,47} = 156.24$, $p < 0.001$) and months (ANOVA: $F_{3,45} = 37.80$, $p < 0.001$). Furthermore, it was pronounced in May and August as revealed by the significant interaction term (ANOVA: $F_{3,45} = 62.66$, $p < 0.001$).

Discussion

The morphometric analyses revealed that the morphs are merely separated by hind wing length or hind wing length in combination with any other character as a shape ratio. It was thus, by far, the most important character (Figs 2A, B, 4A, B). The first shape PC explaining 80% of the total variance supports this suggestion, while all other shape axes explain just a marginal portion of variation. The best ratio is hind wing length to length of the mid-femur, which almost perfectly distinguishes between *bipunctata* and *kraussi*. The traditionally used standard ratio of tegmen length to hind wing length (Lehmann 2004; Baur et al. 2006), is much less reliable (Fig. 4B). The differences between the morphs vanish when the importance of hind wing length is suppressed, as in the second shape PC (see Fig. 2A, C).

Isometric size between the morphs is widely overlapping with *bipunctata* being slightly larger on average (Fig. 3). This is consistent with the differences in body size measured as pronotum length and tegmen length found in the Diemeltal in northwest Germany (Schulte 2003). Based on more than 1000 specimens, *bipunctata* was the slightly larger morph compared to *kraussi*. Allometric variation is weak in both morphs and, because of the overlap in size, allometric scaling can be excluded. Some authors suggested the height of the pronotum as a possible difference (Schulte 2003). In Suppl. material 3: Fig. S2, we demonstrate that the variation in pronotum height between individuals excludes it from being a delimitation character.

In conclusion, we did find clear morphometric differences between *bipunctata* and *kraussi* only in hind wing length and all ratios including this variable. This is in agreement with results by Schulte (2003) who used specimens from northwest Germany and Sardet et al. (2015) who analysed French specimens. This means that the differences in wing length are consistent, regardless of the geographic origin.

Nadig's intermediate specimens and the subspecies hypothesis

Our analyis shows that the specimens from the Engadin, determined as intermediates ("Zwischenformen") by Nadig (1991), actually fall into either the *bipunctata* or the *kraussi* cluster. This is most evident from the scatterplot of isosize versus the best ratio (Fig. 5A) and, to a lesser degree, also from isosize versus the standard ratio (Fig. 5B).

Based on his observation, Nadig (1991) proposed to classify *bipuncata* and *kraussi* as subspecies. However, the definition of a subspecies, as suggested by most authors (Mayr 1963; Mallet 2007; Braby et al. 2012), also requires a geographical separation of

populations. Even though there are areas where only *kraussi* (the Southern Alps, as well as the Western Balkan) or *bipunctata* is found (Northern German Depression from the Netherlands towards Poland [this article], as well as Siberia and Scandinavia [Lehmann 2004]), there is a large area of sympatry in Central Europe (Fig. 6), thus eliminating the subspecies hypothesis. Syntopic populations are, furthermore, documented from all over the shared distribution range, with changing distribution ratio (see Schulte 2003; Lehmann and Landeck 2011; Sardet et al. 2015a; Moser and Baur 2021).

Habitat differentiation

The morphs show a preference for slightly different habitats, with *kraussi* preferring shorter and less dense vegetation cover (Fig. 8). Fischer (1948) had already reported differential micro-habitat usage of *bipunctata* and *kraussi*, with the distribution of *bipunctata* in generally higher vegetation and less exposed than *kraussi*. We found the same in a sympatric population in Southern Brandenburg. Overall, *kraussi* seems to prefer drier, warmer climatic conditions and is often associated with limestone and open space with low vegetation, while *bipunctata* shows a preference for denser vegetation and higher plants (Figs 9, 10), which is in accordance with other observations (Zuna-Kratky et al. 2017). Where the habitat preferences overlap, the morphs meet in sympatry. These shifted preferences help to explain the altitudinal differentiation with *bipunctata* occurring at higher altitudes in the mountains (Fig. 7). Consistent with these habitat preferences, *kraussi* occurs more in the South than *bipunctata* (Fig. 6). In the syntopic populations, we recorded dominance of either *bipunctata* or *kraussi*, as reported in literature (Schulte 2003; Sardet et al. 2015; Moser and Baur 2021). This might be influenced by the prevailing climatic conditions, with *kraussi* being more common in warmer regions and *bipunctata* dominating in cooler climate.

The question whether *kraussi* and *bipunctata* represent different species or should be interpreted as infraspecific morphs is still open. The lack of genetic differentiation (see Hawlitschek et al. 2017) is equally congruent with *bipunctata* and *kraussi* being two young species or representing ecomorphs of a single species. Polymorphism, especially regarding wing length, is a well-known phenomenon in Tetrigidae, for example, in the well-studied *Tetrix subulata* (Steenman et al. 2013, 2015; Lehmann et al. 2018). To complicate the situation, a macropterous morph is documented for *bipunctata* (Devriese 1996; Schulte 2003; this study). As all known Tetrigidae are either mono- or dimorphic (e.g. Günther 1979; Devriese 1996), this would make the *bipunctata*-complex the only documented case with three wing morphs. However, this is not impossible, as other insects are able to develop several morphs per species (West-Eberhard 2003). Unfortunately, we lack any studies on the processes triggering the difference between *kraussi* and *bipunctata* and the forma macroptera as well. The mechanisms for the development of the forma macroptera, on the one hand and the switch between the morphs *bipunctata* and *kraussi* on the other hand, might differ and be based on distinct genetic backgrounds.

More research is needed to distinguish between the two possibilities that *bipunctata* and *kraussi* are genetically young species or infraspecific ecomorphs. However, this is a prime example how even modern species concepts can reach their limits. What we can exclude is their status as subspecies. Missing evidence concerns the genetic and developmental mechanisms behind the wing length. Crossing experiments could, furthermore, be informative to study reproductive barriers and hybrid disadvantage. We recommend that *bipunctata* and *kraussi* are considered as separate units until the species question can be answered more precisely.

Acknowledgements

We thank Elsa Obrecht (NMBE) for critical reading of the manuscript. Estée Bochud (NME) created the map in Figure 6, for which we would like to thank her very much. Our special thanks to Katharina Gatz, for allowing the use of her microhabitat data. For the loan of specimen, we are grateful to the following curators in alphabetic order: the late Christiane Amédégnato (MNHN), B.J.H. Brugge and Willem Hogenes (ZMA), Jürgen Deckert, Claudia Hömberg and Michael Ohl (ZMB), Rolf Franke (SMNG), Eckhard Groll (DEI), the late Alfred Kaltenbach (NMW), Dietmar Klaus (NKML), Miss Riemann (NHMV), Klaus Schönitzer (ZSM) and Peter Schwendinger (MHNG). Daniel Roesti, Wasen i.E., accompanied H. Baur on one of the excursions in the Bernese Alps. We thank the private collectors Stanislav Gomboc, Alfred Karle-Fendt, Ingmar Landeck and Martin Muth for loan of and Carola Seifert and Reinhold Treiber for donating specimens.

References

Ali RF, Neiber MT, Walther F, Hausdorf B (2016) Morphological and genetic differentiation of *Eremina desertorum* (Gastropoda, Pulmonata, Helicidae) in Egypt. Zoologica Scripta 45: 48–61. https://doi.org/10.1111/zsc.12134

Anichini M, Kuchenreuther S, Lehmann GUC (2017) Allometry of male sound-producing structures indicates sexual selection on wing size and stridulatory teeth density in a bush-cricket. Journal of Zoology 301: 271–279. https://doi.org/10.1111/jzo.12419

Bartels PJ, Nelson DR, Exline RP (2011) Allometry and the removal of body size effects in the morphometric analysis of tardigrades. Journal of Zoological Systematics and Evolutionary Research 49: 17–25. https://doi.org/10.1111/j.1439-0469.2010.00593.x

Bartlett JW, Frost C (2008) Reliability, repeatability and reproducibility: analysis of measurement errors in continuous variables. Ultrasound in Obstetrics and Gynecology 31: 466–475. https://doi.org/10.1002/uog.5256

Baur B, Baur H, Roesti C, Roesti D (2006) Die Heuschrecken der Schweiz. 1. Haupt, Bern, 352 pp. https://books.google.ch/books/about/Die_Heuschrecken_der_Schweiz.html?id=e8NJAAAACAAJ&redir_esc=y

Baur H, Leuenberger C (2011) Analysis of ratios in multivariate morphometry. Systematic Biology 60: 813–825. https://doi.org/10.1093/sysbio/syr061

Baur H, Leuenberger C (2020) Multivariate Ratio Analysis (MRA): R-scripts and tutorials for calculating Shape PCA, Ratio Spectra and LDA Ratio Extractor. Zenodo. https://doi.org/10.5281/zenodo.3890195

Baur H, Kranz-Baltensperger Y, Cruaud A, Rasplus J-Y, Timokhov AV, Gokhman VE (2014) Morphometric analysis and taxonomic revision of Anisopteromalus Ruschka (Hymenoptera: Chalcidoidea: Pteromalidae)–an integrative approach. Systematic Entomology 39: 691–709. https://doi.org/10.1111/syen.12081

Bellmann H, Rutschmann F, Roesti C, Hochkirch A (2019) Der Kosmos Heuschreckenführer. Frankh-Kosmos Verlags-GmbH, Stuttgart, 430 pp.

Braby MF, Eastwood R, Murray N (2012) The subspecies concept in butterflies: has its application in taxonomy and conservation biology outlived its usefulness? Biological Journal of the Linnean Society 106: 699–716. https://doi.org/10.1111/j.1095-8312.2012.01909.x

Buuren S van, Groothuis-Oudshoorn K (2011) mice: Multivariate Imputation by Chained Equations in R. Journal of Statistical Software 45: 1–67. https://doi.org/10.18637/jss.v045.i03

Cigliano MM, Braun H, Eades DC, Otte D (2021) Orthoptera Species File. Version 5.0/5.0. [2021_03_20] http://Orthoptera.SpeciesFile.org

Coyne JA, Orr HA (2004) Speciation. Sinauer, 480 pp.

Dayrat B (2005) Towards integrative taxonomy. Biological Journal of the Linnean Society 85: 407–415. https://doi.org/10.1111/j.1095-8312.2005.00503.x

De Queiroz K (2007) Species concepts and species delimitation. Systematic Biology 56: 879–886. https://doi.org/10.1080/10635150701701083

Default B, Morichon D (2015) Criquets de France, Volume 1, fascicule A et B (Orthoptera: Caelifera). Faune de France, 738 pp. https://www.nhbs.com/faune-de-france-volume-97-criquets-de-france-volume-1-fascicule-a-et-b-orthoptera-caelifera-2-volume-set-book [January 26, 2021]

Devriese H (1996) Bijdrage tot de systematiek, morfologie en biologie van de West-Palearktische Tetrigidae. Nieuwsbrief Saltabel 15: 1–50.

Evenhuis NL (2002) Publication and dating of the two "Bulletins" of the Société Entomologique de France (1873–1894). Zootaxa 70: 1–32. https://doi.org/10.11646/zootaxa.70.1.1

Fischer H (1948) Die schwäbischen *Tetrix*-Arten (Heuschrecken). Bericht der Naturforschenden Gesellschaft Augsburg 1: 40–87.

Fischer J, Steinlechner D, Zehm A, Poniatowski D, Fartmann T, Beckmann A, Stettmer C (2020) Die Heuschrecken Deutschlands und Nordtirols: Bestimmen – Beobachten – Schützen. 2., korrigierte Auflage. Quelle & Meyer, Wiebelsheim, 371 pp.

Gould SJ (1966) Allometry and size in ontogeny and phylogeny. Biological Reviews 41: 587–638. https://doi.org/10.1111/j.1469-185X.1966.tb01624.x

Günther K (1979) Die Tetrigoidea von Afrika südlich der Sahara (Orthoptera: Caelifera). Beiträge zur Entomologie = Contributions to Entomology 29: 7–183. https://doi.org/10.21248/contrib.entomol.29.1.7-183

Harz K (1957) Die Geradflügler Mitteleuropas. Fischer, Jena, 494 pp.

Harz K (1975) Die Orthopteren Europas – The Orthoptera of Europe II. Dr. W. Junk B.V., The Hague, 939 pp. https://doi.org/10.1007/978-94-010-1947-7

Hastie T, Tibshirani R, Friedman J (2009) The elements of statistical learning. 2nd edn. Springer, New York, 745 pp. http://statweb.stanford.edu/~tibs/book/preface.ps [June 26, 2017]

Hawlitschek O, Morinière J, Lehmann GUC, Lehmann AW, Kropf M, Dunz A, Glaw F, Detcharoen M, Schmidt S, Hausmann A, Szucsich NU, Caetano-Wyler SA, Haszprunar G (2017) DNA barcoding of crickets, katydids and grasshoppers (Orthoptera) from Central Europe with focus on Austria, Germany and Switzerland. Molecular Ecology Resources 17: 1037–1053. https://doi.org/10.1111/1755-0998.12638

Hebert PDN, Cywinska A, Ball SL, deWaard JR (2003) Biological identifications through DNA barcodes. Proceedings of the Royal Society of London. Series B: Biological Sciences 270: 313–321. https://doi.org/10.1098/rspb.2002.2218

Huber C, Schnitter PH (2020) Nebria (Pseudonebriola) tsambagarav sp. nov., a new alpine species from the Mongolian Altai (Coleoptera, Carabidae). Alpine Entomology 4: 29–38. https://doi.org/10.3897/alpento.4.50408

Jolicoeur P (1963) 193. Note: The Multivariate Generalization of the Allometry Equation. Biometrics 19: 497–499. https://doi.org/10.2307/2527939

Kevan DKMcE (1953) The status of *Tetrix bipunctatum* (Linn.) (Orthoptera; Tetrigidae) in Britain. – Entomologist's Gazette 4: 205–224.

Klingenberg CP (2008) Morphological Integration and Developmental Modularity. Annual Review of Ecology, Evolution and Systematics 39: 115–132. https://doi.org/10.1146/annurev.ecolsys.37.091305.110054

Klingenberg CP (2016) Size, shape, and form: concepts of allometry in geometric morphometrics. Development Genes and Evolution 226: 113–137. https://doi.org/10.1007/s00427-016-0539-2

László Z, Baur H, Tóthmérész B (2013) Multivariate ratio analysis reveals Trigonoderus pedicellaris Thomson (Hymenoptera, Chalcidoidea, Pteromalidae) as a valid species. Systematic Entomology 38: 753–762. https://doi.org/10.1111/syen.12026

Lawrence JF, Nielsen ES, Mackerras IM (1991) Skeletal anatomy and key to orders. In: Naumann ID (Ed.) Insects of Australia: A textbook for students and research workers. Division of Entomology, CSIRO, Carlton, 3–32.

Le NH, Nahrung HF, Morgan JAT, Lawson SA (2020) Multivariate ratio analysis and DNA markers reveal a new Australian species and three synonymies in eucalypt-gall-associated Megastigmus (Hymenoptera: Megastigmidae). Bulletin of Entomological Research 110: 709–724. https://doi.org/10.1017/S000748532000022X

Lehmann AW (2004) Die Kurzflügel-Dornschrecke *Tetrix* (*bipunctata*) *kraussi* Saulcy, 1888: eine missachtete (Unter-) Art. Articulata 19: 227–228.

Lehmann AW, Landeck I (2011) Erstfund der Kurzflügel-Dornschrecke *Tetrix kraussi* Saulcy, 1888 im Land Brandenburg (Orthoptera: Tetrigidae). Märkische Entomologische Nachrichten 13: 227–232.

Lehmann AW, Devriese H, Tumbrinck J, Skejo J, Lehmann GUC, Hochkirch A (2017) The importance of validated alpha taxonomy for phylogenetic and DNA barcoding studies: a comment on species identification of pygmy grasshoppers (Orthoptera, Tetrigidae). ZooKeys 679: 139–144. https://doi.org/10.3897/zookeys.679.12507

Lehmann GUC, Marco H, Lehmann AW, Gäde G (2018) Seasonal differences in body mass and circulating metabolites in a wing-dimorphic pygmy grasshopper – implications for life history? Ecological Entomology 43: 675–682. https://doi.org/10.1111/een.12647

Linnaeus C (1758) Systema naturae per regna tria naturæ, secundum classes, ordines, genera, species, cum characteribus, differentiis, synonymis, locis (10th edn.). Impensis direct Laurentii Salvii, Stockholm, 847 pp. https://www.biodiversitylibrary.org/page/726886

Lougheed SC, Arnold TW, Bailey RC (1991) Measurement error of external and skeletal variables in birds and its effect on principal components. The Auk 108: 432–436.

Mallet J (2007) Subspecies, semispecies, superspecies. Encyclopedia of Biodiversity 5: 1–5. https://doi.org/10.1016/B0-12-226865-2/00261-3

Massa B, Fontana P, Buzzetti FM, Kleukers RMJC, Baudewijn O (2012) Orthoptera. Calderini-Edizioni, Bologna, 563 pp.

Mayr E (1963) Animal species and evolution. Belknap Press of Harvard University Press, Cambridge, [xiv,] 797 pp.

Moser V, Baur H (2021) Morphometric data from: Two species? – Limits of the species concepts in the pygmy grasshoppers of the *Tetrix bipunctata* complex (Orthoptera: Tetrigidae). Zenodo. https://doi.org/10.5281/zenodo.4818525

Mosimann JE (1970) Size allometry size and shape variables with characterizations of the lognormal and generalized gamma distributions. Journal of the American Statistical Society 65: 930–945. https://doi.org/10.1080/01621459.1970.10481136

Nadig A (1991) Die Verbreitung der Heuschrecken (Orthoptera:Saltatoria) auf einem Diagonalprofil durch die Alpen (Inntal-Maloja-Bregaglia-Lago di Como-Furche. Jahresbericht der Naturforschenden Gesellschaft Graubündens 102: 277–378.

Nakagawa S, Schielzeth H (2010) Repeatability for Gaussian and non-Gaussian data: a practical guide for biologists. Biological Reviews of the Cambridge Philosophical Society 85: 935–956. https://doi.org/10.1111/j.1469-185X.2010.00141.x

Pfeifer MA, Niehuis M, Renker C [Eds] (2011) Fauna und Flora in Rheinland-Pfalz Beiheft Die Fang- und Heuschrecken in Rheinland-Pfalz. GNOR, Landau, 678 pp.

Pimentel RA (1979) Morphometrics, the Multivariate Analysis of Biological Data. Kendall/Hunt Pub. Co, Dubuque, Iowa, 276 pp.

R Core Team (2021) R: A Language and Environment for Statistical Computing. R Foundation for Statistical Computing, Vienna. https://www.R-project.org/

Rebrina F, Anichini M, Reinhold K, Lehmann GUC (2020) Allometric scaling in two bushcricket species (Orthoptera: Tettigoniidae) suggests sexual selection on song-generating structures. Biological Journal of the Linnean Society 131: 521–535. https://doi.org/10.1093/biolinnean/blaa122

Sardet E, Dehondt F, Mora F (2015a) *Tetrix bipunctata* (L., 1758) et *Tetrix kraussi* Saulcy, 1889 en France: répartition nationale, biométrie, écologie, statut et sympatrie (Orthoptera: Caelifera, Tetrigoidea, Tetrigidae). Matériaux Orthoptériques et Entomocénotiques 20: 15–24.

Sardet É, Braud Y, Roesti C, Koch V (2015b) Cahier d'identification des Orthoptères de France, Belgique, Luxembourg & Suisse. Biotope éditions, Mèze, 304 pp.

Saulcy F (1888) Notice sur le genre *Tetrix* Latreille. Bulletin de la Société Entomologique de France 6: 135–136.

Schneider C, Rasband W, Eliceiri K (2012) NIH Image to ImageJ: 25 years of image analysis. Nature Methods 9: 671–675. https://doi.org/10.1038/nmeth.2089

Schulte AM (2003) Taxonomie, Verbreitung und Ökologie von *Tetrix bipunctata* (Linnaeus 1758) und *Tetrix tenuicornis* (Sahlberg 1893) (Saltatoria: Tetrigidae). Articulata, Beiheft 10: 1–226.

Seifert B (2002) How to distinguish most similar insect species – improving the stereomicroscopic and mathematical evaluation of external characters by example of ants. Journal of Applied Entomology 126: 445–454. https://doi.org/10.1046/j.1439-0418.2002.00693.x

Selz OM, Dönz CJ, Vonlanthen P, Seehausen O (2020) A taxonomic revision of the whitefish of Lakes Brienz and Thun, Switzerland, with descriptions of four new species (Teleostei, Coregonidae). ZooKeys 989: 79–162. https://doi.org/10.3897/zookeys.989.32822

Sharma S, Ciufo S, Starchenko E, Darji D, Chlumsky L, Karsch-Mizrachi I, Schoch CL (2018) The NCBI BioCollections Database. Database 2018: bay006. https://doi.org/10.1093/database/bay006

Sidlauskas BL, Mol JH, Vari RP (2011) Dealing with allometry in linear and geometric morphometrics: a taxonomic case study in the Leporinus cylindriformis group (Characiformes: Anostomidae) with description of a new species from Suriname. Zoological Journal of the Linnean Society 162: 103–130. https://doi.org/10.1111/j.1096-3642.2010.00677.x

Sites JW, Marshall JC (2004) Operational Criteria for Delimiting Species. Annual Review of Ecology, Evolution and Systematics 35: 199–227. https://doi.org/10.1146/annurev.ecolsys.35.112202.130128

Steenman A, Lehmann AW, Lehmann GUC (2013) Morphological variation and sex-biased frequency of wing dimorphism in the pygmy grasshopper *Tetrix subulata* (Orthoptera: Tetrigidae). European Journal of Entomology 110: e535. https://doi.org/10.14411/eje.2013.071

Steenman A, Lehmann AW, Lehmann GUC (2015) Life-history trade-off between macroptery and reproduction in the wing-dimorphic pygmy grasshopper *Tetrix subulata* (Orthoptera Tetrigidae). Ethology Ecology & Evolution 27: 93–100. https://doi.org/10.1080/03949370.2014.885466

Tumbrinck J (2014) Taxonomic revision of the Cladonotinae (Orthoptera: Tetrigidae) from the islands of South-East Asia and from Australia, with general remarks to the classification and morphology of the Tetrigidae and descriptions of new genera and species from New Guinea and New Caledonia. In: Telnov D (Ed.) Biodiversity, biogeography and nature conservation in Wallacea and New Guinea. Riga, the Entomological Society of Latvia, 345–396.

Wägele JW (2005) Foundations of Phylogenetic Systematics. (1st edn.). Pfeil, F, München, 365 pp.

Warton DI, Wright IJ, Falster DS, Westoby M (2006) Bivariate line-fitting methods for allometry. Biological Reviews 81: 259–291. https://doi.org/10.1017/S1464793106007007

West-Eberhard MJ (2003) Developmental Plasticity and Evolution. Illustrated Edition. Oxford University Press, Oxford, 816 pp. https://doi.org/10.1093/oso/9780195122343.001.0001

Wickham H (2016) ggplot2: elegant graphics for data analysis (2nd edn.). Springer, Huston, Texas, xvi, 260 pp.

Will KW, Mishler BD, Wheeler QD (2005) The perils of DNA barcoding and the need for integrative taxonomy. Systematic Biology 54: 844–851. https://doi.org/10.1080/10635150500354878

Willemse L, Kleukers RMJC, Baudewijn O (2018) The Grasshoppers of Greece. EIS Kennniscentrum Insecten & Naturalis Biodiversity Center, Leiden, 439 pp. https://www.nhbs.com/the-grasshoppers-of-greece-book [January 26, 2021]

Wranik W, Meitzner V, Martschei T (2008) Beiträge zur floristischen und faunistischen Erforschung des Landes Mecklenburg-Vorpommern (Lung M.-V.) Verbreitungsatlas der Heuschrecken Mecklenburg-Vorpommerns. Steffen GmbH, Friedland, 281 pp.

Yeates DK, Seago A, Nelson L, Cameron SL, Joseph L, Trueman JWH (2011) Integrative taxonomy, or iterative taxonomy? Systematic Entomology 36: 209–217. https://doi.org/10.1111/j.1365-3113.2010.00558.x

Zachos FE (2016) Species Concepts in Biology: Historical Development, Theoretical Foundations and Practical Relevance. Springer International Publishing, 220 pp. https://doi.org/10.1007/978-3-319-44966-1

Zuna-Kratky T, Landman A, Illich I, Zechner L, Essl F, Lechner K, Ortner A, Weissmair W, Wöss G (2017) Die Heuschrecken Österreichs. Denisia 39: 1–872.

Appendix 1

Identification and removal of unreliable characters.

As mentioned under Materials and methods, we omitted three characters from all morphometric analyses presented in the results. In the following, we briefly describe the procedure that led to their removal.

Initially, we started with a shape PCA, based on all 20 characters (see Suppl. material 2: Fig. S1). The resulting scatterplot was very similar to the one presented in the results (Fig. 2A), with an almost perfect separation of morphs along shape PC1 and a complete overlap along shape PC2 (Suppl. material 2: Fig. S1A). In addition, the PCA ratio spectrum for shape PC1 was fully congruent with the one of the definitive analysis (compare Suppl. material 2: Fig. S1B and Suppl. material 3: Fig. S2B). Differences eventually arose in the PCA ratio spectrum of the second shape PC, where the coefficients of the three characters pronotum height (prn.h), 2nd pulvillus length (pu2.l) and 3rd pulvillus length (pu3.l) evidently had much too broad confidence intervals (Suppl. material 2: Fig. S1C). These characters dominated the spectrum (also that of the third shape PC, not shown here), but at the same time, did not at all contribute to the differentiation of morphs. We, therefore, suspected that the measurements were unreliable, either due to high measurement error or intraspecific variation

(Baur and Leuenberger 2011). Closer inspection of specimens, indeed, revealed that the latter was prevalent concerning the upper edge of the pronotum. Here, specimens of both morphs showed large individual variation. For measuring pronotum height, we thus had to move the reference points along the body axis, rendering these points clearly non-homologous (Suppl. material 3: Fig. S2, measurement position indicated by a magenta line; note the varying position of these lines relative to the base of the tegmen). The pulvilli, on the other hand, were often worn off and the respective reference points indistinct.

It is well known that a high quality of measurements is crucial in morphometric data, as low reliability may cause serious problems for multivariate data analysis (Lougheed et al. 1991; Bartlett and Frost 2008; Nakagawa and Schielzeth 2010; László et al. 2013). Baur et al. (2014), for instance, demonstrated how badly a single error-prone variable may affect a shape PCA by masking important groupings. Therefore, we think it was not only justified, but also necessary to exclude the three characters from the dataset.

Appendix 2

Overview of measurements of *Tetrix* females, showing minimum, mean, median and maximum in mm.

Morph	Basitarsus length (bt3.l)				Eye breadth (eye.l)				Eye height (eye.h)				5th flagellomere breadth (f5.b)			
	min	mean	median	max	min	mean	median	max	min	mean	median	max	min	mean	median	max
bipunctata	1.10	1.26	1.26	1.44	0.60	0.68	0.68	0.75	0.66	0.76	0.76	0.86	0.12	0.15	0.15	0.17
kraussi	1.08	1.28	1.28	1.47	0.61	0.69	0.69	0.77	0.67	0.77	0.78	0.86	0.11	0.14	0.15	0.16

Morph	5th flagellomere length (f5.l)				Mid femur breadth (fm2.b)				Mid femur length (fm2.l)				Hind femur breadth (fm3.b)			
	min	mean	median	max	min	mean	median	max	min	mean	median	max	min	mean	median	max
bipunctata	0.21	0.26	0.26	0.31	2.98	3.32	3.31	3.73	8.67	9.42	9.41	10.63	9.07	10.53	10.62	11.80
kraussi	0.22	0.27	0.27	0.32	2.96	3.30	3.30	3.71	8.49	9.56	9.61	10.64	8.87	10.51	10.49	11.97

Morph	Hind femur length (fm3.l)				Frons height (fro.h)				Head breadth (hea.b)				Hind wing length (hwi.l)			
	min	mean	median	max	min	mean	median	max	min	mean	median	max	min	mean	median	max
bipunctata	25.50	28.88	28.99	31.99	6.27	6.98	6.98	7.77	6.98	7.69	7.71	8.47	17.17	22.28	22.29	26.98
kraussi	24.25	29.36	29.47	33.34	6.10	6.94	6.96	7.54	6.83	7.73	7.74	8.26	6.45	12.00	12.29	18.27

Morph	Pronotum breadth (prn.b)				Pronotum height (prn.h)				Pronotum length (prn.l)				2nd pulvillus length (pu2.l)			
	min	mean	median	max	min	mean	median	max	min	mean	median	max	min	mean	median	max
bipunctata	12.85	14.64	14.62	16.54	3.49	5.00	4.98	6.59	39.29	45.82	45.80	51.94	0.30	0.40	0.41	0.49
kraussi	12.30	14.31	14.39	15.76	3.22	5.02	4.98	6.93	39.24	45.16	45.20	52.50	0.33	0.42	0.42	0.54

Morph	3rd pulvillus length (pu3.l)				Tegmen breadth (teg.b)				Tegmen length (teg.l)				Vertex breadth (wt.b)			
	min	mean	median	max	min	mean	median	max	min	mean	median	max	min	mean	median	max
bipunctata	0.30	0.42	0.42	0.55	1.88	2.28	2.30	2.63	5.09	7.12	7.13	8.41	3.47	3.88	3.85	4.50
kraussi	0.34	0.44	0.44	0.56	1.67	2.13	2.12	2.61	4.63	6.12	6.09	8.66	3.36	3.89	3.90	4.51

Supplementary material 1

Table S1

Authors: Valentin Moser, Hannes Baur, Arne W. Lehmann, Gerlind U.C. Lehmann

Data type: table

Explanation note: Records of 660 specimen of *Tetrix bipunctata* and *T. kraussi*, based on our surveys in European Museums and private collections, see Table 3 for the list of sources.

The 17 rows coloured represent syntopic occurrences of *Tetrix bipunctata* and *T. kraussi*.

Species: z = Zwischenformen, specimen supposed to be intermediates by Nadig (1991), but turned out to be either *Tetrix bipunctata* or *T. kraussi* in this study.

Date: Collection date as reported on labels, in square brackets we added the unreported centuries [18] or [19] deduced from our knowledge of collectors biographies.

State: English name of the governmental province.

Bundesland / Kanton: German name of the governmental province.

Geographic coordinates and altitudes: extracted with the help of open mapping tools (https://tools.retorte.ch/map/, https://www.mapcoordinates.net).

Comments: Additional information given on labels.

First and second determination: Identifications based on label information.

Authors' determination: Identifications based on the standard ratio of the full hind wing length to tegmen length: ≥ 2.5 = bipunctata, < 2.5 = kraussi (corresponding to the ratio of the protruding part of hind wing length to tegmen length of ≥ 1.5 and < 1.5, respectively).

Collectio: Abbreviations of European Museums and private collections with material studied. Museum codes are unified using the NCBI database (https://www.ncbi.nlm.nih. gov/biocollections/), see also Sharma et al. (2018). An exception is the Naturhistorisches Museum Bern, where we take the code used by the Museum NMBE instead of the NCBI code NHMBe (compare Table 3).

Collection number: Individual codes assigned by the Collectio Lehmann [CL], the Muséum d'Histoire Naturelle, Geneva (MHNG) or Naturhistorisches Museum Bern (NMBE).

Link: https://doi.org/10.3897/zookeys.1043.68316.suppl1

Supplementary material 2

Figure S1

Authors: Valentin Moser, Hannes Baur, Arne W. Lehmann, Gerlind U.C. Lehmann

Data type: (measurement/occurrence/multimedia/etc.)

Explanation note: Shape principal component analysis (shape PCA) of 273 females of *Tetrix bipunctata* and *kraussi*. **A:** analysis including 20 variables, scatterplot of first against second shape PC. **B:** PCA ratio spectrum for first shape PC. **C:** PCA ratio spectrum for second shape PC. Horizontal bars in the ratio spectra represent 68% bootstrap confidence intervals based on 1000 replicates.

Link: https://doi.org/10.3897/zookeys.1043.68316.suppl2

Supplementary material 3

Figure S2

Authors: Valentin Moser, Hannes Baur, Arne W. Lehmann, Gerlind U.C. Lehmann

Data type: (measurement/occurrence/multimedia/etc.)

Explanation note: Variation in pronotum shape (lateral view) of some *Tetrix* females included in the morphometric analyses. **A–D:** *bipunctata*; **E–H:** kraussi. The position where pronotum height was measured is indicated by a magenta line.

Link: https://doi.org/10.3897/zookeys.1043.68316.suppl3

ZooKeys 1043: 61–85 (2021)
doi: 10.3897/zookeys.1043.65829
https://zookeys.pensoft.net

RESEARCH ARTICLE

A peer-reviewed open-access journal
ZooKeys
Launched to accelerate biodiversity research

Revision of the genus *Coccidula* Kugelann (Coleoptera, Coccinellidae)

Karol Szawaryn[1], Oldřich Nedvěd[2,3], Amir Biranvand[4], Tomasz Czerwiński[1], Romain Nattier[5]

1 *Museum and Institute of Zoology, Polish Academy of Sciences, Wilcza 64, 00-679 Warszawa, Poland* **2** *Faculty of Science, University of South Bohemia, Branišovská 1760, CZ-37005 České Budějovice, Czech Republic* **3** *Czech Academy of Sciences, Biology Centre, Institute of Entomology, České Budějovice, Czech Republic* **4** *Department of Entomology, College of Agricultural Sciences, Shiraz Branch, Islamic Azad University, Shiraz, Iran* **5** *Institut de Systématique, Evolution et Biodiversité (ISYEB), Muséum national d'Histoire naturelle, CNRS, Sorbonne Université, EPHE, Université des Antilles, 57 rue Cuvier, CP 50, 75231, Paris Cedex 05, France*

Corresponding author: Karol Szawaryn (k.szawaryn@gmail.com)

Academic editor: J. Poorani | Received 11 March 2021 | Accepted 5 May 2021 | Published 11 June 2021

http://zoobank.org/B6FC6D94-EC85-4EFC-8CEF-6F2D7E67059D

Citation: Szawaryn K, Nedvěd O, Biranvand A, Czerwiński T, Nattier R (2021) Revision of the genus *Coccidula* Kugelann (Coleoptera, Coccinellidae). ZooKeys 1043: 61–85. https://doi.org/10.3897/zookeys.1043.65829

Abstract

The genus *Coccidula* Kugelann includes five species distributed in the Holarctic, with one species in North America and four in Palearctic region. *Coccidula* belongs to the tribe Coccidulini which historically was treated as a separate subfamily within ladybird beetles, but recent studies confirmed its placement as a tribe within the broadly defined subfamily Coccinellinae. All species are revised and a **new synonymy** of *Lithophilus naviauxi* Duverger with *C. litophiloides* Reitter is proposed. Light and electron microscopy pictures support morphological descriptions. An identification key to all species is also provided.

Keywords

Coccinelloidea, ladybirds, morphological revision, new synonym, taxonomy

Introduction

The classification of ladybird beetles (Coccinellidae) has changed dynamically in the last decade mainly due to molecular approaches. Although several studies have been conducted at the family level, none of them gave robust classification of the family (Seago et al. 2011; Robertson et al. 2015). Historically, the family was divided into six or seven subfamilies (Sasaji 1968; Kovář 1996) but more recent treatments based on morphology and molecules support just two, Microweiseinae and Coccinellinae (Ślipiński 2007; Seago et al. 2011; Robertson et al. 2015). However, recent analysis of a large molecular dataset (Che et al. 2021) revealed the existence of the third monotypic subfamily Monocoryninae.

The genus *Coccidula* Kugelann, 1798 was traditionally placed in the subfamily Coccidulinae (Sasaji 1968; Kovář 1996), nonetheless, in the new classification of ladybirds it was proposed to be one of the tribes (Coccidulini) within the broadly defined subfamily Coccinellinae. Seago et al. (2011) synonymized this tribe with Scymnini, however, after the analyses by Robertson et al. (2015) and Che et al. (2021) both are once again treated as independent tribes. Coccidulini are one of the most problematic groups of ladybirds as in the traditional classification they contain numerous genera with just superficial external similarity based mainly on hairy body surface and relatively long antennae. Consequently, in all molecular analyses they do not form a monophyletic group (Seago et al. 2011; Robertson et al. 2015; Che et al. 2021). The tribe is distributed worldwide with moderate diversity in the Palearctic (Kovář 2007) and African regions (Fürsch 2007; Tomaszewska 2010), rich in South America (Gordon 1994), but the most diverse fauna occurs in South Asia, Australia and neighboring regions (e.g., Ślipiński 2007; Poorani and Ślipiński 2009; Tomaszewska 2010; Tomaszewska and Ślipiński 2011; Szawaryn and Leschen 2019). The largest and most widely distributed is the genus *Rhyzobius* Stephens, 1831 with more than 100 recognized species (Tomaszewska 2010; Czerwiński et al. 2020) and numerous undescribed species mainly from New Guinea. Interestingly it is also the only genus of Coccidulini with known fossil representatives from the Eocene period discovered in Oise (Kirejtshuk and Nel 2012) and Baltic ambers (Szawaryn and Tomaszewska 2020).

Coccidula is a small genus distributed in the Holarctic, with one species in North America and four in Eurasia. Historically numerous species and varieties have been described based mostly on differences in color pattern, but most of them were subsequently synonymized when genitalia were examined. Gordon (1985) revised the North American species; however, the Palearctic species have not been revised until now. As Coccidulini has never been a subject of morphological cladistic analysis there is no hypothesis about its internal relationship available. However, based on recent molecular analyses (Che et al. 2021), *C. scutellata* (Herbst, 1783) and *Rhyzobius litura* (Fabricius, 1787) group in a single clade with the African genus *Epipleuria* Fürsch, 2001 and African species of *Rhyzobius*.

The European species are usually found in wetlands and water banks in low and middle elevations (Bielawski 1959). They live on herbaceous emergent grassy

vegetation such as reeds, feeding on aphids such as *Hyalopterus pruni* (Hemiptera: Aphididae). *Coccidula rufa* is sometimes contrastingly reported also from dry sand dunes and in Finland from cereal fields (Clayhills and Markkula 1974). High prevalence (60–80%) of endosymbiotic bacteria *Rickettsia* and *Wolbachia* was reported from Germany (Weinert et al. 2007). *Coccidula rufa* is univoltine – mating and egg-laying occur in the spring and summer, eggs are laid in batches on reed stems and foliage, larvae develop through the spring and summer, and a new generation of adults emerges in July. All species may be locally and temporally abundant.

The tribe Coccidulini needs comprehensive revision. In the current work we present a morphological revision of all currently known species of *Coccidula*, the type genus for the tribe. This revision is a first step to understand the morphological diversity of the tribe and may lead to further phylogenetic studies.

Material and methods

Material used of this study is deposited in the following collections:

AJC	Andrzej Jadwiszczak Collection, Poland;
ASC	Alexander Slutsky Collection, Kharkov, Ukraine;
HNHM	Hungarian Natural History Museum, Budapest, Hungary;
NMP	National Museum Prague, Czech Republic;
MIZ	Museum and Institute of Zoology, Warsaw, Poland;
MNHN	Muséum national d'histoire naturelle, Paris, France;
USB	University of South Bohemia, České Budějovice, Czech Republic.

Genitalia were dissected, cleared in a 10% KOH solution, washed in water, and placed in glycerol on slides for further study. Female genitalia were stained with chlorazol black. Measurements were recorded as follows: TL – total body length from apical margin of clypeus to apex of elytra; PL – pronotal length from the middle of anterior margin to the middle of the posterior margin; PW – pronotal width across widest part; EL – elytral length along suture including scutellum; EW – elytral width across both elytra at the widest part. Colour images were taken using either a stereo microscope Leica MZ 16 with a digital camera IC 3D; final images were produced using Helicon Focus 5.0X64 and Adobe Photoshop CS6 software, or a stereo microscope Nikon SMZ 1500 with Lumenera digital camera and QuickPhoto software, composite images with deep focus were generated using Zerene Stacker. The SEM photographs were taken in the Laboratory of Scanning Microscopy, MIZ (Warsaw), using a scanning electron microscope HITACHI S-3400N under low vacuum conditions and on JEOL JSM-7401F in Biology Centre CAS (České Budějovice). Terminology used for morphology follows Ślipiński (2007) and Lawrence et al. (2011). In this paper, we follow the classification proposed by Che et al. (2021).

Taxonomy

Family Coccinellidae Latreille, 1807
Subfamily Coccinellinae Latreille, 1807
Tribe Coccidulini Mulsant, 1846

Coccidula Kugelann, 1798

Coccidula Kugelann, 1798: 421. Type species: *Chrysomela scutellata* Herbst, 1783, by subsequent designation by Crotch 1874.
Strongylus Panzer, 1813: 114.
Cacidula Dejean, 1821: 132. Type species: *Chrysomela pectoralis* Fabricius, 1792 (=*Dermestes rufus* Herbst, 1783).
Cacicula Stephens, 1831: 397.

Diagnosis. Representatives of the genus *Coccidula* with its general body shape may resemble *Tetrabrachys* Kapur, however, it can be separated based on the structure of the tarsi which are tetramerous in both genera but in *Coccidula* the first tarsomere is sub-triangularly broadened apically and the second is elongate and distinctly lobbed, while in *Tetrabrachys* both the first and second are narrow, elongate and without lobes. Moreover, in *Tetrabrachys* the apical maxillary palpomere is widely securiform, and beetles are brachypterous, while in *Coccidula* the apical maxillary palpomere is only slightly widened and the second pair of wings is functional. *Coccidula* is also externally similar to European species of *Rhyzobius* but it can be separated based on the following characters: body almost parallel sided, elytra covered with punctures of two sizes, larger punctures arranged in nine rows (in *C. litophiloides* some of them are reduced), base of the pronotum not bordered, while in *Rhyzobius* the lateral body outline is broadly rounded, the elytra are covered with single sized, randomly arranged punctures, and base of the pronotum with distinct bordering line.

Description. Body elongate-oval, with sides parallel (Fig. 1C–H), body flattened in lateral view, convex in cross-section; dorsum covered with setiferous punctures of two sizes (Figs 7A, 9A), hairs directed forwards on pronotum, backwards on elytra.

Head partially withdrawn into prothorax (Fig. 1C–H); ventral antennal grooves shallow and moderately long, extending to posterior border of an eye (Fig. 3E). Eyes prominent, coarsely facetted (7–8 ommatidia per eye width), ocular canthus distinct, about as long as 4–5 ommatidium diameters; interocular distance about 3× as eye diameter; interfacetal setae present only in basal part; temple behind eye distinctly longer than eye (Fig. 3E). Antennal insertion placed laterally, invisible from above, distance between antennal insertions about same as between eyes; frons around antennal insertions slightly expanded, covering antennal insertions, anterior tentorial pits placed ventrally below antennal insertions. Antennae (Figs 5A, E, 7A, D) longer than maximum head width including eyes, composed of 11 antennomeres (AN); scape simple, without projections, slightly curved; pedicel distinctly narrower than scape, elongate (1.5× longer than wide); AN 3–8 elongate (AN3 ≈ 3.5×; AN8 ≈ 1.3× longer than wide); AN

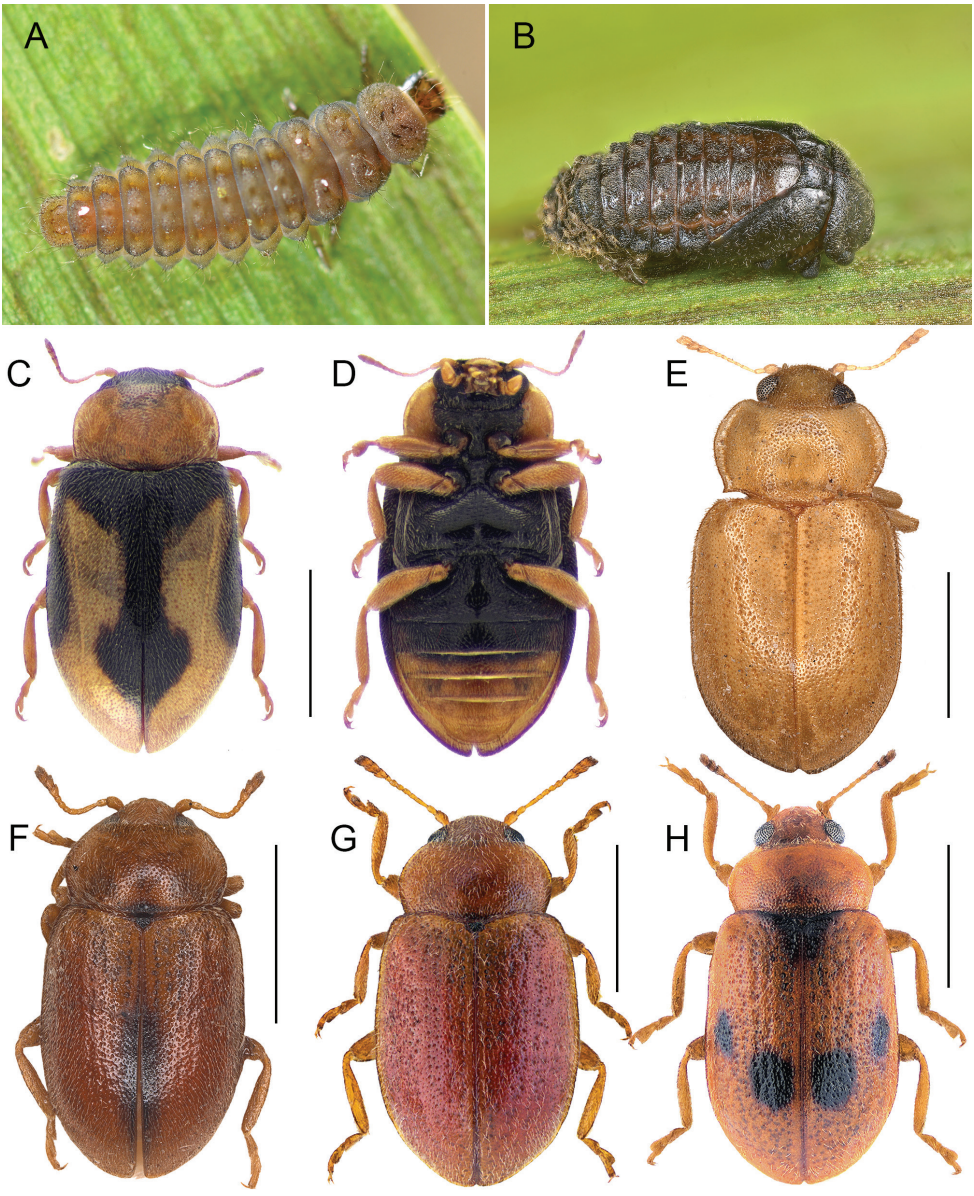

Figure 1. Immature stages and habitus of adult species of *Coccidula* Kugelann **A** *C. rufa* larva **B** *C. rufa* pupa **C** *C. lepida*, dorsal **D** *C. lepida*, ventral **E** *C. litophiloides* **F** *C. reitteri* **G** *C. rufa* **H** *C. scutellata* **A, B** Gilles San Martin, Wikimedia Commons **C, D** Danny Haelewaters **G, H** Udo Schmidt. Scale bars: 1 mm (**C–H**).

9–11 forming a loose, asymmetric club, ultimate AN truncate apically. Frontoclypeus short, transverse, anterior margin straight. Labrum entirely exposed, transverse, anterior margin straight. Mandibles asymmetric, bifid apically (Fig. 10G), molar part with basal tooth; prostheca distinct. Maxillary stipes (Figs 2B, 5C, 9C, 10H) with distinct groove for reception of maxillary palp in repose; palpomere 2 shorter than terminal

(4th) one, slightly broadened apically; palpomere 3 about 2.3× shorter than terminal one, subtriangular; terminal palpomere slightly securiform; lacinia with stiff setae on outer margin in apical half, with several additional spurs on surface (Fig. 10H). Labial palps (Figs 3E, 9C) with 3 palpomeres, inserted ventrally on prementum; palpomere 1 very small, apical palpomere as long as and about as broad as penultimate; distance between palp insertions about 1.5–2× as its width. Prementum subquadrate, transverse apically. Mentum trapezoidal, broadest in anterior part, with horseshoe impression at base (Figs 7C, 9C). Submentum broad, transverse, with suture invisible.

Anterior margin of pronotum weakly, broadly emarginate (Figs 3B, 5B) with anterior corners broadly rounded; lateral margins with moderately (Figs 7B, 9B) to distinctly expanded lateral beads (Fig. 3B), distinctly margined; hind corners sharply pointed; hind margin not bordered. Prothoracic hypomeron smooth, without delimited foveae (Figs 3C, 7C). Prosternum in front of coxae about as long as longitudinal length of procoxal cavity; anterior margin straight or slightly emarginate with distinct border. Prosternal process about 0.4 times of coxal diameter, surface smooth (Fig. 3C) or with lateral carinae (Figs 7C, 9E). Procoxal cavity oval, distinctly bordered anteriorly.

Mesoventrite 1.3× longer than its width at the level of mid coxae (Figs 1D, 5D, 7D); mesal surface with deep emargination for receiving tip of prosternal process (Fig. 2C); anterior margin with completely raised border. Meso-metaventral process narrow (Figs 1D, 2C, 5D, 7E), about 0.5 times of mesocoxal diameter, junction slightly arcuate (Figs 2C, 3D, 5D, 7E, 9D), with suture visible. Metendosternite with stalk sub-quadrate, tendons long, separated by a distance of about width of stalk and situated closer to center (Fig. 10I). Scutellar shield pentagonal (Figs 7B, 9B). Elytra at base wider than pronotum, lateral margins clearly visible from above throughout (Figs 2D, 3A, 5A, 7A) (except *C. scutellata* where it is obscured in basal part, Fig. 9A), surface covered with punctures of double size, smaller irregularly distributed, larger punctures arranged in nine irregular longitudinal rows. Sutural stria absent. Elytral epipleuron narrow, incomplete, reaching base of ventrite 4 (Fig. 1D), with complete bordering line, epipleural foveae absent. Hind wings fully developed or missing (in *C. litophiloides*). Metaventral postcoxal lines roundly joined medially, complete laterally, straight or descending (Figs 2C, 3D, 5D, 7E, 9D). Metaventrite with discrimen visible in posterior 2/3.

Trochanters simple, subtriangular, without projection (figs 7E, 9D). Tibiae slightly expanded apically with one apical spur on forelegs, and two in mid and hind legs. Tarsi consisting of four tarsomeres, second tarsomere truncate apically; tarsal claws cleft apically (Fig. 9G) with single empodial seta present.

Abdomen in both sexes with 6 ventrites (Fig. 1D); ventrite 1 about as long as ventrites 2–4 combined, ventrite 2 longer than ventrite 3, ventrites 3–5 subequal in length. Abdominal postcoxal lines (Figs 7E, 9D) separate medially, recurved and complete, reaching anterior margin of ventrite, posteriorly reaching about half length of ventrite 1. Ventrite 5 in female posteriorly rounded (Fig. 7F), in male truncate (Fig. 9F). Ventrite 6 rounded in both sexes.

Male terminalia. Tegmen (Figs 4A, B, 8A, B, 10A, B) symmetrical; parameres articulated with penis guide. Penis (Figs 4C, 8C, 10C) slender, pointed apically; penis capsule asymmetrical with outer arm reduced, inner arm well developed. Apodeme of

male sternum IX simple, not broadened apically (Figs 8D, 10D). Tergite X broadly rounded, semicircular (Figs 8D, 10D).

Female terminalia. Coxites (Figs 10F) distinctly elongate, subtriangular; styli small but visible, bearing several short setae; infundibulum absent (Figs 4D, 8E, 10E); sperm duct simple. Spermatheca (Figs 4D, 8E, 10E) worm-like, without clear ramus or nodulus; spermathecal accessory gland small, elongate. Proctiger elongate, rounded apically (Fig. 10F).

Immature stages. Larva as in Fig. 1A, pupa as in Fig. 1B.

Distribution. Holarctic: Asia, Europe, Africa (North), North America.

Key to species of *Coccidula* Kugelann

1 Head and epipleurae black (Fig. 1C, D); elytra with humeral area black. Nearctic ..... ***C. lepida*** **LeConte**

– Head and epipleurae testaceous; elytra with humeral area testaceous. Palaearctic ... **2**

2 Pronotum with posterior corners pointed, with an angle much less than 90° (Figs 1G, 3B); pronotal lateral margins broadly explanate (Figs 1E, 3B); prosternal process without carinae (Fig. 3C); elytra with missing or reduced rows of large punctures 2 and 3 (counted from the suture) ..... ***C. litophiloides*** **Reitter**

– Pronotum with posterior corners not distinctly pointed, with an angle around 90° (Figs 1F–H, 7B, 9B); pronotal lateral margins moderately explanate (Figs 1G, 7B, 9B); prosternal process with distinct lateral carinae (Figs 7C, 9E); elytra with all rows of large punctures well visible..... **3**

3 Prosternal process with lateral carinae very distinct, sinuate, roundly joined to the anterior prosternal margin (Fig. 9E); lateral elytral margins in basal part not visible from above (Fig. 9A); metaventral postcoxal lines narrowly separated on metaventral process (Fig. 9D); specimens entirely testaceous or with more than one black macula on elytra (Fig. 1H); penis guide about half length of parameres (Fig. 10A) ..... ***C. scutellata*** **Herbst**

– Prosternal process with lateral carinae straight, sometimes not joined together, extending to level of anterior border of procoxal cavity, not merged to anterior prosternal margin (Figs 5C, 7C); lateral elytral margins in basal part visible from above (Figs 5A, 7A); metaventral postcoxal lines joined on metaventral process (Figs 5D, 7E); specimens entirely testaceous to rufous (Fig. 1G) or with single elongate dark brown to black macula near the elytral suture around middle of elytra (Fig. 1F); penis guide longer than parameres (Figs 6B, 8A)..... **4**

4 Body entirely rufous, sometimes with darker scutellar shield (Fig. 1G); penis guide distinctly curved in lateral view, parameres at base about as broad as in middle (Fig. 8B)..... ***C. rufa*** **(Herbst)**

– Body testaceous with small transverse macula at base of pronotum just above scutellar shield, scutellar shield dark, elytra with single dark brown to black, longitudinal macula on elytral suture around middle of elytra (Fig. 1F); penis guide mildly curved in lateral view, parameres at base distinctly narrower than in middle (Figs 6A, C) ..... ***C. reitteri*** **Dodge**

***Coccidula lepida* LeConte, 1852**
Figs 1C, D, 2A–E

Coccidula lepida LeConte, 1852: 132.
Coccidula occidentalis Horn, 1895: 114.
Coccidula suturalis Weise, 1895: 132.

Material examined. United States of America: America b., 82, coll. Růžička et Vokál, (1: NMP); Alaska, Mi.1249, Alaska Hwy., Dedman Lk., 6.–7.VII.1968, Campbell & Smetana (1: NMP); Vermont, Korschefsky det. (2: MIZ); Canada: SK, Harris Reservoir, Hwy 21, 10 km S, Maple Creek, April 19 2016, drift D. Larson (1 female: NMP). Type material not studied, deposited in Museum of Comparative Zoology, Cambridge, USA.

Diagnosis. *Coccidula lepida* is the only Nearctic species of the genus, and is similar in many characters to *C. scutellata*, but with the head and epipleura black. In the typical form (*C. lepida* described by LeConte), the black elytral pattern resembles an extension of the five fused black maculae on the elytra of *C. scutellata*, with shoulders and epipleura black. Shoulder tubercle distinct, prototum relatively narrow. Male genitalia with penis guide much shorter than parameres. Detailed description of morphology including variability in pattern can be found in Gordon (1985: 656–659).

Description. Length = 2.7–3.5 mm, BL/BW = 1.88–1.96, EL/BW = 1.40–1.42, PW/BW = 0.73.

Body elongate (Fig. 1C), slightly widening in posterior part. Head black. Elytra of typical form, light testaceous with black pattern covering scutellar shield and surrounding portion of elytra through shoulders to lateral margins, covering about 60% of its anterior part; pair of maculae in posterior 3/4 of elytra near suture; in western population fused and connected to scutellar shield over suture. Ventral side (Fig. 1D) black with hypomera and ventrites 3–6 testaceous.

Head and pronotum covered with uniform small setiferous punctures arranged irregularly. Pronotum transverse, broadly rounded laterally, with lateral margin glabrous; pronotum covered with dense setiferous punctures. Posterior pronotal corners not produced (Fig. 2A). Prosternum with anterior margin with bordering line complete. Prosternal process with complete lateral carinae, joined roundly and merged with anterior border of pronotum (Fig. 2B).

Scutellar shield pentagonal, covered with dense setiferous punctures. Elytra (Fig. 2D) covered with two types of punctures, small setiferous punctures irregularly distributed throughout the elytral surface, some of these punctures surrounded by larger depressed circles forming nine irregular longitudinal rows along the whole length of elytra. Shoulder tubercles distinct, but lateral elytral margin of elytra visible from above throughout. Mesoventrite (Fig. 2C) with anterior border interrupted in median part. Metaventrite (Fig. 2C) with postcoxal lines transverse in median part and then descending laterally, continuous on the metaventral process in median part; covered with setiferous punctures very sparsely distributed in central part of sclerite, densely

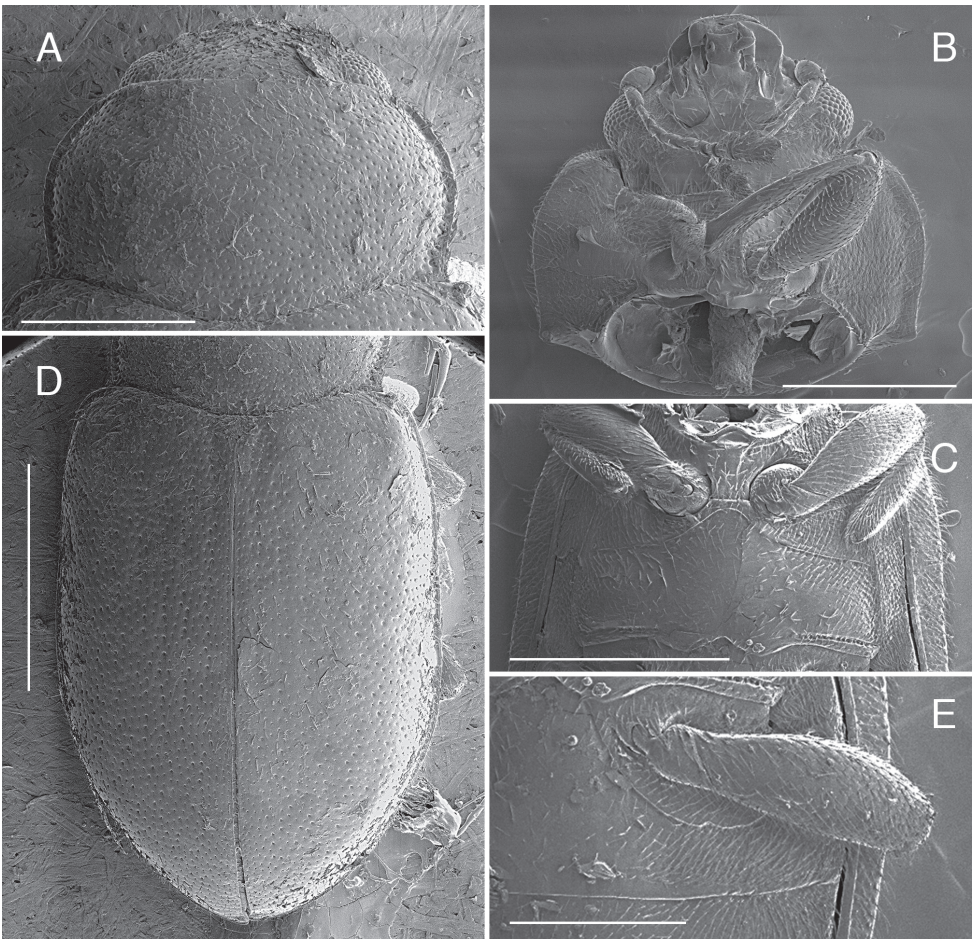

Figure 2. *Coccidula lepida* LeConte SEM illustrations **A** pronotum **B** head and prothorax, ventral **C** meso and metaventrite **D** elytra dorsal **E** ventrite 1. Scale bars: 500 μm (**A–C**); 1 mm (**E, D**).

setose in anterolateral parts, with a single row of large punctures below postcoxal lines and above metacoxae.

Abdominal postcoxal lines (Fig. 2E) complete, widely rounded, reaching about half of the length of the ventrite 1 measured below metacoxa. Ventrites covered with dense setiferous punctures.

Male genitalia. Tegmen in inner view with penis guide subtriangular with pointed apex; short, about two times shorter than parameres. Parameres elongate elliptical, inner surface smooth, with long setae on the inner side and in apical margin. Penis simple with pointed apex. [see Gordon 1985: 657, fig. 539 a–d]

Female genitalia. Sperm duct long, much longer than length of spermatheca. Spermatheca vermiform, broadest in basal part. [see Gordon 1985: 657, fig. 539e]

Type locality. Vermont (USA).

Distribution. North part of North America.

Coccidula litophiloides **Reitter, 1890**
Figs 1E, 3A–E, 4A–D

Coccidula litophiloides Reitter, 1890: 176
Lithophilus naviauxi Duverger, 1983: 83. syn. nov.

Material examined. ***Holotype*.** Azerbaijan, "Caucasus Araxesthal Leder Reitter/ Coll. Reitter/ Coccidula litophiloides 1890/ Holotypus 1890 Coccidula litophiloides Reitter", male (HNHM) (Fig. 11C). ***Holotype*** of *L. naviauxi*, Iran, Vannae, 30-V-77, leg. M. Rapilly, female (MNHN). ***Paratypes*** of *C. litophiloides*. Data same as for the holotype, (7: HNHM). ***Paratypes*** of *L. naviauxi*: Iran, Daran, 9-VI-77, M. Rapilly leg. (2 females: MNHN) (Figs 11A, B). **Other material.** Armenia, Eczmiadzin Cauc, 22 IV 1946, 6399, W. Eichler (2: MIZ); Jerevan město, Razdan, 26–27.5.1988, J. Strejček lgt., (1 male, 1 female: NMP); Iran, Lorestan, 1.1960 leg. A. Warchałowski (1: AJC); Iran, Khorramabad, 19-V-77, M. Rapilly leg. (1: MNHN).

Diagnosis. *Coccidula litophiloides* is very distinctive among *Coccidula* species with large produced posterior pronotal angles, and a prosternal process without carinae (which are present in all remaining species). With its general body shape slightly widening posteriorly and pronotum distinctly widened laterally with broad lateral bead appearing glabrous, it is similar to *C. scutellata*. Male genitalia are distinctive with large, elliptical parameres possessing projections on their inner surfaces, which is also unique among *Coccidula*. Spermatheca, in female genitalia, is distinctly widening apically and has a very short sperm duct, about ¼ of the length of spermatheca.

Description. Length 3.0–3.5 mm, BL/BW = 1.95–1.97, EL/BW = 1.32–1.40, PW/BW = 0.81.

Body elongate, slightly widening in posterior part. Dorsal and ventral side yellow to testaceous (Fig. 1E).

Head and pronotum covered with uniform small setiferous punctures arranged irregularly. Pronotum transverse, broadly rounded laterally (Figs 1E, 3B), with broad, glabrous lateral margin, covered with dense setriferous punctures, with a single row of larger punctures along lateral border. Posterior pronotal corner large, distinctly pointed (Fig. 3B). Prosternum with complete anterior bordering line. Prosternal process without lateral carinae (Fig. 3C).

Scutellar shield pentagonal, covered with dense setiferous punctures. Elytra covered with two types of punctures, small setiferous punctures irregularly distributed throughout elytral surface, some of these punctures surrounded by larger depressed circles, forming irregular longitudinal rows; rows 2 and 3 reduced or missing (Fig. 3A). Elytra more flattened in lateral view than in other *Coccidula*, without shoulder tubercle, lateral elytral margin visible throughout (Fig. 3A). Hind wings missing. Mesoventrite with anterior border complete. Metaventrite with postcoxal lines transverse, descending only laterally, fused on metaventral process in median part, forming continuous arc

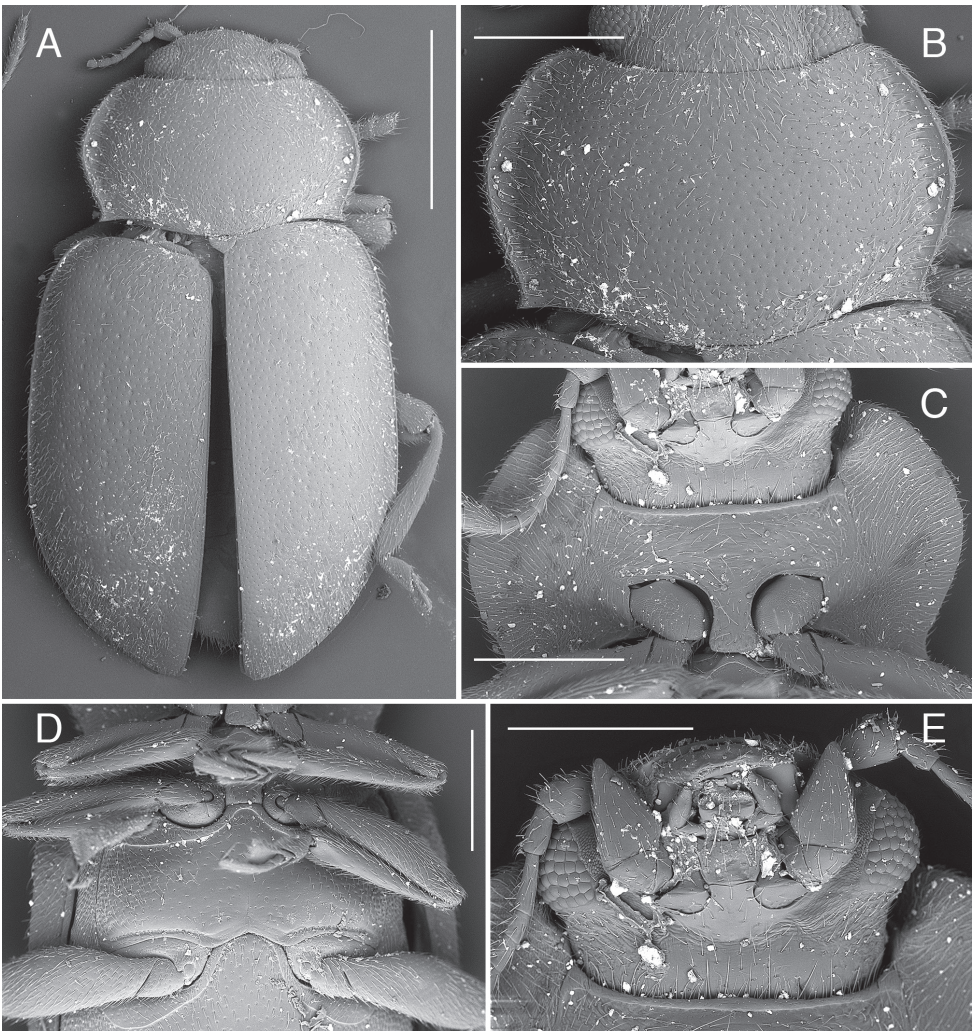

Figure 3. *Coccidula litophiloides* Reitter SEM illustrations, paratype HNHM **A** body, dorsal **B** pronotum **C** head and prothorax, ventral **D** meso and metaventrite **E** head ventral. Scale bars: 1 mm (**A**); 500 μm (**B–D**); 400 μm (**E**).

(Fig. 3D); covered with setiferous punctures very sparsely distributed in central part of sclerite, densely setose in lateral parts, without distinct rows of large punctures below postcoxal lines, large punctures above metacoxae present.

Abdominal postcoxal lines complete, rounded, reaching slightly less than half of length of the ventrite 1 measured below metacoxa. Ventrites covered with dense setiferous punctures.

Male genitalia. Tegmen in inner view with penis guide pentagonal with pointed apex (Fig. 4B); short, slightly longer than half length of parameres (Fig. 4A). Parameres

Figure 4. *Coccidula litophiloides* Reitter **A** tegmen, lateral **B** tegmen, inner **C** penis, lateral **D** spermatheca. Scale bar: 500 μm (**A–D**).

large, elliptical, inner surface with distinct projections (Fig. 4B), with fringe of long setae in apical margin. Penis simple with pointed apex (Fig. 4C).

Female genitalia. Sperm duct short (Fig. 4D), about as long as 1/4 of spermatheca. Spermatheca vermiform, distinctly broadened apically. Accessory gland membranous, longer than sperm duct.

Type locality. Caucasus, Ordubad (Azerbaijan).

Distribution. Armenia, Azerbaijan, Iran

Remarks. Duverger (1983) described *Lithophilus naviauxi* from Iran. After examination of the type specimens (Fig. 1A, B) we noticed that this species does not belong to the genus *Lithophilus* Frölich (=*Tetrabrachys* Kapur). As drawn in the original publication (Duverger 1983), it has antennae with 11 antennomeres (10 in *Tetrabrachys*), and pseudotrimerous tarsi with tarsomere 3 very small and tarsomere 2 distinctly lobed, while in *Tetrabrachys* tarsi are distinctly tetramerous, with tarsomere 3 and 2 elongate, without distinct lobe. Duverger in his paper (1983) described *L. naviauxi* based on just three female specimens of which he illustrated the spermatheca (Duverger 1983: 89, figs 30, 31). However, *C. litophiloides* is also found in Iran. Comparison of the female genitalia of the type material of both taxa, and other available material, together with the lack of a second and third row of large punctures on the elytra, and other morphological features described in the original description of Duverger, led to the conclusion that *L. naviauxi* Duverger falls well within the definition of *C. litophiloides*; thus, we propose to synonymize both species.

***Coccidula reitteri* Dodge, 1938**
Figs 1F, 5A–E, 6A–C

Coccidula suturalis Reitter 1897: 127 nom. nud. (nec. *C. suturalis* Weise, 1895: 132).
Coccidula reitteri Dodge, 1938: 222.

Material examined. ***Holotype.*** Russia, "Quell. d. Jrbut Reitter./ Transbaikal leg. Leder/ Coll. Reitter/ / Coccidula scutellaris m 1896/ Coccidula reitteri Dodge Khnzorian det./ prep. genital R. Bielawski 1956/ Holotypus 1897 Coccidula suturalis Reitter/ Photo ID: HNHM_COL_574", female (HNHM). **Other material.** Russia, "Transbaikalien Leder Reitter/ Coccidula suturalis Rtt. Coll. Reitter/ Coccidula reitteri Dodge, det. Merkl 1984/ prep. genital R. Bielawski 1956" (1 male: HNHM); Listvjanka pr. Bajkal, step, 29.6.1977, H. Karnecka lgt. (1 male, 1 female: NMP).

Diagnosis. *Coccidula reitteri* is very similar to *C. rufa* in external appearance, however, it can be distinguished by the presence of a small black transverse macula on the pronotum just anterior to the scutellar shield, and a longitudinal brown to black macula on the posterior half of the elytra on the elytral suture. Male genitalia are very close to *C. rufa*, however, the upper margin of the penis guide in lateral view is relatively less emarginated and parameres are narrower than in *C. rufa*.

Description. Length = 2.8–3.2 mm, BL/BW = 1.85–1.90, EL/BW = 1.33, PW/BW = 0.77.

Body elongate, parallel sided (Fig. 5A). Pronotum (Fig. 1F) with black transverse macula in front of the scutellar shield. Scutellar shield black. Elytra brown with elongate, dark brown to black macula along the elytral suture in posterior half. Ventral side testaceous with prosternum, mesoventrite, metaventrite, most of the ventrite 1 (except lateral corners), and central part of ventrite 2 black.

Head and pronotum covered with uniform small setiferous punctures arranged irregularly. Pronotum (Fig. 5B) transverse, broadly rounded laterally, with moderately broad, lateral margin without glabrous area; pronotum covered with dense setriferous punctures, with single row of larger punctures along lateral border. Posterior pronotal corners not produced (Fig. 5B). Prosternum with anterior margin with bordering line incomplete in median part, without small sub-rounded impression in center. Prosternal process with lateral carinae straight, joined together roundly at level of anterior border of procoxae, forming sub-triangular pattern (Fig. 5C).

Scutellar shield pentagonal, covered with dense setiferous punctures. Elytra covered with two types of punctures, small setiferous punctures irregularly distributed throughout the elytral surface, some of these punctures surrounded by larger depressed circles forming nine irregular longitudinal rows along whole length of elytra. Lateral elytral margin well visible throughout (Fig. 5A). Mesoventrite with complete anterior border. Metaventrite with postcoxal lines descending laterally, fused on metaventral process in median part, forming continuous arc (Fig. 5D); covered with setiferous punctures very sparsely distributed in central part of sclerite, densely setose in lateral parts, without distinct rows of large punctures below postcoxal lines, large punctures above metacoxae present.

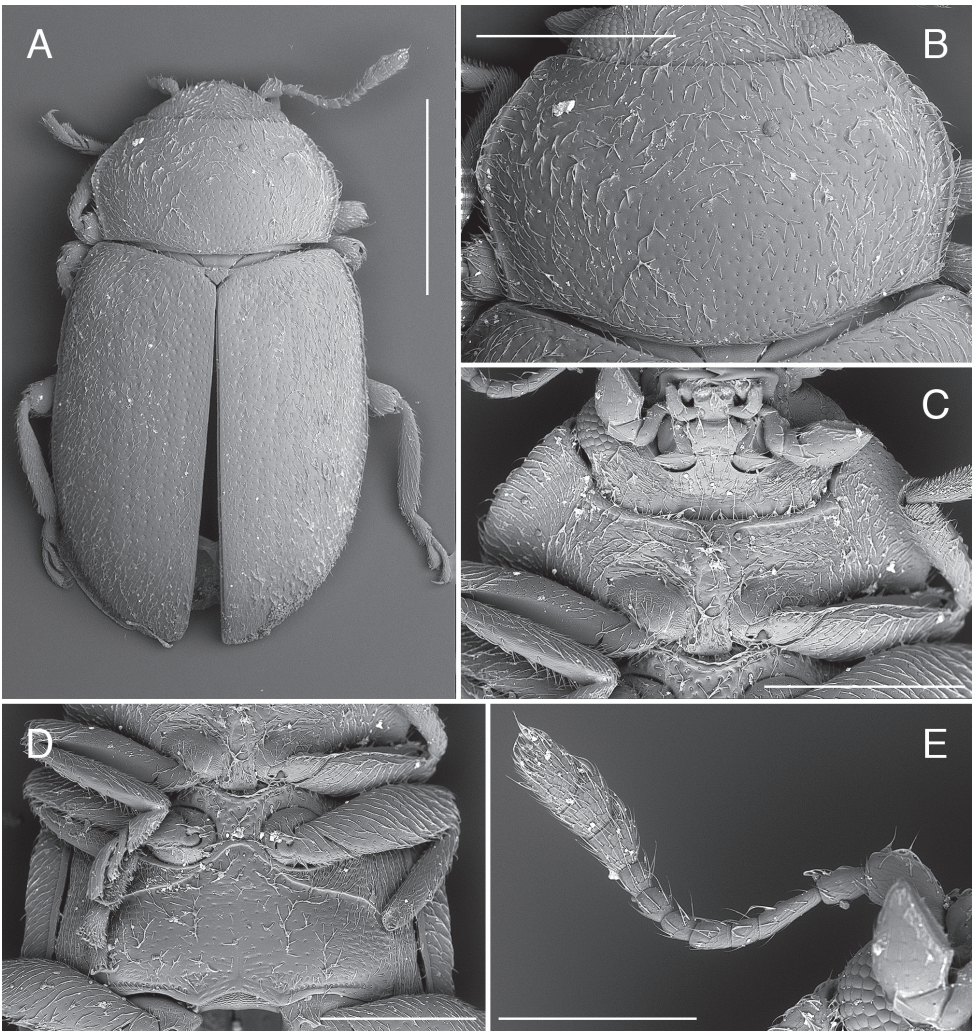

Figure 5. *Coccidula reitteri* Dodge SEM illustrations, HNHM **A** body, dorsal **B** pronotum **C** head and prothorax, ventral **D** meso and metaventrite **E** antenna. Scale bars: 1 mm (**A**); 500 μm (**B–D**); 300 μm (**E**).

Abdominal postcoxal lines complete, arcuate, reaching half of length of ventrite 1 measured below metacoxa. Ventrites covered with sparse setiferous punctures.

Male genitalia. Tegmen in inner view (Fig. 6B) with penis guide broadly rounded in the median or apical part, with rounded apex; in lateral view (Fig. 6C) moderately expanded medially, with upper surface moderately emarginate; long, much longer than parameres. Parameres elongate, parallel sided, with narrow base, inner surface smooth, with fringe of long setae in apical part. Penis simple with pointed apex, with small bump before apex.

Female genitalia. Spermatheca vermiform, not distinctly broadened apically (Fig. 6A).

Type locality. Mongolia, Russia (Krasnoyarsk region, Irkutsk region, Tuva)

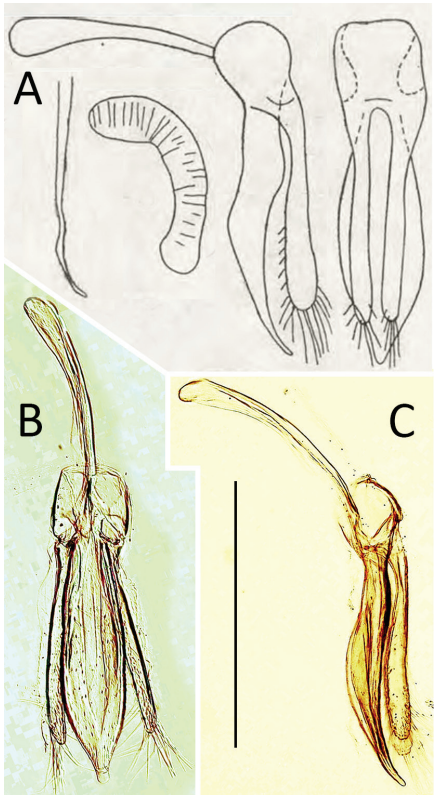

Figure 6. *Coccidula reitteri* Dodge **A** original drawings of male and female genitalia by Bielawski 1984 **B** tegmen, inner **C** tegmen, lateral. Scale bar: 500 μm (**B, C**).

Distribution. Russia (East Siberia).

Remarks. *Coccidula reitteri* is very similar to *C. rufa* in external morphological characters as well as the structure of male and female genitalia (Fig. 6A) (Bielawski 1984); thus, further investigation, preferably of molecular markers, should be conducted to confirm whether it is a separate species or an eastern population of *C. rufa*.

***Coccidula rufa* (Herbst, 1783)**
Figs 1A, B, G, 7A–F, 8A–E

Dermestes rufus Herbst, 1783: 22.
Chrysomela pectoralis Fabricius, 1792: 328.
Silpha rosea Marscham, 1802: 123.
Coccidula conferta Reitter, 1890: 176.
Coccidula rufa var. unicolor Reitter, 1890: 176.
Coccidula rufa var. nigropunctata Reitter, 1900: 220.

Coccidula rufa var. plagiata Gerhardt, 1910: 556.

Material examined. Czech Rep., Zlín, 11.6.1999, lgt. L. Bureš (1: NMP); Mladá Boleslav, 25.4.1987, lgt. Nedvěd (1 male USB); Dvořiště, 9.8.1989, lgt. Nedvěd (1: USB); Kokořínský důl, 9.8.1995, lgt. J. Řehounek (1: USB); Kyrgyzstan, Toktogul, 26 VI 2003, leg. A. Lasoń, WJ 2870, (1 male: AJC); Montenegro, Skadar jez.- Virpazar, 5.6.1984, J. Strejček lgt. (1: NMP); Poland, Kampinos Forest near Warsaw, 17.06.2020, leg. D. Marczak, (7: MIZ); Russia, Leningrad-Lachta, IX 1988, J. Strejček lgt., (1: NMP); Ukraine, Kharkiv region, Dergachevsky district, Boliboki vill., 50°9'16.57"N, 36°3'58.87"E, 1.5.2017, lgt. A. Slutsky (1: ASC); Uzbekistan, Buchara/ Coccidula unicolor Rtt./ Coll. Reitter/ MIZ PAN Warszawa 27/1955/1 (1: MIZ). Type material not studied, deposited in Museum für Naturkunde, Berlin, Germany.

Diagnosis. *Coccidula rufa* is most similar in external appearance to *C. reitteri*, however it can be separated by the uniform testaceous coloration of the dorsal surface (*C. reitteri* possesses dark macula near the elytral suture). From uniformly colored specimens of *C. scutellata* it can be separated by the shape of carinae on the prosternal process. Male genitalia are also very distinctive: in *C. scutellata* penis guide is small, about half length of parameres, while in *C. rufa* it is longer than parameres. Spermatheca in female genitalia of *C. rufa* is vermiform, not widening apically, while in *C. scutellata* it is distinctly widened in apical part.

Description. Length = 2.5–3.2 mm, BL/BW = 1.88–2.00, EL/BW = 1.38–1.44, PW/BW = 0.80–0.82.

Body elongate, parallel sided. Elytra of typical (European) form testaceous without maculae (Fig. 1G), only scutellar shield dark brown to black. Ventral side testaceous with prosternal process, mesoventrite, metaventrite, most of the ventrite 1 (except lateral corners), and central part of ventrite 2 black.

Head and pronotum covered with uniform small setiferous punctures arranged irregularly. Pronotum transverse, broadly rounded laterally, with moderately broad, lateral margin without glabrous area (Fig. 7B); pronotum covered with dense setiferous punctures, with a single row of larger punctures along lateral border. Posterior pronotal corners not produced (Fig. 7B). Prosternum with anterior margin with incomplete bordering line in median part, with a small sub-rounded impression in center. Prosternal process with lateral carinae straight, joined together roundly at level of anterior border of procoxae, forming sub-triangular pattern (Fig. 7C).

Scutellar shield pentagonal, covered with dense setiferous punctures. Elytra covered with two types of punctures, small setiferous punctures irregularly distributed throughout elytral surface, some of these punctures surrounded by larger depressed circles forming nine irregular longitudinal rows along whole length of elytra. Lateral elytral margin well visible throughout (Fig. 7A). Mesoventrite with complete anterior border. Metaventrite with postcoxal lines descending laterally, fused on metaventral process in median part, forming continuous arc (Fig. 7E), covered with setiferous punctures very sparsely

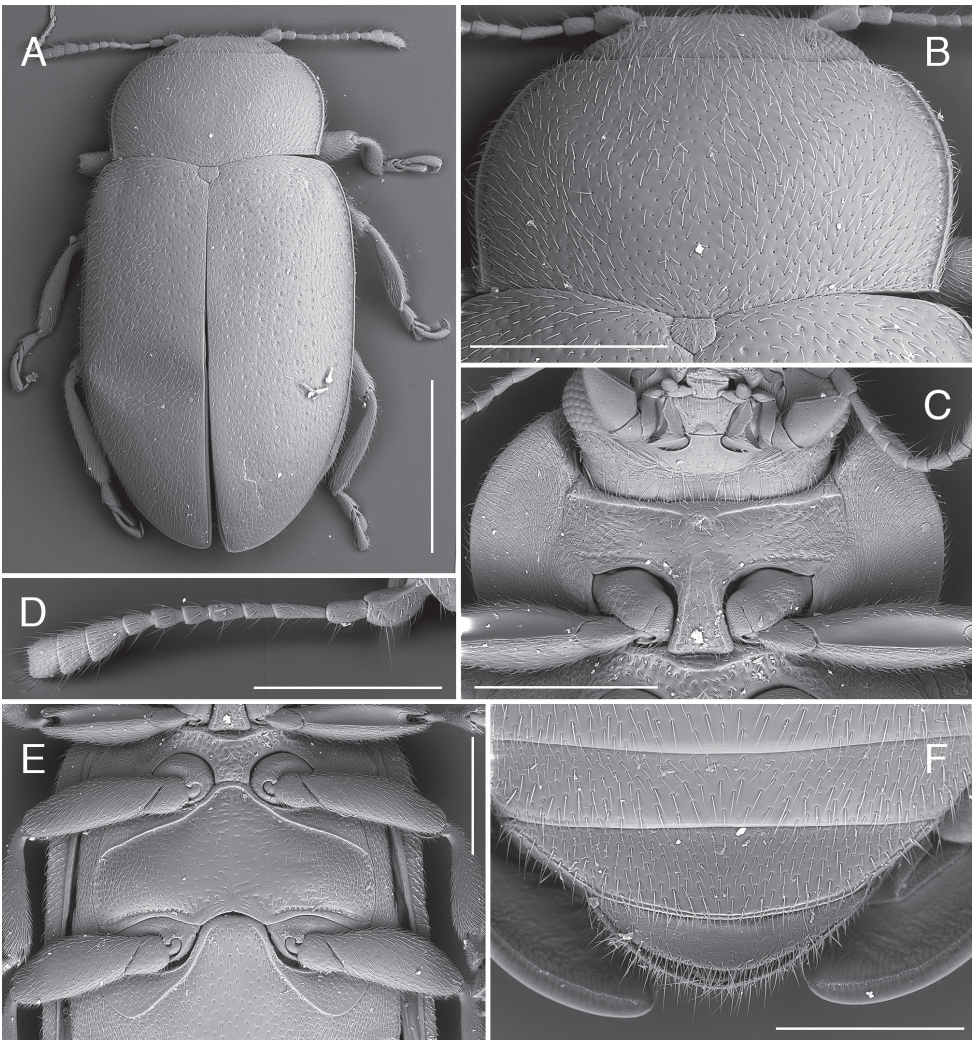

Figure 7. *Coccidula rufa* (Reitter) SEM illustrations **A** body, dorsal **B** pronotum **C** head and prothorax, ventral **D** antenna **E** mesoventrite, metaventrite and ventrite 1 **F** ventrites 4–6, female. Scale bars: 1 mm (**A**); 500 μm (**B, C, E, F**); 400 μm (**D**).

distributed in central part of sclerite, densely setose in lateral parts, without distinct rows of large punctures below postcoxal lines, large punctures above metacoxae present.

Abdominal postcoxal lines complete, arcuate, reaching half of length of ventrite 1 measured below metacoxa. Ventrites covered with sparse setiferous punctures.

***Male genitalia*.** Tegmen in inner view (Fig. 8A) with penis guide sub-parallel to broadly rounded, with rounded apex; in lateral view (Fig. 8B) expanded medially, with deeply emarginated upper margin; long, much longer than parameres. Parameres elongate, parallel sided, with just slightly narrower base, inner surface smooth, with fringe

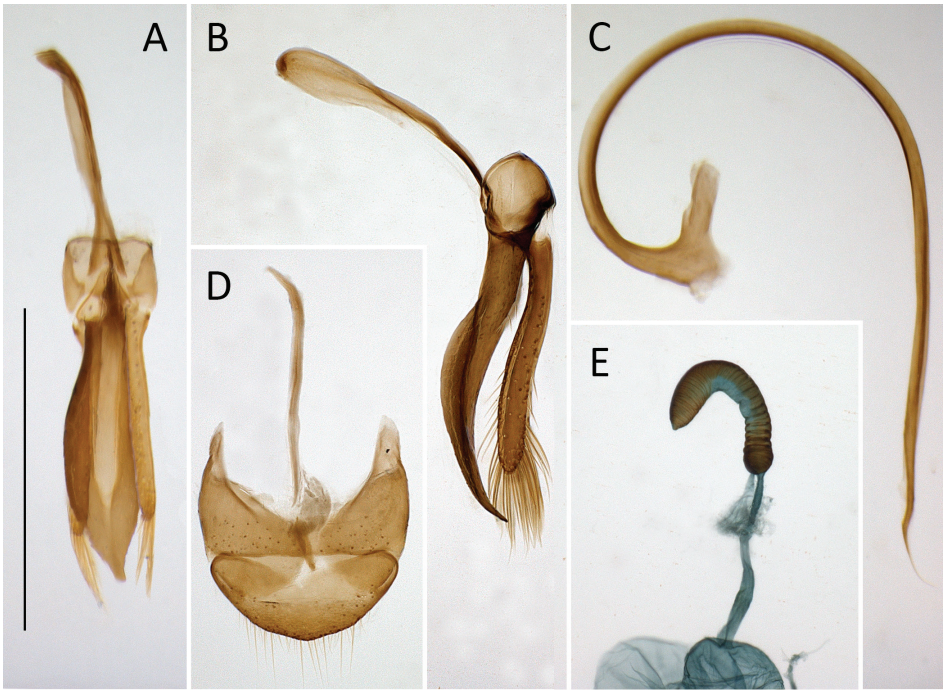

Figure 8. *Coccidula rufa* (Reitter) **A** tegmen, inner **B** tegmen, lateral **C** penis, lateral **D** male genital segment, dorsal **E** spermatheca. Scale bar: 500 μm (**A–E**).

of long setae in apical part. Penis simple with sharply pointed and curved apex, with small bump before apex (Fig. 8C).

Female genitalia. Sperm duct long, longer than spermatheca (Fig. 8E). Spermatheca vermiform, not distinctly broadened apically. Accessory gland membranous, much shorter than sperm duct.

Type locality. Berlin (Germany)

Distribution. Europe (all countries), Africa: Morocco, Asia: Afghanistan, China, Russia (Siberia), Iran, Kazakhstan, Kyrgyzstan, Mongolia, Turkey, Uzbekistan.

Coccidula scutellata (Herbst, 1783)

Figs 1H, 9A–G, 10A–I

Chrysomela scutellata Herbst, 1783: 58.
Nitidula quinquepunctata Fabricius, 1787: 52.
Silpha melanophthalma Gmelin, 1790: 1627.
Nitidula bipunctata Gmelin, 1790: 1630
Coccidula scutellata: Kugelann 1798: 421.
Coccidula scutellata var. subrufa Weise, 1879: 131.
Coccidula scutellata var. arquata Weise, 1879: 131.

Coccidula scutellata var. aethiops Krauss, 1902: 92.

Material examined. Armenia, Erevan, 9.06.1987, leg. V. Karasjov (5: AJC); Czech Rep., Praha-Kyje, 21.1.1945, lgt. Günnther, (1: NMP); Plzeň, 20.7.1978, lgt. V. Mach, (2: USB); Kokořínský důl, 28.8.1994, lgt. J. Řehounek (1: USB); Loučeň, 17.8.1994, lgt. J. Řehounek (1: USB); France, St. Cucufa, VI 65, MD, Ch. 'Duverger det., J.P. Coutanceau det. 2004' (1: MNHN); Poland, Kampinos Forest near Warsaw, 17.06.2020, leg. D. Marczak (11: MIZ); Slovakia, Bratislava, 27.4.36, lgt. O. Kavan (1: NMP); Ukraine, Kharkiv region, Kharkiv district, Bobrovka vill., reserve "Aleshkina balka", 2017-04-28, lgt. A. Slutsky (1: ASC). Type material not studied, deposited in Museum für Naturkunde, Berlin, Germany.

Diagnosis. *Coccidula scutellata* is the most variable species in body coloration. Typical forms with five black maculae on the elytra can be easily distinguished from other *Coccidula* species, however uniformly colored testaceous forms are externally similar to *C. rufa*. They can be easily distinguished by the shape of carinae on prosternal process, which are straight and form a sub-triangular pattern in *C. rufa*, and are sinuate and broadly rounded apically, and fused with anterior border of prosternum in *C. scutellata*. Moreover, *C. scutellata* has a more distinct shoulder tubercle, and relatively narrower protnotum. Also, the male genitalia are distinctive, with penis guide longer than parameres in *C. rufa* and much shorter in *C. scutellata*. Spermatheca, in female genitalia, is broadened apically in *C. scutellata*, while in *C. rufa* it is almost uniform in diameter.

Description. Length = 2.8–4.2 mm, BL/BW = 1.85–2.05, EL/BW = 1.36–1.46, PW/BW = 0.70–0.75.

Body elongate, slightly widening in posterior part. Elytra of typical (European) form testaceous with five black maculae (Fig. 1H), one large covering scutellar shield and surrounding portion of elytra, and four sub-oval maculae in the median part, two of which are placed close to elytral suture and remaining two, close to lateral margin. Sometimes macula surrounding scutellar shield extends along elytral suture, sometimes maculae placed in median part of elytra are fused, forming single band. Various forms with reductions of this pattern are also present to completely testaceous forms without any trace of black color. Ventral side testaceous with prosternal process, mesoventrite, metaventrite, most of ventrite 1 (except lateral corners), and central part of ventrite 2 black.

Head and pronotum covered with uniform small setiferous punctures arranged irregularly. Pronotum transverse, broadly rounded laterally, with broad, glabrous lateral margin (Fig. 9B); pronotum covered with dense setiferous punctures, with single row of larger punctures along lateral border. Posterior pronotal corners not produced. Prosternum with anterior margin with bordering line complete. Prosternal process with complete lateral carinae in form of sinuate line, joined roundly and merged with anterior border of pronotum (Fig. 9E).

Scutellar shield pentagonal, covered with dense setiferous punctures. Elytra covered with two types of punctures, small setiferous punctures irregularly distributed throughout elytral surface, some of these punctures surrounded by larger depressed circles forming nine irregular longitudinal rows along whole length of elytra. Shoulder

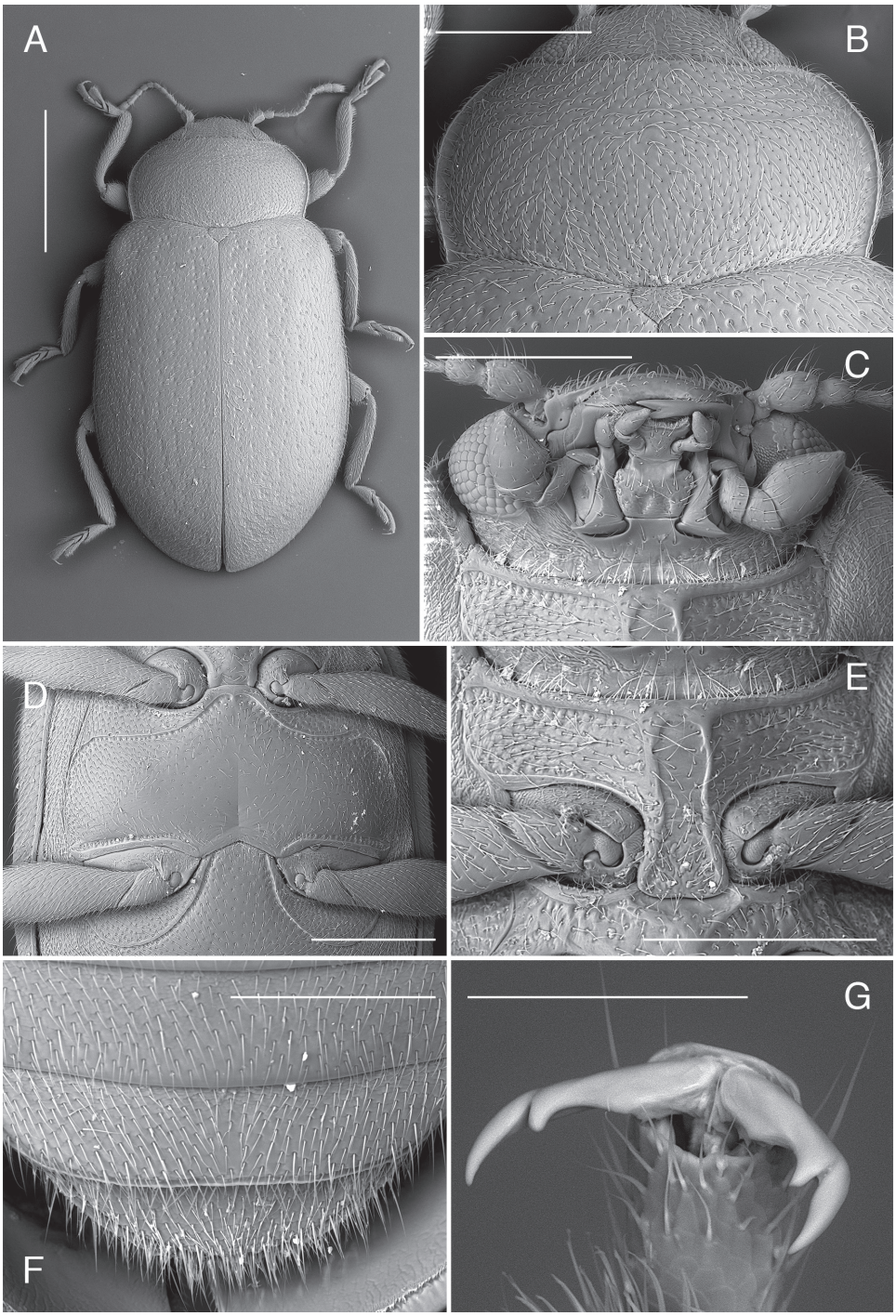

Figure 9. *Coccidula scutellata* (Reitter) SEM illustrations **A** body, dorsal **B** pronotum **C** head, ventral **D** mesoventrite, metaventrite and ventrite 1 **E** prosternum **F** ventrites 4–6, male **G** pro-tarsal claw. Scale bars: 1 mm (**A**); 500 μm (**B, D, E**); 400 μm (**C, F**); 100 μm (**G**).

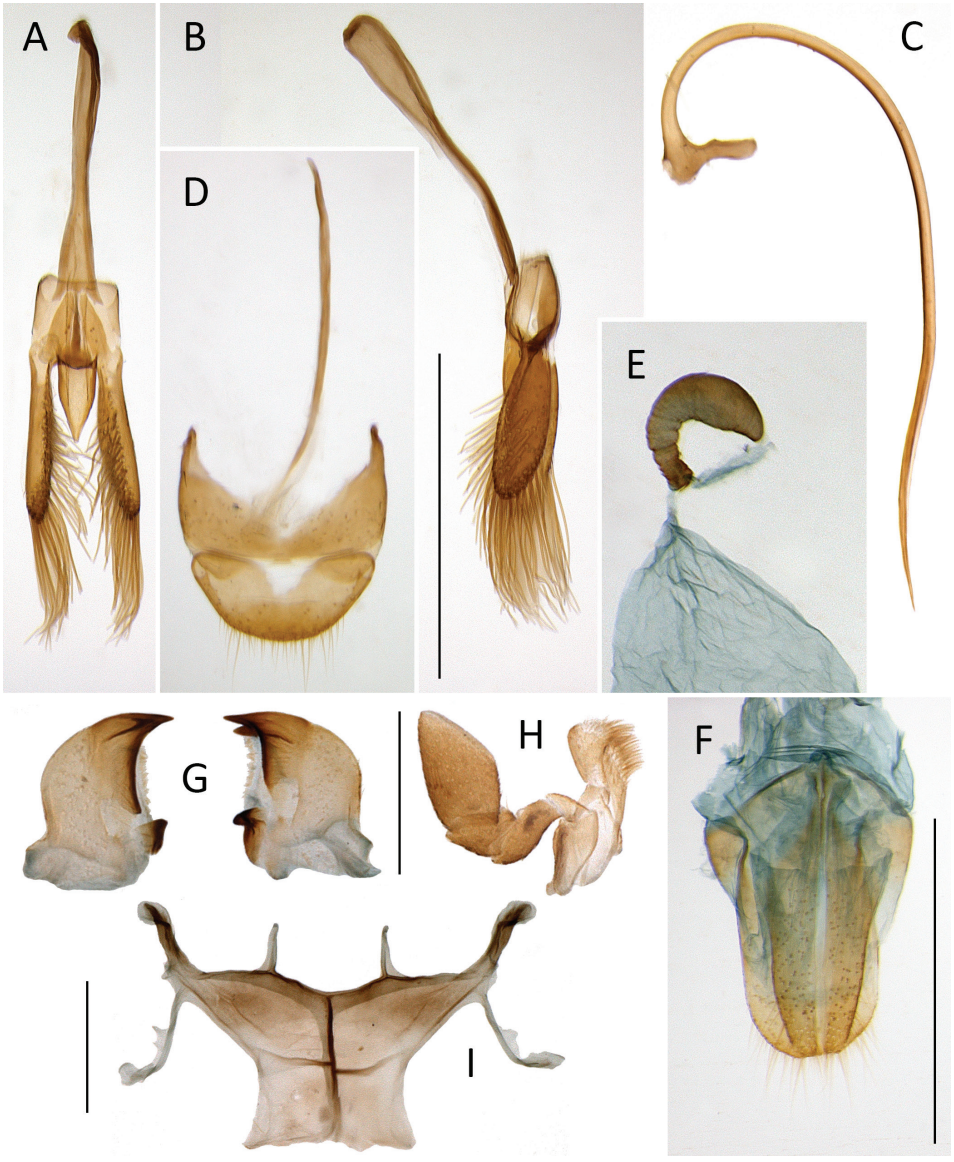

Figure 10. *Coccidula scutellata* (Reitter) **A** tegmen, inner **B** tegmen, lateral **C** penis, lateral **D** male genital segment, dorsal **E** spermatheca **F** female genitalia **G** left and right mandibles **H** maxilla **I** metendosternite. Scale bars: 500 µm (**A–F**); 200 µm (**G–I**).

tubercles distinct, lateral elytral margin of elytra not visible from above in anterior part (Fig. 9A). Mesoventrite with anterior border interrupted in median part. Metaventrite with postcoxal lines transverse in median part and then descending laterally, not fused on metaventral process in median part (Fig. 9D). Covered with setiferous punctures very sparsely distributed in central part of sclerite, densely setose in lateral parts, with single row of large punctures below postcoxal lines and above metacoxae.

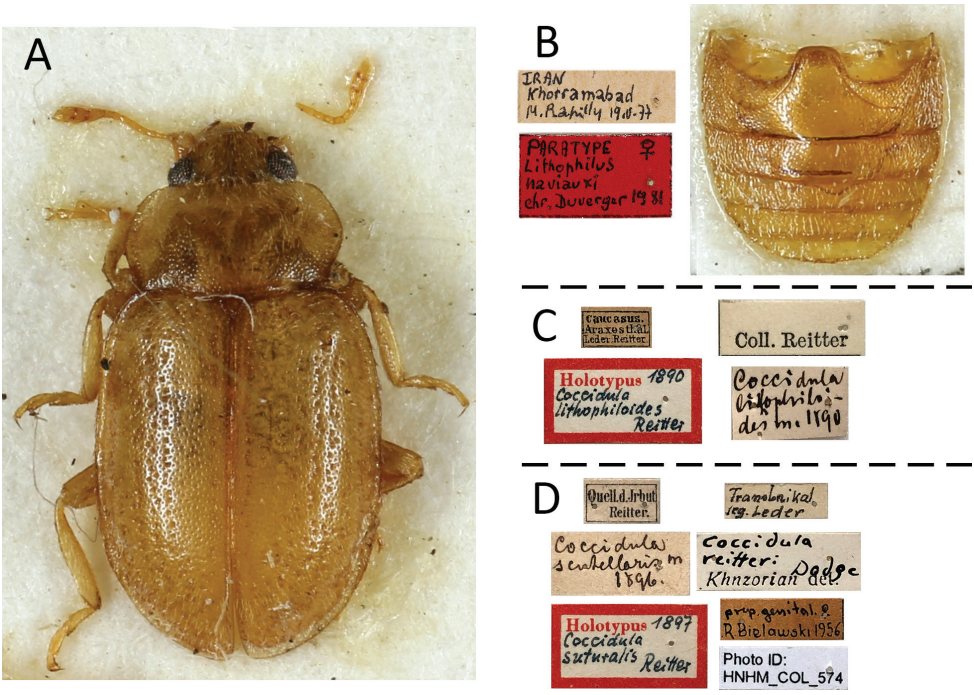

Figure 11. *Lithophilus naviauxi* Duverger **A** paratype MNHN, dorsal **B** paratype labels and abdomen **C** *Coccidula litophiloides* Reitter, holotype labels **D** *Coccidula suturalis* Reitter, holotype labels.

Abdominal postcoxal lines complete, rounded, reaching slightly more than half of length of ventrite 1 measured below metacoxa. Ventrites covered with dense setiferous punctures.

Male genitalia. Tegmen in inner view (Fig. 10A) with penis guide subtriangular with pointed apex; short, about two times shorter than parameres. Parameres elongate elliptical (Fig. 10B), inner surface smooth, with long setae on inner surface and in apical margin. Penis simple with pointed apex (Fig. 10C).

Female genitalia. Sperm duct short, about as long as half of length of spermatheca (Fig. 10E). Spermatheca vermiform, distinctly broadened apically. Accessory gland membranous, longer than sperm duct.

Type locality. Pomerania (Germany, Poland)

Distribution. Europe (all countries), Africa: Morocco, Asia: Kazakhstan, Russia (West Siberia).

Acknowledgements

We thank Otto Merkl and Tamás Németh (HNHM), Andrzej Jadwiszczak (Olsztyn, Poland), Lukáš Sekerka (NMP) and Alexander Slutsky (Kharkov, Ukraine) for a loan of specimens used in this study. Dawid Marczak (Warsaw, Poland) is thanked for providing fresh specimens of European *Coccidula* for analyses. Magdalena Kowalewska-

Groszkowska (MIZ) is acknowledged for her help with the SEM illustrations, and Biology Centre CAS – The Laboratory of Electron Microscopy for making part of SEM images. Danny Haelewaters (USA), David Larson (USA), Vincent Nicolas (France), Gilles San Martin (Belgium) and Udo Schmidt (Germany) are acknowledged for providing habitus photos. The study was partially supported by grant number 20-10003S provided by the Grant agency of Czech Republic to O. Nedvěd. The reviewer and the Editor are acknowledged for their valuable comments on the earlier version of this manuscript.

References

Bielawski R (1959) Chrząszcze – Coleoptera. Biedronki – Coccinellidae. Klucze do Oznaczania Owadów Polski, XIX 76: 1–92.

Bielawski R (1984) Coccinellidae (Coleoptera) of Mongolia. Annales Zoologici 38(14): 281–460.

Che L, Zhang P, Deng S, Escalona HE, Wang X, Li Y, Pang H, Vandenberg N, Ślipiński A, Tomaszewska W, Liang D (2021) New insights into the phylogeny and evolution of lady beetles (Coleoptera: Coccinellidae) by extensive sampling of genes and species. Molecular Phylogenetics and Evolution Molecular Phylogenetics and Evolution 156: 107045. https://doi.org/10.1016/j.ympev.2020.107045

Clayhills T, Markkula M (1974) The abundance of coccinellids on cultivated plants. Annales Entomologicae Fennicae 40: 49–55.

Crotch GR (1874) A revision of the coleopterous family Coccinellidae. E. W. Janson, London, 311 pp. https://doi.org/10.5962/bhl.title.8975

Czerwiński T, Szawaryn K, Tomaszewska W (2020) Three new species of the genus *Rhyzobius* Stephens, 1829 from New Guinea (Coleoptera: Coccinellidae: Coccidulini). European Journal of Taxonomy 692: 1–17. https://doi.org/10.5852/ejt.2020.692

Dejean PFMA (1821) Catalogue de la collection de coléoptères de M. le Baron Dejean. Crevot, Paris, [viii +] 138 pp. https://doi.org/10.5962/bhl.title.11259

Dodge HR (1938) *Coccidula suturalis* synonymy (Coleop.: Coccinellidae). Entomological News and Proceedings of the Entomological Section of the Academy of Natural Sciences of Philadelphia 49: 221–222.

Duverger C (1983) Contribution à la connaissance des Coccinellidae d'Iran. Nouvelle Revue d'Entomologie, Nouvelle Série 13(1): 73–93.

Fabricius JC (1787) Mantissa insectorum sistens eorum species nuper detectas adiectis characteribus genericis, differentiis specificis, emendationibus, observationibus. Tom I. Hafhiae: Chist. Gottl. Profit, [xx +] 348 pp. https://doi.org/10.5962/bhl.title.36471

Fabricius JC (1792) Entomologia systematica emendata et aucta. Secundum classes, ordines, genera, species adjectis synonymis, locis, descriptionibus, observationibus. Tom I. Pars I. Hafhiae: Christ. Gottl. Proft, [xx +] 330 pp. https://doi.org/10.5962/bhl.title.122153

Fürsch H (2007) New species of *Epipleuria* Fürsch and *Rhyzobius* Stephens from southern Africa (Coleoptera: Coccinellidae: Coccidulini). Annals of the Transvaal Museum 44: 11–24.

Fürsch H (2001) Die Gattung *Epipleuria* gen. n. (Coleoptera, Coccinellidae, Coccidulinae). Mitteilungen der Münchner Entomologischen Gesellschaft 91: 5–33.

Gerhardt J (1910) Neujeiten der schlesischen Kaferfauna aus dem Jahre 1909. (Col.). Deutsche Entomologische Zeitschrift 1910: 554–557. https://doi.org/10.1002/mmnd.4801910507

Gmelin JF (1790) Caroli a Linné Systema Naturae per regna tria naturae, secundum classes, ordines, genera, species, cum characteribus, differentiis, synonymis, locis. Editio decima tertia, aucta, reformata. Tomus I Pars IV. Classis V. Insecta. Lipsiae: Georg Enanuel Beer, 1517–2224.

Gordon R (1994) South American Coccinellidae (Coleoptera). Part IV: Definition of Exoplectrinae Crotch, Azyinae Mulsant, and Coccidulinae Crotch; a taxonomic revision of Coccidulini. Revista Brasileira de Entomologia 38(3/4): 681–775.

Gordon RD (1985) The Coccinellidae (Coleoptera) of America north of Mexico. Journal of the New York Entomological Society 93(1): 1–912.

Herbst JFW (1783) Kritisches Verzeichniss meiner Insektensammlung. Archiv der Insectengeschichte. Herausgegeben von Johann Caspar Füessly 4: 1–72.

Horn GH (1895) Studies in Coccinellidae. Transactions of the American Entomological Society 22: 81–114.

Kirejtshuk AG, Nel A (2012) The oldest representatives of the family Coccinellidae (Coleoptera: Polyphaga) from the lowermost Eocene Oise amber (France). Zoosystematica Rossica 21: 131–144. https://doi.org/10.31610/zsr/2012.21.1.131

Kovář I (1996) Phylogeny. In: Hodek I, Honěk A (Eds) Ecology of Coccinellidae. Kluwer Academic Publishers, Dordrecht, 19–31. https://doi.org/10.1007/978-94-017-1349-8_2

Kovář I (2007) Coccinellidae. In: Löbl I, Smetana A (Eds) Catalogue of Palaearctic Coleoptera. Volume 4. Elateroidea, Derodontoidea, Bostrichoidea, Lymexyloidea, Cleroidea, Cucujoidea. Apollo Books, Stentrup, 71–74, 568–630.

Krauss H (1902b) Coleopterologische Beitrâge zur Fauna Austriaca. III. Wiener Entomologische Zeitung 21: 89–92.

Kugelann JG (1798) Verzeichniss der Käfer Preussens. Entworfen von Johann Gottlieb Kugelann Apotheker in Osterode. Ausgearbeitet von Johann Karl Wilhelm Illiger. Mit einer Vorrede von Hellwig und dem angehängten Versuch einer natürlichen Ordnung und Gattungsfolge der Insecten. Johann Jacob Gebauer, Halle, 500 pp. https://doi.org/10.5962/bhl.title.125071

Lawrence JF, Ślipiński A, Seago A, Thayer M, Newton A, Marvaldi A (2011) Phylogeny of the Coleoptera based on adult and larval morphology. Annales Zoologici 61: 1–217. https://doi.org/10.3161/000345411X576725

LeConte JL (1852) Remarks upon the Coccinellidae of the United States. Proceedings of the Academy of Natural Sciences of Philadelphia 6: 129–145.

Marsham T (1802) Entomologia Britannica, sistens insecta britanniae indigena, secundum methodum linnaeanam disposita. Tomus I. Coleoptera. Londini: Wilks et Taylor, J. White, [xxxi +] 548 pp. https://doi.org/10.5962/bhl.title.65388

Mulsant E (1846) Histoire Naturelle des coléoptĕres de France. Sulcicolles – Sécuripalpes. Maison, Paris, [xxiv +] 280 pp.

Panzer GW (1813) Index Entomologicus sistens omnes Insectorum, Pars I. Eleutherata, 2016 pp.

Poorani J, Ślipiński A (2009) A Revision of the Genera *Scymnodes* Blackburn and *Apolinus* Pope et Lawrence (Coleoptera: Coccinellidae). Annales Zoologici 59(4): 549–584. https://doi.org/10.3161/000345409X484946

Reitter E (1890) Neue Coleopteren aus Europa und den angrenzenden Ländern und Sibirien, mit Bemerkungen über bekannte Arten. Deutsche Entomologische Zeitschrift 3: 145–164. https://doi.org/10.1002/mmnd.48018900323

Reitter E (1897) Fünfzehnter Beitrag zur Coleopteren-Fauna des russischen Reiches. Wiener Entomologische Zeitung 16: 121–127. https://doi.org/10.5962/bhl.part.12846

Reitter E (1900) Neue, von Herrn John Sahlberg auf seinen Reisen in Corfu, Palästina und Zentral-Asien gesammelte Coleopteren. Wiener Entomologische Zeitung 19: 217–220. https://doi.org/10.5962/bhl.part.3455

Robertson JA, Ślipiński A, Moulton M, Shockley FW, Giorgi A, Lord NP, McKenna DD, Tomaszewska W, Forrester J, Miller KB, Whiting MF, McHugh J (2015) Phylogeny and classification of Cucujoidea and the recognition of a new superfamily Coccinelloidea (Coleoptera: Cucujiformia). Systematic Entomology 40(4): 745–778. https://doi.org/10.1111/syen.12138

Sasaji H (1968) Phylogeny of the family Coccinellidae (Coleoptera). Etizenia 35: 1–37.

Seago A, Giorgi JA, Li J, Ślipiński A (2011) Phylogeny, classification and evolution of ladybird beetles (Coleoptera: Coccinellidae) based on simultaneous analysis of molecular and morphological data. Molecular Phylogenetics and Evolution 60: 137–151. https://doi.org/10.1016/j.ympev.2011.03.015

Ślipiński A (2007) Australian ladybird beetles (Coleoptera: Coccinellidae): their biology and classification. Department of the Environment and Water Resources, Canberra, [xviii þ] 288 pp.

Stephens JF (1831) Illustrations of British entomology or, a synopsis of indigenous insects: containing their generic and specific distinctions; with an account of their metamorphoses, times of appearance, localities, food, and economy, as far as practicable. Mandibulata. Volume IV. Baldwin and Cradock, London, 413 pp.

Szawaryn K, Leschen RAB (2019) Redescription and notes on the New Zealand ladybird species *Hoangus venustus* (Pascoe, 1875) (Coleoptera: Coccinellidae). Journal of Asia-Pacific Entomology 22(1): 226–232. https://doi.org/10.1016/j.aspen.2018.12.010

Szawaryn K, Tomaszewska W (2020) New and known extinct species of *Rhyzobius* Stephens, 1829 shed light on the phylogeny and biogeography of the genus and the tribe Coccidulini (Coleoptera: Coccinellidae). Journal of Systematic Palaeontology 18(17): 1445–1461. https://doi.org/10.1080/14772019.2020.1769751

Tomaszewska W, Ślipiński A (2011) Revision of the genus *Rodatus* Mulsant, 1850 (Coleoptera: Coccinellidae: Coccidulini). Annales Zoologici 61: 657–684. https://doi.org/10.3161/000345411X622516

Tomaszewska W (2010) *Rhyzobius* (Coleoptera: Coccinellidae) a revision of the world species. Fauna Mundi, volume 2, MIZ PAS, Warszawa, 475 pp.

Weinert LA, Tinsley MC, Temperley M, Jiggins FM (2007) Are we understudying the diversity and incidence of insect bacterial symbionts? A case study in ladybird beetles. Biology Letters 3: 678–681. https://doi.org/10.1098/rsbl.2007.0373

Weise J (1879) Bestimmungs-Tabellen der europaischen Coleopteren II. Coccinellidae. Zeitschrift für Entomologie, Breslau, Neue Folge 7: 88–156.

Weise J (1895) Neue Coccinelliden, sowie Bemerkungen zu bekannten Arten. Annales de la Société Entomologique du Belgique 1895: 120–146.

ZooKeys 1043: 87–102 (2021)
doi: 10.3897/zookeys.1043.58548
https://zookeys.pensoft.net

RESEARCH ARTICLE

A peer-reviewed open-access journal
ZooKeys
Launched to accelerate biodiversity research

Telmatometropsis fredyi gen. nov., sp. nov.: a new water strider from the Colombian Pacific region (Insecta, Hemiptera, Gerridae)

Silvia P. Mondragón-F.[1], Irina Morales[1], Felipe F. F. Moreira[2]

1 *Laboratorio de Entomología, Universidad Pedagógica y Tecnológica de Colombia, Avenida Central del Norte 39-155, Tunja, BY, Colombia* **2** *Laboratório de Biodiversidade Entomológica, Instituto Oswaldo Cruz, Fundação Oswaldo Cruz, Av. Brasil, 4365, Pavilhão Mourisco, sala 214. Manguinhos, Rio de Janeiro, RJ, Brazil*

Corresponding author: Irina Morales (irina.morales@uptc.edu.co)

Academic editor: L. Livermore | Received 11 September 2020 | Accepted 22 March 2021 | Published 11 June 2021

http://zoobank.org/0286F2B8-0E1E-4DC6-B8B0-71652BF1A39D

Citation: Mondragón-F SP, Morales I, Moreira FFF (2021) *Telmatometropsis fredyi* gen. nov., sp. nov.: a new water strider from the Colombian Pacific region (Insecta, Hemiptera, Gerridae). ZooKeys 1043: 87–102. https://doi.org/10.3897/zookeys.1044.58548

Abstract

A new genus of Gerridae (Insecta, Hemiptera, Heteroptera) in the subfamily Trepobatinae, *Telmatometropsis* **gen. nov.**, with a single included species, *T. fredyi* **sp. nov.**, is described from the Colombian Pacific region. Representatives of the new genus were collected in mangrove lagoons of Buenaventura Bay, Valle del Cauca Department. The new genus can be diagnosed by the relative proportions of the antennomeres, the shape of the male fore tarsus, and by the black markings on the head, thorax and abdomen.

Keywords

Aquatic insects, Gerromorpha, Neotropical Region, taxonomy

Introduction

Gerridae comprises over 750 described species in more than sixty genera and eight subfamilies, of which almost 150 species have been recorded from the Neotropical Region (Polhemus and Polhemus 2008). Representatives of the family are semiaquatic bugs that spend almost their entire lives skating on the water surface of lentic and lotic

environments (Andersen 1982; Schuh and Slater 1995). Most gerrids live in freshwater, but a handful inhabit the open ocean (Andersen 1998) and others occupy estuarine brackish waters (Cheng 1976). According to Molano-Rendón and Morales (2017), the subfamilies Halobatinae, Rhagadotarsinae and Trepobatinae have species with marine habits. For example, some species of the genus *Rheumatobates* Bergroth, 1892 inhabit estuarine brackish waters on the Caribbean and Pacific coasts of Central and South America, and species of *Halobates* Eschscholtz, 1822 are almost exclusively marine, with five species living on the open ocean (Andersen and Cheng 2004; Cheng 2006).

The subfamily Trepobatinae is represented in the Neotropical Region by the genera *Halobatopsis* Bianchi, 1896; *Lathriobatoides* Polhemus, 2004; *Metrobates* Uhler, 1871; *Ovatametra* Kenaga, 1942; *Telmatometra* Bergroth, 1908; *Telmatometroides* Polhemus, 1991; *Trepobates* Uhler, 1894; and *Trepobatoides* Hungerford & Matsuda, 1958 (Polhemus and Polhemus 2002). *Telmatometroides* differs from the others by antennomere III shorter than two times the length of antennomere II; interocular space with a dark longitudinal stripe; extensive black markings on posterior part of mesosternum; row of five or six short, stout, black spinose setae on hind tarsomere I; and mid femur shorter than mid tibia and hind femur (Polhemus 1991; Moreira et al. 2018). Currently, *Telmatometroides* is a monospecific genus, including only *T. rozeboomi* (Drake & Harris, 1937), which is recorded from Costa Rica to Ecuador (Pacheco-Chaves et al. 2018).

We recently noticed that some of the specimens deposited in the collection of Universidad Pedagógica y Tecnológica de Colombia, Tunja, Colombia, and identified as *T. rozeboomi* did not agree with the features mentioned in the description of this species, especially regarding the relative proportions of the antennomeres and the disposition of black markings on the head and body. A more detailed examination also showed a modification on the male fore tarsus that is not reported for any Neotropical genus of Trepobatinae, thus revealing an undescribed genus and species from the Colombian Pacific region that are herein described.

Methods

Type specimens have been deposited in the following collections: Colección de Insectos, Museo de Historia Natural "Luis Gonzalo Andrade", Universidad Pedagógica y Tecnológica de Colombia, Tunja, Colombia (**UPTC**); and Coleção Entomológica do Instituto Oswaldo Cruz, Fundação Oswaldo Cruz, Rio de Janeiro, Brazil (**CEIOC**). For comparison with the new genus, we examined photographs of the holotype of *Telmatometroides rozeboomi*, which is deposited in the National Museum of Natural History, Smithsonian Institution, Washington, D.C., United States of America (**NMNH**). Micrographs of the new species were taken using a Zeiss EVO MA10 scanning electron microscope. A Leica S9I stereo microscope with integrated camera was used to obtain the photographs and measurements of 10 specimens of each sex (including the holotype). All measurements are given in millimeters. They are abbreviated as follows in Tables 2 and 3: body length (BL), body width (BW), head width through eyes

(HW), lengths of antennomeres I–IV (ANT I, ANT II, ANT III, ANT IV), pronotum length on midline (PL), abdomen length on midline (AL), femoral length (FEM), tibial length (TIB), and lengths of tarsomeres I–II (TAR I, TAR II). The software QGIS (3.4) was used to generate the geographic distribution map.

Results

***Telmatometropsis* gen. nov.**
http://zoobank.org/3C030D62-5C05-466A-AD9A-1FA9E5AA241A
Figs 1–8

Type species. *Telmatometropsis fredyi* Mondragón-F., Morales & Moreira sp. nov., by present designation and monotypy.

Diagnosis. The new genus is similar to *Telmatometroides* (Fig. 9), sharing with it the long ocular setae, the median and lateral longitudinal black stripes on the mesonotum, male abdominal tergum VIII with a central notch on the posterior margin (stronger on *T. rozeboomi*), mid tarsomere I with a few bristles at the base, the hind femur with five dorsal trichobothria, the male abdominal laterotergites with patches of light setae, and the occupation of estuarine brackish waters. *Telmatometropsis* gen. nov. differs from *Telmatometroides* and all other genera of Neotropical Trepobatinae by the modified fore tarsomere II of the male, which is strongly curved in lateral view, flattened laterally, and apically bifid, with a shorter and a longer portion. The relative proportions of the antennomeres are also unique to the new genus, with article III clearly longer than article I, more than twice as long as article II, but shorter than article IV. Further comparison with other genera of Neotropical Trepobatinae is given in Table 1 and in an updated key to Neotropical Trepobatinae genera provided below.

Description. ***Measurements.*** Male body length 2.90–3.21, width (across suture between meso- and metanotum) 1.07–1.21; female body length 3.30–3.91, width 1.44–1.52. ***Color.*** Ground color of body pale yellow with extensive black and silvery markings dorsally, legs largely pale yellow (Fig. 1A). ***Structural characteristics.*** Eyes elongate, with a pair of long ocular setae (Fig. 1B). Head with four pairs of trichobothria (Fig. 1C). Antenna shorter than body length; antennomere I thickest, curved laterally at base, longer than antennomere II; antennomere II shortest, thicker than antennomeres III and IV; antennomere III longer than antennomere I; antennomere IV longest (Fig. 1A, B). Labium long, extending to mesosternum. Pronotum short, trapezoid (Fig. 1C). Mesonotum about three times as long as pronotum, posterior margin slightly concave (Fig. 1A, B). Fore femur subequal in length to fore tibia, slightly curved at the base in dorsal view; fore tibia with apicolateral row of short, distinctive setae (Fig. 3A); fore tarsus covered with short yellow setae; fore tarsomere I about one third the length of fore tarsomere II; male fore tarsomere II strongly curved in lateral view, flattened laterally, apically bifid with a shorter and a longer portion; claws directed mesally (Fig. 3A–E). Mid femur about two-thirds the length of mid

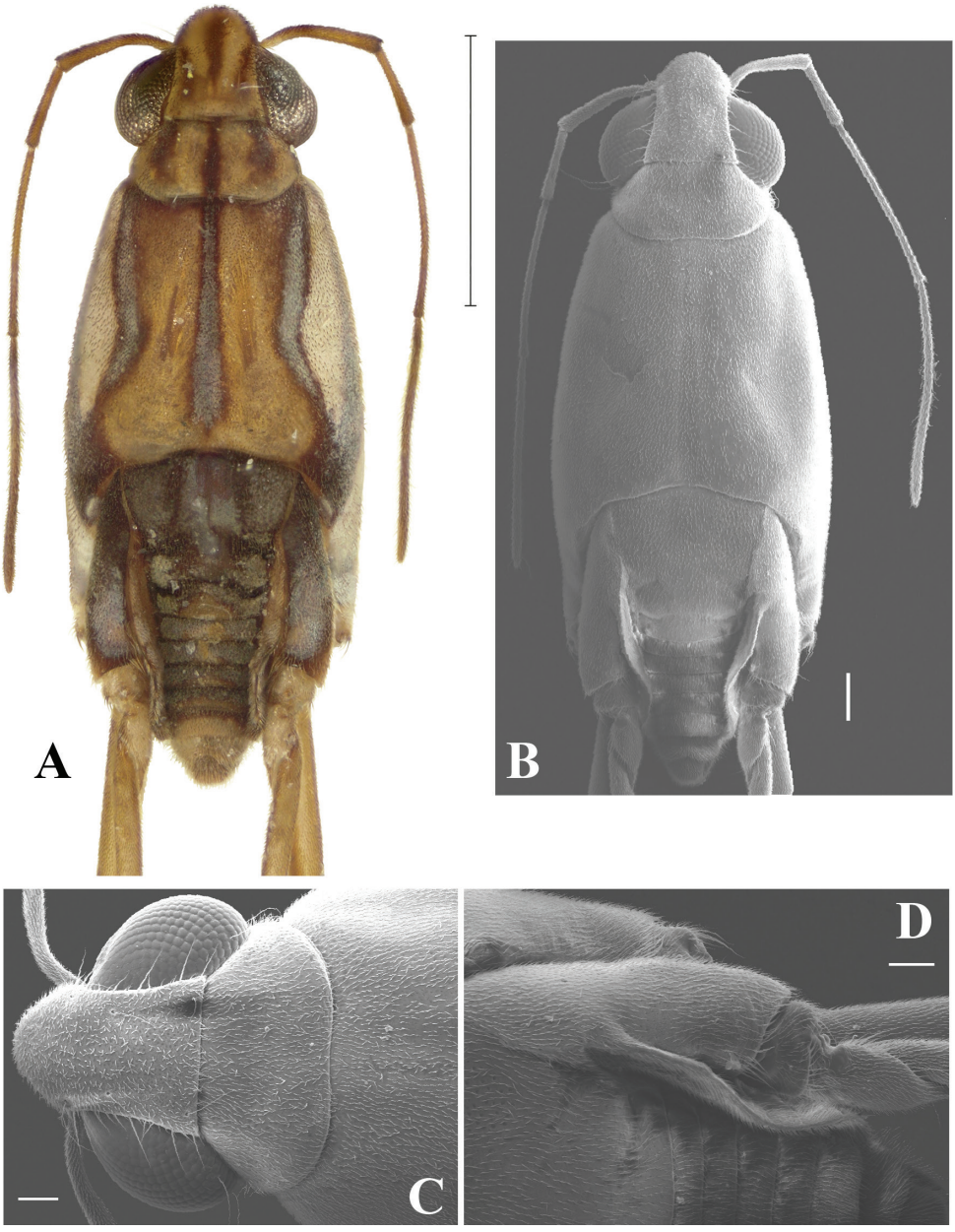

Figure 1. *Telmatometropsis fredyi* gen. nov, sp. nov., male **A** dorsal view **B–D** Scanning electron micrographs **B** dorsal view **C** head, pronotum and anterior portion of mesonotum, dorsal view **D** apex of thorax and base of abdomen, dorsal view. Scale bars: 1 mm (**A**); 400 μm (**B**); 100 μm (**C, D**).

tibia; mid tibia less than twice the length of mid tarsus, about as long as medial length of body from anterior margin of pronotum to apex of abdomen, occasionally almost as long as body; mid tarsus shorter than mid femur, article I subequal to article II or a little longer. Hind femur longer than mid femur; hind tibia about two-thirds the length

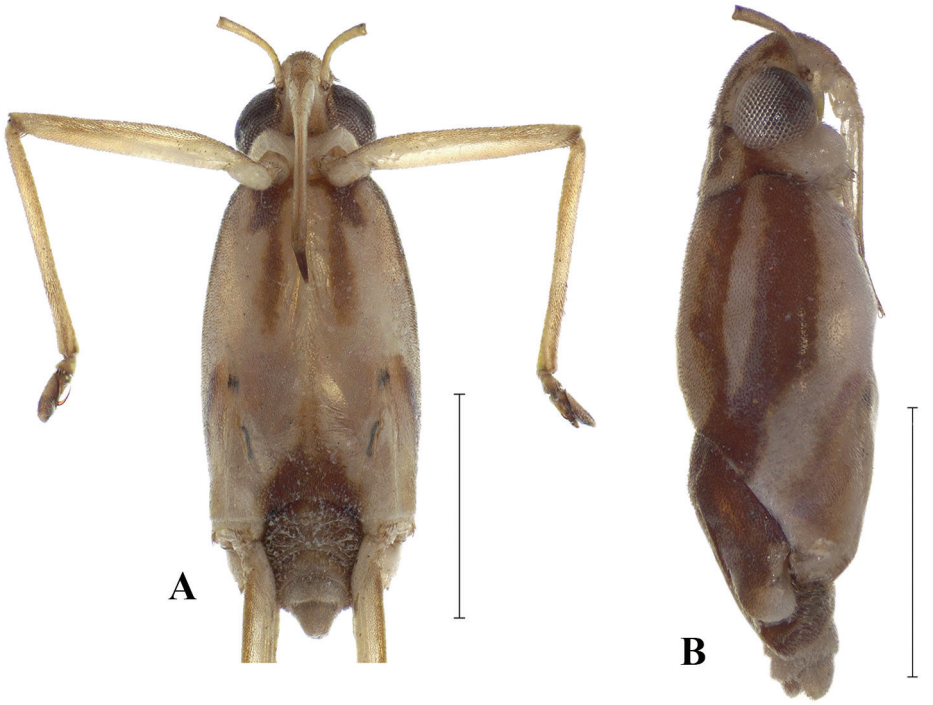

Figure 2. *Telmatometropsis fredyi* gen. nov, sp. nov., male **A** ventral view **B** lateral view. Scale bars: 1 mm.

Table 1. Comparison of *Telmatometropsis* gen. nov. with other genera of Neotropical Trepobatinae. Data on other genera were obtained from Drake and Harris (1932), Kenaga (1941, 1942), Hungerford and Matsuda (1958), Andersen (1982), Polhemus (1991), Nieser (1993), Nieser and Melo (1999), and Aristizábal-García (2017), but not exhaustively concerning measurements.

	Habitat	Ground color	Interocular marks	Mesonotal marks	BL	ANT III/ ANT I	ANT III/ ANT II	ANT III/ ANT IV
Telmatometropsis	Marine	Yellow	Present	Median+lateral	2.90–3.90	1.25–1.85	2.05–2.40	0.72–0.90
Halobatopsis	Freshwater	Yellow/brown	Present/ absent	Median+lateral/ absent	3.40–4.60	0.68–0.77	1.33–1.42	0.79–1.12
Lathriobatoides	Freshwater	Yellow/brown	Absent	Absent	2.60–3.20	1.10–1.20	1.70	1.10–1.20
Metrobates	Freshwater	Black	Present	Median/ median+lateral	3.00–5.00	0.22–0.30	0.73–0.84	0.67–1.29
Ovatametra	Freshwater	Yellow/brown	Present	Median+lateral	2.00–3.10	0.70	1.20	0.64–0.71
Telmatometra	Freshwater	Yellow/brown	Present/ absent	Median+lateral/ lateral	3.30–5.50	1.20–1.40	2.20–2.40	1.00–1.42
Telmatometroides	Marine	Yellow	Present	Median+lateral	3.15–3.70	1.10–1.20	1.40–1.50	0.94
Trepobates	Freshwater/ marine	Yellow/ brown/black	Present	Variable	3.00–5.50	0.70	1.10–1.20	0.84–0.97
Trepobatoides	Freshwater	Yellow/brown	Present	Median+lateral	3.57–4.45	0.40	1.20	0.68–0.70

of hind femur, densely covered with setae; hind tarsus about half the length of hind tibia, article I longer than article II.

Etymology. The generic name refers to its resemblance to the genus *Telmatometroides.*

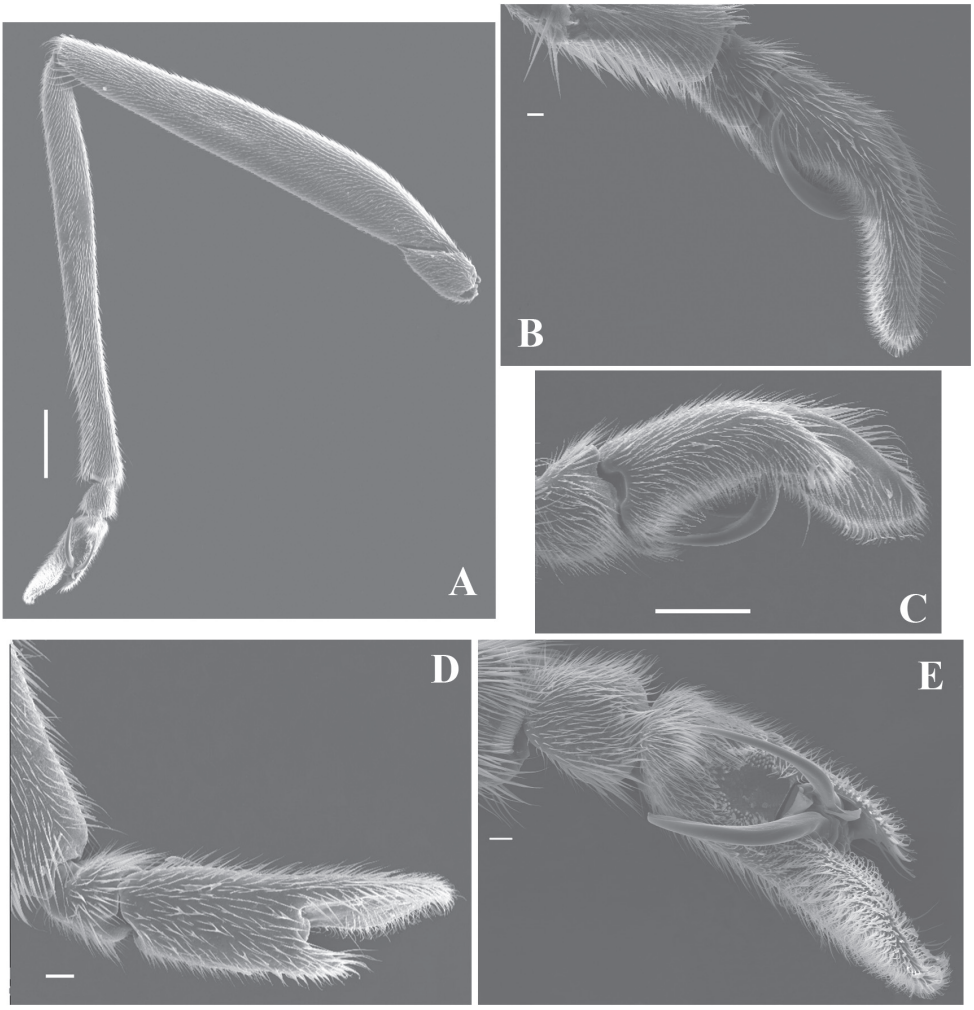

Figure 3. *Telmatometropsis fredyi* gen. nov, sp. nov., male, scanning electron micrographs **A** fore leg, ventral view **B–E** fore tarsus **B** external lateral view **C** internal lateral view **D** dorsal view **E** ventral view. Scale bars: 200 μm (**A**); 300 μm (**B**); 20 μm (**C**); 60 μm (**D**); 40 μm (**E**).

***Telmatometropsis fredyi* sp. nov.**
http://zoobank.org/707ddb44-4b8c-493b-9372-2efd98ffcf0c
Figs 1–8, Tables 2, 3

Description. Male. [For measurements see Table 2.] ***Color.*** Ground color yellow. Head dorsally pale yellow, with three longitudinal brown stripes between eyes; stripes connected posteriorly (Fig. 1A). Venter of head light brown (Fig. 2A). Eye golden brown. Antenna yellowish-brown to brown. Labial articles I–III light brown with brown longitudinal stripe; article IV dark brown. Pronotum pale yellow, with a dark brown median stripe throughout length and laterally with a pair of dark brown

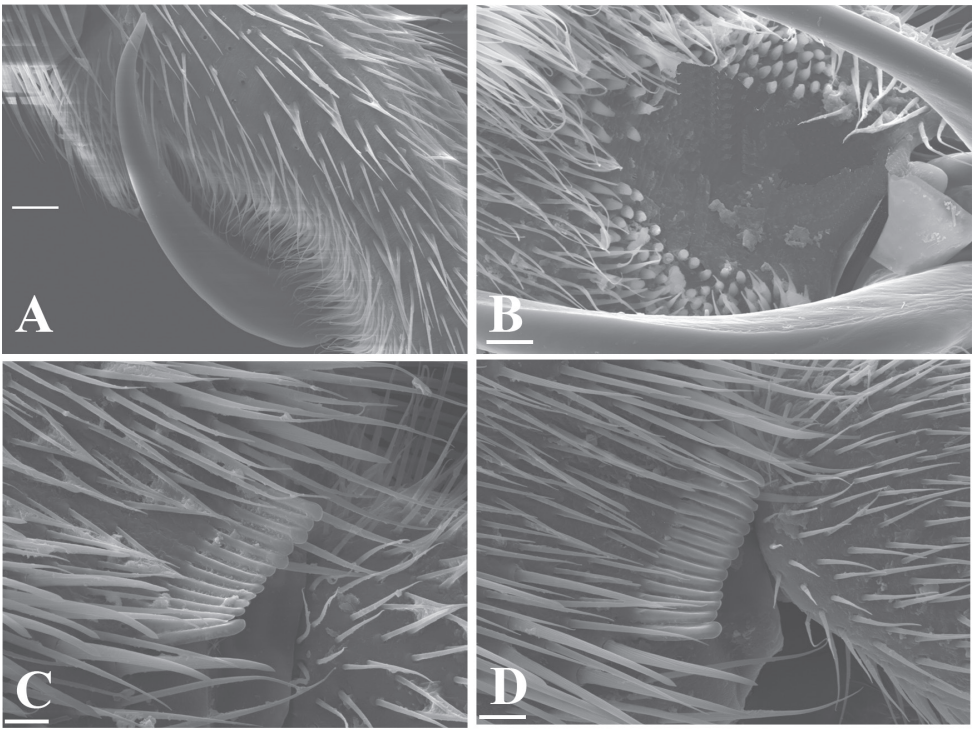

Figure 4. *Telmatometropsis fredyi* gen. nov, sp. nov., scanning electron micrographs **A–C** male **A** fore pretarsal claw, lateral view **B** fore tarsomere II, area with cuticular pegs adjacent to pretarsal claw insertion, ventral view **C** apex of fore tibia with grooming structures, ventral view **D** female, apex of fore tibia with grooming structures, ventral view. Scale bars: 20 μm (**A**); 10 μm (**B, C, D**).

longitudinal stripes reaching slightly beyond middle of length. Mesonotum pale yellow, covered with silvery pilosity, with brown spots on anterior margin, a dark brown median stripe almost reaching posterior margin, and a pair of dark brown longitudinal stripes laterally; lateral stripes posteriorly narrowed and connected to mesopleural stripes (Fig. 2B). Metanotum velvety, dark brown with central subtriangular spot of dense silvery pubescence and two lateral spots of silvery pubescence. Mesopleura covered with silvery pubescence, with a longitudinal dark brown stripe on its ventralmost portion; stripe posteriorly connected to mesonotal stripe. Meso- and metacetabula with pruinose patches. Prosternum pale yellow; mesosternum pale yellow with two longitudinal brown spots (Fig. 2A); metasternum with posterior subtriangular dark brown spot (Fig. 2A). Abdominal mediotergite I dark brown, with silvery pubescence on posterolateral corners; mediotergite II dark brown, with central yellow spot posteriorly and silvery pubescence on posterolateral corners; mediotergites III–VI dark brown, covered with pruinose layer, with central yellow spots varying in size; mediotergites VII–VIII pale yellow, covered with abundant pubescence of same color; mediotergite VII dark brown on anterior margin. Abdominal laterotergites yellow, with patches of light setae. Abdomen laterally dark brown. Foreleg: coxa pale yellow; trochanter pale yellow, with

Table 2. Measurements of male morphological structures of *Telmatometropsis fredyi* sp. nov.

Structure	Male 1	Male 2	Male 3	Male 4	Male 5	Male 6	Male 7	Male 8	Male 9	Male 10	Maximum	Minimum	Average
BL	3.17	3.01	3.20	3.02	3.04	2.90	3.05	3.21	3.18	2.90	3.21	2.90	3.07
BW	1.13	1.09	1.11	1.07	1.21	1.13	1.13	1.19	1.12	1.12	1.21	1.07	1.13
HW	0.28	0.28	0.32	0.31	0.32	0.29	0.31	0.35	0.32	0.31	0.35	0.28	0.31
ANT I	0.48	0.40	0.47	0.45	0.40	0.44	0.48	0.44	0.47	0.47	0.48	0.40	0.45
ANT II	0.29	0.31	0.35	0.30	0.32	0.33	0.34	0.32	0.32	0.31	0.35	0.29	0.32
ANT III	0.70	0.71	0.75	0.71	0.74	0.68	0.72	0.68	0.71	0.66	0.66	0.75	0.71
ANT IV	0.85	0.80	0.95	0.95	0.97	0.94	0.91	0.84	0.85	0.87	0.97	0.80	0.89
PL	0.30	0.27	0.32	0.28	0.31	0.30	0.32	0.30	0.31	0.31	0.32	0.27	0.30
AL	1.23	1.10	1.10	1.03	1.03	1.16	1.21	1.23	1.27	1.12	1.27	1.03	1.15
Fore leg													
FEM	1.10	1.13	1.11	1.02	1.07	1.16	1.14	1.14	1.16	1.16	1.16	1.02	1.12
TIB	1.10	1.19	1.14	1.12	1.12	1.15	1.16	1.12	1.16	1.11	1.19	1.10	1.14
TAR I	0.10	0.06	0.07	0.07	0.10	0.08	0.08	0.09	0.09	0.09	0.10	0.06	0.08
TAR II	0.27	0.32	0.31	0.31	0.26	0.31	0.29	0.28	0.31	0.34	0.34	0.26	0.30
Mid leg													
FEM	1.82	1.83	1.77	1.75	1.79	1.82	1.86	1.74	1.86	1.75	1.86	1.74	1.80
TIB	2.64	2.64	2.61	2.46	2.69	2.55	2.66	2.61	2.62	2.62	2.69	2.46	2.61
TAR I	0.93	0.87	0.87	0.63	0.88	0.81	0.87	0.80	0.82	0.88	0.93	0.63	0.84
TAR II	0.68	0.71	0.73	0.52	0.79	0.73	0.70	0.73	0.50	0.68	0.79	0.50	0.68
Hind leg													
FEM	2.27	2.19	2.21	2.19	2.22	2.22	2.24	2.25	2.10	2.23	2.27	2.10	2.21
TIB	0.93	0.92	0.93	0.89	0.91	0.81	0.92	0.88	0.92	0.92	0.93	0.81	0.90
TAR I	0.22	0.21	0.22	0.21	0.22	0.19	0.21	0.21	0.22	0.21	0.22	0.19	0.21
TAR II	0.27	0.27	0.27	0.26	0.28	0.25	0.26	0.26	0.26	0.27	0.28	0.25	0.27

Table 3. Measurements of female morphological structures of *Telmatometropsis fredyi* sp. nov.

Structure	Female 1	Female 2	Female 3	Female 4	Female 5	Female 6	Female 7	Female 8	Female 9	Female 10	Maximum	Minimum	Average
BL	3.30	3.62	3.65	3.54	3.56	3.46	3.47	3.91	3.85	3.42	3.91	3.30	3.58
BW	1.50	1.50	1.51	1.52	1.51	1.47	1.44	1.50	1.50	1.46	1.52	1.44	1.49
HW	0.34	0.34	0.36	0.35	0.35	0.36	0.37	0.36	0.36	0.36	0.37	0.34	0.36
ANT I	0.49	0.55	0.53	0.54	0.53	0.55	0.54	0.54	0.55	0.51	0.55	0.49	0.53
ANT II	0.35	0.34	0.36	0.35	0.34	0.37	0.33	0.36	0.36	0.34	0.37	0.33	0.35
ANT III	0.74	0.71	0.74	0.73	0.78	0.81	0.68	0.83	0.79	0.73	0.83	0.68	0.75
ANT IV	0.91	0.79	0.95	1.02	0.97	0.95	0.91	1.00	0.93	0.91	1.02	0.79	0.93
PL	0.29	0.32	0.33	0.30	0.31	0.33	0.34	0.34	0.32	0.30	0.34	0.29	0.32
AL	1.53	1.71	1.72	1.70	1.72	1.63	1.64	1.90	1.82	1.60	1.90	1.53	1.70
Fore leg													
FEM	1.12	1.08	1.17	1.13	1.18	1.19	1.14	1.14	1.14	1.18	1.19	1.08	1.15
TIB	1.04	1.07	1.10	1.07	1.09	1.08	1.09	1.10	1.13	1.10	1.13	1.04	1.09
TAR I	0.10	0.09	0.09	0.11	0.12	0.10	0.12	0.08	0.08	0.10	0.12	0.08	0.10
TAR II	0.34	0.43	0.43	0.37	0.40	0.41	0.40	0.40	0.43	0.39	0.43	0.34	0.40
Mid leg													
FEM	2.08	2.11	2.10	2.10	2.20	2.22	2.06	2.16	2.00	2.09	2.22	2.00	2.11
TIB	3.14	2.98	3.11	3.15	3.14	3.21	3.13	3.07	2.77	3.07	3.21	2.77	3.08
TAR I	1.09	0.96	1.07	1.07	1.00	1.09	1.02	1.02	0.96	1.06	1.09	0.96	1.03
TAR II	0.71	0.81	0.83	0.86	0.70	0.89	0.84	0.84	0.69	0.85	0.89	0.69	0.80
Hind leg													
FEM	2.60	2.52	2.63	2.46	2.67	2.63	2.63	2.67	2.67	2.61	2.67	2.46	2.61
TIB	1.15	1.11	1.14	1.17	1.15	1.13	1.12	1.12	1.05	1.14	1.17	1.05	1.13
TAR I	0.26	0.26	0.28	0.27	0.27	0.27	0.27	0.27	0.25	0.27	0.28	0.25	0.27
TAR II	0.33	0.32	0.33	0.34	0.33	0.35	0.34	0.35	0.33	0.31	0.35	0.31	0.33

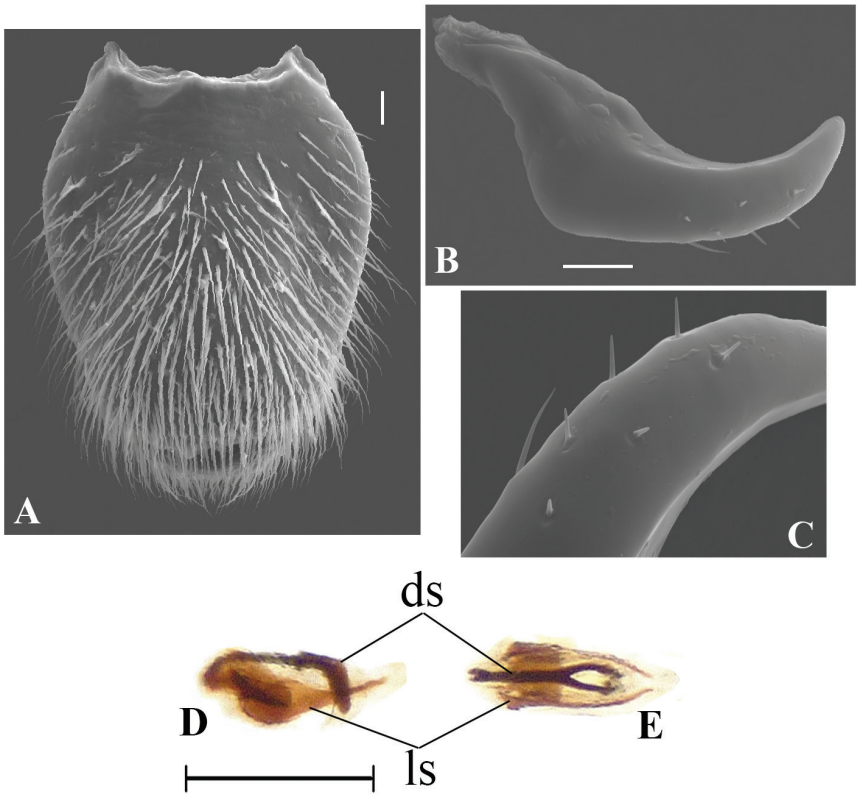

Figure 5. *Telmatometropsis fredyi* gen. nov, sp. nov., male, scanning electron micrographs **A** proctiger, dorsal view **B** paramere, lateral view **C** detail of paramere setiferation **D–E** sclerites **D** lateral view **E** dorsal view. Abbreviations: sclerite (ls), dorsal sclerite (ds). Scale bars: 40 μm (**A**); 20 μm (**B**); 0.25 mm (**D–E**).

brown lateral fringe; femur dorsally brown, ventrally pale yellow, mesal margin larerally yellow, with longitudinal white line; tibia brown; tarsus dark brown. Mid leg: coxa pale yellow; trochanter brown; femur dorsally brown, ventrally pale yellow; tibia with basal half brown and apical half dark brown; tarsus dark brown. Hind leg: coxa pale yellow; trochanter pale yellow; femur dorsally brown, ventrally pale yellow with dark brown apex; tibia and tarsus dark brown. ***Structure.*** Head with frons rounded. Antennomere I curved laterally; antennomere II shortest; antennomere IV longest (Fig. 1A, B). Fore leg: femur widened in basal half, ventrally flattened (Fig. 3A), with ventrolateral row of 4–7 small bristles; apex of tibia with long black bristles laterally and grooming structures (Fig. 4C); tarsomere I 1/4 of tarsomere II length; tarsomere II strongly curved in lateral view, flattened laterally, and apically bifid, with a shorter and a longer portion, with cuticular subconical pegs (Fig. 4B); claws long, strongly curved back (Figs 3B, C, E, 4A). Mid tarsomere I with few bristles at base. Hind femur with five dorsal trichobothria. Abdominal laterotergites elevated at approximately 45° (Fig. 1A, B, D). Abdominal segment VIII dorsally with a small central notch on posterior margin (Fig. 1A, B).

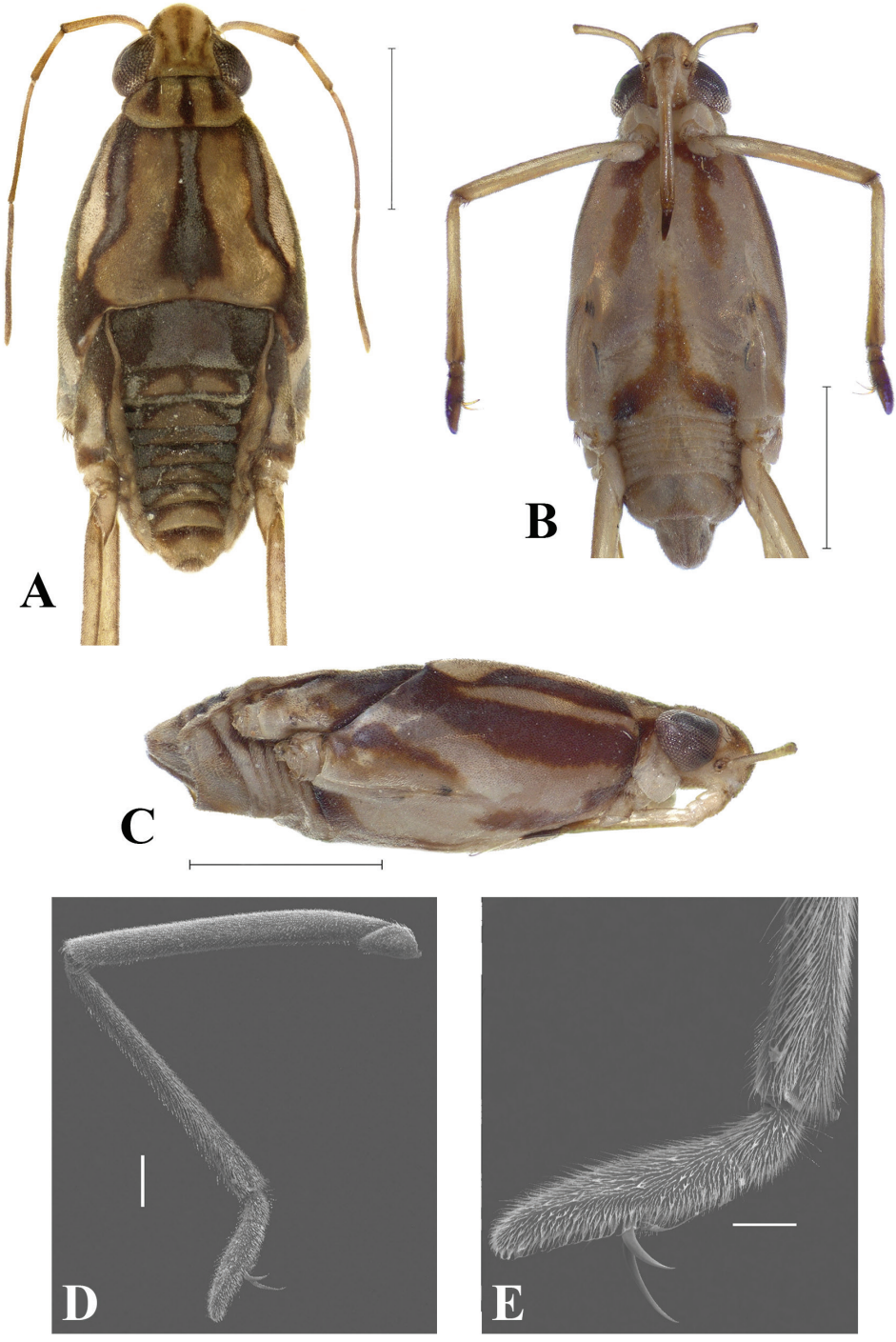

Figure 6. *Telmatometropsis fredyi* gen. nov, sp. nov., female **A** dorsal view **B** ventral view **C** lateral view **D–E** scanning electron micrographs **D** fore leg, ventral view **E** apex of fore tibia and fore tarsus, ventral view. Scale bars: 1 mm (**A, B, C**); 200 μm (**D**); 100 μm (**E**).

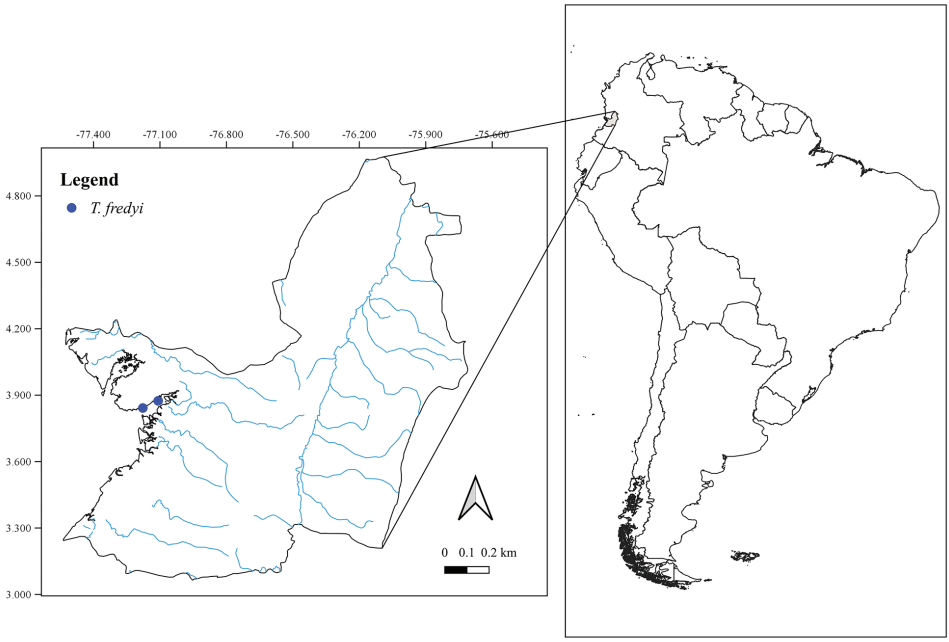

Figure 7. Geographical distribution of *Telmatometropsis fredyi* gen. nov, sp. nov.

Figure 8. Type locality of *Telmatometropsis fredyi* sp. nov.; mangrove lagoons in Buenaventura Bay, Valle del Cauca, Colombia.

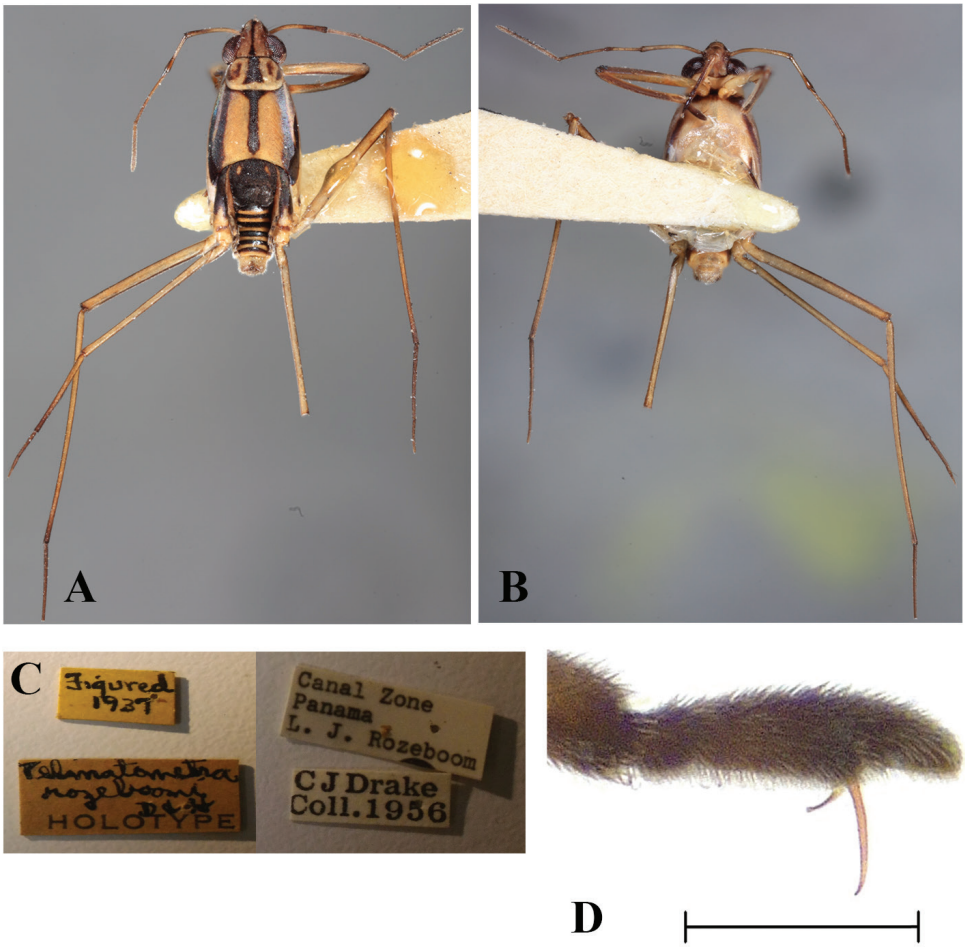

Figure 9. Apterous holotype male, *Telmatometroides rozeboomi* (Drake & Harris, 1937) **A** dorsal view **B** ventral view **C** labels **D** fore tarsus, internal lateral view. Scale bar: 0.25 mm.

Paramere with apex curved up and rows of bristles close to apex (Fig. 5B, C); proctiger oval, covered with setae (Fig. 5A); sclerites as in Fig. 5 D–E.

Female. [For measurements see Table 3.] Similar in color and structure to male, but larger and more robust (Fig. 6A–C). Central spot on metanotum quadrate (Fig. 6A). Spot on metasternum inverted "T"-shaped (Fig. 6B). Abdominal mediotergites dark brown, with central yellow spots; mediotergites II–IX with pruinose patches laterally (Fig. 6C); laterotergites without patches of light setae (Fig. 6A). Fore leg: femur slightly curved at the base (Fig. 6D), with 3–7 bristles; tibia with grooming structures (Fig. 4D); tarsomere II cylindrical, flattened laterally (Fig. 6E). Abdominal laterotergites elevated by almost 90° (Fig. 6A).

Type material. ***Holotype.*** Colombia • apterous male; Valle del Cauca, Buenaventura, La Bocana, lagoon, 8.XI.2003; Molano & Camacho leg. (UPTC-In-00001). ***Para-***

types. 1 apterous female; Valle del Cauca, Buenaventura, La Bocana, lagoon, 4.XI.2004, Molano & Morales leg. (UPTC-In-00002). 5 apterous males and 5 apterous females, same data as for holotype (UPTC-In-00003). 2 apterous males and 2 apterous females; Valle del Cauca, Buenaventura, La Bocana, lagoon, 4.XI.2004, Molano & Morales leg. (CEIOC 76834). 1 apterous female; Valle del Cauca, Buenaventura, Santa Clara, 17.V.2004, Camacho & Molano leg. (UPTC-In-00004). 4 apterous males and 12 apterous females; Valle del Cauca, Buenaventura, La Bocana, lagoon, 4.XI.2004, Molano & Morales leg. (UPTC-In-00208). 2 apterous males and 8 apterous females; Valle del Cauca, Buenaventura, La Bocana, lagoon, 8.XI.2003, Molano & Camacho leg. (UPTC In-00209). 1 apterous male and 1 apterous female; Valle del Cauca, Buenaventura, Punta Arenas, mangrove lagoons, 26.I.1986, M.R. Manzano leg. (UPTC-In-00210).

Etymology. The new species is named in honor of Professor Fredy Molano, who made a great contribution to the knowledge of Gerromorpha from Colombia.

Habitat notes. The species inhabits mangrove lagoons in Buenaventura Bay, Valle del Cauca Department, Pacific region of Colombia (Figs 7, 8).

Key to the genera of Neotropical Trepobatinae

Modified from Moreira et al. 2018.

1	Antennomere II longer than antennomere III; antennomeres II–III of male distally widened ..... ***Metrobates***
–	Antennomere II subequal in length or shorter than antennomere III; antennomeres II–III of male not distally widened **2**
2	Antennomere III 10–85% longer than antennomere I **3**
–	Antennomere III 40–80% of length of antennomere I **6**
3	Antennomere III shorter than two times the length of antennomere II **4**
–	Antennomere III longer than two times the length of antennomere II **5**
4	Interocular space with a dark longitudinal stripe ..... ***Telmatometroides***
–	Interocular space without a dark longitudinal stripe ..... ***Lathriobatoides***
5	Antennomere IV not the longest; male fore tarsus unmodified, cylindrical; freshwater habitats ..... ***Telmatometra***
–	Antennomere IV the longest; male fore tarsus modified (Fig. 2); marine habitats ..... ***Telmatometropsis*** **gen.nov.**
6	Antennomere I much longer than antennomeres II–III together ..... ***Trepobatoides***
–	Antennomere I at most as long as antennomeres II–III together **7**
7	Mid tibia distinctly shorter than length of body ..... ***Ovatametra***
–	Middle tibia almost as long as or slightly longer than length of body **8**
8	Eye in lateral view not extending beyond half of propleuron; hind tibia distinctly shorter than two times the length of hind tarsus ..... ***Trepobates***
–	Eye in lateral view extending beyond half of propleuron; hind tibia longer than two times the length of hind tarsus ..... ***Halobatopsis***

Discussion

The municipality of Buenaventura has a monomodal precipitation regime, with a tendency to bimodality. The highest precipitation values occur between the months of September and October, while the lowest values are observed between February and March, with an average annual precipitation of 7400 mm and an average temperature of 25.9 °C. These very particular climatological characteristics generate a very humid and warm climate (Enriquez et al. 2014). Several freshwater bodies flow to Buenaventura Bay, such as the Dagua River, and the Aguadulce, Pichido, El Corral, and San Joaquín streams. These different estuaries with a large number of drains constitute a deltaic system in the area. The bay is geomorphologically characterized by the vegetated intertidal platforms, which correspond to muddy plains of fine sediments and abundant organic matter, where mainly mangrove-type vegetation grows (*Avicennia germinans* (L.) Stearn (Lamiales: Acanthaceae), *Laguncularia racemosa* (L.) Gaertn. (Myrtales: Combretaceae), *Rhizophora mangle* L., and *R. harrisonii* Leechm. (Malpighiales: Rhizophoraceae)) (Álvarez et al. 2016). It is in such places that the type specimens of *Telmatometropsis fredyi* sp. nov. were collected.

The new genus herein described has a unique feature, the strongly modified male fore tarsomere II, which in other Neotropical trepobatines is elongated and cylindrical. The distribution of *Telmatometropsis* gen. nov. partially overlaps with that of *Telmatometroides*. However, these two genera apparently do not share the same microhabitats, since they have not been collected together. The new genus probably also occurs in the departments of Chocó and Nariño, both in the Colombian Pacific region and where several mangroves are found.

Acknowledgements

We thank Dr. Enrique Vera, Dr. Yaneth Pineda and Jazmith Espinosa (INCITEMA–UPTC) for allowing us to access the scanning electron microscope at UPTC; and Drs. Carla Fernanda Burguez Floriano and Thomas J. Henry (NMNH) for providing photos of the holotype and labels of *Telmatometroides rozeboomi*. To Alfonso Ignacio Ardila Hernandez for providing photographs of the habitat of the new species. We express our gratitude to the university directorate of research, UPTC (DIN) and the project "Análisis biogeográfico de la región Andina colombiana a través de áreas de endemismo de chinches semiacuáticas (Hemiptera: Gerromorpha), SGI 2907". FFFM benefited from grants provided by Fundação Carlos Chagas Filho de Amparo à Pesquisa do Estado do Rio de Janeiro (E-26/#203.207/2017, E-26/#201.066/2020) and Conselho Nacional de Desenvolvimento Científico e Tecnológico (#301942/2019-6). Finally, we thank the reviewers and editor Laurence Livermore, who gave valuable suggestions to improve this paper.

References

Álvarez M, Bermúdez-Rivas C, Niño D (2016) Caracterización de la geomorfología costera y sus coberturas vegetales asociadas, a través de sensores remotos en la Bahía de Buenaventura, Valle del Cauca. Boletín Científico CIOH (34): 49–63. https://doi.org/10.26640/22159045.426

Andersen NM (1982) The Semiaquatic Bugs (Hemiptera: Gerromopha) Phylogeny, Adptations, Biogeography and Classification. Entomograph 3, Scandinavian Science Press LTD Klampenborg, 455 pp.

Andersen NM (1998) Marine water striders (Heteroptera, Gerromorpha) of the Indo–Pacific: cladistic biography and Cenozoic paleogeography. In: Hall R, Holloway JD (Eds) Biogeography and Geological Evolution of SE Asia. Backhuys Publishers, Leiden, 341–354.

Andersen NM, Cheng L (2004) The marine insect *Halobates* (Heteroptera: Gerridae) biology, adaptations, distribution and phylogeny. Oceanography and Marine Biology: An Annual Review 42: 119–180. https://doi.org/10.1201/9780203507810.ch5

Aristizábal-García H (2017) Hemípteros Acuáticos y Semiacuáticos del Neotrópico. Academia Colombiana de Ciencias Exactas Físicas y Naturales, Bogotá–Colombia, 984 pp.

Bergroth E (1892) Note on the water-bug, found by Rev. L. Zabriskie. Insect Life 4: e321.

Bergroth E (1908) Family Gerridae, subfamily Halobatinae. Ohio Naturalist 8: 371–382.

Bianchi V (1896) On two new forms of the heteropterous family Gerridae. Annuaire du Musée Zoologique de l'Académie Impériale des Sciences de St. Pétersbourg 1: 69–76.

Cheng L (1976) Marine Insects. North–Holland Publishing Company. Amsterdam, The Netherlands, 581 pp.

Cheng L (2006) A bug on the ocean waves (Heteroptera, Gerridae, *Halobates* Eschscholtz). Denisia 19: 1033–1040. https://www.zobodat.at/pdf/DENISIA_0019_1033-1040.pdf

Drake CJ, Harris HM (1932) A survey of the species of *Trepobates* Uhler (Hemiptera, Gerridae). Bulletin of the Brooklyn Entomological Society 27: 113–123.

Drake CJ, Harris HM (1937) Notes on some American Halobatinae (Gerridae, Hemiptera). Revista de Entomologia 7: 357–362.

Enriquez O, Guzmán A, Narváez G (2014) Análisis del comportamiento de la precipitación en el municipio de Buenaventura (Valle del Cauca, Colombia) en condiciones de desarrollo de los fenómenos El Niño y La Niña. Cuadernos de Geografía, Revista Colombiana de Geografía 23(1): 165–178. https://doi.org/10.15446/rcdg.v23n1.41090

Eschscholtz F (1822) Entomographien. Erste Lieferung. Berlin, 128 pp. https://doi.org/10.5962/bhl.title.65315

Hungerford HB, Matsuda R (1958) A new genus of Gerridae (Hemiptera) from South America. The Florida Entomologist 41(3): 125–129. https://doi.org/10.2307/3492062

Kenaga EE (1941) The genus *Telmatometra* Bergroth (Hemiptera: Gerridae). The University of Kansas Science Bulletin 27(9): 169–183.

Kenaga EE (1942) A new genus in the Halobatinae (Gerridae – Hemiptera). Journal of the Kansas Entomological Society 15(4): 136–141.

Molano-Rendón F, Morales I (2017) Chinches patinadoras marinas (Hemiptera: Heteroptera: Gerromorpha): diversidad de los hábitats oceánicos del Neotrópico. Biota Colombiana 18(1): 172–191. https://doi.org/10.21068/c2017.v18n01a10

Moreira FFF, Rodrigues HDD, Sites RW, Cordeiro ISR, Magalhães OM (2018) Chapter 7 – Order Hemiptera. In: Hamada N, Thorp JH, Rogers DC (Eds) Thorp and Covich's Freshwater Invertebrates (4th Edn.). Volume III. Keys to Neotropical Hexapoda. Academic Press, London, 175–216. https://doi.org/10.1016/B978-0-12-804223-6.00007-X

Nieser N (1993) Two new South American taxa of *Metrobates* (Heteroptera: Gerridae). Storkia (2): 21–25.

Nieser N, Melo AL (1999) A new species of *Halobatopsis* (Heteroptera: Gerridae) from Minas Gerais (Brazil), with a key to species. Entomologische Berichten 59: 97–102.

Pacheco-Chaves B, Cordeiro IRS, Moreira FFF, Springer M (2018) The water striders (Hemiptera: Heteroptera: Gerridae) of Costa Rica: new species, checklist, and new records. Zootaxa 4471(3): 493–522. https://doi.org/10.11646/zootaxa.4471.3.4

Polhemus JT (1991) Two New Neotropical Genera of Trepobatinae (Gerridae: Heteroptera). Journal of the New York Entomological Society 99(1): 78–86.

Polhemus JT (2004) Nomenclatural notes on homonomy and synonymy in the Gerromorpha (Heteroptera: Gerridae, Hydrometridae). Journal of the New York Entomological Society 112: 212–213. https://doi.org/10.1664/0028-7199(2004)112[0212:NNOHAS]2.0.CO;2

Polhemus JT, Polhemus DA (2002) The Trepobatinae (Gerridae) of New Guinea and surrounding regions, with a review of the World fauna. Part 6. Phylogeny, biogeography, World checklist, bibliography and final taxonomic addenda. Insect Systematics and Evolution 33: 253–290. https://doi.org/10.1163/187631202X00154

Polhemus JT, Polhemus DA (2008) Global diversity of true bugs (Heteroptera; Insecta) in freshwater. Hydrobiologia 595: 379–391. https://doi.org/10.1007/s10750-007-9033-1

Schuh R, Slater J (1995) True Bugs of the World (Hemiptera: Heteroptera): Classification and Natural History. Comstock Publishing Associates, Nueva York, 336 pp.

Uhler PR (1871) Notices of some Heteroptera in the collection of Dr. T. W. Harris. Proceedings of the Boston Society of Natural History 14: 93–109.

Uhler PR (1894) On the Hemiptera-Heteroptera of the Island of Grenada, West Indies. Proceedings of the Zoological Society of London (1894): 167–224.

ZooKeys 1043: 103–116 (2021)
doi: 10.3897/zookeys.1043.61344
https://zookeys.pensoft.net

SHORT COMMUNICATION

A peer-reviewed open-access journal
ZooKeys
Launched to accelerate biodiversity research

Transfer of *Westermannia difficilis* Dohrn to the genus *Polauchenia* McAtee & Malloch (Hemiptera, Heteroptera, Reduviidae, Emesinae, Emesini)

Hélcio R. Gil-Santana[1], Jürgen Deckert[2]

1 *Laboratório de Diptera, Instituto Oswaldo Cruz, Av. Brasil, 4365, 21040-360, Rio de Janeiro, RJ, Brazil*
2 *Leibniz Institute for Evolution and Biodiversity Science, Museum für Naturkunde, Berlin, Germany*

Corresponding author: Hélcio R. Gil-Santana (helciogil@uol.com.br, helciogil@ioc.fiocruz.br)

Academic editor: L. Livermore | Received 24 November 2020 | Accepted 22 March 2021 | Published 11 June 2021

http://zoobank.org/C4AD2420-58A4-42AD-8096-22AC6D01C6CF

Citation: Gil-Santana HR, Deckert J (2021) Transfer of *Westermannia difficilis* Dohrn to the genus *Polauchenia* McAtee & Malloch (Hemiptera, Heteroptera, Reduviidae, Emesinae, Emesini). ZooKeys 1043: 103–116. https://doi.org/10.3897/zookeys.1043.61344

Abstract

Based on the examination of its lectotype (here designated), *Westermannia difficilis* Dohrn, 1860 (Hemiptera, Heteroptera, Reduviidae, Emesinae, Emesini), currently included in *Dohrnemesa* Wygodzinsky, 1945, is transferred to the genus *Polauchenia* McAtee & Malloch, 1925 with the resulting new combination: *Polauchenia difficilis* (Dohrn, 1860), **comb. nov.** An updated key to the species of *Polauchenia* is provided.

Keywords

Assassin bugs, Colombia, Neotropical region, Venezuela

Introduction

There are about 30 genera of Emesinae classified in four tribes in the Neotropics (Wygodzinsky 1966; Maldonado 1990; Gil-Santana et al. 2015; Castro-Huertas et al. 2020).

When describing *Westermannia difficilis*, Dohrn (1860) provided a very short description of the species, apparently based on a single specimen from Colombia and deposited in "Berliner Museum", but he did not mention the gender of the specimen.

Dohrn (1863) presented a redescription of *W. difficilis*, including more details of its coloration and stated that this species was based on one specimen deposited in the Berliner Museum, but again, its gender was not mentioned. Champion (1899) mentioned a "single specimen" of *W. difficilis* Dohrn, 1860, from Panama, which was thought to probably belong to *Emesa* Fabricius, 1803 by Wygodzinsky (1945), who later (Wygodzinsky 1966) stated that judging by Champion's figure, it probably represented another species of the "*difficilis* group" of *Dohrnemesa* Wygodzinsky, 1945.

Because *Westermannia* Dohrn, 1860 was preoccupied by a Hübner's genus of the same name in Lepidoptera ([1821]) (McAtee and Malloch 1925), Kirkaldy (1904) proposed a new name, *Westermannias*, to replace it. McAtee and Malloch (1925) synonymized *Westermannia* and *Westermannias* with *Emesa*, including "*difficilis* (*Westermannia*) Dohrn" and "*tenerrima* (*Westermannia*) Dohrn" as unplaced species in the genus *Emesa*. McAtee and Malloch (1925) argued that they were unable to place these species in their keys without a fuller knowledge of the characters of their types.

When describing *Dohrnemesa*, Wygodzinsky (1945) commented about the difficulties in establishing the systematic position of *Westermannia difficilis* because the types were not examined again. However, he considered that, considering the generic synonyms of *Westermannia* and *Westermannias* with *Emesa* proposed by McAtee and Malloch (1925), there was no reason to worry too much with the species previously included in these genera, because they might eventually be included in *Dohrnemesa* in the future.

Wygodzinsky (1945) considered *Dohrnemesa* close to *Polauchenia* McAtee & Malloch, 1925 and pointed out that the main differences between them were the absence of tubercles or spined humeri and the presence of a free short vein emitted from the base of the basal cell of the forewing in *Dohrnemesa*. In the key to genera of the Emesini presented by Wygodzinsky (1966), the presence or absence of a short free vein at the base of the basal cell of the forewing, in *Dohrnemesa* and *Polauchenia*, respectively, is the main character that separates these genera. Additionally, based on this characteristic alone, Wygodzinsky (1966) transferred *Polauchenia reimoseri* Wygodzinsky, 1950 to *Dohrnemesa*, assuming that the possession of two veins emitted from the base of the basal cell indicated that this species belonged to the latter genus (Gil-Santana and Ferreira 2017). The new combination, *Dohrnemesa difficilis* was also established by Wygodzinsky (1966), although he did not mention his reasons to include this species in *Dohrnemesa*. On the other hand, he divided *Dohrnemesa* in two groups, claiming that the species of the "*difficilis* group" would have the fore lobe subglobular, abruptly narrowed behind and distinctly separated from petiole, and a strongly widened abdomen with flaring connexival segments.

In the current work, we confirm that the lectotype (here designated) of *Westermannia difficilis* Dohrn, 1860, a species currently included in *Dohrnemesa* Wygodzinsky, 1945, does not belong to this genus but to *Polauchenia* McAtee & Malloch, 1925, resulting in the new combination: *Polauchenia difficilis* (Dohrn, 1860), comb. nov. The main differences are that in *P. difficilis*, comb. nov. the base of basal cell is pointed, emitting a single longitudinal vein, with the absence of a short free vein at

this base and the humeri are spined. Both differences are sufficient to show that *P. difficilis*, comb. nov. does not belong to *Dohrnemesa* but to *Polauchenia*. Additionally, as commented below, several other diagnostic characteristics of *Polauchenia* are present in the specimen examined.

Material and methods

For the present study, the male lectotype (here designated) of *Westermannia difficilis* Dohrn, deposited in the Hemimetabola Collection of the Museum für Naturkunde Berlin, Leibniz Institute for Evolution and Biodiversity Science, Berlin, Germany (MFNB), was directly examined (Figs 1–2, 4–14).

The photos of the lectotype (here designated) of *W. difficilis* Dohrn, 1860 were taken with a Canon EOS 6D (Fig. 1) and M50 (Figs 2–12, 14) with a MP-E 65 mm f/2.8 1–5× macro lens attached. Multiple focal planes were merged using the automontage software Helicon Focus Pro.

Figure 13 was produced by drawing the outline of the margins and veins of the forewing directly from its photograph (Fig. 12), using CorelDRAW Graphics Suite 2020.

General morphological terminology mainly follows Wygodzinsky (1966). However, the [visible] segments of the labium are numbered as II to IV, given that the first segment is lost or fused to the head capsule in Reduviidae (Weirauch 2008; Schuh et al. 2009).

When describing label data, a slash (/) separates the lines and a double slash (//) different labels.

Results

Taxonomy

Subfamily Emesinae
Tribe Emesini

***Polauchenia difficilis* (Dohrn, 1860), comb. nov.**
Figs 1, 2, 4–14

Westermannia difficilis Dohrn, 1860: 251 [description], 1863: 47–48 [redescription]; Stål 1872: 125 [checklist]; Walker 1873: 150 [catalog]; Lethierry and Severin 1896: 71 [catalog]; Champion 1899: 164, pl. 10, figs 8, 8a [record of a supposed specimen from Panama]; McAtee and Malloch 1925: 46–47 [as "unplaced species" listed among species of *Emesa*]; Wygodzinsky 1945: 252 [discussion about the

future possibility of its placement in *Dohrnemesa*], 1949: 34 [catalog, as Emesinae *incertae sedis*].

Dohrnemesa difficilis; Wygodzinsky 1966: 231, 237 [citation, key; checklist, statement that *W. difficilis* figured by Champion 1899 from Panama is not the same species]; Gil-Santana and Ferreira 2016: 584 [citation], 2017: 203, 229 [citation, key].

Type material examined. *Westermannia difficilis*, male lectotype (here designated): [handwritten label]: *Leptol*. / *difficilis* / Dohrn // [blue underlined handwritten label]: Columb; Moritz. // [printed label]: 3326 // [printed label]: [at right side]: QR CODE, [at left side]: http://coll.mfn-berlin.de/u/ /123b88 // [printed red label]: LECTOTYPE / *Westermannia difficilis* Dohrn, 1860 / designated by H. R. Gil-Santana & / J. Deckert 2020 (MFNB).

Notes. In the old catalogue of the Berliner Museum the specimen examined here was registered under the number 3326 and named as *Leptolemus difficilis* Dohrn (Fig. 3). The name of the genus "*Leptolemus*" [apparently abbreviated as "*Leptol*."] can also be read on the label attached to the type specimen (Fig. 2). In the same catalogue, other species, *Leptolemus tenerrima* was also listed just above *L. difficilis* (Fig. 3). However, when describing these two species, Dohrn (1860) included them in *Westermannia*, described in the same occasion too. As far as it seems, the name *Leptolemus* is a manuscript name which was never applied as a published name to any Emesinae or other Reduviidae (e.g., Lethierry and Severin 1896; Wygodzinsky 1966; Maldonado 1990).

The collector of the specimen, Moritz (Johann Wilhelm Karl Moritz 1797–1866), collected in the Caribbean islands and Venezuela, but there is a disagreement among some authors if he collected in Colombia. It is possible that the records of his collecting from Colombia originated from the confusion between Venezuela and Colombia, parts of the former having once belonged to the ancient vice-kingdom of "Nueva Granada" (Papavero 1973). In this case, there is a possibility that the lectotype (here designated) of *W. difficilis* was collected in Venezuela and not in Colombia as stated in his collecting data.

Diagnosis. *Polauchenia difficilis*, comb. nov. can be separated from other species of the genus by the combination of characters presented in the key below. *Polauchenia difficilis*, comb. nov. shares similarities with *P. paraprotentor* Gil-Santana & Ferreira, 2017 but differs from this species in several characteristics, such as: the pale markings of the antenna, middle and hind femora are simple (*P. paraprotentor*) or bordered by darker markings (*P. difficilis*, comb. nov.), those on antenna narrow, with the pale annuli as long or only slightly longer (*P. paraprotentor*) or quite longer (four and seven times) than the width of the segment (*P. difficilis*, comb. nov.); fore coxa with a median pale annulus (*P. difficilis*, comb. nov.) or two pale annuli at submedian basal portion and approximately midportion of distal half of the segment (*P. paraprotentor*); distal portion of forewings with (*P. difficilis*, comb. nov.) or without (*P. paraprotentor*) a large whitish subdistal marking; petiole approximately 1.5 (*P. paraprotentor*) or 1.3 (*P. difficilis*, comb. nov.) times as long as fore lobe; humeri spined (*P. difficilis*, comb. nov.) or not (*P. paraprotentor*); spine of scutellum obliquely directed upwards (*P. difficilis*, comb.

Figures 1–3. 1, 2 *Polauchenia difficilis* (Dohrn, 1860), comb. nov., male lectotype (here designated) **1** lateral view, right side **2** labels **3** old catalogue of the Berliner Museum, page excerpt, arrow points to the record of *Leptolemus difficilis* Dohrn in it.

nov.) or backwards (*P. paraprotentor*); spines of scutellum and metanotum mostly pale (*P. difficilis*, comb. nov.) or brownish (*P. paraprotentor*).

Redescription. Male. Measurements (mm): total length: to tip of abdomen 10.0; to tip of forewings 10.6. *Coloration*: brownish to light brown, with yellowish to pale markings or portions (Figs 1, 4–12, 14). Head brownish; clypeus and labrum paler; pale small spots around the eye: in front of the midpoint of its anterior margin, and a pair behind its posterior margin, above and below the level of the anterior spot; the former slightly larger and just behind transverse sulcus; a pale whitish median small area behind transverse sulcus; a median longitudinal dorsal narrow pale whitish stripe on posterior half of postocular region; apices of labial segments II and III and base of labial segment IV pale white to pale yellow; segment IV somewhat paler (Figs 1, 4, 5, 8–10). First antennal segments (others absent) pale brownish with basal portion and four pale annuli; the latter bordered by contiguous basal and distal darkened annuli, forming a set of bicolored annuli; the two distal set of annuli with the pale portion somewhat larger than the two basal ones; the pale portion of the annuli approximately four and seven times the width of the segment in the basal and distal annuli, respectively while the

Figures 4–7. *Polauchenia difficilis* (Dohrn, 1860), comb. nov., male lectotype (here designated) **4** dorsoposterior view **5** anteroventral view **6, 7** ventroposterior views.

darkened basal and distal annuli are narrower, slightly longer to twice longer the width of the segment, respectively (Figs 1, 4, 5, 8, 9). Thorax: brownish, anterior collar paler; prothoracic supracoxal lobes pale whitish on its anterior margin; a rounded pale spot

above the latter; petiole paler laterally, on the portion just behind the fore lobe and more extensively on distal portion (Figs 1, 8–10). Hind lobe of pronotum: a pair of contiguous pale whitish longitudinal stripes on anterior portion, the medial (submedian) stripes approximately half longer than the lateral ones, running approximately on the basal third of the hind lobe; lower margin pale at approximately its anterior two-thirds; humeral tubercles, including their spines pale (Figs 1, 5, 8). Spines of scutellum and metanotum pale, with their tips somewhat darkened (Figs 1, 4, 7, 8, 14). Meso- and metapleura generally dark brownish; meso- and metathoracic supracoxal lobes pale whitish on their posterior margin (Figs 1, 8, 14). Legs: fore coxa light brownish with a median annulus and approximately the apical fourth pale whitish; middle and hind coxae brownish with their distal margin somewhat paler; fore trochanter with approximately basal half pale and distal half brownish; middle and hind trochanters pale with an ill-defined median brownish spot (Figs 1, 8, 9, 11). General coloration of fore femora brownish, with four narrow annuli and apex, more extensively, pale; larger spiniferous processes with their basis whitish and the distal spine blackish (Figs 1, 9, 11). Middle and hind femora generally pale with six large dark annuli, which are bordered by contiguous narrower darker annuli, forming a set of bicolored large annuli, the first at base of the femora, somewhat smaller, the following ones separated by a distance approximately equivalent to the total length of each annulus (including their darker extremities), the more distal, far from apex by approximately the same equivalent distance (Figs 1, 4–6, 8, 14). Fore tibia mostly pale brownish with approximately the basal fourth and a submedian basal annulus pale; on the basal fourth, a small pair of dark spots on dorsal and ventral surfaces approximately at midpoint of this pale portion (Figs. 1, 9, 11). Middle and hind tibiae pale, a subbasal, small, dark spot on dorsal surface followed by two large faintly dark annuli, bordered by contiguous, narrow, darker annuli, the more distal somewhat larger, after them, a small, dark annulus approximately as far as the distance between the previous large annuli; all these markings on the basal half and basal third of the segment of middle and hind tibia, respectively; apices of both tibiae darkened towards apices (Figs 1, 4–8, 14). Fore tarsi pale brownish, second tarsomere paler (Fig. 11); middle and hind tarsi absent. Forewing brownish with most veins paler to whitish; a few oblique ill-defined, small, pale stripes or markings on basal half, between veins; a large, curved, whitish stripe running over Pcu cross vein, distal vein of basal cell and basal portion of discal cell; a diffuse texture formed by small, irregular, whitish spots or transverse lines inside discal cell and a narrow, longitudinal, submedian, oblique, somewhat irregular line along discal cell, except at its basal portion, and two larger, oblique, whitish stripes over distal veins of the discal cell, which join a large whitish spot, which runs transversely obliquely towards apex, subdistally between lateral margins of the wing and medially attaining the apex of the wing at its median portion; this large whitish marking is speckled with brownish spots at median portion; the lateral portions to this large whitish marking are otherwise brownish and speckled by several whitish markings; the tip of the wing is shortly brownish at its median portion (Figs 1, 8, 12). Hind wings hyaline; veins somewhat darker (Figs 6–8). Abdomen generally brownish with scattered, ill-defined, pale and dark markings and

Figures 8–11. *Polauchenia difficilis* (Dohrn, 1860), comb. nov., male lectotype (here designated) **8** ventrolateral view, left side **9** fore lobe of pronotum, head and right fore leg, lateral view **10** head, fore lobe and petiole of pronotum, lateral view **11** left fore leg detached from the specimen, lateral view. Scale bars: 0.5 mm (**9, 10**); 0.26 mm (**11**).

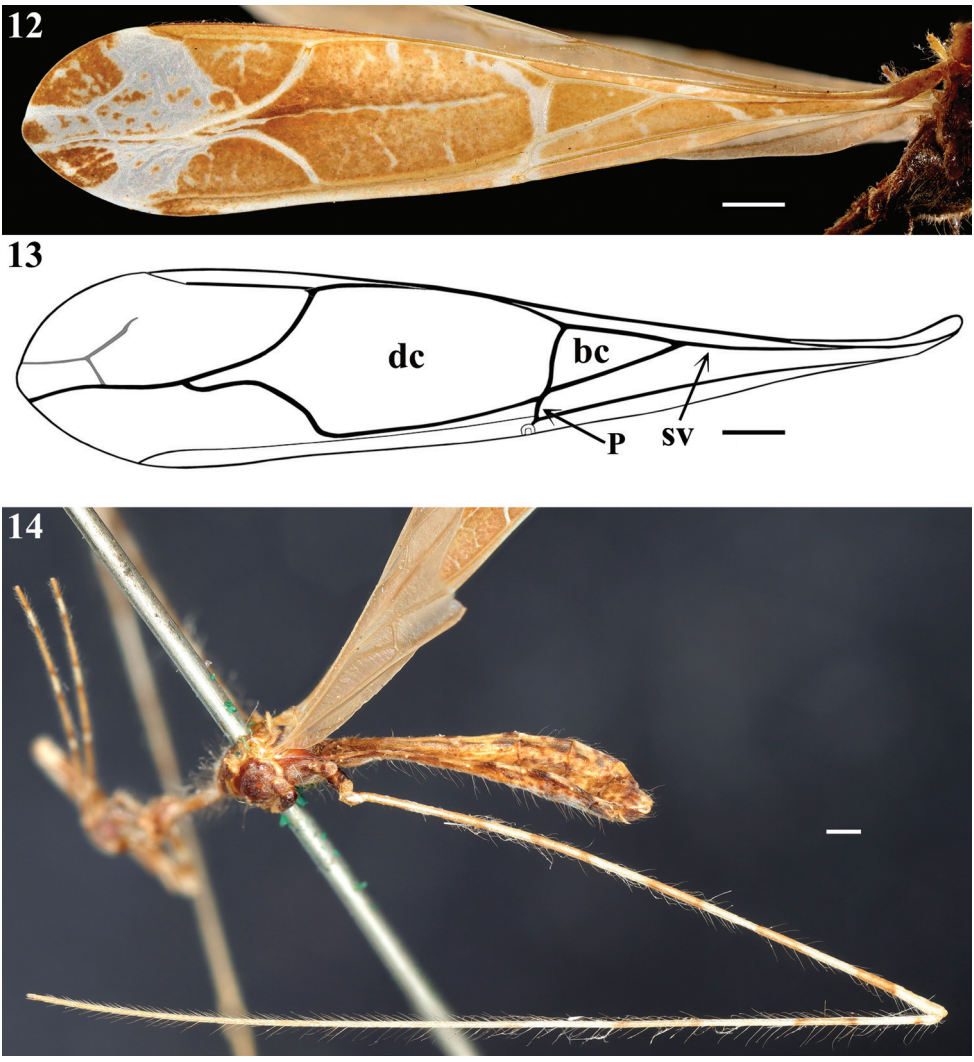

Figures 12–14. *Polauchenia difficilis* (Dohrn, 1860), comb. nov., male lectotype (here designated) **12, 13** forewing **13** schematic outline **14** meso and metathorax, abdomen and left hind leg, lateral view. Abbreviations: bc basal cell, dc discal cell, P Pcu cross vein, sv single vein emitted from the basal cell. Scale bars: 0.5 mm (**12–14**).

spots, respectively; connexivum pale with distal dark spots, which are proportionally larger in relation to the pale basal portion on the last three segments; sternites additionally with thin, interrupted and ill-defined pale lines; posterolateral margins of sternite VIII pale whitish; genital capsule dark with parameres pale (Figs 1, 4–8, 14). *Vestiture*: integument covered with very numerous and long thin setae, and with a short and very dense pubescence formed by thin, curved or adpressed setae (Figs 1, 8–11, 14). Fore femur: posteroventral series beginning at the base of the article and ending far from

apex, composed of about 11 large and medium-sized spiniferous processes, the most basal of which with its apex slightly inclined toward apex of article. A sparse series of very long, darker and strong setae accompanies the posteroventral series. Lengths of larger processes combined with apical spines about as long as or somewhat shorter than the diameter of segment. Fore tibiae with numerous stiff setae on subapical dorsal depression (Figs 9, 11). Forewing almost completely glabrous, with a few scattered short thin setae at basal portion and a few scattered somewhat longer ones along costal vein (Fig. 12). Hind wings glabrous. *Structure*. Integument moderately shiny. Head (Figs 1, 4, 5, 8–10): elongated; anteocular portion longer than postocular. Transversal (interocular) sulcus deep, situated somewhat anteriorly to middle of eyes. Eyes globose, reaching dorsal outline of head at interocular sulcus and not reaching ventral outline of head; a pair of very short tubercles just behind interocular sulcus. Antenna inserted closer to apex of head than to the eyes; first antennal segment thin, slender; others absent. First two visible labial segments thicker than the distal segment; apex of segment III slightly posteriorly to level of midportion of eye; segment IV ending close to midpoint of stridulitrum at its anterior portion. Thorax (Figs 1, 4–14): pronotum pedunculate; petiole approximately 1.3 times as long as fore lobe, the latter semioval; humeral rounded tubercle with a short acute spine. Spines of scutellum and metanotum somewhat elongated, obliquely directed upwards, apices acute, the latter somewhat longer than the former. Fore legs slender; fore coxae elongated, approximately 1.3 times longer than petiole; fore tibiae thinner and slightly shorter than fore femora, somewhat curved; slightly depressed in dorsal portion subapically; somewhat thickened at apex. Mid and hind legs very long, slender, slightly curved; tibiae somewhat thinner and longer than femora. Fore tarsus short, three-segmented, slender; other absent. Forewings slender; basal cell triangular, with a single directed vein emitted from its base and with Pcu cross vein meeting it slightly posterior to the level of its apical portion; pterostigma ending somewhat far from apex of the wing. Abdomen: slender, slightly enlarged towards posterior half. Last tergite narrowed towards apex, subtriangular, posterior margin rounded, with a short prolongation posteriorly, covering most of the genital capsule. Eighth sternite covering approximately half of the pygophore, ventrally.

Discussion

The transfer of *D. difficilis* to *Polauchenia* is in accordance with the aforementioned assertion that *Dohrnemesa* can be separated from *Polauchenia* by the absence/presence of spined humeri and the presence/absence of a free short vein emitted from the base of the basal cell of the forewing in the former and latter genus, respectively (Wygodzinsky 1966; Gil-Santana and Ferreira 2017).

Yet, the inclusion of *P. difficilis*, comb. nov. in *Polauchenia* agrees with the following diagnostic features of the genus (McAtee and Malloch 1925; Wygodzinsky 1966;

Forero 2004): medium-sized species (11–20 mm in length); pronotum pedunculate (Figs 1, 8, 10); scutellum and metanotum with a spine (Figs 1, 8); posteroventral series of fore femora beginning at base of article, composed of large and small spiniferous processes bearing relatively slender apical spines; large processes of subequal size, the most basal either straight or slightly inclined toward apex of article; fore tarsi three-segmented (Figs 9, 11); forewings with two cells, base of basal cell pointed, emitting a single longitudinal vein towards axillary region (Figs 1, 12, 13).

Additionally, among other characteristics of *Polauchenia*, the following are noteworthy and also present in *P. difficilis*, comb. nov.: all species are conspicuously marked with light and dark colors (e.g., Figs 1, 8–12); petiole of pronotum ranging from slightly shorter to much longer than fore lobe of pronotum (Figs 1, 8, 10) and series of processes of the fore femora often accompanied by strong elongated setae (Figs 9, 11) (Wygodzinsky 1966; Gil-Santana and Ferreira 2017).

The only small difference is the total length, which was recorded as being 10.6 mm for *P. difficilis*, comb. nov., very close to the minimum stated by previous authors (11 mm), allowing us to state 10.6 mm as the actual minimum of the genus. Moreover, it is noteworthy that Dohrn (1860, 1863) recorded 11 mm as the length of the lectotype of *W. difficilis*. It is not possible to know how accurately A. Dohrn measured the specimen or if he rounded the measurement to an exact number. It is possible that the specimen was originally 11 mm in length when examined by him but due to the passing of time, the specimen may have shortened a little.

In any case, it becomes clear that the transfer of the species studied here from *Dohrnemesa*, the genus where it was currently included (Wygodzinsky 1966) to *Polauchenia* is in accordance with the differences between these genera and the diagnostic characteristics of *Polauchenia*.

On the other hand, some characteristics which Wygodzinsky (1966) believed *P. difficilis*, comb. nov. would have (fore lobe subglobular, abruptly narrowed behind and distinctly separated from petiole; a strongly widened abdomen with flaring connexival segments) are absent in this species. Therefore, it becomes clear that Wygodzinsky (1966) had limited knowledge of the species and certainly never examined the type of *W. difficilis*, providing an additional argument to disregard his placement of *P. difficilis*, comb. nov. in *Dohrnemesa*.

The type specimen of *Westermannia difficilis* was designated here as a lectotype following the Art. 74.1 of ICZN.

Taking into account the taxonomical change proposed here, seven species are now included in *Polauchenia* and nine in *Dohrnemesa* (*D. albuquerquei* Wygodzinsky, 1966, *D. buyassuana* Wygodzinsky, 1958, *D. carvalhoi* Wygodzinsky, 1966, *D. exporrecta* Wygodzinsky, 1958, *D. kuarajucassaba* Gil-Santana & Ferreira, 2017, *D. lanei* Wygodzinsky, 1945, *D. oliveirai* Gil-Santana & Ferreira, 2016, *D. reimoseri* (Wygodzinsky, 1950), *D. santosi* Wygodzinsky, 1945) (Wygodzinsky 1966; Gil-Santana and Ferreira 2016, 2017).

Key for the species of *Polauchenia*, modified from Wygodzinsky (1966) and Gil-Santana and Ferreira (2017)

1 Postocular region of the head with a median spine, besides a pair of lateral spined tubercles ..... ***unicornis*** **Maldonado, 1968**

– Postocular region of the head without a median spine, with or without a pair of lateral spined or rounded tubercles..... **2**

2 Petiole of pronotum quite longer, at least 1.3 times as long as the fore lobe **3**

– Petiole of pronotum little, if any longer than fore lobe..... **6**

3 Petiole of pronotum approximately 1.3–1.5 times as long as fore lobe; length 10.6–14 mm..... **4**

– Petiole of pronotum at least twice longer than the length of fore lobe; length 15 mm or longer..... **5**

4 Petiole of pronotum approximately 1.5 times as long as the fore lobe; length 14 mm; pale markings of the antenna, middle and hind femora simple .... ***paraprotentor*** **Gil-Santana & Ferreira, 2017**

– Petiole of pronotum approximately 1.3 times as long as the fore lobe; length 10.6 mm; pale markings of the antenna, middle and hind femora bordered by darker markings ..... ***difficilis*** **(Dohrn, 1860)**

5 Length 17.5 mm; females (males unknown) brachypterous, the forewing reaching at about middle of abdomen..... ***marcapata*** **Wygodzinsky, 1966**

– Length not more than 15 mm; female slightly brachypterous, forewing reaching far posterior to the middle of abdomen..... ..... ***protentor*** **McAtee & Malloch, 1925**

6 Length 11 mm; postocular region of the head without projections, spines of scutellum and metanotum yellowish ..... ***schubarti*** **Wygodzinsky, 1950**

– Length 16 mm; postocular region of the head with a pair of spined conical tubercles; spines of scutellum blackish..... ..... ***biannulata*** **McAtee & Malloch, 1925**

Acknowledgements

We are very grateful to Catarina Lopes (Instituto Oswaldo Cruz, Rio de Janeiro, Brazil), an anonymous reviewer, and Laurence Livermore for their valuable comments and suggestions.

References

Castro-Huertas V, Forero D, Grazia J (2020) Evolution of wing polymorphism and genital asymmetry in the thread-legged bugs of the tribe Metapterini Stål (Hemiptera, Reduviidae, Emesinae) based on morphological characters. Systematic Entomology 46(1): 28–43. https://doi.org/10.1111/syen.12445

Champion GC (1899) Insecta Rhynchota. Hemiptera–Heteroptera, Fam. Reduviidæ, Subfam. Emesinæ Vol II. In: Godman FD, Salvin O (Eds) Biologia Centrali Americana. Taylor and Francis, London, 162–175. [pl. X] https://www.biodiversitylibrary.org/page/594873

Dohrn A (1860) Beiträge zu einer monographischen Bearbeitung der Familie der Emesina. Linnaea Entomologica 14: 206–255. [+ 1 pl.] https://www.biodiversitylibrary.org/page/44713025

Dohrn A (1863) Beiträge zu einer monographischen Bearbeitung der Familie der Emesina (Zweites Stück). Linnaea Entomologica 15: 42–63. https://www.biodiversitylibrary.org/page/44063429

Forero D (2004) Capítulo 5. Diagnosis de los gêneros neotropicales de la família Reduviidae (Hemiptera: Heteroptera), y su distribución em Colombia (excepto Harpactorinae). In: Fernández F, Andrade G, Amat G (Eds) Insectos de Colombia Vol. 3. Universidad Nacional de Colombia, Bogotá DC, 128–275.

Gil-Santana HR, Ferreira RL (2016) A new species of *Dohrnemesa* from Brazil, with notes on the male of *D. carvalhoi* and on *D. albuquerquei* (Hemiptera: Heteroptera: Reduviidae: Emesinae). Zootaxa 4173(6): 583–595. https://doi.org/10.11646/zootaxa.4173.6.6

Gil-Santana HR, Ferreira RL (2017) A new species of *Dohrnemesa* and a new species of *Polauchenia* from Brazil (Hemiptera: Heteroptera: Reduviidae: Emesinae). Zootaxa 4338(2): 201–240. https://doi.org/10.11646/zootaxa.4338.2.1

Gil-Santana HR, Forero D, Weirauch C (2015) Assassin bugs (Reduviidae excluding Triatominae). In: Panizzi AR, Grazia J (Eds) True Bugs (Heteroptera) of the Neotropics, Entomology in Focus 2. Springer Science+Business Media, Dordrecht, 307–351. https://doi.org/10.1007/978-94-017-9861-7_12

ICZN [International Comission on Zoological Nomenclature] (1999) International code of zoological nomenclature. Fourth Edition. London: The International Trust for Zoological Nomenclature. https://www.iczn.org/the-code/

Kirkaldy GW (1904) Bibliographical and nomenclatorial notes on the Hemiptera. No. 3. The Entomologist 37: 279–283. https://doi.org/10.5962/bhl.part.2885

Lethierry L, Severin G (1896) Catalogue général des Hémiptères. Tome III. Hétéroptères. R. Friedländer & Fils, Libraires-Éditeurs, Berlin, 275 pp. https://www.biodiversitylibrary.org/page/15708236

Maldonado CJ (1990) Systematic catalogue of the Reduviidae of the world. Caribbean Journal of Science, Special publication No. 1, University of Puerto Rico, Mayagüez, 694 pp.

McAtee WL, Malloch JR (1925) Revision of the American bugs of the reduviid subfamily Ploiariinae. Proceedings of the United States National Museum 67: 1–153. https://doi.org/10.5479/si.00963801.67-2573.1

Papavero N (1973) Essays on the history of Neotropical Dipterology, with special reference to collectors (1750–1905). Vol. 2. Universidade de São Paulo, São Paulo, 217–446. https://www.biodiversitylibrary.org/item/181269

Schuh RT, Weirauch C, Wheeler WC (2009) Phylogenetic relationships within the Cimicomorpha (Hemiptera: Heteroptera): a total-evidence analysis. Systematic Entomology 34: 15–48. https://doi.org/10.1111/j.1365-3113.2008.00436.x

Stål C (1872) Enumeratio Reduviinorum Americae. In: Enumeratio Hemipterorum. Kongliga Svenska Vetenskaps-Akademiens Handlingar 10: 66–128. https://www.biodiversitylibrary.org/page/12796979

Walker F (1873) Catalogue of the specimens of Hemiptera Heteroptera in the Collection of the British Museum (Part VIII). Printed for the Trustees of the British Museum, London, 220 pp. https://www.biodiversitylibrary.org/page/12840212

Weirauch C (2008) From four- to three- segmented labium in Reduviidae (Hemiptera: Heteroptera). Acta Entomologica Musei Nationalis Pragae 48: 331–344.

Wygodzinsky P (1945) Notas e descrições de "Emesinae" neotropicais (Reduviidae, Hemiptera). Revista Brasileira de Biologia 5: 247–262.

Wygodzinsky P (1949) Elenco sistematico de los reduviiformes americanos. Instituto de Medicina Regional de la Universidad Nacional de Tucumán, Monografia 1: 1–102.

Wygodzinsky P (1966) A monograph of the Emesinae (Reduviidae, Hemiptera). Bulletin of the American Museum of Natural History 133: 1–614. http://digitallibrary.amnh.org/handle/2246/1675

ZooKeys 1043: 117–131 (2021)
doi: 10.3897/zookeys.1043.67730
https://zookeys.pensoft.net

RESEARCH ARTICLE

A peer-reviewed open-access journal
ZooKeys
Launched to accelerate biodiversity research

Drawing the Excalibur bug from the stone: adding credibility to the double-edged sword hypothesis of coreid evolution (Hemiptera, Coreidae)

Royce T. Cumming[1,2,3], Stéphane Le Tirant[1]

1 *Montreal Insectarium, 4581 rue Sherbrooke est, Montréal , H1X 2B2, Québec, Canada* **2** *Richard Gilder Graduate School, American Museum of Natural History, New York, NY 10024, USA* **3** *Biology, Graduate Center, City University of New York, NY, USA*

Corresponding author: Royce T. Cumming (phylliidae.walkingleaf@gmail.com)

Academic editor: N. Sinichenkova | Received 22 April 2021 | Accepted 22 May 2021 | Published 14 June 2021

http://zoobank.org/4C659B8F-36DB-47F6-A285-F60424573BB7

Citation: Cumming RT, Le Tirant S (2021) Drawing the Excalibur bug from the stone: adding credibility to the double-edged sword hypothesis of coreid evolution (Hemiptera, Coreidae). ZooKeys 1043: 117–131. https://doi.org/10.3897/zookeys.1043.67730

Abstract

A new genus and species of exaggerated antennae Coreidae is described from Myanmar amber of the Late Cretaceous (Cenomanian stage). *Ferriantenna excalibur* **gen. et sp. nov.** appears related to another Cretaceous coreid with exaggerated antennae, *Magnusantenna* Du & Chen, 2021, but can be differentiated by the fourth antennal segment which is short and paddle-like, the undulating shape of the pronotum and mesonotum, and the shorter and thicker legs. The new coreid, with elaborately formed antennae and simple hind legs instead of the typical extant coreid morphology with simple antennae and elaborately formed hind legs, begs the question: why were the elaborate features of the antennae lost in favor of ornate hind legs? Features that are large and showy are at higher risk of being attacked by predators or stuck in a poor molt and subjected to autotomy and are therefore lost at a higher rate than simple appendages. We hypothesize that because elaborate antennae play an additional significant sensory role compared to elaborate hind legs, that evolutionarily it is more costly to have elaborate antennae versus elaborate hind legs. Thus, through the millenia, as coreid evolution experimented with elaborate/ornate features, those on the antennae were likely selected against in favor of ornate hind legs.

Keywords

Autotomy, Burmese, Cenomanian, Cretaceous, extinct, fossil, leaf-footed bugs, Mesozoic

Introduction

The coreids (leaf-footed bugs) are a diverse group of hemipterans with a cosmopolitan distribution (of ~3100 species in ~260 genera; Henry 2017) and are known for their often-elaborate expansions and ornamentation of their hind femora and hind tibiae, and in some cases the humeral angles of the pronutum are even exaggerated (Fig. 1; Dolling 2006). These adaptations have been reported as being used for intraspecific competition/display (Eberhard 1998; Procter et al. 2012) and sensorial capabilities (for features on the antennae; Gonzaga-Segura et al. 2013). The superfamily Coreoidea as a whole has been recovered as monophyletic with an age of ~125 mya within recent fossil calibrated phylogenetic analyses (Johnson et al. 2018). Interestingly, while the Coreoidea has been recovered as monophyletic, the current internal taxonomic organizations have not (Forthman et al. 2019). When many of the morphological features which have been used in analyses in the past were reviewed alongside these recent large-scale molecular analyses it was found that most clades had few synapomorphies which define them, and most morphological features were found to be homoplastic (Forthman et al. 2019).

The first reported Coreidae species from Cretaceous Burmese amber was the recently described *Magnusantenna wuae* Du & Chen, 2021 (Fig. 2C), and was only the fifth species of coreid described from the Cretaceous (the others being impression fossils, not amber inclusions; Du et al. (2021)). Du et al. (2021) presented the first coreid from the Cretaceous with expansions on the antennae, a feature that is also seen in a few extant coreid species (Fig. 1D), but what was notable about their description was that the antennae were far more elaborate than any known extant species.

Unfortunately, with the fossil record of coreids rather fragmented and often from partial or nymphal specimens this still leaves a great deal of confusion surrounding their evolutionary history. Thankfully with nymphal antennae morphology rather stable into adulthood (Du et al. 2021) recent and herein described fossilized nymphs present a unique opportunity to understand the possible origin of elaborate morphological features.

Materials and methods

The amber containing the holotype specimen was collected from the well-known Hukawng Valley in northern Myanmar, a prolific site of amber excavation (Grimaldi et al. 2002). The age of this amber deposit is estimated to be ~98.79 ± 0.62 million years old, within the Cenomanian stage of the Cretaceous (Shi et al. 2012). The holotype specimen described herein was morphologically reviewed using a 2x-225x trinocular boom stand stereo microscope (#ZM-4TW3-FOR-20MBI3) and photographs were taken with the attached high-speed 20MP camera (#MU2003-BI-CK) (AmScope,

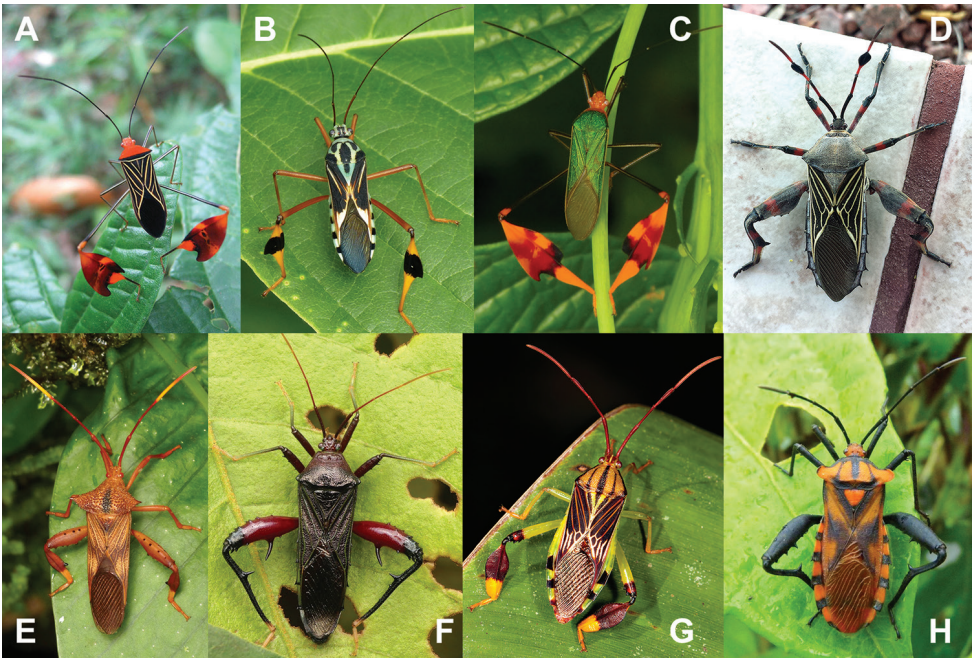

Figure 1. Examples of ornamentation in live extant coreids. Images **A–C, G** with expansions on the hind tibiae. Images **D–H** with hind leg spination **D** with expansions to the third antennal segment. Images **B, C, E–H** photographed by Andreas Kay (Ecuador), other images with appropriate citations given individually **A** *Anisocelis flavolineata* from Veraguas Province, Panama, photographed by Dirk van der Made (Netherlands) **B** Unidentified Coreidae from Ecuador **C** *Anisoscelis foliacea* from Ecuador **D** *Thasus* sp. from Santa Cruz County, Arizona, USA, photographed by Alan Schmierer (USA) **E** Unidentified Coreidae from Ecuador **F** Unidentified Coreidae from Ecuador **G** *Melucha quinquelineata* from Ecuador **H** *Piezogaster* cf. *humeralis* from Ecuador.

Irvine, USA). Illumination was from a 6-Watt LED dual gooseneck illuminator lit by an #85-265VAC/50-60Hz lighting unit (AmScope, Irvine, USA). Measurements were taken using AmLite digital camera software for Mac OS X 10.8 64-bit which was calibrated with a microscope stage calibration slide (#MR095), 0.01mm div. (AmScope, Irvine, USA). Adobe Photoshop Elements 13 (Adobe Inc., San Jose, USA) was used as post-processing software.

Illustrations were done by scientific illustrator Liz Sisk (Washington D.C., USA) using either photographs of the holotype, photographs saved from various online sources illustrating non-type specimens or recreated from the photographs/illustration presented in Du et al. (2021) in order to present side-by-side images of a uniform style.

The holotype specimen is deposited within the Montreal Insectarium, Montreal, Quebec, Canada (IMQC).

Systematic paleontology

Class Insecta Linnaeus, 1758
Order Hemiptera Linnaeus, 1758
Family Coreidae Leach, 1815
Subfamily Coreinae Leach, 1815

Genus *Ferriantenna* gen. nov.
http://zoobank.org/40E251C3-987F-4F74-A89B-6545E487EDC8

Type species. *Ferriantenna excalibur* gen. et sp. nov., herein designated

Taxonomic remarks. The taxonomic placement of this genus is rather uncertain, largely owing to the lack of adult specimens to allow review of genitalia, wing venation, and presence or lack of ocelli. Morphologically this genus appears to be closely related to *Magnusantenna* Du & Chen, 2021 based upon the elaborate antennae, square head shape, and long abdomen with parallel margins. Based upon this assumed close relationship we tentatively place this new genus and species within the Coreinae alongside *Magnusantenna* but would not be surprised if a taxonomic adjustment is necessary once adult specimens are hopefully one day recovered. Additional higher taxonomic possibilities, which can be ruled out, are Yuripopovinidae due to the lack of a distinct collar in our new taxon (Azar et al. 2011). Further, Yuripopovinidae typically have cylindrical antennomeres in cross section (although the recently described *Reticulatitergum hui* Du et al. 2019 does have a terminal antennomere which is flattened and rather similar in shape to our *Ferriantenna* gen. nov. (Fig. 2A; Du et al. 2019)). An additional clade which can have similar general habitus morphology are the Alydidae (particularly the Micrelytrinae which can have thin parallel-sided bodies and long legs very similar to *Magnusantenna wuae*; Fig. 2C). The Alydidae can be differentiated from Coreidae by the length of the bucculae, with the bucculae shorter, not extending posteriorly beyond the base of the antennae in Alydidae but longer in Coreidae, extending posteriorly beyond the base of the antennae (Swanson 2011). Within *Magnusantenna wuae* Du et al. (2021) clearly state that the bucculae are long extending posteriorly beyond the base of the antennae and therefore due to this feature would fit within Coreidae. Unfortunately, the amber piece that our *Ferriantenna* gen. nov. is within is too thick to clearly see the ventral surface of the head, but it does appear that the bucculae are longer than the base of the antennae and therefore more likely a Coreidae than an Alydidae.

The general morphological features of this genus fit well within Coreinae, namely the expanded antennal segments, the length ratios of the various antennomeres (the second and third segments of similar lengths), the smooth pronotum, and the straight femora and tibiae (Schuh and Slater 1995). At present there are three other subfamilies recognized within the coreids: Hydarinae, Meropachyinae, and Pseudophloeinae (CoreoideaSF Team 2021). The following features characterize each of the other subfamilies and help to add credibility to this genus being placed within Coreinae. Hydarinae

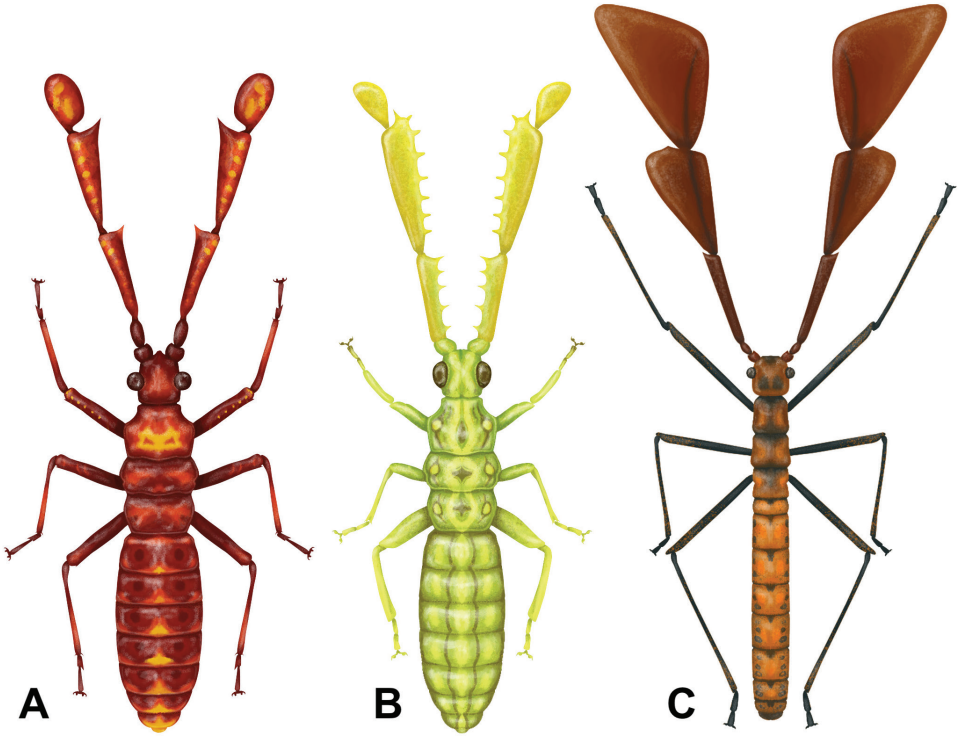

Figure 2. Artist recreation of the presently known three Cretaceous coreids with elaborate antennae. Illustrations by Liz Sisk (USA). Dorsal habitus scaled to same uniform length to highlight the antennae to body ratios. Colorations are artistic recreations based upon extant coreids rather than the actual specimen, whose color was not preserved in the amber **A** *Ferriantenna excalibur* gen. et sp. nov. **B** *Ferriantenna* "club-like antennae" **C** *Magnusantenna wuae*.

have the third antennomere more than twice as long as the second (in *Magnusantenna* and *Ferriantenna* gen. nov. these segments are similar in length (Packauskas 1994)). The subfamily Pseudophloeinae is difficult to morphologically distinguish from other coreids as different authors consider different features significant for differentiation (e.g., Packauskas 1994; Moulet 1995; Schuh and Slater 1995; Hamouly et al. 2010; Schuh and Weirauch 2020). Due to the multiple morphological features which liken our genus to Coreinae we are fairly confident that these fossils do not fall within Pseudophloeinae. Meropachyinae are a small subfamily restricted to the western hemisphere and have a distal spine on the apex of the metatibiae and the metafemora are prominently thickened, notably broader than the pro- and mesofemora (Packauskas 1994; Brailovsky and Barrera 2009). Coreinae has repeatedly been recovered as paraphyletic with regards to Meropachyinae and based upon the typical Meropachyinae leg morphology we expect these fossil coreids do not fall within this clade but likely somewhere else within the Coreinae (Forthman et al. 2019, 2020; Kieran et al. 2019). Review of spermatheca within Coreidae by Pluot-Sigwalt and Moulet (2020) found

that Hydarinae and Pseudophloeinae are morphologically unique but that Coreinae and Meropachyinae were similar, adding credibility to phylogenetic results which don't recover Coreinae and Meropachyinae as unique (Kieran et al. 2019; Forthman et al. 2019, 2020).

Within the Coreinae there are several tribes which have an antennomere that is enlarged (e.g., Nematopini or Chariesterini with only the singular third antennomere flattened; Fig. 1D; CoreoideaSF Team 2021). This similarity alone does not warrant a tribal placement and the authors hope that eventually fossils of adult specimens are recovered to help determine a more accurate taxonomic placement as no extant tribe fits morphologically well.

Diagnosis. Antennae four segmented, long, but not longer than the body (head, thorax, and abdomen). First antennal segment short and robust (slightly longer than wide or about equal in length and width; always shorter than head length); second and third segments ornamented and quite variable in form interspecifically (can be marked throughout with granulation, setation, or prominent tubercles with margins straight or with spination), each at least three times longer than wide, with the third segment slightly wider and longer than the second segment; and the fourth segment is only slightly longer than head length, flat, and paddle-like, lacking intricate features/expansions as present on the second and third segments. Head approximately as long as wide, compound eyes spherical and variable in their size (can be large, occupying most of the lateral margins, or narrower, restricted to the center third and strongly protruding), located on the center of each side of the head. Pronotum with a margin that expands to the posterior third then contracts slightly. Mesonotum gently expands to the midline and then gently contracts to the posterior. Metanotum with margins that can be parallel or slightly rounded. Abdomen slender, notably longer than wide, with parallel margins. Legs stout, not particularly long. Femora approximately two times as wide as the tibiae, but of similar lengths. Tarsi with two segments, bearing two claws.

Differentiation. Several features differentiate the new genus from the assumed closely related genus *Magnusantenna* Du & Chen, 2021. First, the length ratios of the exaggerated antennal segments differ as *Magnusantenna* has the fourth segment approximately as long as, but notably broader than the third segment, versus *Ferriantenna* gen. nov. which has the fourth segment notably shorter than the third segment, appearing paddle-like. Additionally, the thickness and lengths of the legs differentiate these two genera as *Magnusantenna* has long thin legs (such as the hind legs which exceed the apex of the abdomen), versus *Ferriantenna* gen. nov. which has femora which are notably thicker than the tibiae, and specifically for the hind leg it appears that when fully outstretched they fall short or at most reaching the apex of the abdomen but do not exceed it. The thorax and abdomen of *Ferriantenna* gen. nov. are also notably broader than the head width versus *Magnusantenna* which has a very slender and long abdomen, thinner than the width of the quadrate head. Finally, the pro- and mesonotum differ slightly between these two genera as *Magnusantenna* has a pronotum which expands steadily from the anterior to the posterior and the mesonotum is parallel sided, versus *Ferriantenna* gen. nov. which has the pronotum expanding for the

anterior two thirds then slightly contracting, and the mesonotum appears to expand to approximately the middle and then contract to the posterior.

Discussion. Typically, Heteroptera have five instars, as in hemimetabolous insects which they resemble the adults in most morphological features. Our examined specimen which is the type species for this new genus appears to be a fourth instar nymph like was described within Du et al. (2021) based on the following characters they reference from Schuh and Slater (1995): posterior margins of the hind buds not reaching the anterior margin of the first abdominal tergite; ocelli absent; and tarsi two-segmented. As was noted within Du et al. (2021) amber typically does not preserve large inclusions well which is likely why all of these species are being observed as nymphs.

In addition to our herein described species, we have also seen images shared online of an additional species within *Ferriantenna* gen. nov. distinctly different from our *Ferriantenna excalibur* gen. et sp. nov. This second, undescribed *Ferriantenna* species has similar characteristics of the thorax, abdomen, and legs, and the fourth antennomere which is notably smaller and paddle-like (Fig. 2B). This undescribed species however differs in that it has the second and third antennal segments heavily armored with prominent tubercles and granulation, making the antennae appear like a medieval two-handed iron spiked mace (Boeheim 1890) instead of blade-like as is seem in *Ferriantenna excalibur* gen. et sp. nov. This second species, known only from photos shared online of a singular specimen, was being publicly offered for sale on eBay has since been sold. Unfortunately, the specimen could not be traced/examined and therefore we are unaware whether this specimen will end up in a museum collection for research or with a private collector.

The difference in leg lengths between *Magnusantenna* and *Ferriantenna* gen. nov. is likely due to the size of the antennae in relation to the body, as the *Ferriantenna* gen. nov. are notably less expanded and therefore require less leverage to maintain a stable footing, versus *Magnusantenna* which needed the longer legs to create a larger footprint to balance the massive antennae.

Etymology. The generic name is derived from Latin prefix *ferri* (meaning weapon) and Latin *antenna* (meaning yardarm of a ship/sail yard which was the origin of the "feeler or horn" of an insect; https://www.etymonline.com/search?q=antenna). This genus epithet is referring to the weapon-like appearance of the antennae of these insects (Fig. 2A, B). Gender is neuter.

***Ferriantenna excalibur* gen. et sp. nov.**
http://zoobank.org/D28929A-DF04-4038-BB44-B23DAE46BB82
Figures 2A, 3, 4

Material examined. *Holotype*: Amber specimen #BHM10200800678. Flat and round rectangular piece of amber, approximately 1.0 cm by 1.1 cm with high clarity and small debris throughout that does not black visibility of the specimen (Fig. 3C). Specimen partially complete yet well-preserved, likely fourth instar. Missing the ter-

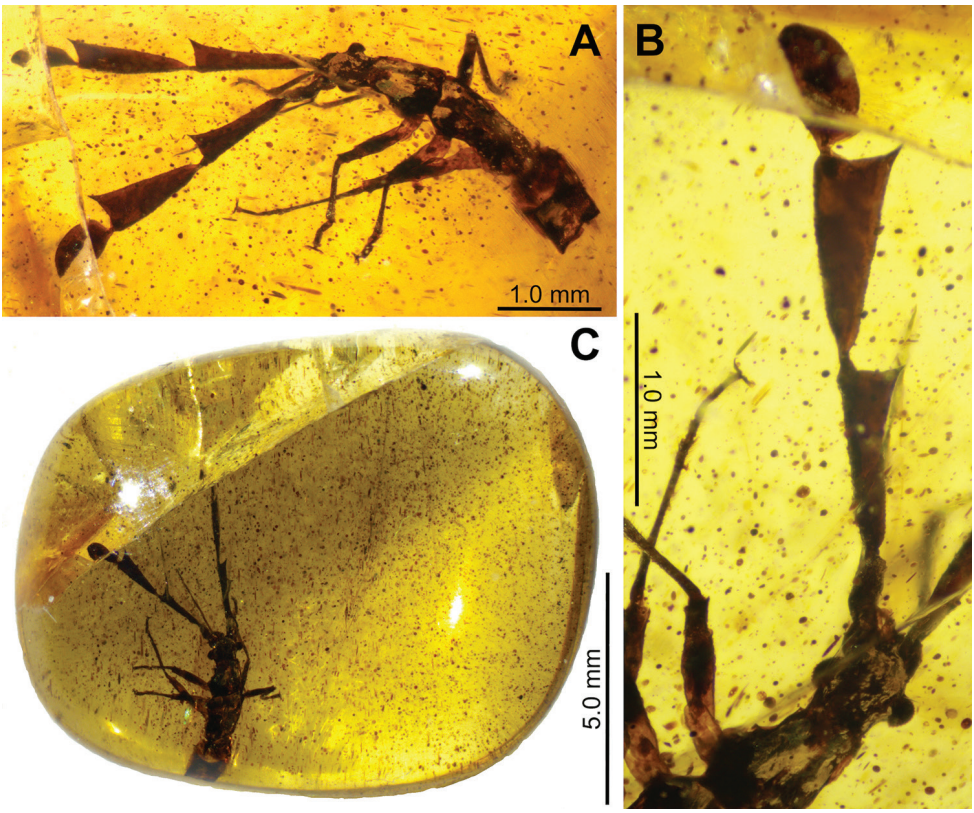

Figure 3. *Ferriantenna excalibur* gen. et sp. nov. holotype **A** dorsolateral habitus **B** left antennae lateral and head dorsal **C** amber specimen #BHM10200800678 showing the inclusion.

minal two or three segments of the abdomen. Deposited in the Montreal Insectarium (IMQC). Unknown sex.

Type locality and horizon. Kachin State, Myanmar; Upper Cretaceous ~98.79 ± 0.62 million years old (Shi et al. 2012). At present we are only aware of this genus and species being found in northern Myanmar from this stratum.

Differentiation. At present this is the only formally described species within this new genus. Refer to the differentiation within the above genus section for discussion on the closely related *Magnusantenna wuae*. We are aware of a second, undescribed *Ferriantenna* gen. nov. species (Fig. 2B) which differs by having the second and third antennomeres which are heavily armored with tubercles, not flattened with each segment narrow at the base and widening gradually to the sharply pointed anterior like is seen in *Ferriantenna excalibur* gen. et sp. nov. (Fig. 2A). The elaborate antennae differentiate these extinct species from all known extant coreids which at most have a single slightly expanded antennal segment.

Description. Mostly complete nymph which appears to be fourth instar. Sex unknown due to the instar stage and missing terminalia of the abdomen. Specimen

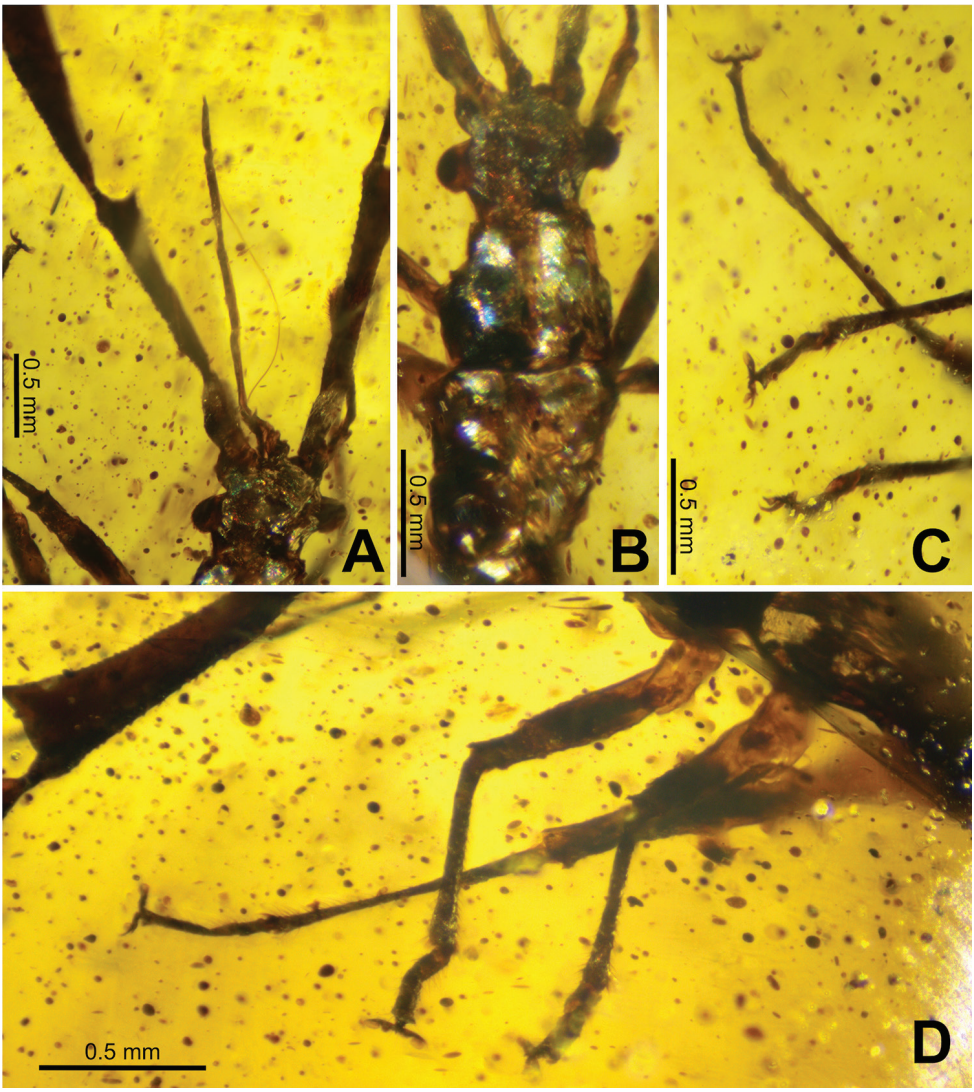

Figure 4. *Ferriantenna excalibur* gen. et sp. nov. holotype **A** extended labium with stylet exposed to the right **B** head, pronotum, and mesonotum, dorsal **C** left tarsi and distal ends of the tibiae **D** legs on the left side, dorsolateral.

complete except for the terminal two or three abdominal segments (Fig. 3A). Overall length (including antennae) 6.87 mm (measured to the end of the abdomen which is missing the terminal segments, so the actual length of the insect is slightly longer).

Head. Antennal socket protruding from the front of the head (Fig. 4B), approximately 0.11 long by 0.20 mm wide, about as wide as the first antennomere. Head subquadrate, 0.50 mm long by 0.46 mm wide (without including compound eyes), including compound eyes head is 0.76 mm wide. Vertex relatively smooth, no notable

textures or structures (Fig. 4B). Clypeus protruding slightly, labrum stout, not prominent. Labium tetramerous, fully extended reaches beyond the apex of the second antennomere, labiomeres one, two, and three similar in length, four approximately half as long as any of the others (Fig. 4A). Apex of the fourth labiomere sharply tapering to a fine point (Fig. 4A). Lengths: first labiomere 0.41 mm, second labiomere 0.51 mm, third labiomere 0.39 mm, fourth labiomere 0.26 mm. Compound eyes prominently protruding but not overly large, located in the center and taking up approximately one third of the lateral head margins (Fig. 4B).

Antennae. Antennae tetramerous (Fig. 3B), length 3.22 mm, approximately equal in length to the damaged holotype body length (if the abdomen were complete the antennae would be slightly shorter in length than the body). First antennomere tubular, with sparse and short setae, 0.28 mm long and 0.14 mm wide. Antennomeres two through four appear to be laterally flattened due to the way the antennae are held in the amber. Second antennomere approximately right triangular in shape, with the anterior wide and the posterior narrow and the triangular expansion raised dorsally. Margins finely granular, with the dorsal margin marked with few fine setae, the ventral margin is marked with slightly longer and more prominent setae. Antennomere surfaces are relatively smooth, with minimal setae and only prominent granulation along the margins. Second antennomere length 1.08 mm and maximum width (on the anterior end) 0.39 mm. Third antennomere similar in shape and texture to the second antennomere but slightly wider throughout the length and on the anterior than the second antennomere; approximately right triangular in shape, with the anterior wide and the posterior narrow with the triangular expansion raised dorsally. Margins finely granular, with the dorsal margin with only fine setae, the ventral margin with slightly longer and more prominent setae. Antennomere surfaces relatively smooth, with minimal setae and fine granulation along the margins. Third antennomere 1.15 mm long and maximum width (on the anterior end) 0.52 mm. Fourth antennomere paddle-shaped and notably smaller than the previous two, with a narrow base expanding into a rounded segment; 0.71 mm long and 0.40 mm at the widest point (in the center). Fourth antennomere surfaces are more setose than the previous two antennomeres, marked throughout by moderate fine granulation. Margins with smaller and finer granulation and setae than on the previous two antennomeres.

Thorax. Pronotum approximately an isosceles trapezium, anterior three fifths gradually expanding to the widest point, then the posterior two fifths converge slightly to the posterior (Fig. 4B). Dorsal surface of pronotum smooth, lacking prominent features. Overall pronotum length 0.73 mm, minimum width (on the anterior) 0.48 mm, width of the posterior 0.66 mm, maximum width on the posterior two fifths 0.72 mm. Mesonotum broader than long, with lateral margins expanding slightly on the anterior half and then contract slightly to the posterior (Fig. 4B). Overall mesonotum length 0.55 mm and greatest width 0.67 mm. Metanotum with anterior and posterior margins the same width, 0.60 mm, overall metanotum length 0.55 mm and maximum width (in the center) 0.65 mm.

Legs. All legs of a similar morphology, only slight differences in length differentiate them (Fig. 4D). All femora of a uniform width, and all tibiae of a uniform width.

Femora tubular, with a surface texture that is mostly smooth, but with a slight granular texture in places but not throughout. At the femora and tibiae joint the femora have a single spine-like projection on each side projecting outward and slightly towards the tibiae (Fig. 4D). Tibiae are half as wide as the femoral widths. Tibiae on the proximal end start out smooth but gradually become heavily setose along the ventral and lateral surfaces. At the apex of the tibiae the setae are rather prominent, and the setae continue on under the tarsomeres, albeit slightly more sparse, not as dense as the apex of the tibiae (Fig. 4C). Tarsi with two tarsomeres, apex with two distinct claws, each with a prominent pulvillus (Fig. 4C). Leg segment lengths: profemora 0.66 mm, mesofemora 0.60 mm, metafemora 0.77 mm, protibiae 0.62 mm, mesotibae 0.58 mm, metatibiae 0.94 mm.

Abdomen. Abdomen notably damaged in the holotype. Disconnected from the body following the second segment, the remainder is mostly crushed, and the terminal two or three segments are missing (Fig. 3A). Greatest width approximately 0.55 mm. Abdomen without notable structures, margins parallel sided with rather smooth transitions from one segment to the next.

Etymology. Noun in apposition, given for Excalibur, the mythical "sword in the stone" which was first described in the epic poem Merlin (about the mythical advisor to King Arthur), written by the French poet Robert de Boron sometime between 1195–1210 (Reeve and Wright 2007) which was a reworking of Geoffrey of Monmouth's "Historia Regum Britanniae", completed c. 1138 (Wright 1985). Within this poem is the first mention of Excalibur being the sword in the stone, which could only be removed by the true king of England. We felt that this specific epithet was fitting as this group of insects with exaggerated antennae were first described as a possible "double edged sword in evolution" as these elaborate antennae went extinct (Du et al. 2021). We felt this witty description, coupled with the insect being trapped in stone (amber) was fitting for such a long lost, and therefore mythical species.

Conclusion

Our understanding of antennae diversity of the region and period is expanded with the description of this new genus and species of elaborately antennaed coreid from Cretaceous amber. These elaborate features have for the most part been lost from the antennae through the millennia and are now primarily found on the hind legs. Extant coreids primarily have the expansions on antennae restricted to a single antennal segment (Fig. 1D), and expansions are notably less elaborate than in extinct coreids (Fig.2). There are several hypotheses we think might have led to this shift.

First, we feel the presence of elaborate structures on the hind legs versus the antennae is likely much more manageable for terrestrial movement due to a lower center of gravity (such as escape from predators of nymphs which cannot fly) and for flight in adults (as it is likely that such large/relatively heavy antennae would be difficult for flight/have significant wind resistance when on the anterior of the individual).

Also, it is most often large, elaborate appendages on insects that are reported as being lost at a higher rate to potential predators or to an imperfect molt than simple limbs/antennae (Maginnis 2008; Emberts et al. 2016). The large and elaborate antennae might have been more likely to be lost than the simple legs of extinct coreids. It is worth noting that in modern coreids the elaborate hind limbs have been reported as significant for sexual selection and overall mimesis, so just like their sensory significant antennae, their hind legs are impactful to overall fitness if lost (Eberhard 1998). Perhaps the elaborate antennae of this ancient coreid lineage were indeed a double-edged sword, as Du et al. (2021) hypothesized and discussed its costs/benefits. By losing these antennae it was evolutionarily prohibitively more costly due to the impact on the ability to find a mate via pheromone signaling, finding potential food sources, or oviposition sites (Elgar et al. 2018), thus leading to the extinction of this lineage.

Perhaps the selection pressures discussed above have acted against having elaborate (potentially likely to be lost) structures on the receptor valuable antennae, and instead the much more expendable hind legs have become the target for evolutionary experimentation for elaborate structures within the coreids. The extinct lace bug *Gyaclavator kohlsi* Wappler, Guilbert, Wedmann, Labandeira, 2015 lends credibility to this idea of evolutionary experimentation leading to elaborate antennae, which are subsequently lost. This fossil Eocene lace bug has an expanded fourth antennomere, a feature previously unknown within Tingidae, which has not survived into extant species (Wappler et al. 2015).

An additional likely possibility/contributing factor is that this lineage of elaborate antennaed coreids fell victim to the Cretaceous–Paleogene (K–Pg) mass extinction which occurred approximately 66 million years ago and marked the end of the Cretaceous (Renne et al. 2013). This period of significant ecological disruption resulted in the extinction of a majority of species with estimates for extinction of marine life as high at ~75% (Jablonski 1994), extensive disruption to terrestrial plant communities (Wilf and Johnson 2004), and massive decline in diversity in terrestrial invertebrates (Wilf et al. 2006).

Typically, only one segment is expanded in extant coreids with the most elaborate antennae (Fig. 1D), but not to such a drastic degree as in the Cretaceous coreids discussed herein. Thus, whatever causes led to the elimination this elaborate antennaed coreid lineage, we are left with only these interesting fossils for speculation as to the function.

Acknowledgements

Thank you to our scientific illustrator Liz Sisk (USA) who did a beautiful job of illustrating these interesting fossils so that their living glory may be appreciated. Thank you to Simon Chen (Canada) for recognizing the importance of the holotype specimen and sending it to the authors. We thank Michel Saint-Germain, head of collections and research and Maxim Larrivé, director of the Montreal Insectarium for their support of our research. Thank you to our peer reviewers for their extremely helpful feedback and suggestions.

References

Azar D, Nel A, Engel MS, Garrouste R, Matocq A (2011) A new family of Coreoidea from the Lower Cretaceous Lebanese Amber (Hemiptera Pentatomomorpha). Polish Journal of Entomology 80: 627–644. https://doi.org/10.2478/v10200-011-0049-5

Boeheim W (1890) Handbuch der Waffenkunde: das Waffenwesen in seiner historischen Entwickelung vom Beginn des Mittelalters bis zum Ende des 18. Jahrhunderts. Verlag Von E. A. Seemann, Leipzig, Germany.

Brailovsky H, Barrera E (2009) New Species of *Merocoris* (*Merocoris*) Perty from Brazil, with Keys to Known Subgenera and Species of the Tribe Merocorini (Hemiptera: Heteroptera: Coreidae: Meropachyinae). Florida Entomologist 92(1): 134–138. https://doi.org/10.1653/024.092.0120

CoreoideaSF Team (2021) Coreoidea Species File Online. Version 5.0/5.0. [March 25th, 2021]. http://Coreoidea.SpeciesFile.org

Dolling WR (2006) Coreidae Leach, 1815. In: Aukema B, Rieger C (Eds) Catalogue of the Heteroptera of the Palaearctic region (Vol. 5), Pentatomorpha II. The Netherlands Entomological Society, Amsterdam, 43–101. https://www.researchgate.net/publication/254899169

Du B-J, Chen R, Tao W-T, Shi H-L, Bu W-J, Liu Y, Ma S, Ni M-Y, Kong F-L, Xiao J-H, Huang D-W (2021) A Cretaceous bug with exaggerated antennae might be a double-edged sword in evolution. iScience 24: e101932. https://doi.org/10.1016/j.isci.2020.101932

Du S-L, Hu Z-K, Yao Y-Z, Ren D (2019) New genus and species of the Yuripopovinidae (Pentatomomorpha: Coreoidea) from mid-Cretaceous Burmese amber. Cretaceous Research 94: 141–146. https://doi.org/10.1016/j.cretres.2018.10.022

Eberhard WG (1998) Sexual Behavior of *Acanthocephala declivis guatemalana* (Hemiptera: Coreidae) and the Allometric Scaling of their Modified Hind Legs. Annals of the Entomological Society of America 91(6): 863–871. https://doi.org/10.1093/aesa/91.6.863

Elgar MA, Zhang D, Wang Q, Wittwer B, Thi Pham H, Johnson TL, Freelance CB, Coquilleau M (2018) Insect Antennal Morphology: The Evolution of Diverse Solutions to Odorant Perception. The Yale journal of biology and medicine 91(4): 457–469. https://www.ncbi.nlm.nih.gov/pmc/articles/PMC6302626/

Emberts Z, St. Mary CM, Miller CW (2016) Coreidae (Insecta: Hemiptera) Limb Loss and Autotomy. Annals of the Entomological Society of America 109(5): 678–683. https://doi.org/10.1093/aesa/saw037

Forthman M, Miller CW, Kimball RT (2019) Phylogenomic analysis suggests Coreidae and Alydidae (Hemiptera: Heteroptera) are not monophyletic. Zoologica Scripta 48: 520–534. https://doi.org/10.1111/zsc.12353

Forthman M, Miller CW, Kimball RT (2020) Phylogenomics of the Leaf-Footed Bug Subfamily Coreinae (Hemiptera: Coreidae). Insect Systematics and Diversity 4(4) (2): 1–15. https://doi.org/10.1093/isd/ixaa009

Gonzaga-Segura J, Valdéz-Carrasco J, Castrejón-Gómez VR (2013) Sense Organs on the Antennal Flagellum of *Leptoglossus zonatus* (Heteroptera: Coreidae). Annals of the Entomological Society of America: 106(4): 510–517. https://doi.org/10.1603/AN12127

Grimaldi DA, Engel MS, Nascimbene PC (2002) Fossiliferous Cretaceous Amber from Myanmar (Burma): Its Rediscovery, Biotic Diversity, and Paleontological Significance. American Museum Novitates 3361: 1–72. https://doi.org/10.1206/0003-0082(2002)361%3C0001:FCAFMB%3E2.0.CO;2

Hamouly HE, Sawaby RF, Fadl HH (2010) Taxonomic review of the subfamily Pseudophloeinae (Hemiptera: Coreidae) from Egypt. Egyptian Journal of Biology 12: 108–124.

Henry TJ (2017) Biodiversity of Heteroptera. In: Foottit RG, Adler PH (Eds) Insect Biodiversity: Science and Society (Vol. I, 2nd Edn.). John Wiley & Sons Ltd., 279–335. https://doi.org/10.1002/9781118945568.ch10

Jablonski D (1994) Extinctions in the fossil record (and discussion). Philosophical Transactions of the Royal Society of London B 344(1307): 11–17. https://doi.org/10.1098/rstb.1994.0045

Johnson KP, Dietrich CH, Friedrich F, Beutel RG, Wipfler B, Peters RS, Allen JM, Petersen M, Donath A, Walden KKO, Kozlov AM, Podsiadlowski L, Mayer C, Meusemann K, Vasilikopoulos A, Waterhouse RM, Cameron SL, Weirauch C, Swanson DR, Percy DM, Hardy NB, Terry I, Liu S, Zhou X, Misof B, Robertson HM, Yoshizawa K (2018) Phylogenomics and the evolution of hemipteroid insects. Proceedings of the National Academy of Sciences of the United States of America 115(50): 12775–12780. https://doi.org/10.1073/pnas.1815820115

Kieran TJ, Gordon ERL, Forthman M, Hoey-Chamberlain R, Kimball RT, Faircloth BC, Weirauch C, Glenn TC (2019) Insight from an ultraconserved element bait set designed for hemipteran phylogenetics integrated with genomic resources. Molecular Phylogenetics and Evolution 130: 297–303. https://doi.org/10.1016/j.ympev.2018.10.026

Maginnis TL (2008) Autotomy in a Stick Insect (Insecta: Phasmida): Predation Versus Molting. Florida Entomologist, 91(1): 126–127. https://doi.org/10.1653/0015-4040(2008)091[0126:AIASII]2.0.CO;2

Moulet P (1995) Hémiptères Coreoidea (Coreidae, Rhopalidae, Alydidae), Pyrrhocoridae, Stenocephalidae Euro-Méditerranéens. Faune de France 81. Fédération Française des Sociétés de Sciences Naturelles, Paris, 336 pp.

Packauskas RJ (1994) Key to the subfamilies and tribes of the New World Coreidae (Hemiptera), with a checklist of published keys to genera and species. Proceedings of the Entomological Society of Washington 96(1): 44–53.

Pluot-Sigwalt D, Moulet P (2020) Morphological types of spermatheca in Coreidae: bearing on intra-familial classification and tribal-groupings (Hemiptera: Heteroptera). Zootaxa 4834(4): 451–501. https://doi.org/10.11646/zootaxa.4834.4.1

Procter DS, Moore AJ, Miller CW (2012) The form of sexual selection arising from male-male competition depends on the presence of females in the social environment. Journal of Evolutionary Biology 25: 803–812. https://doi.org/10.1111/j.1420-9101.2012.02485.x

Renne PR, Deino AL, Hilgen FJ, Kuiper KF, Mark DF, Mitchell WS, Morgan LE, Mundil R, Smit J (2013) Time scales of critical events around the Cretaceous-Paleogene boundary. Science 339(6120): 684–687. https://doi.org/10.1126/science.1230492

Reeve MD, Wright N (2007) Geoffrey of Monmouth. The History of the Kings of Britain: an edition and translation of De gestis Britonum. Boydell Press, Woodbridge, United Kingdom, 392 pp.

Shi G, Grimaldi DA, Harlow GE, Wang J, Wang J, Yang M, Lei W, Li Q, Li X (2012) Age constraint on Burmese amber based on U-Pb dating of zircons. Cretaceous Research 37: 155–163. https://doi.org/10.1016/j.cretres.2012.03.014

Schuh RT, Slater JA (1995) True Bugs of the World (Hemiptera: Heteroptera): Classification and Natural History. Cornell University Press, Ithaca, New York, 337 pp.

Schuh RT, Weirauch C (2020) True bugs of the World (Hemiptera: Heteroptera). Classification and natural history (second edition) Siri Scientific Press, Manchester 768 pp. [+ 32 pls.]

Swanson DR (2011) A Synopsis of the Coreoidea (Heteroptera) of Michigan. The Great Lakes Entomologist 44(2): 139–162 https://scholar.valpo.edu/tgle/vol44/iss2/4

Wappler T, Guilbert E, Labandeira CC, Hörnschemeyer T, Wedmann S (2015) Morphological and Behavioral Convergence in Extinct and Extant Bugs: The Systematics and Biology of a New Unusual Fossil Lace Bug from the Eocene. PLoS ONE 10(8): e0133330. https://doi.org/10.1371/journal.pone.0133330

Wilf P, Johnson KR (2004) Land plant extinction at the end of the Cretaceous: a quantitative analysis of the North Dakota megafloral record. Paleobiology 30(3): 347–368. https://doi.org/10.1666/0094-8373(2004)030%3C0347:LPEATE%3E2.0.CO;2

Wilf P, Labandeira CC, Johnson KR, Ellis B (2006) Decoupled plant and insect diversity after the end-Cretaceous extinction. Science 313(5790): 1112–1115. https://doi.org/10.1126/science.1129569

Wright N (1985) The Historia Regum Britanniae of Geoffrey of Monmouth, 1: Bern, Burgerbibliothek, MS. 568. D.S. Brewer, Cambridge, 238 pp.

ZooKeys 1043: 133–145 (2021)
doi: 10.3897/zookeys.1043.61706
https://zookeys.pensoft.net

RESEARCH ARTICLE

A peer-reviewed open-access journal
ZooKeys
Launched to accelerate biodiversity research

Onthophagus pilauco sp. nov. (Coleoptera, Scarabaeidae): evidence of beetle extinction in the Pleistocene–Holocene transition in Chilean Northern Patagonia

Francisco Tello[1], José R. Verdú[2], Michele Rossini[3], Mario Zunino[4]

1 *Transdisciplinary Center for Quaternary Research (TAQUACH), Universidad Austral de Chile, Valdivia, Chile* **2** *I.U.I. CIBIO, Universidad de Alicante, Alicante, Spain* **3** *Finnish Museum of Natural History (LUOMUS), University of Helsinki, Pohjoinen Rautatiekatu 13, Helsinki, 00014, Finland* **4** *Scuola di Biodiversità, Polo universitario Asti Studi Superiori, Asti, Italy*

Corresponding author: Francisco Tello (ftelloa@yahoo.cl)

Academic editor: Andrey Frolov | Received 5 December 2020 | Accepted 18 April 2021 | Published 15 June 2021

http://zoobank.org/B38C0C9B-D6AA-4473-9839-C6DEF8E9FD3B

Citation: Tello F, Verdú JR, Rossini M, Zunino M (2021) *Onthophagus pilauco* sp. nov. (Coleoptera, Scarabaeidae): evidence of beetle extinction in the Pleistocene–Holocene transition in Chilean Northern Patagonia. ZooKeys 1043: 133–145. https://doi.org/10.3897/zookeys.1043.61706

Abstract

The South American Pleistocene–Holocene transition has been characterized by drastic climatic and diversity changes. These rapid changes induced one of the largest and most recent extinctions in the megafauna at the continental scale. However, examples of the extinction of small animals (e.g., insects) are scarce, and the underlying causes of the extinction have been little studied. In this work, a new extinct dung beetle species is described from a late Pleistocene sequence (~15.2 k cal yr BP) at the paleoarcheological site Pilauco, Chilean Northern Patagonia. Based on morphological characters, this fossil is considered to belong to the genus *Onthophagus* Latreille, 1802 and named *Onthophagus pilauco* **sp. nov.** We carried out a comprehensive revision of related groups, and we analyzed the possible mechanism of diversification and extinction of this new species. We hypothesize that *Onthophagus pilauco* **sp. nov.** diversified as a member of the *osculatii* species-complex following migration processes related to the Great American Biotic Interchange (~3 Ma). The extinction of *O. pilauco* **sp. nov.** may be related to massive defaunation and climatic changes recorded in the Plesitocene-Holocene transition (12.8 k cal yr BP). This finding is the first record of this genus in Chile, and provides new evidence to support the collateral-extinction hypothesis related to the defaunation.

Keywords

Dung beetle, extinction, fossil beetles, new species, Pleistocene, South America

Introduction

The South American Pleistocene–Holocene transition (~16.0–11.0 k cal yr BP) has been characterized by drastic changes in climatic conditions, animal and plant diversity, and types of early-human occupation (Dillehay 1989; Borrero et al. 1998; Dillehay et al. 2015). There is currently no clear paleontological consensus concerning the mechanisms that facilitated these processes and multiple hypotheses seem to provide equally robust explanations for these paleoecological events, which include transformations induced by climatic and anthropogenic factors. The latest hypothesis is based on stochastic changes induced by cosmic impact (i.e., the Younger Dryas bolide-impact hypothesis, ~12.8 k cal yr BP), which resulted in large fires that contributed to a rapid overturn in species, and climatic and environmental conditions in both hemispheres (Firestone et al. 2007). This assumption is supported by evidence of extraterrestrial material and charcoal spherules, which have been found at several paleontological sites distributed across four continents (e.g., Pino et al. 2019; Wolbach et al. 2020).

In addition, the extinction of megafauna caused drastic changes in forest ecosystems, as these animals (e.g., the Gomphotheriidae) were fundamental in the past to support a series of important trophic relations (Owen-Smith 1987; Barnosky et al. 2016; González-Guarda et al. 2017). Thus, megafauna-species-dependent (e.g., parasitic insects and dung beetles) are very likely to have suffered the loss of these large animals. As a consequence, these organisms likely experienced major changes in their community compositions, along with the extinction of many species (Zinovyev 2011; Ashworth and Nelson 2014; Tello et al. 2017). As an example, *Cobboldia russanovi* Grunin, 1973 (Gasterophilidae) was a mammoth-botfly that became extinct at the end of the Pleistocene in Russia due to the loss of its host (Kuzmina and Korotyaev 2019, and references therein).

In South America, most of the evidence of the extinction of dung beetle fauna is based on fossil breeding balls (i.e., ichnospecies) in the early, middle and late Pleistocene (Cantil et al. 2013, Sánchez et al. 2013) and the unique dung beetle fossil remains recovered from Coprinisphaeridae inchnofossils (Zunino 2013). To date, examples of changes in fossil insect assemblages and the collateral extinction of insect species caused by the loss of large mammals in the Pleistocene–Holocene transition are still scarce.

In this study, we analyzed fossil remains from a late Pleistocene sequence collected at the paleoarcheological site Pilauco in Chilean Northern Patagonia. The fossil remains are tentatively classified in the *Onthophagus osculatii* species-complex (Coleoptera: Scarabaeidae: Scarabaeinae) (Rossini et al. 2018a). The extant dung beetle genus *Onthophagus* Latreille, 1802 comprises about 200 valid species in the New World. This number is greatly overshadowed by the impressive diversity of the genus in the Afrotropical, Oriental, and Palearctic regions, which are home to over 1000, 600 and 400 species, respectively. In recent years, scientific expeditions and studies on biodiversity carried out in remote and still unexplored areas of the American continent,

have made it possible to obtain a great deal of information about the natural history of certain specimens, alongside the description of an increasing number of new species. However, the genus *Onthophagus* has never been recorded from Chile (Elgueta 2000; González-Chang and Pinochet 2015). Furthermore, the small number of fossil *Onthophagus* species described so far have been found in Europe, in sites dated from the middle to upper Paleocene (61.6–56 Ma) to middle Miocene (14–13.5 Ma), and a more recent North American fossil dated from the upper Pleistocene (0.068–0.004 Ma) (Tarasov et al. 2016).

The main goals of this study were to analyze the morphology of the fossil remains, to discuss the paleoecological implications and biogeographical distributions of the extant Chilean dung beetle fauna, with emphasis on South American *Onthophagus*, and to suggest a taxonomic placement for these fossil remains.

Study site and paleontological context

The Pilauco archeological and paleontological site is located in the city of Osorno, Chilean Northern Patagonia (40°34'S, 73°07'W) (Fig. 1A). Pilauco is considered to be a well-developed site at which to study the Pleistocene–Holocene transition due to its very obvious stratigraphy, large amount of animal and plant fossil remains, evidence of early-human occupation, and sedimentary record of the Younger Dryas bolide-impact at 12.8k cal yr BP (Pino et al. 2013, 2019, Moreno et al. 2019, Navarro-Harris et al. 2019). The current weather regime in Osorno (11.4 °C mean annual temperature, ~1300 mm precipitation per year) indicates temperate-warm climatic conditions.

Stratigraphy and age

Stratigraphically, the Pilauco site is composed of four principal beds (Fig. 1B) that were deposited in fluvial, colluvial and palustrine environments (Pino et al. 2019). The basal bed (PB-6) is an unconsolidated sandy conglomerate, containing abundant, well-rounded pebbles and boulders. The overlying bed (PB-7) contains most of the extinct megafaunal remains, and is composed of an organic-rich sand with isolated colluvium-derived pebbles. Bed PB-8 is very similar to PB-7, although it contains lower abundances of mammal fossils and lithic artifacts. The Younger Dryas bolide-impact layer can be seen at the interface between beds PB-8 and PB-9, with PB-9 recording major changes in environmental conditions (Pino et al. 2019, 2020). Pino et al. (2019) proposed a Bayesian age model based on 36 accelerator mass spectrometry radiocarbon dates. These dates were calibrated according to the Southern Hemispheric calibration curve (SHIntCal13), providing an age range for Pilauco of between 16,400 and 4340 cal yr BP. According to the age model, the age of the fossil beetle is 15,200 cal yr BP (Fig. 1B), corresponding to the PB-7 bed.

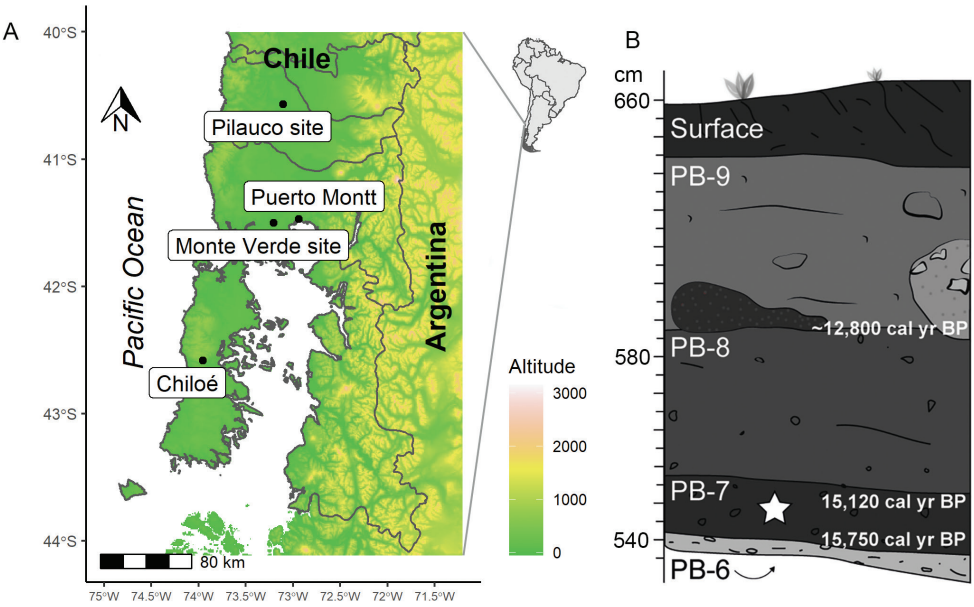

Figure 1. Type locality of *Onthophagus pilauco* sp. nov. **A** shaded elevation map shows Pilauco and Monte Verde sites. Representation of profile of a grid of the Pilauco site **B** symbol (star) indicates the layer in which *Onthophagus pilauco* sp. nov. was collected.

Paleoclimatic, paleoenvironmental and paleofaunistic records

Pollen records have recently indicated that the environment associated with bed PB-7 contained mainly non-arboreal taxa, such as Poaceae, Asteraceae, Solanaceae, and an aquatic flora (Abarzúa et al. 2020). Additionally, arboreal species, such as *Saxegothaea conspicua* Lindl., *Nothofagus dombeyi*-type and *Weinmannia trichosperma* Cav., were present in lesser proportions in the palynological record (Abarzúa et al. 2020). These proxies suggest that the climatic conditions were cold (at least ~4 °C lower) and humid compared to the current climate at the same locality. The presence of slightly arboreal temperate species of modern Chilean Northern Patagonia here between 16.0 and 14.0 k cal yr BP indicates very humid and cold climatic conditions. Additionally, the megafaunal bones at Pilauco correspond to several extinct taxa, including cf. *Notiomastodon platensis* (Ameghino, 1888) (Gomphotheriidae), *Equus* (*Amerhippus*) *andium* (Branco, 1883) (Equidae), *Xenarthra* sp. and cf. *Hemiauchenia paradoxa* (Gervais & Ameghino, 1880) (Camelidae), with the most abundant remains belonging to gomphotherids (Recabarren et al. 2011, Recabarren 2020). As for fossilized beetles, 22 species, belonging to 14 families, have been recorded from the Pilauco site. Among these, Curculionidae, Carabidae, Staphylinidae, Hydrophilidae and Scarabaeidae are the most abundant families (Tello et al. 2017, 2019). According to recent paleo-inferences based on beetle records, Pilauco was dominated by large mammals and climatic transition. When compared with modern beetle assemblages, there was a persistent rich beetle fauna, which included dung beetles and other coprophilous insects (Tello et al. 2017, 2019; Tello and Torres 2020).

Materials and methods

Abbreviations

CEMT Seção de Entomologia da Coleção Zoológica, Universidade Federal de Mato, Grosso, Cuiabá, Brazil;
CMNC Canadian Museum of Nature, Gatineau, Quebec, Canada;
MPDO Museo Pleistocénico de Osorno, Osorno, Chile;
MZ Mario Zunino private collection, Asti, Italy;
MZUF Museo di Storia Naturale dell'Università di Firenze, Florence, Italy;
NMPC Národní Muzeum, Prague, Czech Republic.

Drawings and determination of fossil remains

The fossil beetle remains were recovered from the sediment using an adaptation of the water flotation technique described by Hoganson et al. (1989) (see also Tello and Torres 2020). The remains were collected from grid 18AC, at an elevation of 384 cm in bed PB-7. The age span of this bed is ~16.0 to 14.0 k cal yr BP (Pino et al. 2020). The taxonomic placement suggested for the fossil was made after detailed examination and a comparison with multiple modern specimens of South American *Onthophagus* species deposited in the CEMT, CMNC, MZUF, MZ and NMPC collections. For the taxonomic nomenclature, we followed Rossini et al. (2018a, b). Figure 1A was obtained using R software v4.0.3. Figure 2A, 2B was obtained using a scanning electron microscope (variable pressure, EVO MC10), and Fig. 2C, D was obtained using a Leica M205C camera. All figures were processed using Adobe Photoshop 2019 CC. Type material is deposited in the MPDO insect collection, Osorno, Chile.

Results

Systematic paleontology

Order Coleoptera Linnaeus, 1758
Suborder Polyphaga Emery, 1886
Family Scarabaeidae Latreille, 1802
Genus *Onthophagus* Latreille, 1802

Type species *Onthophagus pilauco* sp. nov.
http://zoobank.org/9B203D54-E27A-432D-8AC8-ED7C33ED2F83
Fig. 2

Description. *Holotype*. Male, minor form. Clypeus sub-trapezoidal and slightly elongated forward, with anterior margin narrowly and slightly reflexed, head margin barely

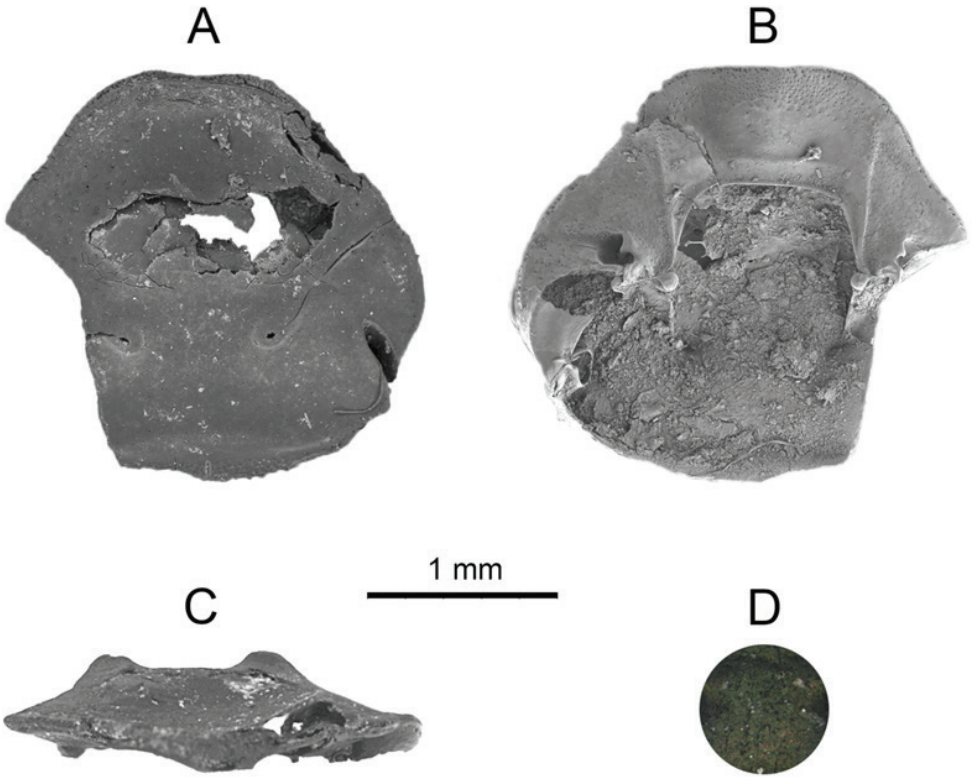

Figure 2. Holotype of *Onthophagus pilauco* sp. nov. **A** dorsal **B** ventral and **C** frontal views **D** detail of the microsculpture.

sinuated at the clypeo-genal junction. Fronto-clypeal region without carina, frons with two close, weak tubercles, strongly advanced in position, in line with the anterior margin of the eyes (Fig. 2A, C). Head surface very finely and evenly punctate. Latero-clypeal region with deeper ocellate punctures. Color dark with metallic green to bronze sheen (Fig. 2D). Pronotum and elytra not found.

Female unknown.

Diagnosis. *Onthophagus pilauco* sp. nov. is considered to be a close relative of *O. confusus* Boucomont, 1932 and *O. insularis* Boheman, 1858, as it shares the following morphological characters with these species: sub-trapezoidal shape of the clypeus; small, slightly deeper cephalic punctation, coupled with very shallow wrinkles in proximity to the genal and clypeal margins. Although the fronto-clypeal region is significantly damaged, there is no indication of a possible carina.

Proposed English and Spanish vernacular names. The Pilauco dung beetle (EN) and estercolero de Pilauco (ES).

Etymology. The name of the new species refers to the archeopaleontological site from which the fossil remains were collected.

Discussion

From our observations, the fossil remains found at Pilauco correspond to a new and extinct species of the genus *Onthophagus*, closely related to the *hircus* group. *Onthophagus pilauco* sp. nov. represents the first record of an endemic species of this genus in Chile. Moreover, this record brings new evidence of beetle extinction related to the Pleistocene–Holocene transition and massive defaunation after a possible cosmic impact and/or YD cooling reversal events.

Morphological delimitation of the fossil record

Despite the beetle remains only being represented by cephalic parts (clypeus, right gena and frons; fronto-clypeal region partly damaged; left gena absent; see Fig. 2A–D), it is clear that they belong to the genus *Onthophagus.* Close scrutiny of the fossil remains, along with an extensive analysis of multiple specimens belonging to extant American *Onthophagus* led us to assign *O. pilauco* to the *O. hircus* group, and more precisely to the *osculatii* species-complex (Rossini et al. 2018a). The two cephalic horn-like tubercles may indicate that the remains belong to a male specimen, probably a minor form. The physical location of the cephalic tubercles is rather unique in the modern American *Onthophagus* fauna. They rise in a very advanced position, in line with the anterior margin of the eyes, and are quite close to each other. The combination of these two characteristics has only ever been found in an undescribed *Onthophagus* from Costa Rica, which was included in the same species group, but in a different taxonomic complex (Rossini, pers. comm. 2020). Close cephalic tubercles are also found in female specimens of species belonging to the *Onthophagus clypeatus, dicranius* and *mirabilis* groups, but they are always situated at the front, and never as advanced as in *O. pilauco*. Also, the shape of the clypeus in these females is always triangular or evenly curved, terminating at the apex with a margin slightly to distinctly emarginated (with two obtuse teeth).

Hypothesis for the speciation and extinction of *Onthophagus pilauco*

Comprehensive knowledge of the Chilean beetle fauna suggests that only a few species (nine) can be considered to be exclusively associated with dung resources (González-Chang and Pinochet 2015). Thus, six species have been assigned to the Scarabaeidae family (excluding the saprophagous Aphodiinae species): two species belonging to Deltochilini tribe: *Megathopa villosa* Escholtz and *Scybalophagus rugosus* (Blanchard); and four species with uncertain taxonomic position (*incertae sedis sensu* Tarasov and Dimitrov 2016): *Tesserodoniella elguetai* Vaz-de Mello & Halffter, *T. meridionalis* Vaz-de Mello & Halffter, *Homocopris punctatissimus* (Curtis), and *H. torulosus* (Escholtz) (González-Chang and Pinochet 2015). The placement of the genus *Homocopris* in a suprageneric group requires further research. Additionally, three dung beetle species

belong to the family Geotrupidae Latreille, 1802, represented in Chile by the subfamily Taurocerastinae: *Frickius costulatus* Germain, *F. variolosus* Germain and *Taurocerastes patagonicus*, which are distributed across central and southern Chile.

The Deltochilini group is distributed in the pantropical zone, being especially diversified in the northern areas of South America. The genus *Tesserodoniella* is related to the Australian genera *Tesserodon* and *Aptenocanthon* and their ancestors probably originated from the Gondwana supercontinent (Vaz-De-Mello and Halffter 2006). In contrast, the extant American *Onthophagus* is a result of migrations to the continent by intercontinental connections, the current remnants of which are known as Beringia components. These migratory processes occurred at different times and under different geographical and climatic conditions, and involved different ancestors, all belonging to the subgenus *Onthophagus sensu stricto* (Rossini et al. 2018a, b, Halffter et al. 2019, Zunino and Halffter 2019). Additionally, after the definitive closure of the Isthmus of Panama (~3 Ma), which eliminated natural barriers, Central America became a permanent bridge from one continent to another, improving migratory conditions for large animals and dung beetles. Therefore, we suggest that the ancestors of *O. pilauco* migrated to South America during the Great American Biotic Interchange, following large mammals at the end of the Pliocene (3 Ma). This migratory mechanism has been suggested for the extant related *hircus* group, which arrived by crossing the Andes via the Huancabamba Depression, similarly to other extinct dung beetles (e.g., *Phanaeus violetae* Zunino, 2013). Intra-continental migratory patterns have also been reported in extant species of dung beetles that have rapidly colonized new habitats following cattle migrations (e.g., *Digitonthophagus gazella* (Fabricius, 1787); see Noriega et al. 2020). Thus, ancestors of the *osculatii* species-complex diverged in situ in Chilean areas, resulting in the evolution of *O. pilauco* (Fig. 3). This speciation hypothesis is supported by several studies on Pleistocene Patagonian landscapes (~180 ka and 26 ka) that have suggested that the rapid contraction and expansion of ice cover has induced drastic changes in biotic distributions and prompted diversification in different groups of organisms (e.g., in amphibians: Nuñez et al. 2020; in mammals: Himes et al. 2008). Moreover, the presence of extant endemic species belonging to the *osculatii* species-complex in western Ecuador and northwestern Peru [*O. confusus* and *O. insularis* (Rossini et al. 2018a)] suggests that *O. pilauco* could be a species endemic to southern Chile.

On the other hand, the extinction of large animals in South American Pleistocene environments has invoked multiple climate- and human-activity-related hypotheses, and interactions between them (Barnosky et al. 2004). The causes of small animal (<60 kg) extinctions, and the implications of changes in species compositions and distributions, are poorly understood. Owen-Smith (1987) proposed the 'keystone herbivore' hypothesis, which provides a framework to explain the simultaneous extinctions of animals not obviously made extinct by the previous causes. Additionally, a possible cosmic impact may have generated the Younger Dryas cooling oscillation (12.8 and 11.0 k cal yr BP), resulting in a rapid defaunation process, including smaller taxa

Figure 3. Artistic reconstruction of *Onthophagus pilauco* sp. nov. and its palaeoenvironment (by Mauricio Alvarez).

(Firestone et al. 2007; Pino et al. 2019; Wolbach et al. 2020). In this case, we suggest that both the rapid climatic changes and the extensive defaunation in South America could be determining factors in the extinction of *O. pilauco* during the Pleistocene–Holocene transition.

Acknowledgements

We would like to thank to Dr Mario Pino for his collaboration in the manuscript revision, and Mario Elgueta for the primary approximation to the taxonomical identities. We are grateful to Fernanda Torres for the creation of the Figure 1B. FT was supported by CONICYT doctoral scholarship Grant #21171980 and Ilustre Municipalidad de Osorno, Osorno, Chile.

References

Abarzúa AM, Martel-Cea A, Lobos V (2020) Vegetation–Climate–Megafauna Interactions During the Late Glacial in Pilauco Site, Northwestern Patagonia. In: Pino M, Astorga G (Eds) Pilauco: A Late Pleistocene Archaeo-paleontological Site. Springer, Cham, 157–173. https://doi.org/10.1007/978-3-030-23918-3_9

Ashworth AC, Nelson RE (2014) The paleoenvironment of the Olympia beds based on fossil beetles from Discovery Park, Seattle, Washington, U.S.A. Quaternary International 341: 243–254. https://doi.org/10.1016/j.quaint.2013.09.022

Ashworth AC, Hoganson J, Gunderson M (1989) Fossil-beetle analysis. In: Dillehay T (Ed.) Monte Verde – a Late Pleistocene Settlement in Chile. – a Late Pleistocene Settlement in Chile. Smithsonian Institution Press, Washington DC, 211–226.

Barnosky AD, Koch PL, Feranec RS, Wing SL, Shabel AB (2004) Assessing the causes of late pleistocene extinctions on the continents. Science 306: 70–75. https://doi.org/10.1126/science.1101476

Barnosky AD, Lindsey EL, Villavicencio NA, Bostelmann E, Hadly EA, Wanket J, Marshall CR (2016) Variable impact of late-Quaternary megafaunal extinction in causing ecological state shifts in North and South America. Proceedings of the National Academy of Sciences 113: 856–861. https://doi.org/10.1073/pnas.1505295112

Borrero LA, Zárate M, Miotti L, Massone M (1998) The Pleistocene-Holocene transition and human occupations in the southern cone of South America. Quaternary International 49–50: 191–199. https://doi.org/10.1016/S1040-6182(97)00063-3

Cantil LF, Sánchez MV, Bellosi ES, González MG, Sarzetti LC, Genise JF (2013) *Coprinisphaera akatanka* sp. nov.: The first fossil brood ball attributable to necrophagous dung beetles associated with an Early Pleistocene environmental stress in the Pampean region (Argentina). Palaeogeography, Palaeoclimatology, Palaeoecology 386: 541–554. https://doi.org/10.1016/j.palaeo.2013.06.021

Dillehay T (1989) Monte Verde. A Late Pleistocene Settlement in Chile. Smithsonian Institution Press, Washington DC, 1071 pp.

Dillehay TD, Ocampo C, Saavedra J, Sawakuchi AO, Vega RM, Pino M, Collins MB, Scott Cummings L, Arregui I, Villagran XS, Hartmann GA, Mella M, González A, Dix G (2015) New Archaeological Evidence for an Early Human Presence at Monte Verde, Chile. Hart JP (Ed.) PLoS ONE 10(12): e0145471. [27 pp.] https://doi.org/10.1371/journal.pone.0141923

Elgueta M (2000) Estado actual del conocimiento de los coleópteros de Chile (Insecta: Coleoptera). PrIBES-2000: Proyecto para Iberoamérica de Entomología Sistemática 17: 145–154.

Firestone RB, West A, Kennett JP, Becker L, Bunch TE, Revay ZS, Schultz PH, Belgya T, Kennett DJ, Erlandson JM, Dickenson OJ, Goodyear AC, Harris RS, Howard GA, Kloosterman JB, Lechler P, Mayewski PA, Montgomery J, Poreda R, Darrah T, Que Hee SS, Smitha AR, Stich A, Topping W, Wittke JH, Wolbach WS (2007) Evidence for an extraterrestrial impact 12,900 years ago that contributed to the megafaunal extinctions and the Younger Dryas cooling. Proceedings of the National Academy of Sciences of the United States of America 104: 16016–16021. https://doi.org/10.1073/pnas.0706977104

González-Chang M, Pinochet D (2015) Escarabajos estercoleros nativos en Chile. Una revisión con énfasis en su ecología. Agro Sur 43: 51–61. https://doi.org/10.4206/agrosur.2015.v43n3-06

González-Guarda E, Domingo L, Tornero C, Pino M, Hernández Fernández M, Sevilla P, Villavicencio N, Agustí J (2017) Late Pleistocene ecological, environmental and climatic reconstruction based on megafauna stable isotopes from northwestern Chilean Patagonia. Quaternary Science Reviews 170: 188–202. https://doi.org/10.1016/j.quascirev.2017.06.035

Himes CMT, Gallardo MH, Kenagy GJ (2008) Historical biogeography and post-glacial recolonization of South American temperate rain forest by the relictual marsupial *Dromiciops gliroides*. Journal of Biogeography 35: 1415–1424. https://doi.org/10.1111/j.1365-2699.2008.01895.x

Kuzmina SA, Korotyaev BA (2019) A new species of the weevil genus *Phyllobius* Germar, 1824 (Coleoptera: Curculionidae: Entiminae) from the Pleistocene of northeastern. Invertebrate Zoology 16: 154–164. https://doi.org/10.15298/invertzool.16.2.04

Moreno K, Bostelmann JE, Macías C, Navarro-Harris X, De Pol-Holz R, Pino M (2019) A late Pleistocene human footprint from the Pilauco archaeological site, northern Patagonia, Chile. Chiang T-Y (Ed.) PLoS ONE 14(4): e0213572. [16 pp.] https://doi.org/10.1371/journal.pone.0213572

Navarro-Harris X, Pino M, Guzmán-Marín P, Lira MP, Labarca R, Corgne A (2019) The procurement and use of knappable glassy volcanic raw material from the late Pleistocene Pilauco site, Chilean Northwestern Patagonia. Geoarchaeology 34: 592–612. https://doi.org/10.1002/gea.21736

Noriega J, Floate KD, Génier F, Reid CAM, Kohlmann B, Horgan FG, Davis ALV, Forgie SA, Aguilar C, Ibarra MG, Vaz-de-Mello F, Ziani S, Lobo JM (2020) Global distribution patterns provide evidence of niche shift by the introduced African dung beetle *Digitonthophagus gazella*. Entomologia Experimentalis et Applicata eea.12961: 776–782. https://doi.org/10.1111/eea.12961

Nuñez JJ, Suárez-Villota EY, Quercia CA, Olivares AP, Sites Jr JW (2020) Phylogeographic analysis and species distribution modelling of the wood frog *Batrachyla leptopus* (Batrachylidae) reveal interglacial diversification in south western Patagonia. PeerJ e9980: 1–29. https://doi.org/10.7717/peerj.9980

Owen-Smith N (1987) Pleistocene Extinctions: The Pivotal Role of Megaherbivores. Paleobiology 13: 351–362. https://doi.org/10.1017/S0094837300008927

Pino M, Abarzúa AM, Astorga G, Martel-Cea A, Cossio-Montecinos N, Navarro RX, Lira MP, Labarca R, LeCompte MA, Adedeji V, Moore CR, Bunch TE, Mooney C, Wolbach WS, West A, Kennett JP (2019) Sedimentary record from Patagonia, southern Chile supports cosmic-impact triggering of biomass burning, climate change, and megafaunal extinctions at 12.8 ka. Scientific Reports 9: 1–27. https://doi.org/10.1038/s41598-018-38089-y

Pino M, Chávez-Hoffmeister M, Navarro-Harris X, Labarca R (2013) The late Pleistocene Pilauco site, Osorno, south-central Chile. Quaternary International 299: 3–12. https://doi.org/10.1016/j.quaint.2012.05.001

Pino M, Martel-Cea A, Vega RM, Fritte D, Soto-Bollmann K (2020) Geology, Stratigraphy, and Chronology of the Pilauco Site. In: Pino M, Astorga G (Eds) Pilauco: A Late Pleistocene Archaeo-paleontological Site. Springer, Cham, 33–53. https://doi.org/10.1007/978-3-030-23918-3_3

Recabarren O (2020) The Proboscidean Gomphotheres (Mammalia, Gomphotheriidae) from Southernmost South America. In: Pino M, Astorga G (Eds) Pilauco: A Late Pleistocene Archaeo-paleontological Site. Springer, Cham, 55–68. https://doi.org/10.1007/978-3-030-23918-3_4

Recabarren O, Pino M, Cid I (2011) A new record of *Equus* (Mammalia: Equidae) from the Late Pleistocene of central-south Chile. Revista chilena de historia natural 84: 535–542. https://doi.org/10.4067/S0716-078X2011000400006

Rossini M, Vaz-de-Mello FZ, Zunino M (2018a) A taxonomic revision of the New World *Onthophagus* Latreille, 1802 (Coleoptera: Scarabaeidae: Scarabaeinae) of the *osculatii* species-complex, with description of two new species from South America. Journal of Natural History 52: 541–586. https://doi.org/10.1080/00222933.2018.1437230

Rossini M, Vaz-De-Mello FZ, Zunino M (2018b) Toward a comprehensive taxonomic revision of the "*hirculus*" group of american *Onthophagus* Latreille, 1802 (Coleoptera, Scarabaeidae, Scarabaeinae). European Journal of Taxonomy 432: 1–21. https://doi.org/10.5852/ejt.2018.432

Sánchez MV, Genise JF, Bellosi ES, Román-Carrión JL, Cantil LF (2013) Dung beetle brood balls from Pleistocene highland palaeosols of Andean Ecuador: A reassessment of Sauer's Coprinisphaera and their palaeoenvironments. Palaeogeography, Palaeoclimatology, Palaeoecology 386: 257–274. https://doi.org/10.1016/j.palaeo.2013.05.028

Tarasov S, Dimitrov D (2016) Multigene phylogenetic analysis redefines dung beetles relationships and classification (Coleoptera: Scarabaeidae: Scarabaeinae). BMC Evolutionary Biology 16: 1–19. https://doi.org/10.1186/s12862-016-0822-x

Tarasov S, Vaz-de-Mello FZ, Krell FT, Dimitrov D (2016) A review and phylogeny of Scarabaeine dung beetle fossils (Coleoptera: Scarabaeidae: Scarabaeinae), with the description of two *Canthochilum* species from Dominican amber. PeerJ 4:e1988: 1–35. https://doi.org/10.7717/peerj.1988

Tello F, Torres F (2020) Fossil Coleoptera from the Pilauco Site: An Approach to Late Pleistocene Microenvironments. In: Pino M, Astorga G (Eds) Pilauco: A Late Pleistocene Archaeo-paleontological Site. Springer, Switzerland, 195–212. https://doi.org/10.1007/978-3-030-23918-3_12

Tello F, Arriagada G, Pino M (2019) First record of the family Histeridae (Insecta: Coleoptera) in a late Pleistocene sequence from Chile. Ameghiniana 57: 63–67. https://doi.org/10.5710/AMGH.06.12.2019.3260

Tello F, Elgueta M, Abarzúa AM, Torres F, Pino M (2017) Fossil beetles from Pilauco, south-central Chile: An Upper Pleistocene paleoenvironmental reconstruction. Quaternary International 449: 58–66. https://doi.org/10.1016/j.quaint.2017.05.046

Vaz-de-Mello FZ, Halffter G (2006) A new dung beetle genus with two new species from Chile (Coleoptera: Scarabaeidae: Scarabaeinae). Zootaxa 1193: 59–68. https://doi.org/10.11646/zootaxa.1193.1.4

Wolbach WS, Ballard JP, Mayewski PA, Kurbatov A, Bunch TE, LeCompte MA, Adedeji V, Israde-Alcántara I, Firestone RB, Mahaney WC, Melott AL, Moore CR, Napier WM, Howard GA, Tankersley KB, Thomas BC, Wittke JH, Johnson JR, Mitra S, Kennett JP, Kletetschka G, West A (2020) Extraordinary Biomass-Burning Episode and Impact Win-

ter Triggered by the Younger Dryas Cosmic Impact ~12,800 Years Ago: A Reply. The Journal of Geology 128: 95–107. https://doi.org/10.1086/706265

Zinovyev E (2011) Sub-fossil beetle assemblages associated with the "mammoth fauna" in the Late Pleistocene localities of the Ural Mountains and West Siberia. ZooKeys 100: 149–169. https://doi.org/10.3897/zookeys.100.1524

Zunino M (2013) Primer hallazgo de un escarabajo en un ichnofósil Coprinisphaeridae: *Phanaeus violetae* n. sp. (Coleoptera: Scarabaeinae) de una bola de cangahua del Ecuador. Acta Zoológica Mexicana (N.S.) 29: 219–226. https://doi.org/10.21829/azm.2013.291397

Zunino M, Halffter G (2019) About the origin of American *Onthophagus* (Coleoptera: Scarabaeidae). A critical appraisal of a recent paper by Breeschoten et al. (2016) on phylogenetics and biogeography. Molecular Phylogenetics and Evolution 133: 141–141. https://doi.org/10.1016/j.ympev.2019.01.001

ZooKeys 1043: 147–191 (2021)
doi: 10.3897/zookeys.1043.64438
https://zookeys.pensoft.net

RESEARCH ARTICLE

A peer-reviewed open-access journal
ZooKeys
Launched to accelerate biodiversity research

Taxonomy of three species of the genus *Spinoncaea* (Copepoda, Oncaeidae) in the North Pacific Ocean with focus on morphological variability

Kyuhee Cho[1], Chailinn Park[2,3], Ruth Böttger-Schnack[4]

1 *Marine Ecosystem Research Center, Korea Institute of Ocean Science & Technology, Busan, Republic of Korea* **2** *Global Ocean Research Center, Korea Institute of Ocean Science & Technology, Busan, Republic of Korea* **3** *Department of Ocean Science, University of Science and Technology, Daejeon, Republic of Korea* **4** *GEOMAR Helmholtz-Centre for Ocean Research Kiel, Kiel, Germany*

Corresponding authors: Kyuhee Cho (chokh@kiost.ac.kr); Ruth Böttger-Schnack (rboettgerschnack@geomar.de)

Academic editor: Danielle Defaye | Received 15 February 2021 | Accepted 15 May 2021 | Published 15 June 2021

http://zoobank.org/E4AD2746-040E-4CD6-ABCA-5806FFA422CF

Citation: Cho K, Park C, Böttger-Schnack R (2021) Taxonomy of three species of the genus *Spinoncaea* (Copepoda, Oncaeidae) in the North Pacific Ocean with focus on morphological variability. ZooKeys 1043: 147–191. https://doi.org/10.3897/zookeys.1043.64438

Abstract

Three species of *Spinoncaea* Böttger-Schnack, 2003 are newly recorded in three locations of the equatorial and temperate Pacific Ocean collected by using a net of 60 µm mesh size. For all three species, morphological characters and patterns of ornamentation were analyzed in detail and illustrations of both sexes, also including form variants of the females, are provided. For the first time, information about the variability of various continuous (morphometric) characters are given, such as the spine lengths on the rami of the swimming legs or the proportions of urosomites. The complementary morphological descriptions of the Pacific specimens focus on similarities or modifications of characters as compared to earlier descriptions of these species from the type locality and various other localities. For *S. ivlevi* (Shmeleva, 1966), originally but insufficiently described from the Adriatic Sea, the Pacific material is similar in most aspects to the comprehensive redescription of the species from the Red Sea and from the type locality, except for a difference in the morphometry of the distal endopod segment on the antenna, which is discussed here. For *S. tenuis* Böttger-Schnack, 2003, and *S. humesi* Böttger-Schnack, 2003, the Pacific material mostly coincides with the characteristic features as described in the original account from the Red Sea. For all three species, differences and/or additions in ornamentation details were found in Pacific specimens (e.g., on the intercoxal sclerite of the first swimming leg or on the genital somite of the male) and females with aberrant morphology were detected. Genetic analyses based on 12S srRNA revealed for two species, *S. ivlevi* and *S. humesi*, little or no differences in genetic sequences between Pacific specimens and those recorded

from the Mediterranean Sea, thus demonstrating that specimens from both locations are conspecific. For *S. tenuis*, for which no comparable genetic data are available, 12S srRNA amplification was unsuccessful as was the amplification of mitochondrial COI (barcoding) for all three species. The applicability of using COI amplification for barcoding of oncaeid copepods is discussed.

Keywords
Molecular, morphological modification, Pacific, taxonomy, zooplankton

Introduction

Species of Oncaeidae Giesbrecht, 1893 [1892] are abundant in marine ecosystems of temperate, tropical, and polar regions and in the whole water column (Metz 1995; Böttger-Schnack et al. 2001; Nishibe and Ikeda 2004; Razouls et al. 2005–2021 at http://copepodes.obs-banyuls.fr/en). More than 170 years of taxonomic studies has led to the identification of 113 species ranging from small to large sizes of between 0.17–1.4 mm female body length (Razouls et al. 2005–2021; Walter and Boxshall 2021). All these species are distinguished by morphological analysis using traditional descriptive taxonomy, but they include many sister species, making it difficult to identify them clearly (Böttger-Schnack and Schnack 2013, 2015, 2019).

The genus *Spinoncaea* was established by Böttger-Schnack (2003) to accommodate species of the *ivlevi*-group as defined in a preliminary phylogenetic study of Oncaeidae (Böttger-Schnack and Huys 2001). The typical characteristics of the genus are (1) the modification of caudal rami seta III into a strong spiniform element, (2) the undulate or lobate hyaline frill at the posterior margin of the urosomites and (3) the reduced number of six elements on the maxillule. *Spinoncaea ivlevi* (Shmeleva, 1966), the type species of this genus, was originally described from the Adriatic Sea. Thereafter, Malt (1982) provided a taxonomical report from the Atlantic. In 2003, Böttger-Schnack published a detailed morphological re-analysis of the species, including all the mouthparts, based mainly on copepod material from the Red Sea as compared to specimens from the type locality (Adriatic Sea) and including specimens from various regions in the Indian and Pacific Oceans (cf. Böttger-Schnack 2003: table 3). In the same account, two new species, *S. humesi* Böttger-Schnack, 2003 and *S. tenuis* Böttger-Schnack, 2003 were described, which differed from *S. ivlevi* in the spine count on P2 exopod-3 (*S. humesi*) and/or proportional lengths of the female urosome as well as modifications of caudal setae. Overall, the three described species are very similar in morphology and include some intraspecific variability as observed within as well as between different regions (Böttger-Schnack 2003). Also, females of *S. ivlevi* and *S. tenuis* exhibited two form variants each, which differed mainly in body proportions, especially in the urosomites, and slightly in endopodal spine lengths (Böttger-Schnack 2003). As for *S. ivlevi*, the detection of form variants hampered an unambiguous assignment of either form to the genuine species from the Adriatic Sea (Böttger-Schnack 2003).

Recently, a taxonomic study of the family Oncaeidae has been performed in the NE equatorial Pacific Ocean and one species of *Spinoncaea* identified as *S. ivlevi* was reported (Cho 2011). However, there was some doubt about the identification as the females in Cho's study showed morphological differences from the genuine *S. ivlevi* female in the proportional length of the female urosome, the length of the second endopod segment of the antenna, and the length ratio of the distal exopod segment to the distal spine on P2–P4.

As a part of a new and ongoing taxonomical study on the oncaeid copepods in the temperate and tropical Pacific, we obtained new copepod material of *Spinoncaea* from the northeastern and northwestern equatorial Pacific as a supplement to the copepod material sampled earlier (Cho 2011) and we also included samples taken in the Korea Strait. All three *Spinoncaea* species were found and examined in great detail. The present paper provides redescriptions of the morphological characters of the three species of *Spinoncaea* in these locations of the Pacific Ocean. Particular attention was paid to the variability of continuous morphological characters, such as e.g., the spine lengths on the rami of the swimming legs, as well as the occurrence of form variants among the females. In comparison to the earlier descriptions by Böttger-Schnack (2003) morphological differences and additions will be provided and the importance of information on the morphological variability within these species will be discussed. In addition, we performed genetic analysis to test the hypothesis that species with morphological variation will show genetic differences. To compare the sequences of *Spinoncaea* species with those obtained by Böttger-Schnack and Machida (2011) from the Mediterranean Sea, specimens from the Pacific were analyzed by the genetic regions of the mitochondrial cytochrome c oxidase subunit 1 (mtCOI) and 12S small ribosomal RNA (12S srRNA).

Material and methods

The copepod material was collected in three different regions and years in the Pacific Ocean, in the tropical northeastern (EP-1; 21 August 2009, EP-2; 19 March 2019) and northwestern (WP-1; 27 March 2016, WP-2; 4 April 2016) Pacific, and in the Korea Strait (KS; 7 October 2008) (Fig. 1). A conical net (60 cm mouth diameter, 60 μm mesh size) was used to sample different integrated vertical depth layers in the epipelagic zone between 0–100 m and 0–200 m. A station list with geographic positions, dates and depth layers sampled is given in Table 1. Each net sample was preserved in 99.9% ethyl alcohol immediately after collection on board. In the laboratory, oncaeids were sorted out from the preserved zooplankton samples under a stereomicroscope (Semi 2000-C; Carl Zeiss, Germany). Specimens were dissected with tungsten needles, mounted in lactophenol: glycerin (1:5), and sealed with transparent nail-varnish. Some specimens were mounted in fluoromount-G (SouthernBiotech, Birmingham, USA) on H-S slides (Double slide plate, BSDS-011R; Biosolution, Republic of Korea) (cf. Shirayama et al. 1993). For the purpose of morphometries and

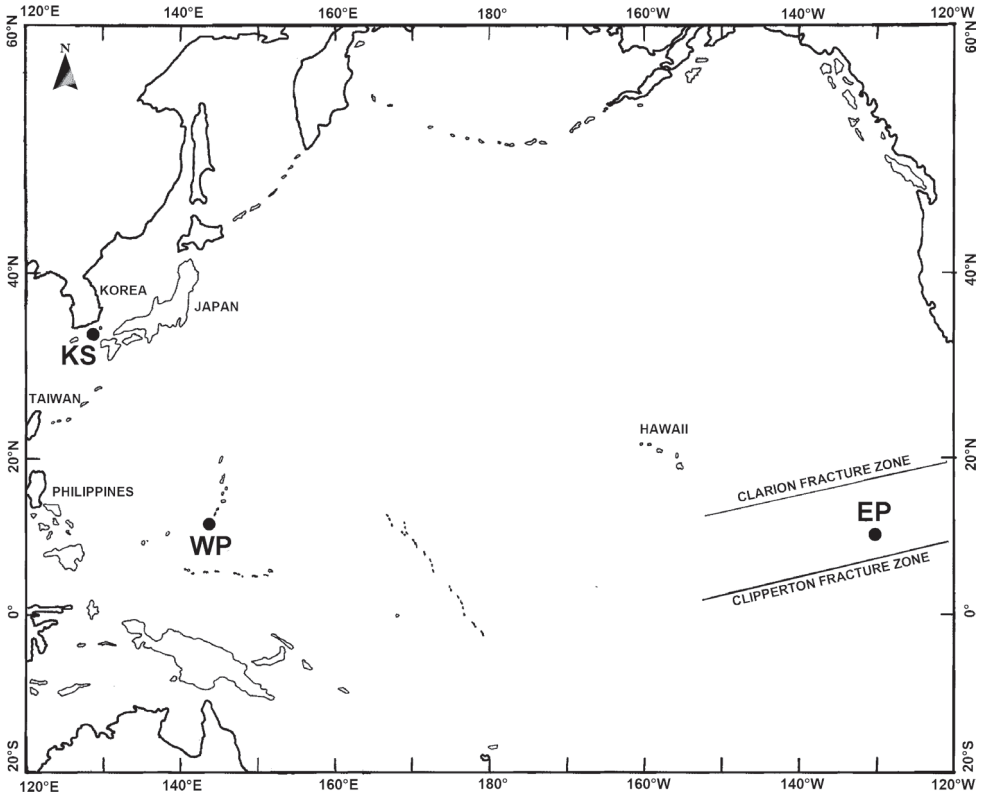

Figure 1. Location of the sampling stations in the northeastern equatorial Pacific (EP), the northwestern equatorial Pacific (WP), and the Korea Strait (KS).

Table 1. Sample locations for species of *Spinoncaea* in the equatorial and temperate Pacific Ocean.

Region	Station	Date	Geographical position	Sampling depth (m)
Northeastern Pacific	EP-1	21 August 2009	10°23'N, 131°20'W	100
	EP-2	19 March 2019	9°52'1.38"N, 131°45'38.28"W	200
Northwestern Pacific	WP-1	27 March 2016	13°23'46.44"N, 143°55'0.6"E	150
	WP-2	4 April 2016	13°20'3.42"N, 144°20'2.7"E	150
Korea Strait	KS	7 October 2008	33°44'50.50"N, 128°15'39.02"E	110

illustrations a differential interference contrast light microscope (DM2500; Leica, Wetzlar, Germany or BX51; Olympus, Tokyo, Japan) with a drawing tube was used. To prepare specimens for scanning electron microscope analysis (S-4300; Hitachi, Tokyo, Japan), specimens were fixed with 2% Glutaraldehyde and 2% OsO_4, dehydrated with graded ethanol, substituted with t-BuOH, dried by freeze dryer (ES-2030; Hitachi, Tokyo, Japan), mounted on stubs using copper tape, coated with platinum using an ion sputter (E-1045; Hitachi, Tokyo, Japan), and then photographed. Some specimens were deposited in the collection of National Institute of Biological Resources (**NIBR**), Incheon, Korea and the accession numbers are written in parentheses next to the specimens.

The morphological terminology used in the text and figures was adopted from Huys et al. (1996). Abbreviations:

Al antennule;
A2 antenna;
ae aesthetasc;
P1–P6 first to sixth thoracopod;
exp exopod;
enp endopod;
exp (enp)-1 (2, 3) to denote the proximal (middle, distal) segment of a three-segmented ramus.

Body sizes of individuals were measured laterally from the anterior margin of the prosome to the posterior margin of the caudal rami, not considering the various degrees of telescoping of somites. The length to width ratio of the caudal rami, the anal somite, and the genital (double-)segment was measured in dorsal view. The variability of individual spine lengths on the exo- and endopod segments of the swimming legs was examined by calculating (1) on the exopods of P2–P4 (1a) the length of the distal exopod segment in relation to the length of the distal spine; (1b) the length of the outer spine on the proximal exopod segment in relation the outer spine on the middle exopod segment; (1c) the length ratio of the outer spine on the proximal exopod segment compared to the length of the outer spines on the distal exopod segment; (2) on the endopods of P2–P4, the length of the outer subdistal and/or outer distal spine on the distal segment in relation to the length of the distal spine. If possible, both the left and right sides of the swimming legs were measured for each specimen. Scale bars in the figures are indicated in micrometers (μm).

Total genomic DNA was extracted from presorted single individuals with DNeasy Blood & Tissue Kit (Qiagen, Hilden, Germany) following the protocol of Cornils (2014). PCR amplifications were performed targeting mitochondrial COI and the 12S small ribosomal RNA genes. Two sets of primers, mtCOI primers [LCO1490, HCO2198 (Folmer et al. 1994)] and 12S srRNA primers [L13337-12S (Machida et al. 2002), H13842-12S (Machida et al. 2004)] were used for gene amplification. PCR reactions were carried out in 20 μl containing 5 μl of template, 0.2 μl of 2.5 unit Z-Taq (Takara, Kusatsu, Japan), 1 μl of each primer (5 μM), 2 μl of dNTP (2.5 mM each), 2 μl of 10X buffer, 0.6 μl of DMSO (99%), and 8.2 μl of sterile distilled water. The cycling profile was denaturation at 94 °C for 5 sec, annealing at 48 °C for 5 sec, and extension at 72 °C for 10 sec, for 40 cycles in the C1000 Touch Thermal Cycler (Bio-Rad, California, USA). PCR products were stained with Loanding STAR (Dyne Bio, Seongnam, Republic of Korea) and electrophoresed in 1.5% agarose gel. Positive PCR products were purified with AccuPrep PCR/Gel Purification Kit (Bioneer, Daejeon, Republic of Korea) and sent to Macrogen (Seoul, Republic of Korea) for sequencing.

DNA sequences were compared against known species from the NCBI GenBank nucleotide database using BLASTn. All sequences were edited using BioEdit 7.0.5.3 software (Hall 1999). Edited sequences were aligned by ClustalW using MEGA 7 software (Kumar et al. 2016). The phylogenetic tree was constructed by Maximum-likelihood with Kimura two-parameter distance in MEGA 7 software.

Results

Systematics

Order Cyclopoida Burmeister, 1834
Family Oncaeidae Giesbrecht, 1893 [1892]

Genus *Spinoncaea* Böttger-Schnack, 2003

The morphology of the three *Spinoncaea* species from the Pacific agrees in general with the (re)-description of these species from the Red Sea (Böttger-Schnack 2003), but a number of additions, modifications and/or supplements were found, which are specified in the following for each species and form variant. As the variability of morphometric data was studied for the Pacific specimens only (Tables 3, 4), the respective individual values of Red Sea specimens are mentioned only when outside the range of values from the Pacific.

***Spinoncaea ivlevi* (Shmeleva, 1966)**
Figs 2–7, 16

Oncaea ivlevi Shmeleva, 1966: 932–933, figs 1.1–1.11 (Adriatic).
Oncaea ivlevi: Shmeleva 1969: 5–8, 27, figs 3a–i, 4a–h (Adriatic, tropical Atlantic).
Oncaea ivlevi: Malt 1982: 186–187, 193, figs 3a–k, 4a–d (temperate Atlantic).
Spinoncaea ivlevi: Böttger-Schnack 2003: 193–207, figs 2–7 (Red Sea, Mediterranean Sea, Indian and Pacific oceans).

Material examined. 1. Robust form. (1) Northwestern Pacific (a) 13°23'46.44"N, 143°55'0.60"E (WP-1), 27 March 2016: Five females and four males dissected on several slides, respectively. Four dissected females (NIBRIV0000882743–882746) and four dissected males (NIBRIV0000882747–882750) were deposited in the NIBR; (b) 13°20'3.42"N, 144°20'2.7"E (WP-2), 4 April 2016: Six females dissected on several slides, respectively. Four dissected females (NIBRIV0000882751–882754), one undissected female (NIBRIV0000882755) and one undissected male (NIBRIV0000882756) mounted on H-S slide, respectively, and five undissected females and three undissected males in alcohol vial (NIBRIV0000882757) were deposited in the NIBR. (2) Northeastern Pacific, 10°30'N, 131°20'W (EP-1), 21 August 2009: Six females (NIBRIV0000882758–882763) and four males (NIBRIV0000882764–882767) dissected on several slides, respectively. All dissected specimens, one undissected female (NIBRIV0000882768) and one undissected male (NIBRIV0000882769) on respective H-S slide, and five undissected females and two undissected males in alcohol vial (NIBRIV0000882770) were deposited in the NIBR. (3) Korea Strait, 33°44'50.50"N, 128°15'39.02"E (KS), 7 October 2008: Three females (NIBRIV0000882771–882773) and one male dissected (NI-

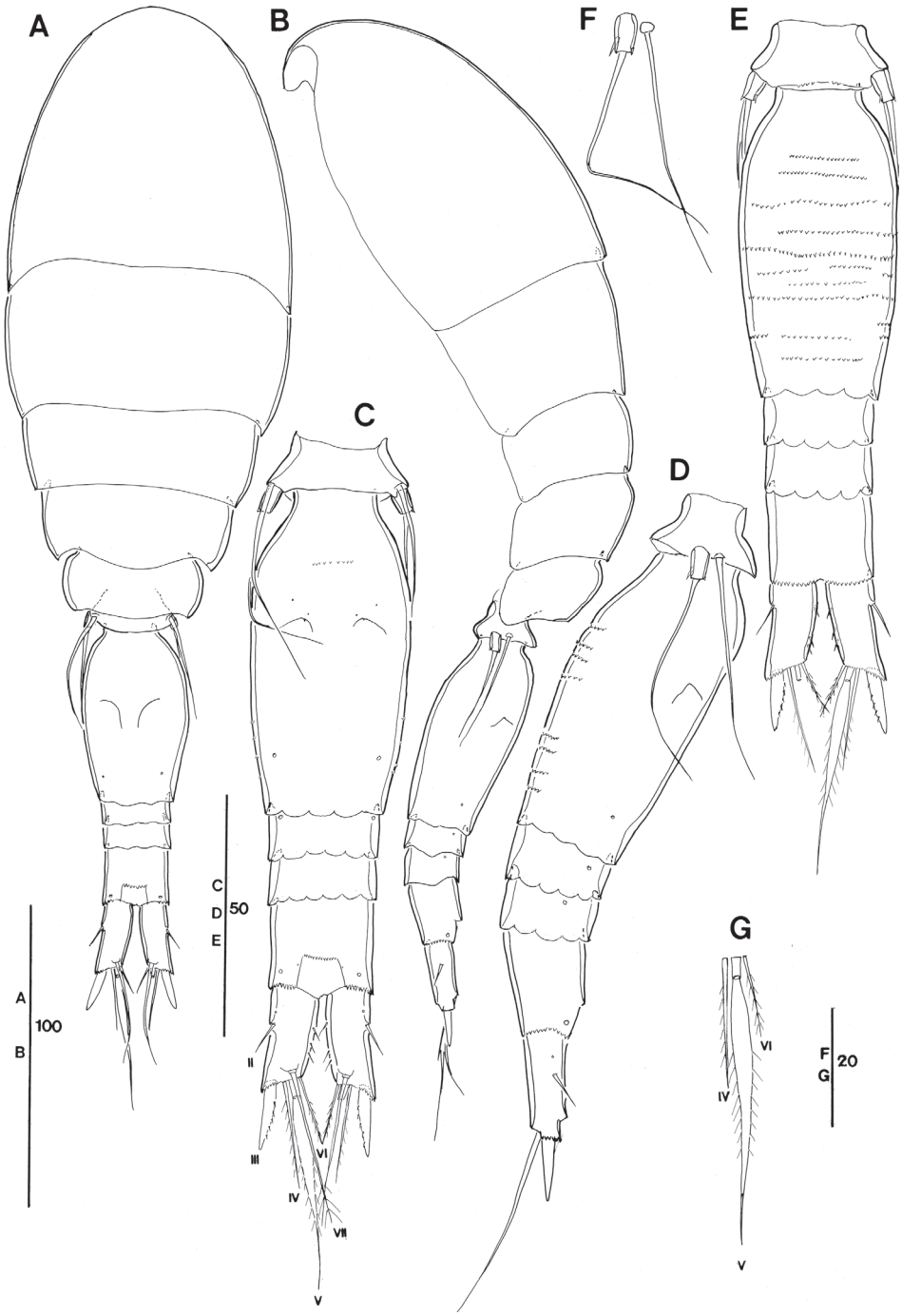

Figure 2. *Spinoncaea ivlevi* (Shmeleva, 1966), female, robust form (northwestern equatorial Pacific) **A** habitus, dorsal (caudal seta V on right side missing) **B** habitus, lateral **C** urosome, dorsal, setae on caudal rami are numbered using Roman numerals (seta V on right side missing) **D** urosome, lateral (seta V on right side missing) **E** urosome, ventral **F** leg 5, lateral **G** caudal setae IV–VI shown separately. Scale bars in μm.

BRIV0000882774) on H-S slide, respectively. All dissected specimens and two undissected females and two undissected males in alcohol vial (NIBRIV0000882775) were deposited in the NIBR.

2. Elongate form. (1) Northwestern Pacific, 13°23'46.44"N, 143°55'0.60"E (WP-1), 27 March 2016: One female (NIBRIV0000882776) dissected on two slides. This specimen was deposited in NIBR. (2) Northeastern Pacific, 10°30'N, 131°20'W (EP-1), 21 August 2009: Three females (NIBRIV0000882777–882779) dissected on one slide or three slides, respectively. Two females (aberrant) (NIBRIV0000882780) dissected on H-S slide. The morphometric data provided in Tables 3 and 4 included only four specimens (three normal females and one aberrant female). All dissected specimens except for one specimen of aberrant female and one undissected aberrant female (in alcohol, NIBRIV0000882781) were deposited in the NIBR.

Description. Female (robust form, Figs 2–4, 6, 7D, E, 16A–D, Tables 3, 4). Body length (in lateral view, telescoping of somites not considered) range 318–373 μm in Pacific specimens (Table 3), showing a wider size range than in the Red Sea (330–340 μm, Böttger-Schnack 2003: 193).

Prosome 1.9 × length of urosome, excluding caudal rami, 1.6 × urosome length, including caudal rami (Fig. 2B), calculated by not correcting for the telescoping of somites. Variation of prosome to urosome length (including CR) ratio 1.5–1.7 in Pacific specimens (Table 3). The respective values provided for Red Sea specimens are not comparable as they were based on length data corrected for the telescoping of somites. When calculating the body proportions of the female from Böttger-Schnack's fig. 2A by not correcting for the telescoping of somites, the respective ratio of prosome to urosome length (incl. CR) would account to 1.5, which is within the range of values for Pacific specimens.

P5-bearing somite with paired row of midventral spinous processes (Fig. 2E), variable in number, generally two or three processes, difference per body side may appear as in Fig. 2E: four (right) and two (left). No such variation was mentioned for the Red Sea specimens.

Posterior margin of genital double-somite and postgenital somites with undulate hyaline frill (Fig. 2C, E), as typical for *Spinoncaea* species, shown in detail in Fig. 16D.

Genital double-somite (Figs 2C, D, E, 16D) 2.0 × as long as maximum width in specimen figured (measured in dorsal aspect) and ~ 1.5 × as long as postgenital somites combined; variation in length to width ratio 1.6–2.0 in Pacific specimens (Table 3), surface ornamentation and pore pattern as figured (Figs 2E, 16D).

Anal somite approximately as wide as long, with insignificant variation in length to width ratio (Table 3), ornamentation as figured (Fig. 2C, E).

Caudal ramus (Fig. 2A, C, G) with length to width ratio 1.9–2.2 measured along inner margin and 2.4–2.9 measured along outer margin (Table 3). Caudal seta II with a single long spinule (as in male, e.g., Fig. 16E), which is difficult to discern, and which was not reported for Red Sea specimens, and seta IV with ornamentation being unipinnate, while it is bipinnate in Red Sea specimens. Variation in length ratios among setae II, III, and IV as given in Table 3, denoting a smaller ratio for seta III:II (1.3–1.9) than in the Red Sea (2.2; Böttger-Schnack 2003: fig. 2F).

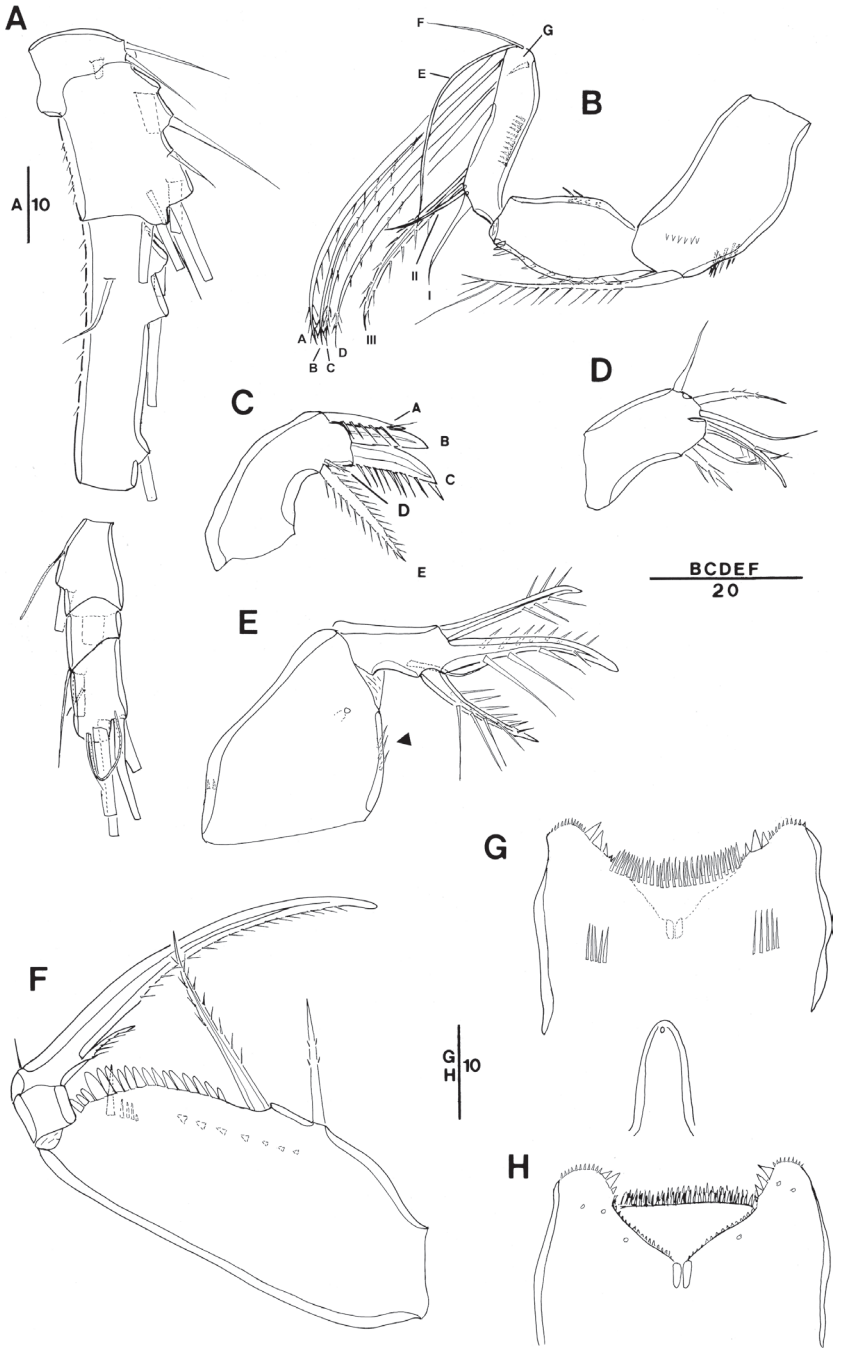

Figure 3. *Spinoncaea ivlevi* (Shmeleva, 1966), female, robust form (northwestern equatorial Pacific) **A** antennule (separated between segments 3 and 4) **B** antenna, distal elements on distal endopod segment numbered using capital letters, lateral elements indicated by Roman numerals **C** mandible, individual elements indicated by capital letters **D** maxillule **E** maxilla, arrow indicating spinules on syncoxa, **F** maxilliped, posterior, syncoxa missing **G** labrum, anterior **H** labrum, posterior. Scale bars in μm.

Table 2. Swimming legs armature formula. Roman numerals indicate spines, Arabic numerals represent setae. Differences in spine count are marked in bold. (a) *S. ivlevi* and *S. tenuis*, (b) *S. humesi*.

Leg	Coxa	Basis	Exopod	Endopod
P1	0–0	1–I	I-0; I-1; III,I,4	0–1; 0–1; 0,I,5
P2	0–0	1–0	I-0; I-1; **III[(a)]/II[(b)]**,I,5	0–1; 0–2; 0,II,3
P3	0–0	1–0	I-0; I-1; II,I,5	0–1; 0–2; I,II,2
P4	0–0	1–0	I-0; I-1; II,I,5	0–1; 0–2; I,II,1

Antennule 6-segmented (Fig. 3A) with armature formula: 1-[3], 2-[8], 3-[5], 4-[2+ae], 5-[2 (ae not discernible)], 6-[5+(1+ae)], typical for *Spinoncaea* species.

Antenna 3-segmented, armature as for Red Sea specimens, including the absence of seta IV on the lateral armature of the distal endopod segment (Fig. 3B, setae I–III indicated). Distal endopod segment reflexed (Fig. 3B), 3.0–3.9 × longer than wide (Table 3), somewhat longer than reported for Red Sea specimens (ca 3:1; discussed under "Remarks"). Ornamentation of elements differing slightly from Red Sea specimens in (1) the coxobasis with a long seta at inner distal corner is ornamented with long spinules unilaterally along entire length, including a single very long spinule at distal part, but only a short row of small spinules at anterior half (Fig. 3B), while in specimens from the Red Sea this seta is ornamented with strong spinules bilaterally and lacking a single long spinule (Böttger-Schnack 2003: fig. 3A), and on (2) the proximal endopod segment is lacking single strong spine on expanded outer margin in specimen figured (Fig. 3B), but is present in specimen from Korea Strait (Fig. 6A), as specified for Red Sea specimens.

Labrum (Figs 3G, H, 16A) showing variable ornamentation on anterior surface, paired row of long setules in specimen figured (Fig. 3G, indicated by white arrow in Fig. 16A) as specified for Red Sea specimens, additional row of setules indicated in specimen from Korea Strait (Fig. 6C).

Mandible (Fig. 3C) gnathobase with five elements, with dorsal element D shortest and inserting near base of seta E, as typical for *S. ivlevi* (cf. Böttger-Schnack 2003: 191) difficult to discern in some specimens from the Pacific.

Maxillule (Figs 3D, 16B) with six elements [innermost element on outer lobe absent, as typical for *Spinoncaea* species]; ornamentation of middle and innermost element on inner lobe as well as of element next to innermost on outer lobe (Fig. 16B) slightly modified as compared to Red Sea specimens.

Maxilla (Fig. 3E) with additional ornamentation on syncoxa showing rows of short spinules along outer margin and long spinules along inner margin (arrowed in Fig. 3E), not reported earlier for Red Sea specimens.

Maxilliped (Fig. 3F, syncoxa missing) with basis ornamented with fringe of short spatulated spinules between distal seta and articulation with endopod, as illustrated for Red Sea specimens (Böttger-Schnack 2003: fig. 3G, but erroneously described as "… between proximal seta and articulation with endopod;.." in text on p 200).

Swimming legs 1–4 (Fig. 4A–D) with armature formula shown in Table 2. Intercoxal sclerite of P1 ornamented with paired long, fine setules (Figs 4a, 16C), which were not discernible in some specimens. Outer seta on basis of P1 slightly shorter than

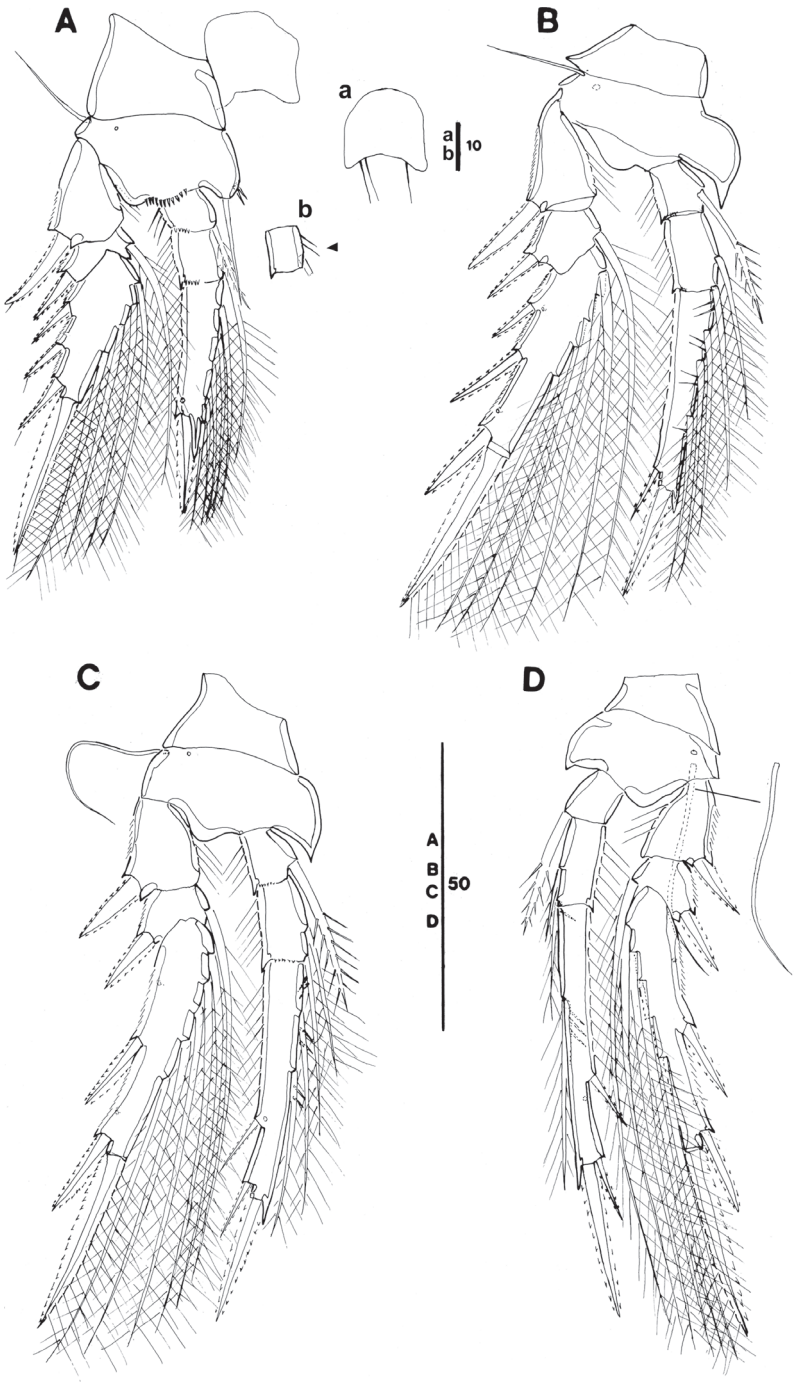

Figure 4. *Spinoncaea ivlevi* (Shmeleva, 1966), female, robust form (northwestern equatorial Pacific) **A** P1, anterior [a: ornamentation on intercoxal sclerite of another specimen, b: second endopod segment shown separately, strong setules on inner margin arrowed] **B** P2, posterior **C** P3, anterior **D** P4, anterior, seta on basis figured separately. Scale bars in μm.

Table 3. Variation in morphometric traits for three species of *Spinoncaea* (both sexes, including form variants of female *S. ivlevi*) from three locations in the Pacific Ocean (WP = western equatorial Pacific; EP = eastern equatorial Pacific; KS = Korea Strait; n = number of specimens examined) Abbreviations: A2 = antenna; AS = anal somite; CR = caudal ramus, for numbering of setae see Fig. 2C; DES = distal endopod segment; DS = distal spine; G(D)S = genital (double-)somite; in = inner margin; out = outer margin; L = length; PGS = postgenital somites; Pro = prosome; Uro = urosome; W = width.

		S. ivlevi								*S. tenuis*				*S. humesi*		
		female					male			female		male		female	male	
		WP		EP		KS	WP	EP	KS	EP	KS	EP	KS	EP	WP	KS
		robust	elongate	robust	elongate	robust										
n		11	1	6	4	3	4	4	1	8	1	3	1	3	2	1
Total length (µm)		327–360	305	318–373	330–345	343–344	306–329	307–331	298	320–355	329	310–325	292	344–348	285/295	292
Pro:Uro including CR		1.5–1.7	1.4	1.5–1.7	1.3	1.5–1.6	1.3–1.5	1.5–1.6	1.4	1.5–1.7	1.3	1.5	1.4	1.3–1.4	1.1/1.2	1.3
AS L:W		1.0–1.1	1.3	1.0–1.1	1.2–1.4	1.0–1.1	0.9–1.1	0.9–1.0	0.9	1.1–1.3	1.2	1.0	1.2	1.2–1.3	1.2	1.2
CR	L:W (in)	1.9–2.2	2.0	1.9–2.2	2.0–2.1	2.1	1.8–1.9	1.7–2.0	1.8	1.8–2.5	2.5	1.9–2.2	2.4	2.3–2.5	2.1/2.2	2.5
	L:W (out)	2.4–2.9	2.5	2.4–2.6	2.6–2.8	2.4	2.3–2.7	2.3–2.5	2.4	2.3–2.9	3.0	2.2–2.6	2.8	2.8–3.1	2.6/2.9	3.2
	Setae III:II	1.5–1.9	2.0	1.3–1.7	1.6–2.0	1.3–1.6	1.6–1.9	1.2–1.9	1.4	1.0–1.5	1.1	1.2–1.5	1.2	1.6–1.7	1.6/1.8	1.3
	Setae IV:III	1.2–1.8	1.7	1.5–1.7	1.2–1.3	1.8–1.9	1.3–1.5	1.2–2.0	1.8	1.4–2.3	2.2	1.7–1.9	2.0	1.2–1.6	1.4/1.5	1.6
G(D)S (dorsal view)	L:W	1.8–2.0	2.0	1.6–1.9	1.9–2.2	1.8	1.8–1.9	1.8–1.9	1.8	1.8–2.3	2.2	1.8–1.9	2.0	1.9–2.0	1.7/1.9	2.1
G(D)S L : PGS L		1.4–1.5	1.7	1.7	1.4–1.5	1.6	2.3–2.5	2.0	2.1	1.5–2.1	1.9	2.6–2.7	2.4	1.4–1.5	2.1/2.2	2.3
G(D)S Max W: Min W (posterior portion)		1.2–1.5	1.5	1.4–1.5	1.4–1.6	1.3–1.5	-	-	-	1.5–2.1	1.8	-	-	1.7–2.0	-	-
A2 DES L:W		3.4–3.9	2.2	3.0–3.8	3.4–3.9	3.2–3.9	3.2–3.9	3.6–3.8	-	3.3–4.1	4.1	3.6–4.0	3.8	3.7–4.3	3.8–4.1	3.5

Table 4. Variation in proportional spine lengths on P2–P4 for three species of *Spinoncaea* (both sexes, including form variants of female *S. ivlevi*) from three locations of the Pacific Ocean (WP = western equatorial Pacific; EP = eastern equatorial Pacific; KS = Korea Strait, n = number of specimens measured) Abbreviations: DS = distal spine; L = length; MS = middle spine; ODS = outer distal spine; OSDS = outer subdistal spine; PS = proximal spine; SP = spine; W = width.

		S. ivlevi								*S. tenuis*				*S. humesi*		
		female					**male**			female		male		female	male	
		WP		EP		KS	WP	EP	KS	EP	KS*	EP	KS*	EP	WP	KS*
		robust	**elongate***	**robust**	**elongate**	**robust**										
n		11	1	6	4	3	4	4	1	8	1	3	1	3	2	1
P2 L ratio exp-3:DS		1.03–1.38	1.13	1.19–1.32	1.03–1.20	1.1–1.29	1.07–1.28	1.20–1.30	1.19	0.92–1.09	0.98	1.02–1.07	1.0/1.03	1.04–1.12	1.04–1.23	1.13/1.16
P3 L ratio exp-3:DS		1.21–1.52	1.21	1.09–1.38	1.06–1.19	1.22–1.43	1.17–1.57	1.23–1.32	1.28	0.95–1.07	0.98	1.01–1.12	1.05/1.06	1.14–1.21	1.13–1.19	1.19/1.22
P4 L ratio exp-3:DS		1.26–1.49	1.26/1.60	1.31–1.41	1.20–1.30	1.26–1.43	1.23–1.52	1.33–1.49	damaged	0.96–1.13	0.97	1.00–1.04	0.99	1.11–1.20	1.06–1.28	1.28/1.48
L ratio spines on P2 exp	SP exp-1:SP exp-2	1.24–1.57	1.46	1.33–1.63	1.32–1.43	1.43–1.74	1.44–1.77	1.31–1.55	1.39	1.29–1.47	1.27	1.36–1.52	1.21/1.33	1.31–1.42	1.25–1.32	1.25/1.26
	SP exp-1:PS exp-3	1.36–1.76	1.46	1.36–1.79	1.46–1.72	1.43–1.64	1.53–1.83	1.42–1.57	1.45	1.28–1.72	1.32	1.40–1.70	1.33/1.45	1.13–1.26	1.04–1.15	1.13/1.19
	SP exp-1:MS exp-3	1.00–1.16	0.97	0.95–1.16	1.03–1.07	1.02–1.11	0.86–1.17	1.03–1.29	1.07	0.97–1.14	1.00	1.00–1.17	1.10/1.22			
	SP exp-1:ODS exp-3	0.90–1.13	0.88	0.92–1.10	0.88–0.95	0.90–1.18	0.88–1.15	0.89–1.15	0.91	0.82–1.17	0.85	0.85–0.94	0.97/1.03	0.94–1.13	0.93–1.00	0.89/0.96
L ratio spines on P3 exp	SP exp-1:SP exp-2	1.05–1.38	1.14	1.10–1.22	1.16–1.30	1.14–1.35	1.00–1.37	1.03–1.43	1.03	1.06–1.21	1.10/1.13	1.07–1.26	1.42/1.44	1.14–1.26	1.15–1.30	1.24/1.25
	SP exp-1:PS exp-3	0.85–1.11	0.89	0.89–1.00	0.97–1.06	0.93–1.03	0.83–1.10	0.97–1.03	0.94	0.88–1.00	1.10	0.83–0.85	1.17	1.07–1.31	1.15–1.20	1.14/1.35
	SP exp-1:ODS exp-3	0.83–1.03	0.89	0.87–1.05	0.82–1.00	0.83–0.95	0.66–0.97	0.94–1.11	0.83	0.77–0.94	0.91/0.92	0.81–0.83	1.06/1.10	1.00–1.06	1.00–1.08	1.07/1.09
L ratio spines on P4 exp	SP exp-1:SP exp-2	0.90–1.18	0.92/1.02	1.01–1.12	0.86–1.13	0.94–1.06	0.85–1.25	0.96–1.17	0.96	0.88–1.21	1.04	1.05–1.19	1.04	1.04–1.08	1.05–1.28	0.81/0.83
	SP exp-1:PS exp-3	0.82–1.07	0.73/0.90	0.87–1.06	0.80–0.93	0.84–0.97	0.86–0.93	0.87–1.08	0.86	0.75–0.97	0.92	0.82–1.02	1.10	1.00–1.27	1.00–1.17	0.94/1.14
	SP exp-1:ODS exp-3	0.72–0.92	0.69/0.79	0.83–0.97	0.70–0.93	0.78–0.94	0.72–1.04	0.79–1.00	0.78	0.65–0.88	0.76	0.74–0.78	0.91/0.93	0.81–0.93	0.78–1.00	0.81/0.83
L ratio spines on P2 enp-3	ODS:DS	0.45–0.63	0.51/0.56	0.43–0.57	0.49–0.58	0.52–0.55	0.50–061	0.45–0.59	damaged	0.42–0.53	0.47/0.50	0.45–0.55	0.53/0.56	0.42–0.51	0.50–0.55	0.51
L ratio spines on P3 enp-3	OSDS:DS	0.39–0.56	0.42	0.37–0.48	0.35–0.53	0.47–0.53	0.43–0.54	0.39–0.56	0.42	0.34–0.52	0.38/0.40	0.32–0.43	0.43	0.38–0.43	0.37–0.41	0.37/0.41
	ODS:DS	0.44–0.64	0.42/0.51	0.43–0.56	0.42–0.55	0.48–0.54	0.42–0.51	0.41–0.55	0.45	0.39–0.50	0.40/0.46	0.42–0.51	0.51/0.52	0.42–0.44	0.42–0.50	0.45/0.51
L ratio spines on P4 enp-3	OSDS:DS	0.30–0.49	0.38	0.30–0.48	0.28–0.45	0.41–0.47	0.30–0.47	0.32–0.43	0.37	0.25–0.33	0.27/0.34	0.25–0.32	0.34	0.35–0.38	0.34–0.38	0.26/0.31
	ODS:DS	0.36–0.50	0.42	0.32–0.48	0.33–0.52	0.42–0.51	0.39–0.53	0.36–0.48	0.43	0.29–0.38	0.36/0.38	0.28–0.41	0.42	0.39–0.41	0.40–0.43	0.34/0.37

* = data from the left/right legs of one specimen; if there is only one datum, it means that the values are the same or only one side was measured.

in Red Sea specimens and naked. Anterior surrounding of bases of spines on exopodal and endopodal segments (= small spinules) not discerned in Pacific specimens.

Exopods with general characteristics as for Red Sea specimens, including a reduced length of spine on middle segment (= exp-2) of P2 and P3 (Fig. 4B, C) and of proximal spine on distal segment (= exp-3) of P2 (Fig. 4B); variability of proportional spine lengths, however, indicates that extent of size reduction of spine on exp-2 differs between legs: most obvious on P2, less obvious on P3 and insignificant on P4 (Table 4). Distal spine on P1 slightly longer, on P2–P4 shorter than distal exopod segment, variability of respective length ratios (Table 4) indicating that the respective size difference is less obvious in P2 as compared to P3 and P4.

Endopods with length ranges of outer subdistal spine and outer distal spine relative to distal spine given in Table 4 generally similar to Red Sea specimens (Böttger-Schnack 2003: fig. 4A–D).

P5 (Fig. 2C, D, F) with length to width ratio of exopod segment 1.6, as for Red Sea specimens.

P6 (Fig. 2C) represented by operculum closing off each genital aperture; possibly armed with a short spinule, which is difficult to discern in Pacific specimens.

Female (elongate form, Fig. 7A–C, Tables 3, 4). Body length range 305–345 μm, based on five specimens from tropical northeastern and northwestern Pacific, not significantly different from robust form (Table 3).

Prosome 1.3–1.4 × length of the urosome (incl. CR), smaller than in the robust form (1.5–1.7, Table 3).

Genital double-somite with shape slightly different from robust form, degree of tapering being stronger (Fig. 7A) than in robust form (Fig. 2C). Length to width ratio of the genital double-somite (1.9–2.2) slightly larger than in robust form (1.6–2.0), but values overlap (Table 3).

Anal somite with length to width ratio larger in elongate form (1.2–1.4) than in robust form (1.0–1.1) (Table 3); longer than CR (measured along outer margin) while in the robust form the anal somite is shorter than the CR (cf. Fig. 2A, C, E).

Caudal ramus with ranges in length to width ratio overlapping between the two female form variants (Table 3).

Antennule (not figured) 6-segmented. Armature formula as for *S. ivlevi* robust form.

Antenna (not figured) 3-segmented, armature as for *S. ivlevi* robust form. Distal endopod segment with variation of length to width (Table 3).

Mandible, maxillule, maxilliped (not figured) similar to those of the robust form.

Swimming legs variable in proportional lengths of endopodal and exopodal spines on P2–P4 as given in Table 4, showing similar ranges of variation among both forms of the species (cf. Table 4).

Male (Figs 5, 16E, Tables 3, 4). Body length range 298–331 μm in Pacific specimens (Table 3). Sexual dimorphism in antennule, maxilliped, P6, and in genital segmentation, slight modification in setal length of P5.

P5-bearing somite with paired row of midventral spinous processes (Fig. 5D), variable in number, generally two or three processes.

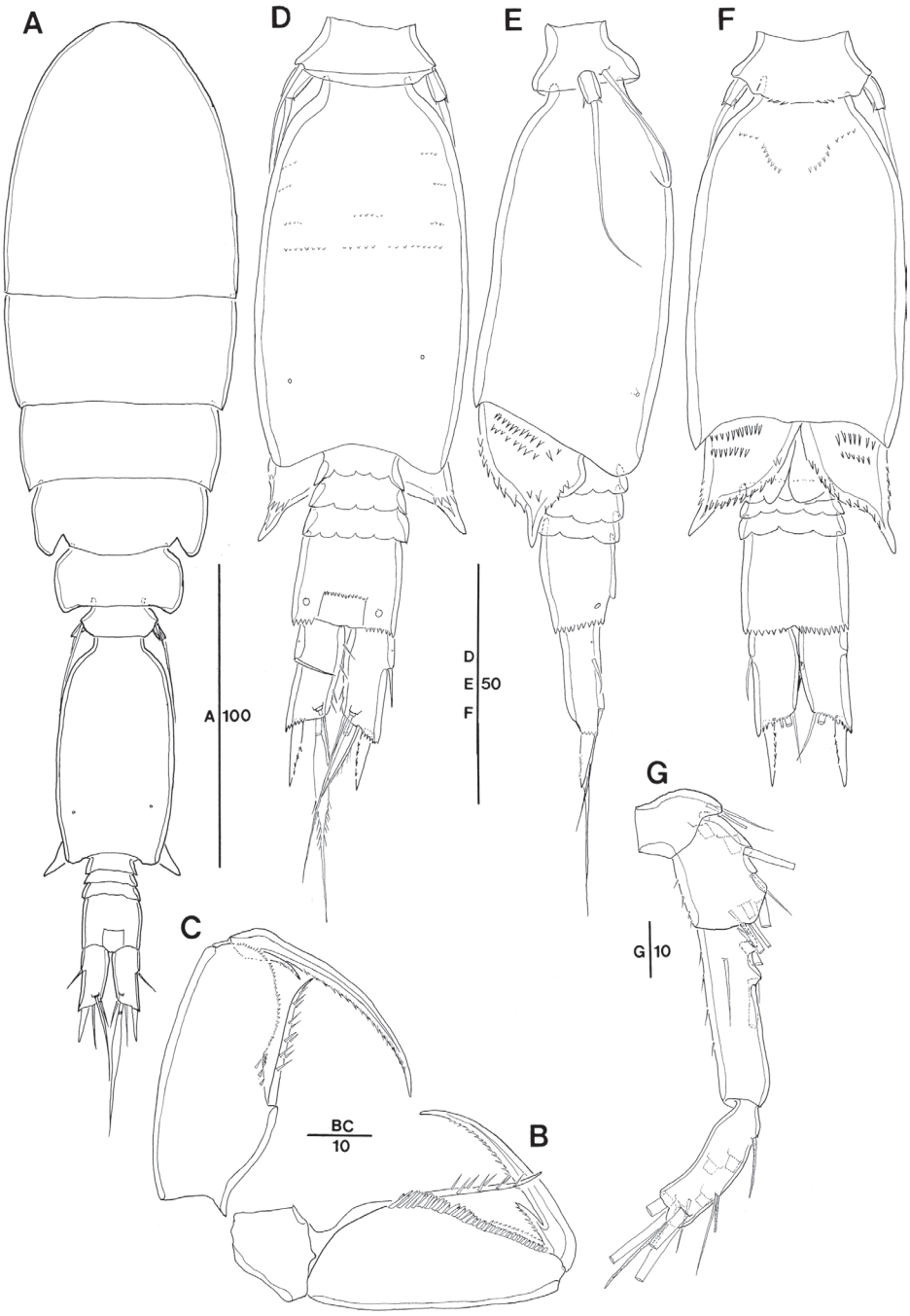

Figure 5. *Spinoncaea ivlevi* (Shmeleva, 1966), male (northwestern equatorial Pacific) **A** habitus, dorsal (caudal seta V on left side missing) **B** maxilliped, posterior **C** maxilliped, anterior, syncoxa missing **D** urosome, dorsal (caudal seta IV on left side and seta V on right side missing, seta VII on left side omitted) **E** urosome, lateral **F** urosome, ventral (caudal seta IV on left side and seta V on right side missing, seta IV on right side and seta V on left side omitted) **G** antennule. Scale bars in μm.

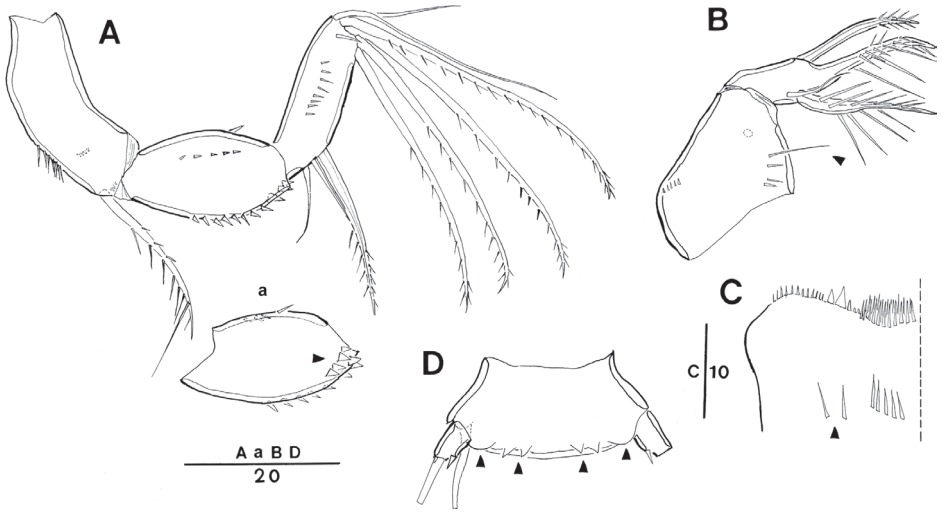

Figure 6. *Spinoncaea ivlevi* (Shmeleva, 1966), female, robust form (Korea Strait) **A** antenna [a: first endopod segment of right antenna, additional broad spinules arrowed] **B** maxilla, long setule arrowed **C** labrum, anterior, additional setules arrowed **D** P5-bearing somite, ventral, midventral spinous processes and weakly pronounced ventrolateral lobes arrowed. Scale bars in μm.

Caudal rami (Fig. 5A, D, F) with length to width ratio 1.7–2.0 measured along inner margin and 2.3–2.7 measured along outer margin (Table 3). Caudal setae with variations in proportional lengths of caudal setae III:II and setae IV:III as given in Table 3, similar to female. CR seta II ornamented with single long spinule in some specimens (Fig. 16E), not noted for specimens from Red Sea.

Dorsal surface of genital somite ornamented with pattern of minute denticles or spinules (Fig. 5D), which are less distinct than in Red Sea specimens (Böttger-Schnack 2003: fig. 5D), ventral surface with spinule pattern on anterior part (Fig. 5F) not observed in Red Sea specimens (Böttger-Schnack 2003: fig. 5E). Surface of genital flaps covered with several rows of strong denticles or spinules (Fig. 5E, F), few denticles also observed on inner distal part (Fig. 5D) not observed in Red Sea specimens (Böttger-Schnack 2003: fig. 5D).

Antennule (Fig. 5G) 4-segmented, armature formula: 1-[3], 2-[8], 3-[4], 4-[9+2ae+(1+ae)], aesthetascs very small and slender, segment 4 with small middle aesthetasc close to seta present, which is not discernible in the female. Ornamentation as figured.

Antenna (not figured) with variation in length to width ratio of distal endopod segment similar to female (Table 3).

Maxilliped (Fig. 5B, C) 3-segmented, comprising syncoxa, basis and 1-segmented endopod, armature and ornamentation as figured. Basis with only one long seta within longitudinal cleft, corresponding to distal seta in female, proximal seta absent (Fig. 5C). Endopod represented by long curved claw, tip of claw without hyaline apex.

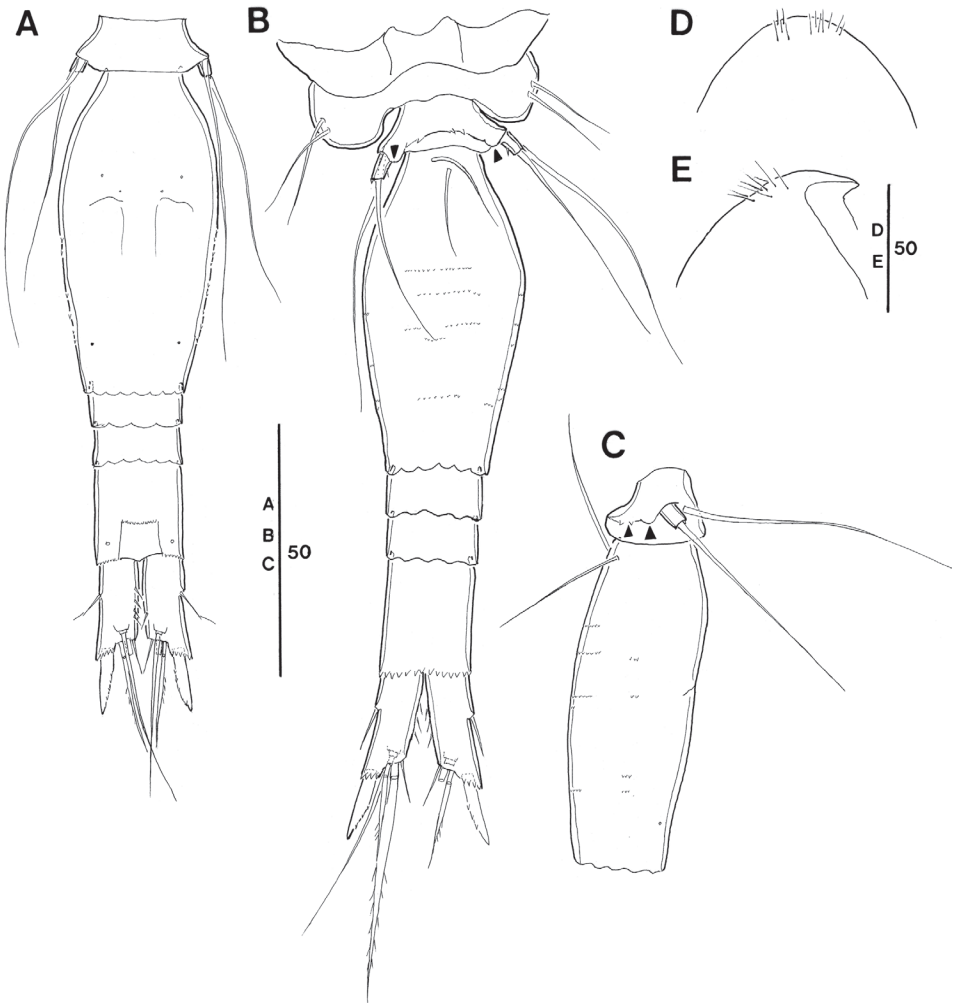

Figure 7. *Spinoncaea ivlevi* (Shmeleva, 1966), female, elongate form, general (northwestern equatorial Pacific) **A** urosome, dorsal, caudal seta V on both sides missing; elongate form, aberrant (northeastern equatorial Pacific) **B** P4-bearing somite and urosome, ventral, showing ornamentation on P4 and P5-bearing somites and genital double-somite, ventrolateral lobes arrowed, caudal seta V on left side missing **C** P5-bearing somite and genital double-somite, lateral, showing 2 long setules on ventral side of double-somite, midventral spinous process and ventrolateral lobe arrowed. *Spinoncaea ivlevi* (Shmeleva, 1966), female, robust form, variation, (northwestern equatorial Pacific) **D** setular patch on tip of cephalosome, dorsal **E** setular patch on cephalosome, lateral. Scale bars in µm.

Swimming legs 1–4 with armature and ornamentation as in female. Variability in length ratios of outer spine on exp-1 relative to outer spines on exp-2 and exp-3 of P2–P4, and length ratios of outer subdistal spine and outer distal spine relative to distal spine on enp-3 of P2–P4 given in Table 4, not significantly different from female.

P5 (Fig. 5E, F) exopod with general shape and armature as in female; exopodal seta and outer basal seta somewhat shorter than in female.

P6 (Fig. 5F) represented by posterolateral flap closing off genital aperture on either side, ornamented as described above, posterolateral corners well discernible in dorsal aspect (Fig. 5A, D).

Remarks. Böttger-Schnack (2003) provided a comprehensive redescription of *S. ivlevi* from the Red Sea and various other regions and included a detailed discussion of Shmeleva's descriptions of the species in 1966 (original account) and in 1969 and of that record by Malt (1982). Therefore, these papers are not further discussed in the present paper and the data presented by Böttger-Schnack (2003) were mainly used as a reference for comparison with the Pacific specimens. However, one detail of Shmeleva's original illustration is noteworthy, as the shape of the distal endopod segment on the antenna is much more slender in both sexes (Shmeleva 1966: fig. 1.4; 1969: figs 3d, 4c) than figured in Böttger-Schnack's account for the robust form of the female (2003: fig. 3A). In specimens of both female form variants from the Pacific the distal endopod segment of the antenna appears to be relatively longer and more slender than figured for the Red Sea specimens, showing a range of variation in length to width ratio of 3.0–3.9 in Pacific (cf. Table 3), while this ratio is described as "about three times longer than wide" in the Red Sea (Böttger-Schnack 2003: 198). As the figure of the specimen from the Korea Strait (Fig. 6A) also shows a somewhat stronger reflexed orientation of the distal segment compared to the specimen from the equatorial Pacific (Fig. 3B), the length to width ratio may be underestimated. But the respective figure (Fig. 6A) does not give clear evidence about its actual length to width ratio, because the strongly reflexed orientation of the distal antennary segment makes it difficult to measure it from this figure.

Some other differences between our study and Böttger-Schnack's redescription were detected in the presence of few long fine setules on the intercoxal sclerite of P1 in both sexes (Figs 4a, 16C), and the distinct ornamentation of the ventral anterior surface of the genital somite in the male (Fig. 5F). The first character mentioned has so far been found only in one other *Spinoncaea* species, *S. tenuis* (cf. Böttger-Schnack 2003: fig. 14A), and is recorded for *S. ivlevi* in the present account for the first time, but seemed to be variable, being present in most but not all specimens examined from the three locations in the Pacific (e.g., eight of eleven females and three of four males in the northwestern Pacific).

Additional or different ornamentation details found in the Pacific specimens of *S. ivlevi*, not mentioned and/or not figured by Böttger-Schnack (2003) included mainly details on the surface of elements such as on the maxilla (syncoxa with additional spinule pattern, Fig. 3E), or small details on setae, such as on the inner seta on the coxobasis of the antenna (Figs 3B, 6A) and on the middle element on the outer lobe of the maxillule (Figs 3D, 16B). These delicate ornamentation details can be discerned much better under a scanning electronic microscope as used in the present study than under a light microscope.

Despite the ornamentation differences between the redescription (Böttger-Schnack 2003) and the present account, specimens from the equatorial and temperate Pacific

Ocean were regarded as conspecific with *S. ivlevi* because our specimens showed basic morphological characters of *S. ivlevi*, such as:

(1) the mandible showing the full set of 5 elements,
(2) the length to width ratio of the caudal ramus,
(3) the proportional lengths of caudal setae,
(4) the shape of caudal seta IV, which is setiform and not dilated as in *S. tenuis*,
(5) the shape and ornamentation of the female genital double-somite, and
(6) the paired row of long setules on the anterior surface of the labrum.

In addition, the results of the molecular genetic analysis, which are presented, also supports this opinion, and is briefly discussed below.

Similar to the report from the Red Sea (Böttger-Schnack 2003), females of *S. ivlevi* exhibited two form variants in the equatorial northeastern and northwestern Pacific. Taking into consideration the variability of morphological characters of the two variants as examined in the present account (Tables 3, 4), the following differences between the two female forms reported by Böttger-Schnack (2003: 204) could be confirmed for specimens from the Pacific: (1) the length to width ratio of the anal somite, which is larger in the elongate form (1.2–1.4) than in robust form (1.0–1.1), (2) the length ratio of prosome to urosome which is smaller in the elongate form (1.3–1.4) than in the robust form (1.5–1.7), and (3) the shape of the genital double-somite, which shows a stronger degree of tapering in the elongate form (Fig. 7A) as compared to the robust form (Fig. 2C). On the other hand, the difference between the two forms in the length to width ratio of the genital double-somite indicated in Böttger-Schnack´s study (2003: 204) was not confirmed, because the respective values in the Pacific specimens overlapped. (Table 3). Also, the variability of the length to width ratio of the caudal ramus is similar for both variants, and the range of values of proportional spine lengths of endopodal and exopodal spines on P2–P4 overlap between the two forms, including the values of these spines calculated from the robust form in Böttger-Schnack (2003: fig. 4B–D). The P5-bearing somite of the elongate form from the equatorial Pacific exhibits one pair of weakly developed ventrolateral lobes (Fig. 7B, C), which is not mentioned in the descriptive text of Böttger-Schnack (2003), but was shown in her fig. 6b. In the robust form, these lobes were not observed in specimens from the two locations in the equatorial Pacific areas (cf. Fig. 2E), but were weakly pronounced in specimens from the Korea Strait (Fig. 4D, arrowed).

In the Pacific, individual variation between specimens was found e.g., in the number of midventral spinous processes on the P5-bearing somite, either two or three in both sexes, and some individuals also had different numbers between left and right side (Fig. 2E). It is common that there is no fringe of long setules on outer margin of proximal endopod segment of P4 in *S. ivlevi*, but in some individuals this fringe was present (not figured). Furthermore, individual variation in ornamentation appeared (1) in the caudal seta II in some individuals, ornamented with a single long spinule in both sexes, (2) in the ornamentation on the dorsal anterior surface of the genital double-somite of females (cf. Fig. 2C),

Table 5. The morphological abnormalities of *S. ivlevi* from three locations in the Pacific Ocean Abbreviations: RF1, RF2 = female robust form; EF1, EF2, female elongate form; M = male; for abbreviation of locations see Tables 3, 4.

Specimens	Figure	Morphological abnormalities or variation
WP-RF1	Fig. 7D, E	- a patch of long setules on the anterior part of the cephalosome - the reduced length on both enp-3 of P1 with modified setae
WP-RF2	Fig. 7D, E	- a patch of long setules on the anterior part of the cephalosome
WP-RF3	not figured	- a long setule (or a seta) on the dorsal anterior surface of the genital double-somite
WP-M1	not figured	- reduced length of both enp-3 of P4 with modified spines and OSDS absent
EP-EF1	Fig. 7B, C	- two pairs of extremely long setules on both sides of the P4-bearing somite in ventral view - two extremely long setules on the ventral anterior surface of the genital double-somite
EP-EF2 and EP-EF3	Fig. 7B	- two pairs of extremely long setules on both sides of the P4-bearing somite in ventral view
KS-RF1	not figured	- one inner seta and one outer spine absent on the right exp-3 of P2
KS-M1	not figured	- abnormal shape of distal endopod segment on the antenna with aberrant setae

not observed in all specimens. One of the robust females from the Korea Strait (Fig. 6A–D) showed intraspecific variation in the outer distal part of the first endopod segment of the antenna with broad and more numerous spinules (arrowed in Fig. 6a), in additional setules on the anterior surface of the labrum (Fig. 6C), in one of the spinules on the inner margin of the syncoxa of the maxilla being relatively long (arrowed in Fig. 6B), and in the weak development of the ventrolateral lobes on the P5-bearing somite (Fig. 6D).

A number of morphological aberrations found in some specimens of *S. ivlevi* were summarized in Table 5. In the northwestern Pacific Ocean, three out of eleven robust female form variants and one out of four males showed abnormalities. Two aberrant specimens were ornamented with a patch of long setules on the anterior part of the cephalosome (Fig. 7D, E) and the other one robust female was ornamented with a very long setule on the dorsal anterior surface of the genital double-somite. In the northeastern Pacific Ocean, three out of six elongate females showed a pair of extremely long setules on both sides of the P4-bearing somite in ventral view (e.g., Fig. 7B), and one of them had also two extremely long setules on the ventral anterior surface of the genital double-somite (Fig. 7B). In the Korea strait, one robust female showed an atypical spine count on the right leg of P2, with only two outer spines on P2 exp-3 [typical for the spine count on P2 exp-3 of *S. humesi*] and with an inner setal count of four setae instead of five setae, while the armature on the right leg was normal. One male from the Korea strait showed imperfect and/or flawed segmentation of endopod segments on the antenna, and the distal part of abnormal distal segment has aberrant four setae.

Spinoncaea tenuis Böttger-Schnack, 2003

Figs 8–11

Spinoncaea tenuis Böttger-Schnack, 2003: 215–225, figs 12–16 (Red Sea, Mediterranean, Arabian Sea, Pacific Ocean).

Material examined. (1) Northeastern Pacific (a) 10°30'N, 131°20'W (EP-1), 21 August 2009: One female (habitus of *S. tenuis* female in Fig. 8A, B) and one male (habitus

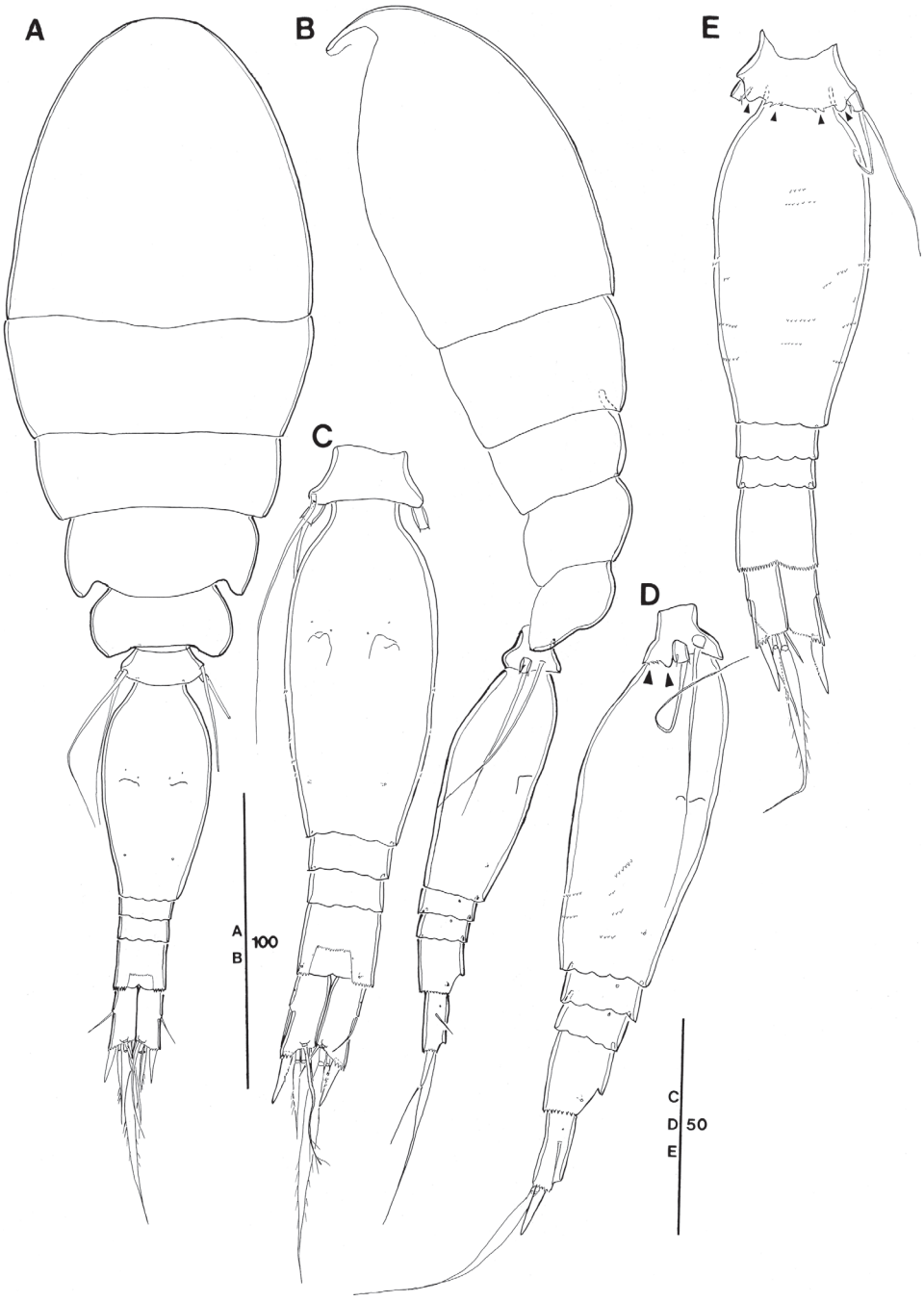

Figure 8. *Spinoncaea tenuis* Böttger-Schnack, 2003, female (northeastern equatorial Pacific) **A** habitus, dorsal (outer basal seta and exopodal seta of P5 on right side damaged, caudal seta V on left side missing) **B** habitus, lateral **C** urosome, dorsal (outer basal seta and exopodal seta of P5 on right side missing, caudal seta V on left side missing) **D** urosome, lateral, midventral spinous processes and ventrolateral lobe arrowed **E** urosome, ventral, midventral spinous processes and ventrolateral lobes arrowed (caudal setae IV and VI on left side omitted and seta V missing). Scale bars in μm.

of *S. tenuis* male in Fig. 11A) undissected on H-S slide, respectively. Five females and two males dissected on several slides, respectively. Three females dissected on H-S slide, respectively. Six dissected females (NIBRIV0000882784–882789) and one dissected male (NIBRIV0000882790) and one undissected female (NIBRIV0000882782) and one undissected male (NIBRIV0000882783) on respective H-S slide were deposited in the NIBR. (b) 9°52'1.38"N, 131°45'38.28"W (EP-2), 19 March 2019. Two undissected females and two undissected males in alcohol vial (NIBRIV0000882791) were deposited in the NIBR. (2) Northwestern Pacific, 13°20'3.42"N, 144°20'2.7"E (WP-2), 4 April 2016. One undissected male in alcohol vial (NIBRIV0000882792) was deposited in the NIBR. (3) Korea Strait, 33°44'50.50"N, 128°15'39.02"E (KS), 7 October 2008: One female (NIBRIV0000882793) and one male (NIBRIV0000882794) dissected on H-S slide, respectively. All dissected specimens and one undissected female (in alcohol, NIBRIV0000882795) were deposited in the NIBR.

Description. Female (Figs 8–10, Tables 3, 4). Body length in lateral view (telescoping of somites not considered) (Fig. 8B) 320–355 μm in Pacific specimens (Table 3), somewhat larger than in the Red Sea (280–300 μm, Böttger-Schnack 2003: 215).

Prosome 1.7 × length of urosome, excluding caudal rami, 1.5 × urosome length including caudal rami in specimens figured (Fig. 8B), calculated by not correcting for the telescoping of somites. Variation of prosome to urosome length (including CR) 1.3–1.7 in Pacific specimens (Table 3), single value from Korea Strait smallest. The respective values provided for Red Sea specimens (1.5 incl. CR; Böttger-Schnack 2003: fig. 12A, calculated by not correcting for telescoping of somites) are within the range of values from the Pacific.

P5-bearing somite with paired midventral spinous processes variable in number (two or three processes) and one pair of ventrolateral lobate processes (arrowed in Fig. 8D, E). Variation in number of midventral spinous processes was not mentioned for Red Sea specimens and ventrolateral lobes were not described, but are vaguely discernible from Böttger-Schnack (2003: fig. 12I).

Genital double-somite (Fig. 8C, D, E) 2.1 × as long as maximum width in specimen figured (measured in dorsal aspect) and ~ 2.1 × as long as postgenital somites combined; variation in length to width ratio 1.8–2.3 in Pacific specimens (Table 3), respective values from Red Sea fall within this range. Largest width measured at 2/5 the distance between anterior and posterior margin, similar to Red Sea specimens, where it is "about halfway". Ventral surface with few rows of minute spinules in some specimens (Fig. 8E), difficult to discern; this ornamentation was not mentioned for Red Sea specimens. Paired genital apertures located dorsally at about same position as in Red Sea specimens, armature difficult to discern. Weakly pronounced undulate hyaline frill on posterior margin of genital double-somite and postgenital somites and pore pattern as figured (Fig. 8D, E).

Anal somite (Fig. 8C) length to width ratio ranging between 1.1–1.3 (Table 3), ornamentation as figured (Fig. 8C, D, E).

Caudal ramus (Fig. 8A, C) length to width ratio 1.8–2.5 measured along inner margin and 2.3–3.0 measured along outer margin (Table 3). Caudal seta III ornamented with few minute spinules along medial margin (Fig. 8C), not observed in Red Sea

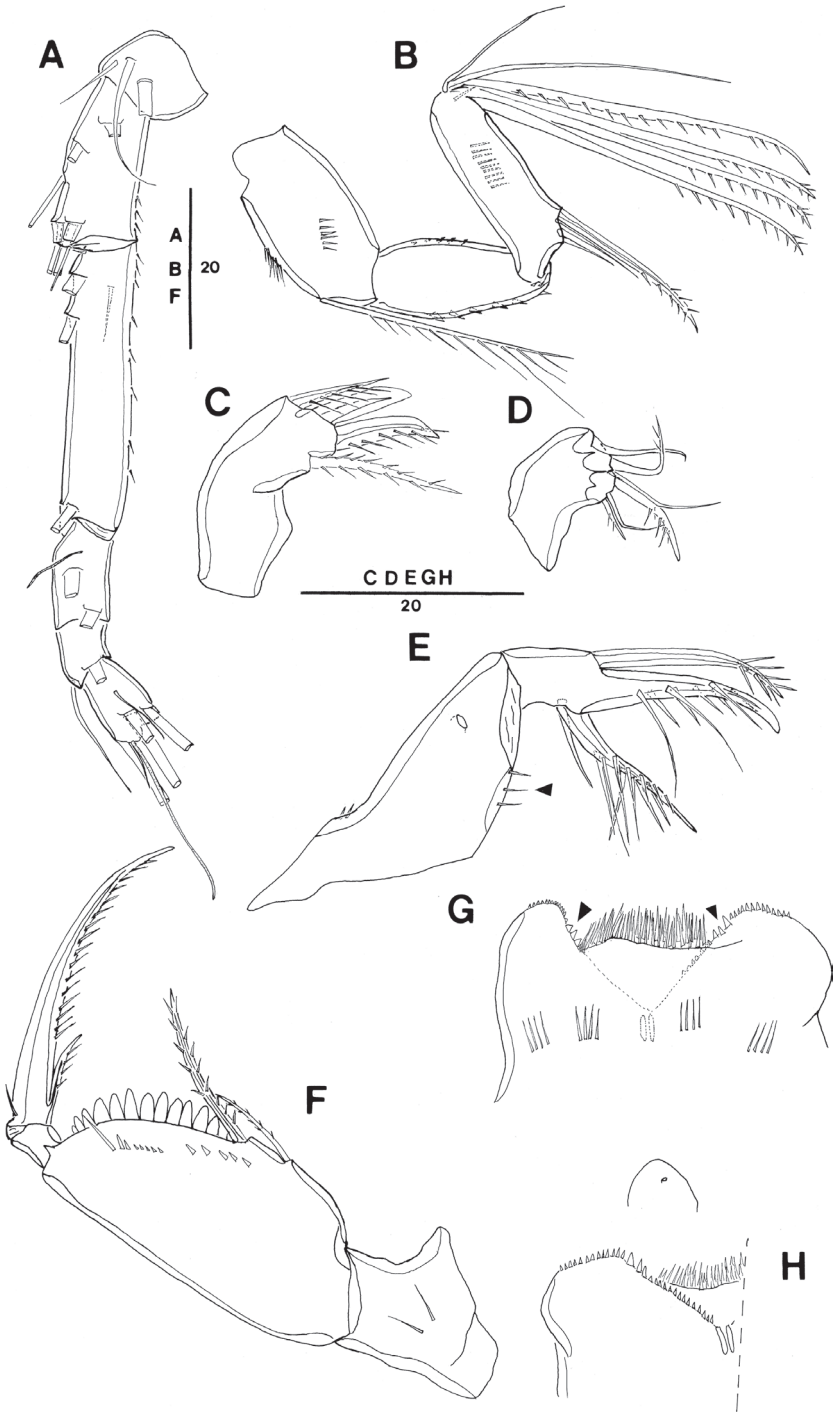

Figure 9. *Spinoncaea tenuis* Böttger-Schnack, 2003, female (northeastern equatorial Pacific) **A** antennule **B** antenna **C** mandible **D** maxillule **E** maxilla, arrows indicating spinules **F** maxilliped, anterior **G** labrum, anterior, arrows indicating three marginal teeth **H** labrum, posterior. Scale bars in µm.

specimens. Length ratio between seta IV and III 1.4–2.3 (Table 3), seta IV unipinnate, not bipinnate as in Red Sea specimens (Böttger-Schnack 2003: fig. 12C).

Antennule 6-segmented (Fig. 9A). Armature formula and ornamentation as for *S. ivlevi*.

Antenna 3-segmented, armature and ornamentation as figured (Fig. 9B). Distal endopod segment with length to width ratio 3.3–4.1 in Pacific specimens (Table 3), seta II longer than seta I (as illustrated for Red Sea specimens, Böttger-Schnack 2003: fig. 13A, but erroneously described as being "shorter than seta I" in text on p. 217).

Labrum with ornamentation as figured (Fig. 9G, H). including difference to *S. ivlevi* in (1) size of three marginal teeth along distal (ventral) margin on each lobe (arrowed in Fig. 9G) being somewhat smaller than in *S. ivlevi*, and (2) presence of two paired rows of long setules on anterior surface (Fig. 9G), not only a single paired row as in *S. ivlevi*.

Mandible with armature and ornamentation as figured. (Fig. 9C), small element D on gnathobase absent, as typical for *S. tenuis* (cf. Böttger-Schnack 2003: 218, fig. 13D).

Maxillule (Fig. 9D) similar to *S. ivlevi*, except for middle element on inner lobe naked.

Maxilla (Fig. 9E) with additional ornamentation on surface of syncoxa (arrowed in Fig. 9E), not reported earlier for Red Sea specimens.

Maxilliped as figured (Fig. 9F), surface of syncoxa ornamented with few spinules (arrowed in Fig. 9F), which was not recorded for Red Sea specimens.

Swimming legs 1–4 (Fig. 10A–D), with armature as in *S. ivlevi* (Table 2). Intercoxal sclerites of P1 ornamented with paired long, fine setules (but only one paired setule shown in Fig. 10A), which are difficult to discern. Ornamentation on inner portion of basis in P1–P3 as figured (Fig. 10A–C).

Exopods with variability of proportional spine lengths given in Table 4, respective values from the Red Sea fall within this range (Böttger-Schnack 2003: fig. 14A–D), except for the proportional lengths of outer spines on P3, which are larger in Pacific specimens than in the Red Sea specimens. Distal spine slightly longer than (P1) or almost equal in length (P2–P4) to distal exopod segment, similar to Red Sea specimens (Böttger-Schnack 2003: fig. 14A–D).

Endopods. Length ranges of outer subdistal spine and outer distal spine relative to distal spine on P2–P4 enp-3 as given in Table 4 generally similar to Red Sea specimens (Böttger-Schnack 2003: fig. 14A–D).

P5 (Fig. 8C, D, F) exopod 1.7 × longer than wide, armature and ornamentation as figured.

P6 (Fig. 8C) as figured, possibly armed with a short spinule, which is difficult to discern.

Male (Fig. 11, Tables 3, 4). Body length 292–325 μm (Table 3). Sexual dimorphism in antennule, maxilliped, P6, and in genital segmentation, slight modification in setal length of P5. Pore pattern on prosome not discerned.

P5-bearing somite with paired row midventral spinous processes variable in number as in female and one pair of ventrolateral lobate processes (Fig. 11C).

Caudal rami (Fig. 11A, B, C, G) with length to width ratio 1.9–2.4 measured along inner margin and 2.2–2.8 measured along outer margin (Table 3), ornamenta-

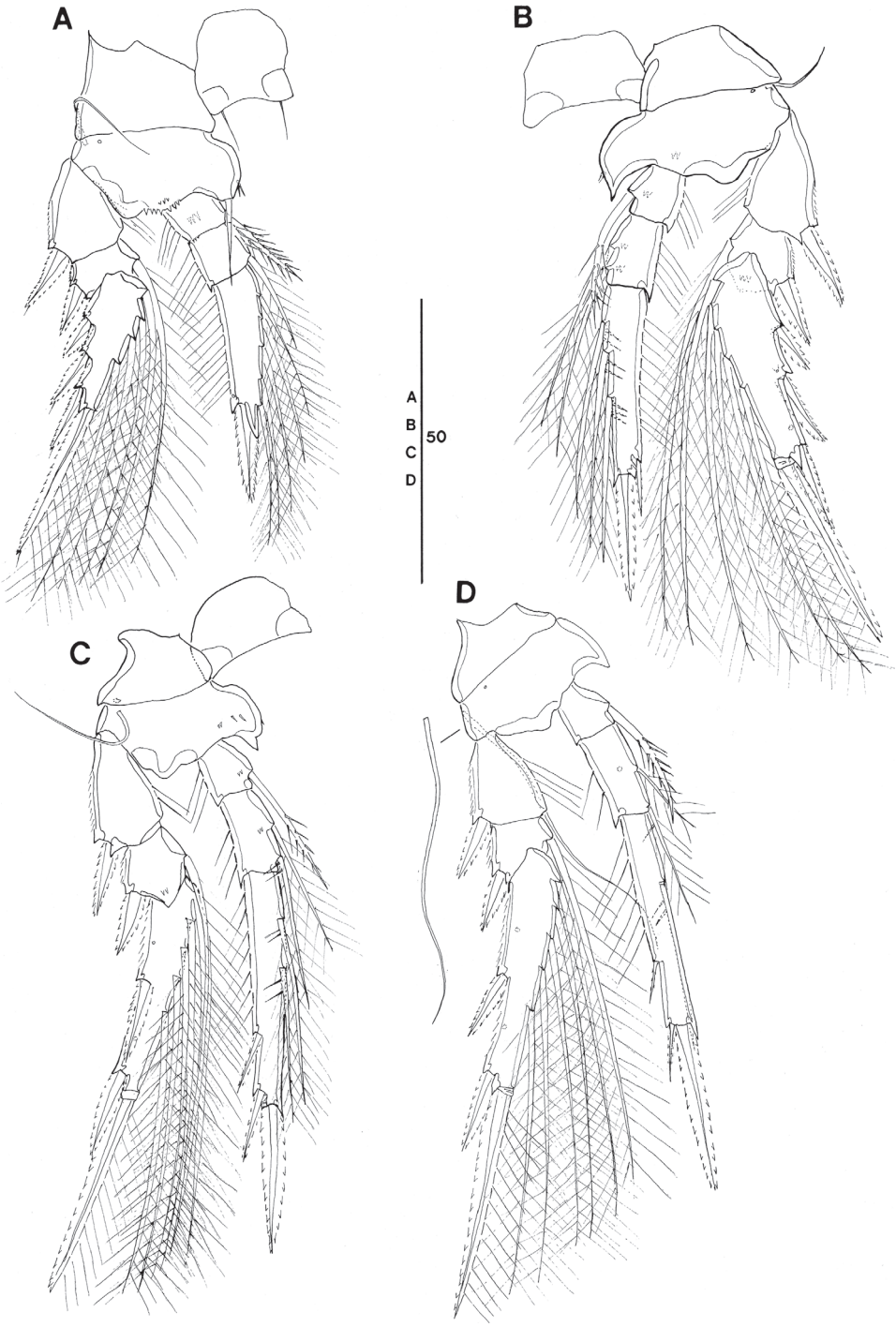

Figure 10. *Spinoncaea tenuis* Böttger-Schnack, 2003, female (northeastern equatorial Pacific) **A** P1, anterior **B** P2, anterior **C** P3, posterior **D** P4, anterior, intercoxal sclerite not figured, seta on basis figured separately. Scale bars in µm.

tion as figured (Fig. 11D). Caudal setae with proportional lengths as in female, variation in length ratios as given in Table 3.

Antennule (Fig. 11E) 4-segmented, armature as for *S. ivlevi*.

Antenna (not figured) with variation in length to width ratio of distal endopod segment similar to female (Table 3).

Maxilliped (Fig. 11D) 3-segmented, armature and ornamentation as figured.

Swimming legs 1–4 with armature and ornamentation as in female. Variability in proportional spine lengths on rami given in Table 4, values of equatorial Pacific fall within the range of females, but proportional lengths of exopodal spines on P2 and P4 from Korea Strait larger than those of females.

P5 (Fig. 11F) with exopodal seta and outer basal seta somewhat shorter than in female.

P6 (Fig. 11C) with ornamentation pattern as figured.

Remarks. Böttger-Schnack (2003) reported two variants of female *S. tenuis* which differed in geographical distribution. The typical form appeared in the entire Red Sea and in the northern Arabian Sea, while the elongate form was found in the Mediterranean Sea and in the NW Pacific (Kuroshio Extension); specimens from the NE Pacific (Monterey), on the other hand, showed intermediate values between both forms. In the present study, females from the NE equatorial Pacific also displayed intermediate values in morphological characters between the two forms of *S. tenuis*, which are as follows: (1) the length to width ratio of the genital double-somite has a wide range (1.8–2.3), including values of both form types; (2) the position of the genital apertures is at 2/5 of distance from the anterior margin as in the elongate form (from the Adriatic Sea); (3) the basal seta on P4 is more similar to the typical Red Sea form, reaching as far as the middle of the distal exopod segment, whereas this seta is much longer in the elongate form (from the Adriatic Sea), reaching beyond the tip of the distal spine on the exopod segment (cf. Böttger-Schnack 2003: fig. 16C); (4) the outer basal seta on P5 reaching as far as 4/5 the distance from the anterior margin of the genital double-somite in our Pacific specimens, but extending almost beyond the posterior margin of the genital double-somite in the elongate form (from the Adriatic Sea), (5) the length to width ratio of the caudal ramus measured along inner or outer margin in our specimens (1.8–2.5 or 2.3–2.9 ×, respectively) is larger than in the typical form from the Red Sea (1.9–2.0 or 2.1–2.3 ×) at least for ratio of the outer margin, and the range of values corresponds approximately to those of the elongate form from the Adriatic Sea (1.8–2.4 or 2.2–2.6 ×) and the NE Pacific (off Monterey, California) (2.1 or 2.4–2.7 ×) (Böttger-Schnack 2003: table 8).

In terms of ornamentation details, which are described for the typical form only, our Pacific specimens differed from the typical *S. tenuis* mainly by some details such as: (1) (1a) on the syncoxa of the maxilla and (1b) on the proximal element of the maxilliped; (2) short spinule(s) on the inner margin of bases on P2 and P3; (3) ornamentation with few minute spinules along the medial margin of CR seta III; and (4) variable number of midventral spinous processes on the P5-bearing somite.

Unlike the females, males of *S. tenuis* could not clearly be classified into form types in Böttger-Schnack's account. When compared to the typical form from the Red Sea, specimens from the equatorial Pacific are similar in morphology, except for

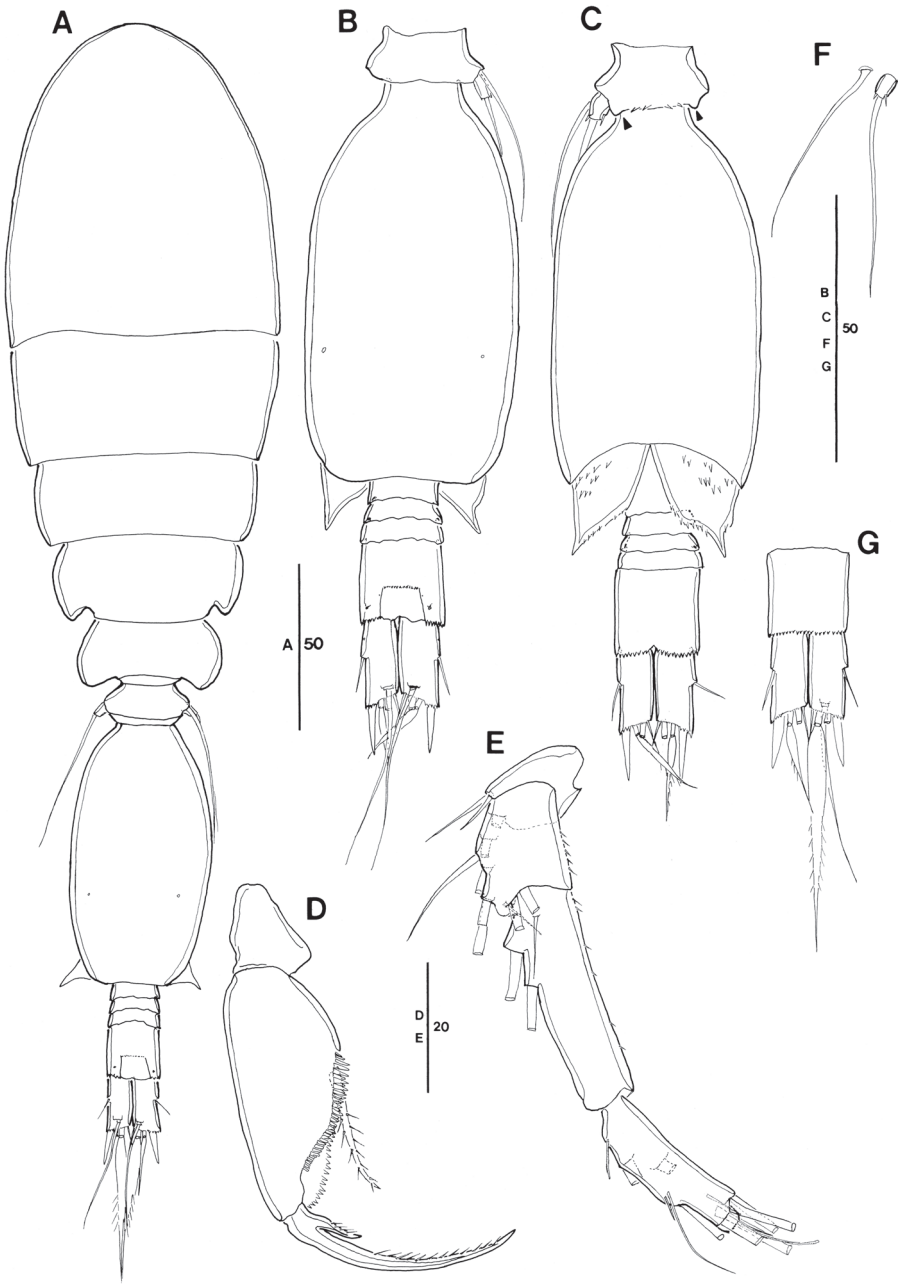

Figure 11. *Spinoncaea tenuis* Böttger-Schnack, 2003, male (northeastern equatorial Pacific) **A** habitus, dorsal (outer basal seta on left side of P5-bearing somite missing) **B** urosome, dorsal (P5 and the outer seta of P5-bearing somite on left side missing, caudal seta V on both sides missing) **C** urosome, ventral, ventrolateral lobes on P5-bearing somite arrowed (P5 and the outer seta of P5-bearing somite on left side missing, caudal seta V on both sides missing) **D** maxilliped, anterior **E** antennule **F** P5 exopod and outer basal seta, lateral **G** Anal somite and caudal ramus of another specimen, ventral. seta IV on left side and seta V on right side omitted. Scale bars in μm.

some minor differences including (1) the length to width ratio of the genital somite, which is longer than in our specimens (1.8–2.0 ×) than in the Red Sea specimens (1.7 ×), (2) the caudal rami (inner 1.9–2.2 ×, outer 2.2–2.6 ×) were slightly longer than in the Red Sea specimens (inner 1.9 ×, outer 2.3 ×), and (3) the length ratio of caudal setae VII and IV, respectively, with seta VII being 1.6–1.9 × longer than seta IV in the Pacific specimens, whereas seta VII is only 1.4 × the length of seta IV in the Red Sea specimens. Also, the number of paired midventral spinous processes on the P5-bearing somite differs, showing only two processes in the Pacific, as compared to three processes in the Red Sea specimens. However, as the male specimen from the Korea Strait also showed three paired processes (not figured), and differences among individuals of *S. tenuis* females (two or three processes) were apparent, this ornamentation seems to be due to individual variation, and cannot be regarded as a regional difference.

According to Böttger-Schnack (2003), some slight morphological differences occurred between males of *S. tenuis* from the Red Sea and the Adriatic Sea (e.g., the proportional lengths of the genital somite and the caudal rami), but the determination of an elongate male appeared to be ambiguous. In our case, the above mentioned two characters are intermediate between the typical form (from the Red Sea) and the elongate form (from the Adriatic Sea) and the range of these values could be perceived as a variation among individuals (cf. Table 3). However, the single male of *S. tenuis* from the Korea Strait (not figured) seemed to be similar to the elongate form from the Adriatic Sea, as it differed from specimens from the equatorial Pacific specimens in the following characters (Table 3): (1) smaller body length: 292 μm; (2) the genital somite being slightly longer than in the equatorial Pacific, with a length to width ratio of 2.0:1; (3) the length to width ratio of the caudal rami being greater/higher (inner 2.4 ×, outer 2.8 ×) than in the equatorial Pacific (Table 3); (4) the anal somite slightly longer than in the equatorial Pacific, 1.2 × longer than wide; and (5) the outer basal seta on P5 reaching the posterior margin of the genital somite. In summary, the observed variation of features for *S. tenuis* in the Pacific indicates that the previously described form types of this species are not clearly separated; however, distinct form types may occur due to regionally reduced ranges of variation in the morphological details described here.

The female of *S. tenuis* can easily be confused with the elongate form of female *S. ivlevi* from the Pacific Ocean, due to the shape of the genital double-somite. However, as Böttger-Schnack (2003) mentioned the distinction between *S. tenuis* and *S. ivlevi* elongate form from the equatorial Pacific are: (1) the number of elements on the mandible (four in *S. tenuis*, but five in *S. ivlevi* elongate form) and (2) the number of spinules patches on the anterior surface of the labrum (two pairs in *S. tenuis*, but one pair in *S. ivlevi* elongate form, generally). Further morphometric differences between females of the two species may be found in (3) the proportional lengths of caudal setae III: II, which is smaller in *S. tenuis* (1.0–1.5 ×) as compared to *S. ivlevi* elongate form (1.6–2.0 ×) and (4) the length ratio between the distal spine and distal exopod segment on P2–P4, with the distal spine being almost equal in length to the distal segment in *S. tenuis*, whereas the spine is shorter than the segment in *S. ivlevi* elongate form (esp. on P4) (Table 4). Further minor differences between the two species are found in the

patterns of the ornamentation on the ventral surface of the genital double-somite, as the elongate form of *S. ivlevi* (Fig. 7B) has a larger number of spinular rows than *S. tenuis* (Fig. 8E) and the ornamentation on the inner margin of caudal ramus, which is absent in *S. tenuis*, but is present in *S. ivlevi* elongate form.

Spinoncaea humesi **Böttger-Schnack, 2003**

Figs 12–15

Spinoncaea humesi Böttger-Schnack, 2003: 208–215, figs 8–11 (Red Sea, Mediterranean, Indian and Pacific oceans).

Material examined. (1) Northeastern Pacific, 9°52'1.38"N, 131°45'38.28"W (EP-2), 19 March 2019. Three females dissected on three or seven slides, respectively. Two dissected females (NIBRIV0000882796–882797) and two undissected females (in alcohol, NIBRIV0000882798) were deposited in the NIBR. (2) Northwestern Pacific (a) 13°23'46.44"N, 143°55'0.60"E (WP-1), 27 March 2016: Two males dissected on one or three slides, respectively. All dissected specimens (NIBRIV0000882799–882800) were deposited in the NIBR. (b) 13°20'3.42"N, 144°20'2.7"E (WP-2), 4 April 2016. One undissected male in alcohol (NIBRIV0000882801) was deposited in the NIBR. (3) Korea Strait, 33°44'50.50"N, 128°15'39.02"E (KS), 7 October 2008: One dissected male (NIBRIV0000882802) on H-S slide, and one undissected female and one undissected male in alcohol vial (NIBRIV0000882803) were deposited in the NIBR.

Description. Female (Figs 12–14, Tables 3, 4). Body length in lateral view (telescoping of somites not considered) (Fig. 12B) 344–348 μm in northeastern Pacific (Table 3), somewhat larger than in the Red Sea (310–320 μm, Böttger-Schnack 2003: 208).

Prosome 1.7 × length of urosome, excluding caudal rami, 1.3–1.4 × urosome length including caudal rami (Fig. 12B, Table 3), for comparison with Red Sea see under "Remarks". Integumental pores on prosome difficult to discern, not figured.

P5-bearing somite with three paired midventral spinous processes (Fig. 12D), no variation in number found (but see under "Male").

Genital double-somite (Fig. 12C, D, E) 2 × as long as maximum width in specimen figured (measured in dorsal aspect) and ~ 1.5 × as long as postgenital somites combined; variation in length to width ratio given in Table 3, respective ratios from Red Sea specimens fit into this range; ornamentation of dorsal and ventral surfaces (Fig. 12D, E) as for Red Sea specimens, including weakly developed undulate hyaline frill on posterior margin of genital double-somite and postgenital somites, as well as absence of pores on lateral surface of postgenital somites (Fig. 12E).

Anal somite (Fig. 12C) with length to width ratio 1.2–1.3 (Table 3), similar to Red Sea, but slightly different from other areas reported in Böttger-Schnack's account (1.0–1.2:1, Böttger-Schnack 2003: table 7). One pair of secretory pores present dorsally near posterior margin (Fig. 12C), second pair reported for Red Sea specimens not discerned. Other ornamentation as figured (Fig. 12C–E).

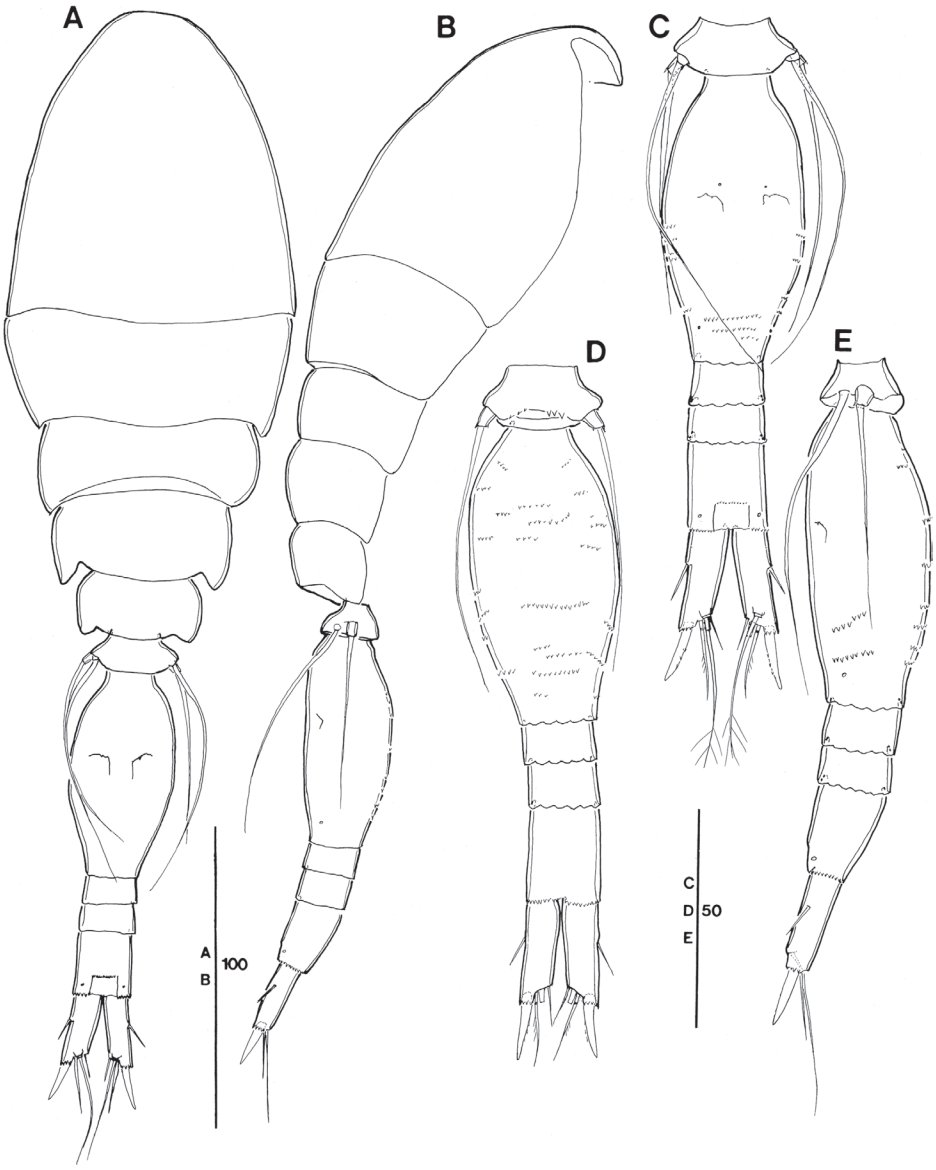

Figure 12. *Spinoncaea humesi* Böttger-Schnack, 2003, female (northeastern equatorial Pacific) **A** habitus, dorsal (caudal seta V missing on both sides) **B** habitus, lateral **C** urosome, dorsal, (caudal seta V missing on both sides) **D** urosome, ventral, (caudal seta V missing on both sides) **E** urosome, lateral. Scale bars in μm.

Caudal ramus (Fig. 12A, C) 2.3–2.5 × longer than wide measured along inner margin and ~ 2.8–3.1 × longer than wide measured along outer margin (Table 3), range of variation similar to ratios reported for Red Sea and other regions (Böttger-Schnack 2003: table 7). Length ratios among setae II, III, and IV with ranges in Pacific specimens given in Table 3, Red Sea data fit into these ranges; seta V missing on both

sides of specimen figured (measurements taken from undissected specimen as follows: seta V ~ 2.7 × longer than seta IV, 1.5 × longer than seta VII).

Antennule (Fig. 13A) with armature formula as for *S. ivlevi*. Ornamentation along inner non-setiferous margin of segments 2 and 3 absent, as specified for Red Sea specimens.

Antenna 3-segmented, armature and ornamentation as figured (Fig. 13B). Endopod segments ~ equal in length (but in Fig. 13B, the proximal endopod segment looks shorter than the distal one, due to its orientation on the slide); distal endopod segment ~ 4 × longer than wide, variation given in Table 3, Red Sea data fit into these ranges; armature and ornamentation as in *S. ivlevi*, except for seta II slightly longer than seta I (for numbering of elements see Fig. 3B).

Labrum with ornamentation as figured (Fig. 13G) including difference to *S. ivlevi* in size of four marginal teeth along distal (ventral) margin on each lobe being smaller than in *S. ivlevi*. Posterior face with two secretory pores on each lobe, which are difficult to discern. Anterior surface of labrum not observed in detail, but overlapping rows of fine spinules covering median concavity on anterior side visible from Fig. 13G.

Mandible with armature and ornamentation as figured (Fig. 13C), small element D on gnathobase absent, as typical for the species.

Maxillule (Fig. 13D) similar to *S. ivlevi*, except for middle element on outer lobe naked.

Maxilla with armature and ornamentation as figured (Fig. 13E), additional ornamentation on syncoxa in Pacific specimens arrowed in Fig. 13E.

Maxilliped with armature and ornamentation as figured (Fig. 13F), similar to Red Sea specimens, including small ornamentation details, such as proximal element on basis unornamented.

Swimming legs (Fig. 14A–D), with armature as in *S. ivlevi* except for spine count on distal exopod segment of P2, showing only two outer spines (Table 2). Intercoxal sclerites unornamented (missing in specimen figured). Surface of coxae and bases with sparse surface ornamentation as figured, outer basal seta on P4 very long, reaching as far as tip of distal exopod segment (Fig. 14D), as typical for the species.

Exopods with variability of proportional spine lengths in Pacific specimens given in Table 4, respectively values from Red Sea generally fit into these ranges, except proportional spine lengths on P2 larger than in the Red Sea specimens.

Endopods with length ranges of outer subdistal spine and outer distal spine relative to distal spine on P2 and P4 given in Table 4 generally similar to Red Sea specimens, except for outer distal spine relative to distal spine on P2 (0.45–0.51) and P3 (0.42–0.44) smaller than Red Sea (0.56 on P2 and 0.48 on P3, calculated from Böttger-Schnack 2003: fig. 10B, C).

P5 (Fig. 12C, E) with exopod 1.4 × longer than wide, shorter than in Red Sea (1.7:1; cf. Böttger-Schnack 2003: 208, fig. 8H, I), armature and ornamentation as figured.

P6 (Fig. 12C) as figured, armature (short spinule) difficult to discern.

Male (Fig. 15, Tables 3, 4). Body length 285–295 µm (Table 3). Sexual dimorphism in antennule, maxilliped, P6, and in genital segmentation, slight modification in setal length of P5. Pore pattern on prosome not discerned.

P5-bearing somite with paired midventral spinous processes variable in number (two or three processes) (Fig. 15D).

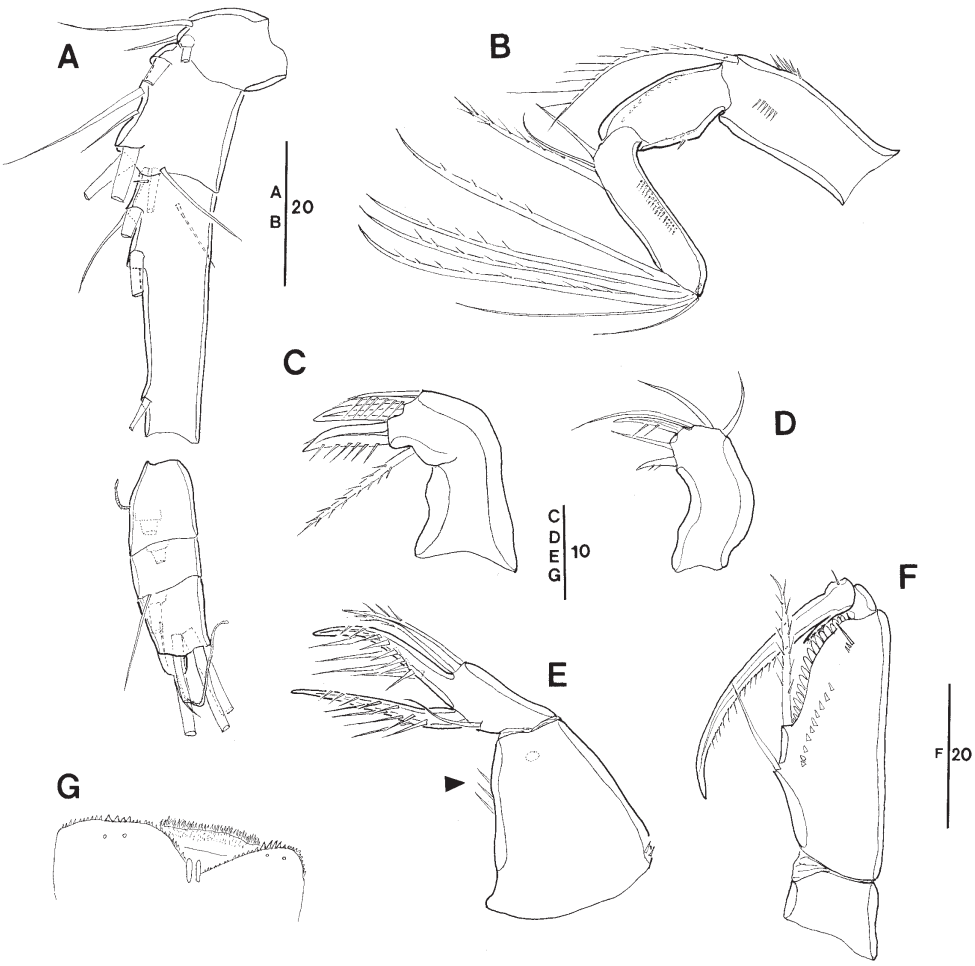

Figure 13. *Spinoncaea humesi* Böttger-Schnack, 2003, female (northeastern equatorial Pacific) **A** antennule (segments 4–6 drawn from another specimen) **B** antenna **C** mandible **D** maxillule **E** maxilla, arrows indicating spinules **F** maxilliped, anterior **G** labrum, posterior, showing some ornamentation on anterior side. Scale bars in μm.

Caudal rami (Fig. 15A, C, D) with length to width ratio 2.1–2.5 measured along inner margin and 2.6–3.2 measured along outer margin (Table 3), [single value from Korea Strait larger than those from western equatorial Pacific,] respective values from Red Sea and other areas (Böttger-Schnack 2003: table 7) fit into this range. Ornamentation details as figured, similar to Red Sea specimens, including absence of surface ornamentation on genital somite (Fig. 15C, D).

Antennule (Fig. 15F) with armature as for *S. ivlevi*. Segments 2 and 3 without ornamentation.

Maxilliped (Fig. 15G, H) 3-segmented, syncoxa missing in specimen figured. Basis and endopod (claw) with armature and ornamentation similar to Red Sea specimen, including ornamentation detail on claw, with pinnules only along distal half of concave margin.

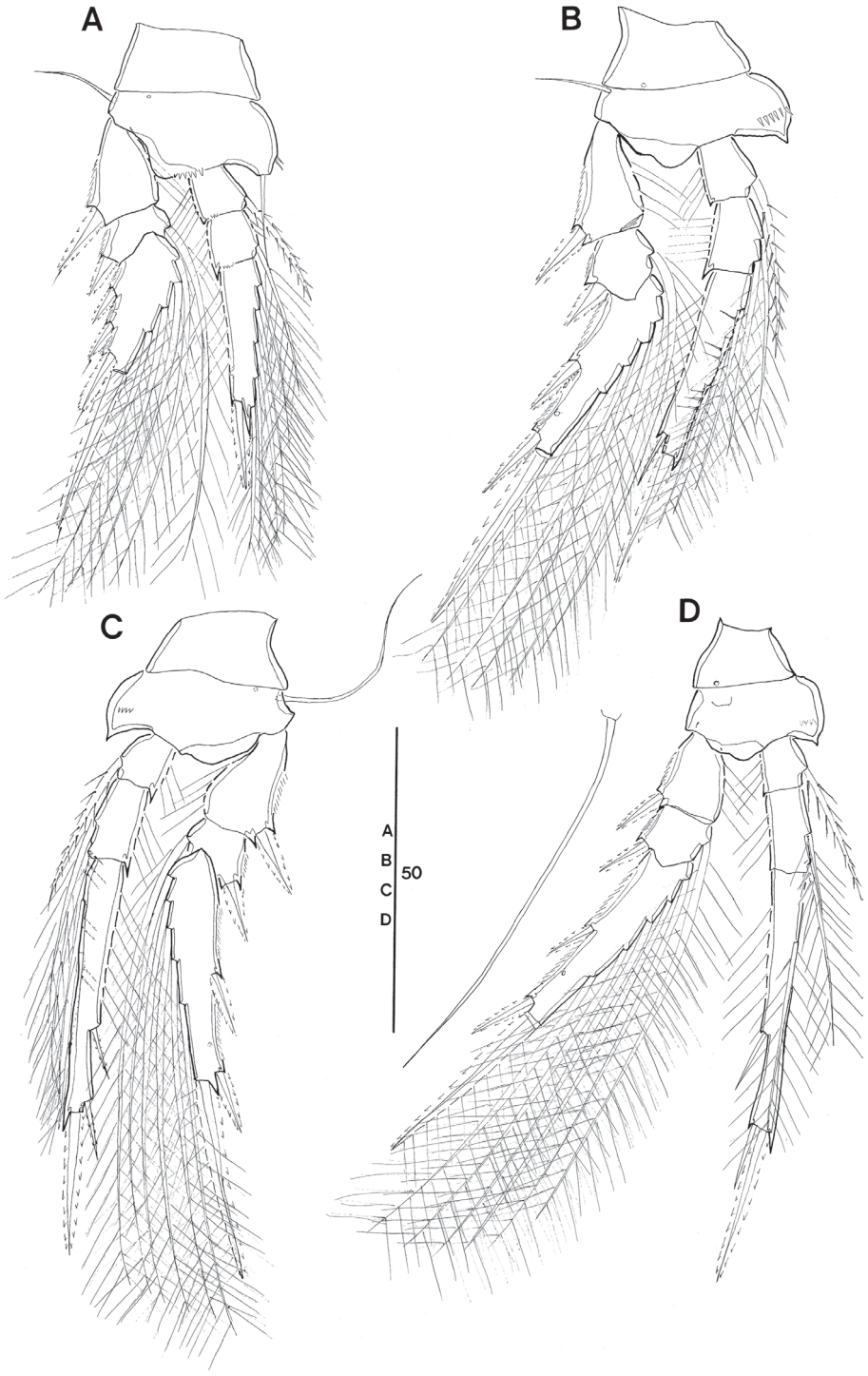

Figure 14. *Spinoncaea humesi* Böttger-Schnack, 2003, female (northeastern equatorial Pacific) **A** P1, anterior **B** P2, posterior **C** P3, anterior **D** P4, posterior, basal seta of another specimen figured separately. Scale bars in µm.

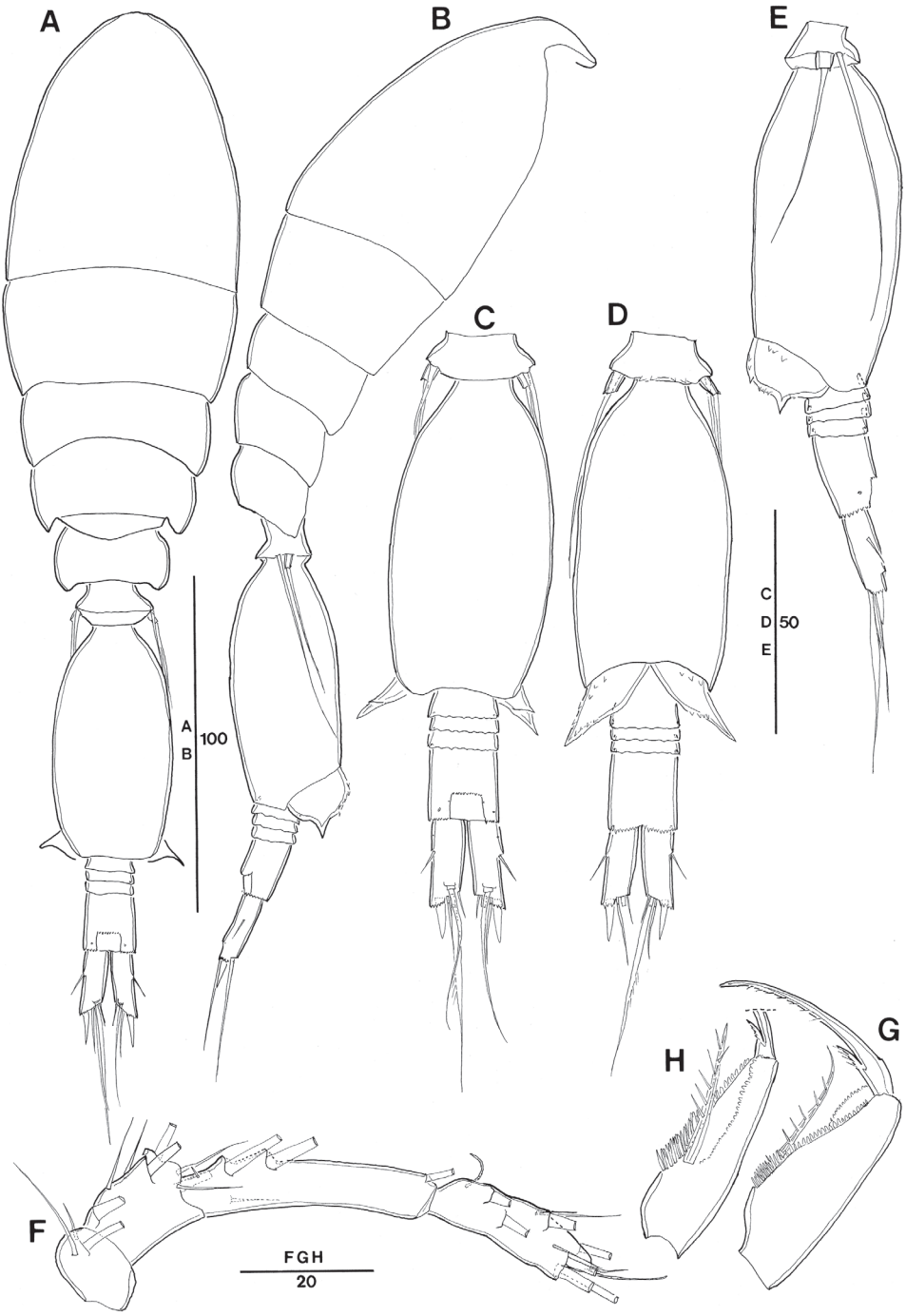

Figure 15. *Spinoncaea humesi* Böttger-Schnack, 2003, male (northwestern equatorial Pacific) **A** habitus, dorsal (caudal seta V on right side missing) **B** habitus, lateral **C** urosome, dorsal (caudal seta V on right side missing) **D** urosome, ventral (caudal seta V on right side missing) **E** urosome, lateral **F** antennule **G** maxilliped, anterior **H** maxilliped, middle. Scale bars in μm.

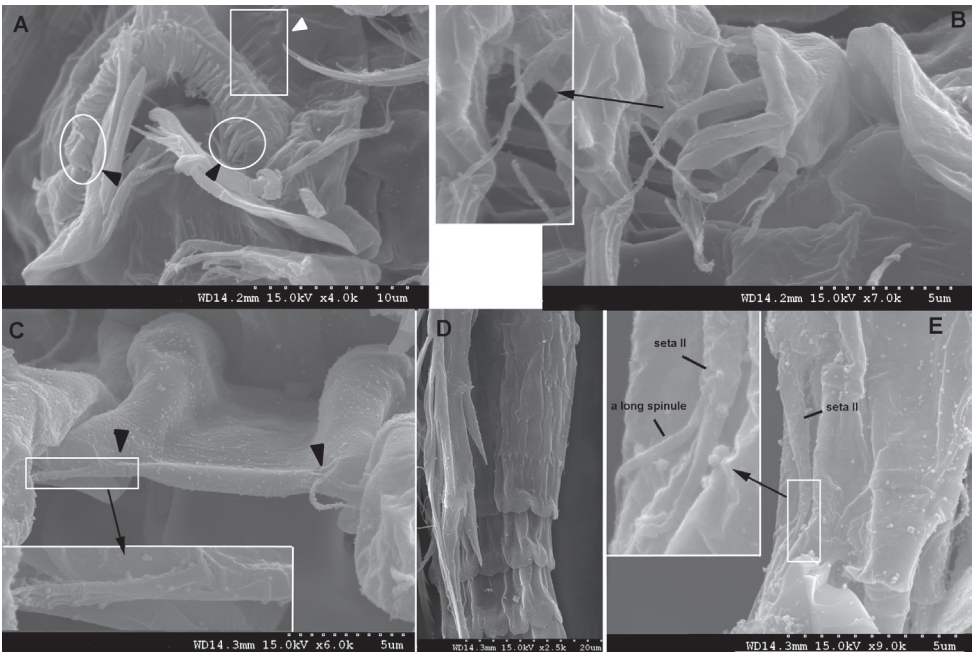

Figure 16. *Spinoncaea ivlevi* (Shmeleva, 1966), female, robust form (northwestern equatorial Pacific) **A** labrum, anterior, white arrow indicating setules (in square), black arrows indicating three marginal teeth (in circle) **B** maxillule, inset showing enlarged second element on outer lobe **C** intercoxal sclerite on P1, black arrows indicating ornamentation with long, fine setule, inset showing enlarged setules **D** posterior part of genital double-somite and postgenital somites showing undulate hyaline frill. *Spinoncaea ivlevi* (Shmeleva, 1966), male (northwestern equatorial Pacific) **E** caudal ramus seta II, inset showing enlarged seta II ornamented with a single long spinule.

Swimming legs 1–4 with the value ranges in spine lengths on rami given in Table 4 not significantly different from female, except for the values of the endopodal spines on P4 from Korea Strait smaller than those of females.

P5 (Fig. 15B, E) with exopodal seta and outer basal seta shorter than in female, outer basal seta also much shorter than in Red Sea specimens (Böttger-Schnack 2003: fig. 11D–F).

P6 (Fig. 15D) with ornamentation as figured.

Remarks. The morphology of both sexes of *S. humesi* from the Pacific agrees in most parts with the original description of the species by Böttger-Schnack (2003). As stated above, the Pacific specimens differ only in a few characters, such as in (1) a somewhat larger body size in the female and (2) the length ratio of the prosome to the urosome in the female, which appears to be slightly larger in the Pacific specimens (1.7:1 and 1.3–1.4:1, excluding and including caudal rami, respectively) as compared to the Red Sea specimens (1.5:1 excluding caudal rami and 1.2:1 including caudal rami, calculated from Böttger-Schnack (2003: fig. 8A). Note, that in the text of Böttger-Schnack (2003: 208) the proportions of the prosome to the urosome are given as 2.0:1 and 1.7:1, respectively, but these were calculated by a different method taking

into account the telescoping of somites, while the telescoping of somites was not considered in the present study. Also, some additional ornamentations were found in the Pacific specimens, such as on the syncoxa of the maxilla of both sexes, the additional ornamentation on the inner portion of the basis of P2–P4 in our Pacific specimens or the number and size of spatulated spinules between proximal seta and articulation with endopod on the maxilliped in female, which are smaller and more numerous than in the specimen from the Red Sea.

The male of *S. humesi* from the Korea Strait agreed in almost all morphological characters with the specimens from the northwestern equatorial Pacific. But it exhibited individual variabilities in the length to width ratio of caudal ramus, the relative length ratio of caudal setae, and the length to width ratio of the genital somite (cf. Tables 3, 4). An additional variation in the male from the Korea Strait was found in the number of midventral spinous processes on the P5-bearing somite, with three paired processes (not figured), as in female, while in the male of the northwestern Pacific only two paired processes were found, as in the male from the Red Sea (Böttger-Schnack 2003: fig. 11E). The number of midventral spinous processes on the P5-bearing somite seems to be a common individual variation seen within both sexes among *Spinoncaea* species.

Spinoncaea humesi can easily be distinguished from the other two species of *Spinoncaea* by the number of spines on P2 exp-3, showing two outer spines in *S. humesi*, but three spines in *S. ivlevi* and *S. tenuis*. Also, the outer basal seta of P5 is extremely long, extending beyond the posterior margin of the genital double-somite in the female, and the shape of genital double-somite is different, being barrel-shaped in *S. humesi*. Other additional characters for species segregation are not further mentioned in the present study because they are described in detail in the remarks section of *S. humesi* by Böttger-Schnack (2003: 214–215).

Key to species of the genus *Spinoncaea*

1	P2 exp-3 with 2 outer spines; genital double-somite barrel-shaped in female ..... ***S. humesi***
–	P2 exp-3 with 3 outer spines; genital double-somite oval-shaped or elongate oval-shaped in female **2**
2	Md with 5 elements; undulate or lobate hyaline frill at posterior margin of urosomites strongly pronounced; inner margin of caudal ramus with row of setules; modified seta III (spine) on caudal ramus very strong ..... ***S. ivlevi***
–	Md with 4 elements; undulate hyaline frill at posterior margin of urosomites weakly pronounced; inner margin of caudal ramus naked; modified seta III (spine) on caudal ramus less strong ..... ***S. tenuis***

The difference described for the mandible is not noticeable without difficult preparation of the mouthparts. Thus, this character is not included in the general identification key for Oncaeidae "OncIdent" of Böttger-Schnack and Schnack (2016–2021).

Molecular analysis

All three species of *Spinoncaea*, including also the two forms of female *S. ivlevi*, were analyzed for mtCOI and 12S srRNA sequences during the present study, but only the 12S srRNA sequences of *S. ivlevi* (robust form) and of *S. humesi* were successfully obtained (Table 6). The mtCOI sequences, which allowed clear discrimination of even the most closely related species (Hill et al. 2001), were not successfully sequenced for the *Spinoncaea* species. The 12S srRNA sequences of *Spinoncaea* species obtained in this study can be found under the GenBank accession numbers MN714702–MN714706. The 12S srRNA sequences for individuals of *S. ivlevi* in the western and

Table 6. Molecular analysis of three *Spinoncaea* species from the northeastern (NE) and northwestern (NW) equatorial Pacific: Collection region, number of individuals analyzed (N), number of DNA successfully isolated (n), and GenBank accession numbers of specimens successfully used for molecular analysis.

Species	N	n	Marker	GenBank accession no.	Collection region
Spinoncaea ivlevi (robust form)	14	2	12S	MN714703, MN714705	NE Pacific
	12	0	COI	–	
	5	2	12S	MN714704, MN714706	NW Pacific
Spinoncaea ivlevi (elongate form)	3	0	COI	–	NE Pacific
	6	0	12S	–	
	4	0	12S	–	NW Pacific
Spinoncaea humesi	3	1	12S	MN714702	NE Pacific
	3	0	12S	–	NW Pacific
Spinoncaea tenuis	10	0	12S	–	NE Pacific
	9	0	COI	–	
	10	0	12S	–	NW Pacific

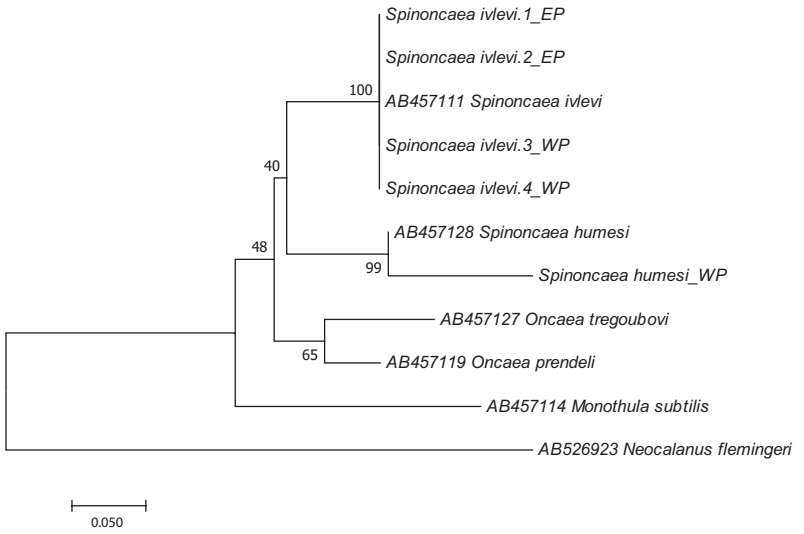

Figure 17. Maximum-likelihood tree from 12S sequences of two *Spinoncaea* species from the Pacific (WP, EP) and species of a clade including *Monothula* and the *ivlevi-tregoubovi* lineage as defined by Böttger-Schnack and Huys (2001). Sequences of compared species were obtained from GenBank as analysed by Böttger-Schnack and Machida (2011) and for the outgroup *Neocalanus flemingeri* by Machida and Tsuda (2010). Bootstrap values from 1000 replications.

the northeastern Pacific Ocean were 100% identical to each other and were in concordance with *S. ivlevi* type sequence collected in the Mediterranean Sea (GenBank accession number AB457111; Böttger-Schnack and Machida 2011). The sequencing result of *S. humesi* from the Pacific was also 99% identical to the type sequence collected in the Mediterranean Sea (GenBank accession number AB457128; Böttger-Schnack and Machida 2011). Each node is strongly supported with high bootstrap values in 12S phylogenetic tree (Fig. 17). Within *S. ivlevi*, the *p*-distances were zero and the *p*-distances of between *S. ivlevi* and *S. humesi* were 0.16.

Discussion

Spinoncaea species are supposed to have a wide geographical distribution in warm-temperate and tropical areas, as they were described from various regions, such as the Mediterranean Sea (including the Adriatic Sea), the Red Sea, the Indian and the Pacific Oceans (Böttger-Schnack 2003). In the Pacific Ocean, however, earlier records mainly refer to higher latitudes (north of ~ 36°N), such as near Japan (Böttger-Schnack 2003; Nishibe and Ikeda 2004; Nishibe et al. 2009) or near California (Böttger-Schnack 2003). In the present study we add the open equatorial Pacific to their distribution, and they are first recorded in Korea's surrounding waters.

Apart from the detailed morphological/taxonomical analysis and documentation (figures) of *Spinoncaea* species from the open equatorial Pacific, for the first time individual variation of numerous morphometric characters was analyzed for all three species, including proportions of body somites (e.g., anal somite, genital (double-)somite) and armature elements, such as the proportional lengths of endopodal and exopodal spines on the swimming legs, which have been found as limited but useful characters for differentiation between species of other oncaeid genera (e.g., *Triconia* Böttger-Schnack, 1999) (Heron et al. 1984; Heron and Bradford-Grieve 1995; Cho et al. 2013, 2017, 2019). The respective data obtained for *Spinoncaea* did in most cases not turn out to be useful for discrimination of the three species in this genus (Tables 3, 4). In some cases, however, the range of variation did not overlap among the species (e.g., the length ratio of distal exopod segment to distal spine on P4; cf. Table 4). Here a larger data set is required to clarify if these measures can be used for the differentiation of the species. Also, the data set will serve as a basis for comparative data with other oncaeid genera to understand the range of intraspecific variation of species in different parts of the world's oceans.

Intraspecific variation among the three species was also found for ornamentation details, such as the number of midventral spinous processes on the P5-bearing somite in both sexes, which, however, is considered a commonly occurring variation in nature.

The morphological descriptions of *Spinoncaea* species by Böttger-Schnack (2003) included also details of ornamentation, but in Pacific specimens we found additional new ornamentation items which have not been reported in previous studies. For all three *Spinoncaea* species some additional ornamentation was found on the inner margin of the maxillary syncoxa, showing 3–5 long spinules. It is uncertain whether

this has been overlooked in previous studies, as specimens from this area had not been described in detail in Böttger-Schnack's study, or whether it newly emerged in specimens from the Pacific. Remarkably, a similar ornamentation on the syncoxa of the maxilla was also found in Pacific specimens of *Oncaea tregoubovi* Shmeleva, 1968 (unpublished thesis of Cho 2011: fig. 38F) and *tregoubovi*-group species (as *Oncaea* sp. 3 in Cho 2011: fig. 42E), based on copepod material collected from the same location in the northeastern equatorial Pacific (EP-1) as in the present study, and it was also found recently in *Oncaea prendeli* Shmeleva, 1966 from the southern Sea off Jeju Island (the East China Sea) (Cho et al. 2020). In earlier (re)descriptions of *O. tregoubovi* and *O. prendeli* from their type locality in the Adriatic Sea (Huys and Böttger-Schnack 2007), a corresponding ornamentation was not described (their figs 3F, 8F, respectively). Another ornamentation detail newly found in *S. ivlevi* from the Pacific was the ornamentation on the intercoxal sclerite on P1 in both sexes as well as the distinct ornamentation on the ventral surface of the genital somite in the male. In particular, the unique pattern in the male may be useful for distinguishing the males of the three *Spinoncaea* species. However, it is not easy to observe the ornamentation of these small sized species, measuring approximately 300 μm in body length, so more careful and precise observation is required and recommended for their examination.

Some specimens of *S. ivlevi* in the present study did not only show abnormal ornamentation items on the cephalosome or the genital double-somite (cf. Fig. 7B–E), but also featured morphological asymmetries and abnormalities on other body parts, such as the swimming legs. The atypical spine count on the right exp-3 of P2 observed in a female (robust form) from the Korea Strait showing two instead of the typical three spines (see above under "Remarks" of *S. ivlevi*) is of particular importance as the spine count of this leg is used for distinguishing *S. ivlevi* (three spines) from *S. humesi* (two spines). Therefore, identification of the two species simply based on leg armature may lead to misidentification and care should be taken to use additional morphological parameters for their distinction/differentiation. Morphological abnormalities in various appendages have also been reported for various other oncaeid species such as an aberrant number of spines on swimming leg 1 in *Oncaea venusta* f. *typica* Farran, 1929 (Böttger-Schnack 2001: fig. 4a); a modified tip of the posterolateral corner on P6 in males of *Triconia hawii* (Böttger-Schnack & Boxshall, 1990) (Böttger-Schnack 1999: fig. 23a–d); *Oncaea media* Giesbrecht, 1891 and *O. waldemari* Bersano & Boxshall, 1996 (Böttger-Schnack 2001: figs 16C, 27E) and *Triconia giesbrechti* Böttger-Schnack, 1999 (Cho et al. 2013: fig. 12F); an abnormal shape of the distal endopod segment of the antenna with an aberrant seta and a reduced number of setae (*Oncaea prolata* Heron, 1977 in Cho 2011: fig. 29I, male); an aberrant process on the outer proximal corner on the basis of P4 (*O. parabathyalis* Böttger-Schnack, 2005, in Böttger-Schnack 2005: fig. 18d, female); and the tumorous growth on the surface of the prosome of female *Triconia derivata* (Heron & Bradford-Grieve, 1995) (Heron and Bradford-Grieve 1995: figs 9h, 10a). Among marine pelagic copepods, the genus *Acartia* Dana, 1846 is a well-known taxon of morphological anomalies, mainly in P5. In a study on the morphological anomalies of *Acartia*, there was no indication found that the occurrence of

anomalies on the P5 was relatively more frequent in the polluted area than in the open sea, and it was tentatively inferred that these anomalies may be a common phenomenon in nature (Brylinski 1984; Behrends et al. 1997). Also, morphological anomalies have been observed at the bases of P3 in *Clausocalanus mastigophorus* (Claus, 1863) collected from the equatorial Atlantic (Melo et al. 2014). It was assumed that this was due to a developmental error or random genetic mutations. Hence, in oncaeid copepods, the observed morphological asymmetries and abnormalities may be a common natural phenomenon as well, but further studies will be needed to provide sufficient information for avoiding any taxonomic confusion.

The present study included molecular genetic analyses with the aim of overcoming taxonomic problems related to morphological variation. The sequence of the mtCOI region could not successfully be obtained for any of the three species of *Spinoncaea* analyzed, supporting previous findings that for oncaeid copepods the 12S gene is a better tool for use in DNA barcoding than the COI gene (Böttger-Schnack and Machida 2011). The 12S srRNA sequences of *Spinoncaea* species from the Pacific did not indicate a genetic difference between species from the Mediterranean Sea and those from the northwestern and/or northeastern equatorial Pacific Ocean. However, morphological variation cannot exclude the possibility that these reflect population differences. And in the case of *Spinoncaea* species, especially *S. ivlevi*, the observed morphological variation from a broad geographical distribution may indicate a high level of gene flow between populations. Thus, mtDNA may not be an accurate indicator of species dispersal due to maternal inheritance of the organelle genome (Bucklin and Frost 2009). Nevertheless, genetic analysis of species with wide distributions and morphological variation in other copepod taxa has indicated the existence of pseudo-sibling species (Staton et al. 2005). In general, mtCOI sequence variation showed greater divergence between conspecific individuals collected in different regions or ocean basins (Bucklin et al. 2003). *Centropages typicus* Krøyer, 1849, showing clear morphological differences in the chela of the fifth thoracopod of the male, between the northwestern and northeastern Atlantic and the Mediterranean Sea showed genetic differences in mtCOI and nuclear rDNA ITS1 (Castellani et al. 2012). Recently, ITS rDNA (internal transcribed spacers of the nuclear ribosomal cistron) was used as a new marker in the molecular phylogeny of Oncaeidae, and this marker was also found to be useful for elucidating the genetic relationship between species (Di Capua et al. 2017). They proposed the use of ITS (especially ITS2) for phylogenetic reconstruction. Therefore, it can be suggested that our results will have to be discussed again in the future with further analysis of other regions of the gene (e.g., nuclear genes).

Recently, there was incongruence between the identified species of *Paracalanus parvus* complex through a comprehensive analysis of progressive molecular method and conventional morphology (Kasapidis et al. 2018). Therefore, considering the high morphological similarity of species belonging to the Oncaeidae, including *Spinoncaea*, the existence of sibling species, and the resulting complexity of taxonomic analyses, molecular analysis will be essential to clarify species identification in this taxon. To observe the relationships between morphological variation and genetic variation requires further analyses in the future taking into consideration various genes.

Acknowledgements

The constructive comments of two reviewers are gratefully acknowledged. This research was supported by the Center for Women In Science, Engineering and Technology (WISET) and WISET Regional Agency of PKNU Grant funded by the Ministry of Science and ICT(MSIT) under the Program for Returners into R&D (Returners into R&D program of Dongnam regional agency No. 2020-008) to K Cho. This research was part of the project titled 'Aquisition of marine bioresources from the high seas and screening of biological potency', funded by the Ministry of Oceans and Fisheries, Korea and by a research program (Contract No. PE99924) of the Korea Institute of Ocean Science and Technology (KIOST).

References

Behrends G, Korshenko A, Viitasalo M (1997) Morphological aberrations in females of the genus *Acartia* (Copepoda, Calanoida) in the Baltic Sea. Crustaceana 70(5): 594–606. https://doi.org/10.1163/156854097X00708

Bersano JGF, Boxshall GA (1994) Planktonic copepods of the genus *Oncaea* Philippi (Poecilostomatoida: Oncaeidae) from the waters off southern Brazil. Nauplius 2: 29–41.

Böttger-Schnack R (1999) Taxonomy of Oncaeidae (Copepoda: Poecilostomatoida) from the Red Sea. I. 11 species of *Triconia* gen. nov. and a redescription of *T. similis* (Sars) from Norwegian waters. Mitteilungen aus dem Hamburgischen Zoologischen Museum und Institut 96: 37–128.

Böttger-Schnack R (2001) Taxonomy of Oncaeidae (Copepoda: Poecilostomatoida) from the Red Sea. II. Seven species of *Oncaea* s. str. Bulletin of the Natural History Museum London (Zoology) 67: 25–84.

Böttger-Schnack R (2003) Taxonomy of Oncaeidae (Copepoda, Poecilostomatoida) from the Red Sea. V. Three species of *Spinoncaea* gen. nov. (*ivlevi*-group), with notes on zoogeographical distribution. Zoological Journal of the Linnean Society 137(2): 187–226. https://doi.org/10.1046/j.1096-3642.2003.00056.x

Böttger-Schnack R (2005) Taxonomy of Oncaeidae (Copepoda: Cyclopoida) from the Red Sea. VII. *Oncaea cristata*, a new species related to the *ovalis*-complex, and a revision of *O. ovalis* Shmeleva and *O. bathyalis* Shmeleva from the Mediterranean. Cahiers de Biologie Marine 46(2): 161–209.

Böttger-Schnack R, Boxshall GA (1990) Two new *Oncaea* species (Copepoda: Poecilostomatoida) from the Red Sea. Journal of Plankton Research 12(4): 861–871. https://doi.org/10.1093/plankt/12.4.861

Böttger-Schnack R, Hagen W, Schnack-Schiel SB (2001) The microcopepod fauna in the Gulf of Aqaba, northern Red Sea: Species diversity and distribution of Oncaeidae (Poecilostomatoida). Journal of Plankton Research 23: 1029–1035. https://doi.org/10.1093/plankt/23.9.1029

Böttger-Schnack R, Huys R (2001) Taxonomy of Oncaeidae (Copepoda, Poecilostomatoida) from the Red Sea. III. Morphology and phylogenetic position of *Oncaea subtilis* Giesbrecht, 1892. Hydrobiologia 453/454: 467–481. https://doi.org/10.1023/A:1013114706718

Böttger-Schnack R, Machida RJ (2011) Comparison of morphological and molecular traits for species identification and taxonomic grouping of oncaeid copepods. Hydrobiologia 666: 111–125. https://doi.org/10.1007/s10750-010-0094-1

Böttger-Schnack R, Schnack D (2013) Definition of species groups of Oncaeidae (Copepoda: Cyclopoida) as basis for a worldwide identification key. Journal of Natural History 47: 265–288. https://doi.org/10.1080/00222933.2012.708453

Böttger-Schnack R, Schnack D (2015) Development of an interactive identification key for Oncaeidae (Copepoda: Cyclopoida). Journal of Natural History 49: 2727–2741. https://doi.org/10.1080/00222933.2015.1022614

Böttger-Schnack R, Schnack D (2019) OncIdent – an interactive identification key for Oncaeidae Giesbrecht, 1983 ["1892"] (Copepoda: Cyclopoida). Marine Biodiversity 49: 1043–1046. https://doi.org/10.1007/s12526-018-0863-z

Böttger-Schnack R, Schnack D (2016–2021) Oncaeidae of the World Ocean – Interactive identification key for female Oncaeidae (Copepoda) – OncIdent2.0. https://rb-schnack.de/login-for-identification-key.html [Accessed April 2021]

Brylinski JM (1984) Anomalies morphologiques chez le genre *Acartia* (Crustacea, Copepoda): Description et essai de quantification. Journal of Plankton Research 6(6): 961–966. [in French, English summary] https://doi.org/10.1093/plankt/6.6.961

Bucklin A, Frost BW (2009) Morphological and molecular phylogenetic analysis of evolutionary lineages within *Clausocalanus* (Copepoda: Calanoida). Journal of Crustacean Biology 29(1): 111–120. https://doi.org/10.1651/07-2879.1

Bucklin A, Frost BW, Bradford-Grieve J, Allen LD, Copley NJ (2003) Molecular systematic and phylogenetic assessment of 34 calanoid copepod species of the Calanidae and Clausocalanidae. Marine Biology 142: 333–343. https://doi.org/10.1007/s00227-002-0943-1

Castellani C, Lindley AJ, Wootton M, Lee CM, Kirby RR (2012) Morphological and genetic variation in the North Atlantic copepod, *Centropages typicus*. Journal of the Marine Biological Association of the United Kingdom 92(1): 99–106. https://doi.org/10.1017/S0025315411000932

Cho K (2011) Study on the taxonomy of family Oncaeidae (Copepoda, Cyclopoida) from the CCFZ (Clarion-Clipperton Fracture Zone; C-C zone) in the northeast equatorial Pacific. PhD Thesis, Hanyang University, Seoul.

Cho K, Kim WS, Böttger-Schnack R, Lee W (2013) A new species of the *dentipes*-subgroup of *Triconia* and a redescription of *T. giesbrechti* and *T. elongata* (Copepoda: Cyclopoida: Oncaeidae) from the tropical Pacific and the Korea Strait. Journal of Natural History 47: 1707–1743. https://doi.org/10.1080/00222933.2013.771757

Cho K, Böttger-Schnack R, Kim WS, Lee W (2017) Two species of the *conifera*-subgroup of *Triconia* (Copepoda, Oncaeidae) from the northeastern equatorial Pacific, with a description of the unknown male of *T. hirsuta*. Zootaxa 4286: 347–369. https://doi.org/10.11646/zootaxa.4286.3.3

Cho K, Böttger-Schnack R, Kim WS, Lee W (2019) Two new species of the *similis*-subgroup of *Triconia* Böttger-Schnack, 1999 (Copepoda, Oncaeidae) and a redescription of *T. denticula* Wi, Shin & Soh, 2011 from the northeastern equatorial Pacific. Zoosystema 41(28): 567–593. https://doi.org/10.5252/zoosystema2019v41a28

Cho K, Kim JG, Lee J (2020) New record of *Oncaea prendeli* (Copepod, Cyclopoida, Oncaeidae) in Korean Waters. Ocean and Polar Research 42(4): 283–292. http://dx.doi.org/10.4217/OPR.2020.42.4.283

Claus C (1863) Die frei lebenden Copepoden mit besonderer Berücksichtigung der Fauna Deutschlands, der Nordsee und des Mittelmeeres. Wilhelm Engelmann, Leipzig, 230 pp. https://doi.org/10.5962/bhl.title.58676

Cornils A (2014) Non-destructive DNA extraction for small pelagic copepods to perform integrative taxonomy. Journal of Plankton Research 37(1): 6–10. https://doi.org/10.1093/plankt/fbu105

Dana JD (1846) Notice of some genera of Cyclopacea. The American Journal of Science and Arts 1(2): 225–230.

Di Capua I, Maffucci F, Pannone R, Mazzocchi MG, Biffali E, Amato A (2017) Molecular phylogeny of Oncaeidae (Copepoda) using nuclear ribosomal internal transcribed spacer (ITS rDNA). PLoS ONE 12(4): e0175662. https://doi.org/10.1371/journal.pone.0175662

Farran GP (1929) Crustacea. Part X. Copepoda. British Antarctic ('Terra Nova') Expedition, 1910. Natural History Reports, Zoology 8(3): 203–306.

Folmer O, Black M, Hoeh W, Lutz R, Vrijenhoek R (1994) DNA primers for amplification of mitochondrial cytochrome c oxidase subunit 1 from diverse metazoan invertebrates. Molecular Marine Biology and Biotechnology 3(5): 294–299.

Giesbrecht W (1891) Elenco dei Copepodi pelagic raccolti dal tenente di vascello Gaetano Chierchia durante il viaggio della R. Corvetta, Vettor Pisani negli anni 1882–1885, e dal tenente di vascello Francesco Orsini nel Mar Rosso, nel 1884. Atti della Reale Accademia del Lincei Rendiconti 4(7): 474–481.

Giesbrecht W (1893 ["1892"]) Systematik und Faunistik der pelagischen Copepoden des Golfes von Neapel und der angrenzenden Meeresabschnitte. Fauna und Flora des Golfes von Neapel 19: 1–831. https://doi.org/10.5962/bhl.title.59541

Hall TA (1999) BioEdit: a user-friendly biological sequence alignment editor and analysis program for Windows 95/98/NT. Nucleic acids symposium series 41: 95–98.

Heron GA (1977) Twenty-six species of Oncaeidae (Copepoda: Cyclopoida) from the Southwest Pacific-Antarctic area. In Pawson DL (Ed.), Biology of the Antarctic Seas, VI. Antarctic Research Series 26: 37–96. https://doi.org/10.1029/AR026p0037

Heron GA, Bradford-Grieve JM (1995) The marine fauna of New Zealand: Pelagic Copepoda: Poecilostomatoida: Oncaeidae. New Zealand Oceanographic Institute Memoir 104: 1–57.

Heron GA, English TS, Damkaer DM (1984) Arctic Ocean Copepoda of the genera *Lubbockia*, *Oncaea*, and *Epicalymma* (Poecilostomatoida: Oncaeidae), with remarks on distributions. Journal of Crustacean Biology 4: 448–490. https://doi.org/10.2307/1548043

Hill RS, Allen LD, Bucklin A (2001) Multiplexed species-specific PCR protocol to discriminate four N. Atlantic *Calanus* species, with a mtCOI gene tree for ten *Calanus* species. Marine Biology 139(2): 279–287. https://doi.org/10.1007/s002270100548

Huys R, Böttger-Schnack R (2007) Taxonomy of Oncaeidae (Copepoda, Cyclopoida) from the Red Sea.- VIII. Morphology and phylogenetic position of *Oncaea tregoubovi* Shmeleva, 1968 and the closely related *O. prendeli* Shmeleva, 1966 from the Mediterranean Sea. Mitteilungen aus dem Hamburgischen Zoologischen Museum und Institut 104: 89–127.

Huys R, Gee JM, Moore CG, Hamond R (1996) Synopses of the British Fauna (New Series) No. 51. Marine and brackish water harpacticoid copepods, Part 1. Field Studies Council, Shrewsbury, 352 pp.

Kasapidis P, Siokou I, Khelifi-Touhami M, Mazzocchi MG, Matthaiaki M, Christou E, Fernandez de Puelles ML, Gubanova A, Di Capua I, Batziakas S, Frangoulis C (2018) Revising the taxonomic status and distribution of the *Paracalanus parvus* species complex (Copepoda, Calanoida) in the Mediterranean and Black Seas through an integrated analysis of morphology and molecular taxonomy. Journal of Plankton Research 40(5): 595–605. https://doi.org/10.1093/plankt/fby036

Krøyer H (1849) Karcinologiske Bidrag (Fortsaettelse). Naturhistorisk Tidsskrift Ser II 2(6): 561–609.

Kumar S, Stecher G, Tamura K (2016) MEGA7: molecular evolutionary genetics analysis version 7.0 for bigger datasets. Molecular biology and evolution 33(7): 1870–1874. https://doi.org/10.1093/molbev/msw054

Machida RJ, Tsuda A (2010) Dissimilarity of species and forms of *Neocalanus* copepods using mitochondrial COI, 12S, nuclear ITS and 28S gene sequences. PLoS ONE 5(4): e10278. https://doi.org/10.1371/journal.pone.0010278

Machida RJ, Miya MU, Nishida M, Nishida S (2002) Complete mitochondrial DNA sequence of *Tigriopus japonicus* (Crustacea: Copepoda). Marine Biotechnology 4(4): 406–417. https://doi.org/10.1007/s10126-002-0033-x

Machida RJ, Miya MU, Nishida M, Nishida S (2004) Large-scale gene rearrangements in the mitochondrial genomes of two calanoid copepods *Eucalanus bungii* and *Neocalanus cristatus* (Crustacea), with notes on new versatile primers for the srRNA and COI genes. Gene 332: 71–78. https://doi.org/10.1016/j.gene.2004.01.019

Malt SJ (1982) New and little known species of Oncaeidae (Cyclopoida) from the northeastern Atlantic. Bulletin of the British Museum (Natural History) Zoology 42: 185–205.

Melo PAMC, Melo Jr M, Araújo M, Neumann-Leitão S (2014) A morphological anomaly in *Clausocalanus mastigophorus* (Claus, 1863) (Copepoda, Calanoida) from St. Peter and St. Paul Archipelago. Brazilian Journal of Biology 74(3): 728–729. https://doi.org/10.1590/bjb.2014.0092

Metz C (1995) Seasonal variation in the distribution and abundance of *Oithona* and *Oncaea* species (Copepoda, Crustacea) in the southeastern Weddell Sea, Antarctica. Polar Biology 15(3): 187–194. https://doi.org/10.1007/BF00239058

Nishibe Y, Ikeda T (2004) Vertical distribution, abundance and community structure of oncaeid copepods in the Oyashio region, western subarctic Pacific. Marine Biology 145(5): 931–941. https://doi.org/10.1007/s00227-004-1392-9

Nishibe Y, Hirota Y, Ueda H (2009) Community structure and vertical distribution of oncaeid copepods in Tosa Bay, southern Japan. Journal of the Marine Biological Association of the United Kingdom 89(3): 491–498. https://doi.org/10.1017/S0025315409003087

Razouls C, de Bovée F, Kouwenberg J, Desreumaux N (2005–2021) Diversity and Geographic Distribution of Marine Planktonic Copepods. Sorbonne University, CNRS. http://copepodes.obs-banyuls.fr/en [Accessed February 03, 2021]

Shirayama Y, Kaku T, Higgins RP (1993) Double-sided microscopic observation of meiofauna using an HS-slide. Benthos Research 44: 41–44. [in Japanese, English summary] https://doi.org/10.5179/benthos1990.1993.44_41

Shmeleva A (1966) New species of the genus *Oncaea* (Copepoda, Cyclopoida) from the Adriatic Sea. Zoologicheskii Zhurnal 45(6): 932–936. [in Russian, English summary]

Shmeleva A (1968) New species of planktonic Copepoda: Cyclopoida from the Adriatic Sea. Zoologicheskii Zhurnal 47(12): 1784–1793. [in Russian, English summary]

Shmeleva A (1969) Espèces nouvelles du genre *Oncaea* (Copepoda, Cyclopoida) de la mer Adriatique. Bulletin de l'Institute Océanographique, Monaco, 68(1393): 1–28. [in French]

Staton JL, Wickliffe LC, Garlitska L, Villanueva SM, Coull BC (2005) Genetic Isolation Discovered among Previously Described Sympatric Morphs of a Meiobenthic Copepod. Journal of Crustacean Biology 25(4): 551–557. https://doi.org/10.1651/C-2600.1

Walter TC, Boxshall G (2021) World of Copepods database. Oncaeidae Giesbrecht, 1893. [Accessed through World Register of Marine Species] http://www.marinespecies.org/aphia.php?p=taxdetails&id=128586 [accessed on 2 March 2021]